EVALUATION OF ANTICANCER ACTIVITY OF *MOMORDICA BALSAMINA* EXTRACTS AND POTENTIAL INTERACTIONS WITH A CONVENTIONAL ANTICANCER DRUG IN COLON CANCER

BY

KHOLOFELO MMANOKO MALEMELA

RESEARCH THESIS

SUBMITTED IN FULFILMENT OF THE REQUIREMENTS FOR THE DEGREE OF

PHILOSOPHIAE DOCTOR (Ph.D.)

IN

BIOCHEMISTRY

IN THE

FACULTY OF SCIENCE AND AGRICULTURE

(SCHOOL OF MOLECULAR AND LIFE SCIENCES)

AT THE

UNIVERSITY OF LIMPOPO, SOUTH AFRICA.

SUPERVISOR: Prof. VG MBAZIMA

Co-SUPERVISOR: Dr S RIEDEL-VAN HEERDEN (SAMRC)

2021

Declaration

I declare that the thesis hereby submitted to the University of Limpopo, for the degree of **Philosophiae Doctor (Ph.D.)** in **Biochemistry** has not been previously submitted by me for a degree at this or any other University; that it is my work in design and execution, and that all material contained therein have been duly acknowledged.

Malemela K.M. (Miss) — Surname and initials (Title)

25 June 2021 — Date.

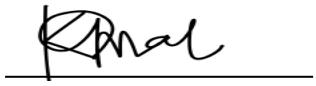

Signature:

Dedication

This work is dedicated to **MYSELF**.

Acknowledgements

- **GOD**.
- My supervisor, **Prof. VG Mbazima**, for the opportunity to be mentored by him. For presenting me with opportunities to expand my technical experience and my research expertise. I am forever grateful.
- My co-supervisor, **Dr S Riedel van Heerden**, for all the help, support and supervision. I am truly grateful.
- My parents, **Margaret Moloko** and **Mahomotjane Piet Malemela** for their unwavering support throughout this journey. The prayers and love that kept me going and afloat.
- My brother, **Katlego Lehumo Malemela**, for his support and encouragement.
- The **South African Medical Research Council (SAMRC) Research Capacity Development Initiative**, for financial support, resources and opportunities presented to learn from others and also expand my research expertise.
- The SAMRC **Biomedical Research and Innovation Platform** for their time and devotion to my work in Cape Town.
- **Thendo Mabuda, Oelfah Patel, Karabo Serala**, **Dolly Kgakishe** and **Nduvho Mohale** for the support, encouragement and mostly keeping me sane.
- The **University of Limpopo**, for its facilities and resources.
- The **Biochemistry, Microbiology and Biotechnology (BMBT)** department of the University of Limpopo for their academic support wherever rendered.

List of conference presentations and publications

1. Pieter Venter, Kholofelo Malemela, Vusi Mbazima, Leseilane J. Mampuru, Christo J.F. Muller and Sylvia Riedel. An RP-LC-TWIMS-HRMS and chemometric approach to differentiate between *Momordica balsamina* chemotypes from three different geographical locations in Limpopo Province of South Africa (Venter *et al*. 2021 *Molecules* **26**x “in press”).
2. R Mabasa, K Malemela, K Serala, M Kgakishe, T Matsebatlela, M Mokgotho, V Mbazima. *Ricinus communis* Butanol Fraction Inhibits MCF-7 Breast Cancer Cell Migration, Adhesion, and Invasiveness(2021). *Integrative Cancer Therapies* 20: 1–11 doi:10.1177/1534735420977684).
3. K Malemela, S Riedel and VG Mbazima. Evaluation of the anticancer activity of *Momordica balsamina* extracts and potential interactions with a conventional anticancer drug in colon cancer. SAMRC Early Career Scientific Convention, Parow, Cape Town, 26 October 2020. Oral presentation.
4. K. Malemela S Riedel, P Venter and VG Mbazima. *Momordica balsamina* induces pro-apoptotic activities associated with cell cycle arrest in HT-29 colon cancer cells. 10th Biomedical Research & Innovation Symposium, Parow Valley, Cape Town, 19 and 20 October 2020. Oral presentation.
5. K Malemela, S Riedel, P Venter and VG Mbazima. Phytochemical profiling of *Momordica balsamina* and potential anticancer activity of the crude methanol and crude water leaf extracts on colon HT-29 cancer cells. 19th Biomedical Research & Innovation Symposium, Parow Valley, Cape Town, 21 October 2019. Poster presentation.
6. K Malemela, S Riedel and VG Mbazima. Evaluation of anticancer activity of *Momordica balsamina* extracts and potential interactions with a conventional anticancer drug in colon cancer. SAMRC Early Career Scientific Convention, Parow, Cape Town, 9 – 11 October 2019. Oral presentation.
7. K Malemela, S Riedel and VG Mbazima. Phytochemical profiling of *Momordica balsamina* and potential anticancer activity of the crude methanol and crude water leaf extracts on colon HT-29 cancer cells. 4th Annual Joint HDI-SAMRC Research Conference, Salt Rock Hotel, Durban, July 25 – 27, 2019. Oral presentation.

8. K Malemela, S Riedel and VG Mbazima. Evaluation of anticancer activity of the *Momordica balsamina* water extract and its potential interactions with a conventional anticancer drug in colon cancer. 3rd Annual Joint HDI-SAMRC Research Conference, Protea Hotel, Techno Park, Stellenbosch, July 25 – 27 2018. Oral presentation.

Table of Contents

List of figures

List of tables

List of abbreviations

5-FU	5-Fluorouracil
A459	Human alveolar adenocarcinoma cell line with basal epithelial morphology
ABC	ATP-binding cassette
ABP	Actin binding protein
ADP	Adenosine diphosphate
AhR	Aryl hydrocarbon receptor
AIF	Apoptosis-inducing factor
ANOVA	Analysis of variance
AO	Acridine orange
Apaf-1	Apoptosis protease activating factor 1
APC	Adenomatous polyposis coli
APC/C	Anaphase promoting complex
ATCC	American type culture collection
Bad	Bcl-2-associated death promoter
Bak	Bcl-2 antagonist killer 1
BAW	Butanol: acetic acid: water
Bax	Bcl-2 associated X, apoptosis regulator
BCA	Bicinchoninic acid assay
Bcl-2	B-cell lymphoma-2
Bcl-B	Bcl-2-like protein similar in amino acid sequence to the Boo protein
Bcl-W	Bcl-2-like protein 2
Bcl-xL	B-cell lymphoma-extra large
Bcl2A1	Bcl-2 related protein A1
BEA	Benzene: ethyl acetate: ammonium hydroxide
BH1/2/3/4	Bcl-2 homology 1/2/3/4
Bid	BH3 interacting-domain death agonist
Bik	Bcl-2-interacting killer
Bim	Bcl-2-like protein 11
Bmf	Bcl-2 modifying factor
BMP	Basic metabolic panel

Bok	Bcl-2-related ovarian killer
BRAF	B-Raf
BSA	Bovine serum albumin
C2C12	Immortalised mouse myoblast cell line
CAD	Caspase activated DNase
CARD	Caspase recruitment domain
CDK	Cyclin-dependent kinase
CDKI	Cyclin-dependent kinase inhibitor
CEA	Carcinoembryonic antigen
CEF	Chloroform: ethyl acetate: formic acid
cIAP-1/2	Cellular Inhibitor of apoptosis-1/2
CIMP	CpG island methylator phenotype
CIN	Chromosomal instability
CPG Island	5'-Cytosine-Phosphate-Guanosine-3' island
CRC	Colorectum cancer
CYP	Cytochrome P450
dATP	Deoxyadenosine triphosphate
DCF	Dichlorodihydrofluorescein
DED	Death effector domain
DFF	DNA fragment factor
DISC	Death-inducing signalling complex
DMEM	Dulbecco's modified eagle's medium
DMSO	Dimethyl sulfoxide
DNA	Deoxyribonucleic acid
DPBS	Dulbecco's phosphate buffered saline
dTMP	Deoxythymidine monophosphate
EC_{50}	Half maximal effective concentration of drug
EDTA	Ethylenediaminetetraacetic acid
EGTA	Ethyleneglycol-bis(beta-aminoethylether)-*N,N,N',N'*-tetraacetic acid
ER	Endoplasmic reticulum
ERK	Extracellular signal-regulated kinase
ESI	Electrospray ionisation
FA	Fatty acid

FAD	Flavin adenine dinucleotide
FADD	Fas-associated death domain
FAO	Food and Agriculture Organisation
FasL	Fas-1 induced apoptosis signal ligand
FasR	Fas-1 induced apoptosis signal receptor
FBS	Foetal bovine serum
FDA	Food and drug administration
FdUMP	Fluorodeoxyuridine monophosphate
FITC	Fluorescein Isothiocyanate
FMN	Flavin mononucleotide
G1	Gap 1
G2	Gap 2
GS	Growth signals
HAS	Human serum albumin
HeLa	Immortalised human cell line, derived from cervical cancer cells
HEPES	4-(2-hydroxyethyl)-1-piperazineethanesulfonic acid
HIF 1-α	Hypoxia-inducible factor 1-alpha
HO-1/2	Heme oxygenase-1/2
HPLC-UV	High-Pressure Liquid Chromatography coupled with an Ultra-Violet detector
Hrk	Harakiri
HRP	Horseradish peroxidase
Hsp	Heat-shock protein
HT-29	Human colorectal adenocarcinoma cell line with epithelial morphology
IAP	Inhibitor of apoptosis
IC_{50}	Half maximal inhibitory concentration
ICAD	Inhibitor of caspase-activated DNase
JC-1	5,5′,6,6′-tetrachloro-1,1′,3,3′-tetraethylbenzimi-dazolylcarbocyanine iodide
KRAS	Kirsten rat sarcoma viral oncogene homolog gene
LC-MS	Liquid Chromatography-Mass Spectrometry
M phase	Mitosis phase

M. balsamina	*Momordica balsamina*
M. charantia	*Momordica charantia*
MAPK	Mitogen-activated protein kinase
MCF-7	Human breast cancer cell line with epithelial luminal morphology
Mcl-1	Myeloid leukaemia cell differentiation protein
MDR	Multidrug resistance protein
MeOH	Methanol
MMP	Mitochondrial membrane potential
MPT	Mitochondrial permeability transition
MS	Mass spectrometry
MS^E	Energy spectra
MSI	Microsatellite instability
MTT	3-(4,5-Dimethylthiazol-2-yl)-2,5-diphenyltetrazolium
NAD	β-nicotinamide adenine dinucleotide
NADH	Nicotinamide adenine dinucleotide
NADPH	Nicotinamide adenine dinucleotide phosphate
NCI	National Cancer Institute
NFκB	Nuclear factor kappa B
NOXA	Phorbol-12-myristate-13-acetate-induced protein 1
O_2	Dioxygen
P-gp	P-glycoprotein
PARP	Poly (ADP-ribose) polymerase
PBS	Phosphate buffered saline
PDA	Photodiode array
PI	Propidium Iodide
PON-2	Paraoxonase 2
PS	Phosphatidylserine
PUMA	p53 upregulated modulator of apoptosis
PVDF	Polyvinylidene fluoride
Q-TOF	Quadruple time-of-flight
RNase	Ribonuclease
ROS	Reactive oxygen species
S phase	DNA synthesis phase

S.D.	Standard deviation
S.E.M	Standard Error and Mean
SAMRC	South African Medical Research Council
SDS	sodium dodecyl sulphate
Smac/Diablo	Second mitochondria-derived activator of caspases/direct IAP-binding protein with low pI
T4	Thyroxine
TLC	Thin-layer chromatography
TNF	Tumour necrosis factor
TNF - α	Tumour necrosis factor-alpha
TNFR	Tumour necrosis factor-alpha receptor
TP53	Tumour protein p53
TRADD	Tumour necrosis factor-alpha receptor-associated death receptor
TRAIL	Tumour necrosis factor-alpha- related apoptosis-inducing ligand
TS	Thymidylate synthase
UK	United Kingdom
USA	United States of America
UV	Ultraviolet
WHO	World Health Organisation
XIAP	X-linked Inhibitor of apoptosis protein

Abstract

Cancer remains one of the leading causes of morbidity and mortality worldwide with an estimated 9.9 million deaths in 2020. Cancer treatment regimens such as chemotherapy and radiotherapy have over the years fallen short due to drug resistance, toxicity, damage to normal healthy cells and tissues surrounding the treatment area. Moreover, they have shown very limited survival benefits for most advanced staged cancers such as colorectal cancer, which in 2020 was responsible for 3 728 deaths with a 6.8% incidence rate. Despite the many efforts in developing alternative chemotherapeutic strategies, cancer of the colon and cancer, in general, remains a burden. For centuries, plants and plant derivatives have been exploited for their nutritional and medicinal properties and now serve as chemical scaffolds or templates for designing and synthesising products with pharmacological importance. Herbal medicines are claimed to enhance therapeutic effects and are often used in combination with chronic medication. However, the concurrent use of herbal medicines and synthetic drugs may affect the pharmacokinetic profile of therapeutic drugs or trigger unexpected and undesirable effects. This study aimed to characterise the leaf extracts (crude water and crude methanol) of *Momordica balsamina* and investigate their potential anticancer activity on HT-29 colon cancer cells. The study also aimed to asses the effect of the extracts on drug metabolising enzymes (CYP450), specifically those which metabolise 5-Fluorouracil (5-FU) prodrugs or are inhibited by 5-FU since it is one of the first-line treatments for colon cancer.

Dried powdered leaves were extracted using water and absolute methanol to obtain crude water and crude methanol extracts, respectively. For characterisation, the extracts were spotted on thin-layer chromatography (TLC) plates and further screened using chemical tests. The ferric ion reducing power assay and Liquid chromatography-mass spectrometry were used to determine the antioxidant activity of the extracts and to identify prominent or abundant compounds in each extract, respectively. To assess the cytotoxic effect of the extracts and 5-FU, HT-29 colon cancer cells and C2C12 muscle cells, which were used as a model for normal cells, were exposed to concentrations that ranged from 0 to 2000 µg/ml for the water (H_2O) extract, 0 to 300 µg/ml for the methanol (MeOH) extract or 0 to 100 µg/ml of 5-FU for 24 and 72 hours, and subjected to the MTT assay. The effect of the extracts on the efficacy of 5-FU was

assessed using the MTT assay by combined treatments of the extract and 5-FU. Genotoxicity of the extracts was assessed on the C2C12 cells using the Muse™ Multi-Colour DNA Damage kit. The generation of intracellular reactive oxygen species (ROS) was assessed by flow cytometry using the DCFH-DA assay. The JC-1 and acridine orange (AO)/propidium iodide (PI) staining assays were used to assess the effect of the extracts on the mitochondrial potential as well as cell and nuclear morphology, respectively. Apoptosis was quantified by flow cytometry using annexin V/PI and caspase activation assessed using the Caspase-8 and Caspase-9 colourimetric assay kits. The pro-apoptotic mechanism(s) was determined by assessing the expression profiles of selected apoptosis regulatory proteins using the human apoptosis antibody array kit. Cell cycle analysis by flow cytometry was conducted to determine the effect of the extract on the cell division cycle. Moreover, to determine the potential of herb-drug interactions, the Vivid® CYP450 Screening kits and P-gp-Glo™ Assay Systems with P-glycoprotein were used to assess the effect on the activity of drug metabolising enzymes and drug transportation, respectively.

The results showed that the MeOH extract possessed fewer polar compounds, higher ferric iron-reducing power, and a relative abundance of flavonol glycosides, cucurbitane-type triterpenoid aglycones, and cucurbitane-type glycosides than the H_2O extract. The MeOH extract was further selectively cytotoxic to the HT-29 colon cancer cells at 24 hours of treatment and selectively induced genotoxicity in HT-29 cells. The H_2O extract, however, was not cytotoxic to the HT-29 cells at all the tested concentrations at 24 and 72 hours of treatment. Analysis of nuclear and cell morphology suggested that the decrease in the percentage viability of MeOH extract-treated cells was associated with apoptotic cell death. Apoptosis was further confirmed by the loss of mitochondrial potential, increase in ROS production, caspase-8 and -9 activities as well as Annexin-V/PI-stained cells. Cell cycle analysis revealed cell cycle arrest at the S phase in MeOH extract-treated cells. Analysis of protein expression profiles revealed that the extract modulated various proteins that play a role in the promotion or inhibition of apoptosis. Moreover, the MeOH extract was shown to inhibit the activity of CYPs 1A2, 2A6, 2C8, and 2C9, while the H_2O extract showed no significant inhibitory effects on the activity of all tested CYPs and 5-FU only significantly inhibited the activity of CYP2C9. However, combinatory treatments with 5-FU and the MeOH extract were shown to have no additive or diminishing effects on

the efficacy of 5-FU on the activity of all the tested CYP enzymes. Treatment with 5-FU (0.008 – 32 µg/ml) and the H_2O extract (0.02 – 200 µg/ml) was shown to stimulate the ATPase activity of P-gp, while the MeOH extract significantly inhibited its activity with concentrations of 0.2, 2, and 20 µg/ml.

In conclusion, the MeOH extract selectively induced cancer cell toxicity, genotoxicity as well as S phase cell cycle arrest and apoptosis via the intrinsic and extrinsic pathways. The anticancer activity of the MeOH leaf extract of *M. balsamina* as well as its antioxidant potential may be attributed to the presence and relative abundance of flavonol glycosides, cucurbitane-type triterpenoid aglycones, and cucurbitane-type glycosides. Although the MeOH extract may potentially reverse the effects of P-gp multidrug resistance by decreasing its activity, its inhibition of the activity of CYPs 1A2, 2A6, 2C8 and, 2C9, which are involved in the metabolism of more than 80% of the drugs in clinical use may suggest that co-administration of the MeOH extract may still result in increased plasma levels of drugs, thereby resulting in toxicity. The H_2O extract, although not pro-apoptotic as the MeOH extract may still have the potential to be developed as a nutraceutical as it was shown to exhibit no adverse drug interactions and because this species is known to possess a wide variety of nutritional and medicinal values.

Chapter 1

1. Introduction

In 2020, cancer was responsible for an estimated 9.9 million deaths and as such is the second leading cause of death around the globe [1, 2]. About 70% of these deaths occur in low-and-middle-income countries [2], like South Africa, where only 15% of the population has access to private healthcare while the rest of the population relies on public healthcare services [3]. This causes a strain on public healthcare as chemotherapy costs continue to rise [3] and consequently, rapid access to treatment favours patients who can afford to pay for or have sufficient medical insurance [4].

Chemotherapeutic treatments currently in use possess intrinsic problems that often result in toxicity in several organs which include, for instance, cardiac, renal and, myelotoxicity caused by anthracyclines such as doxorubicin D [5, 6, 7]. Although several chemically derived drugs such as azacytidine, decitabine, vorinostat and, istodax have been developed and undergone trials showing no adverse side effects, it is extremely costly and demanding to engineer a chemically-derived drug that would selectively distinguish cancer cells from normal cells [5, 8]. Therefore, there is an urgent need to screen plants for novel compounds or analogues and develop an alternative treatment that is less costly and able to discriminate cancer cells from normal cells and induce apoptosis, specifically in cancer cells.

Plants are valuable raw materials and sources for the development of numerous traditional and modern medicines [9]. In some parts of the world, their use as herbal medicine dates back centuries and continues to date as, on a cultural and spiritual perspective, they are trusted more than western medicine [10, 11, 12, 13]. More than 80% of the world's population rely on herbal medicines as a part of their primary healthcare [14]. This is because they are claimed to enhance therapeutic effects and to be free of side effects [15, 16]. Furthermore, herbal medicines are commercially promoted as complementary and alternative medicine (CAM) as they present an alternative approach in the treatment of many diseases which include cancer [17].

Plant-derived nutraceuticals are said to be advantageous as they improve the overall health of patients [18]. However, patients with cancer are advised against the use of such supplements [19], as some can cause a risk of recurrence [20, 21, 22, 23, 24], while some

may prevent the cellular oxidative damage in cancer cells that is required for radiation therapy and chemotherapy treatments to be effective [25]. The occurrence of tumour resistance to the current therapeutic agents has prompted research on exogenous antioxidants which have shown the capability to prevent damage caused by free radicals associated with the development of cancer [26]. These exogenous antioxidants are primarily from plants and hence the introduction of phytotherapy, which makes use of extracts of natural origin as medicine and nutritional supplement therapy in cancer treatment [26, 27]. Although large-scale randomised trials on cancer prevention have shown both beneficial and adverse effects of nutritional supplement therapy amongst cancer patients, many still practice nutritional supplement therapy as it is perceived to have low risk, provide anticancer and anti-toxicity agents [28, 29, 30].

In practice, herbal medicines are used concurrently with therapeutic drugs without considering the potential of adverse herb-drug interactions [31]. Most herbal medicines contain a variety of bioactive compounds whose active constituents may affect the pharmacokinetic profile of therapeutic drugs or trigger unexpected and undesirable effects [32, 33, 34], such as gastrointestinal disturbances [35], blood loss [36], seizures [37], hypoglycemia [38], hepatotoxicity [39], and organ fibrosis [40]. Only a fraction of plant metabolites has so far successfully entered the pharmaceutical production chain for widespread clinical use [41], although several herbal medicines have been established with therapies showing promising potential [14]. Many more potential drug candidates remain untested and are used with poor monitoring, with little knowledge about their mode of action, adverse reactions, and interaction with other drugs as well as functional foods. Thus, there is a need for a detailed investigation of these herbs as well as herb-drug interactions (HDI) [14].

Momordica species are vegetable crops found mostly in African and Asian countries where their leaves are consumed as a vegetable [42]. In the Limpopo and Mpumalanga provinces of South Africa, as well as eSwatini, the leaves are boiled and consumed as tea or cooked to serve as a relish. The seeds, fruit, and leaves of this plant species are traditionally used for the treatment of diabetes [42] and are said to possess antitumour activities [43]. Furthermore, this species contains a wide variety of minerals and amino acids [44], making it a potential herbal supplement or part of a healthy diet. Although *Momordica* spp. are widely used, there is still a lack of scientific

documentation on safety and biological effects, especially how for instance plant extracts interact with metabolising enzymes within the body or how they may interact with other therapeutic drugs. Moreover, to the best of our knowledge, there is a lack or no experimental studies investigating the effect of the *M. balsamina* crude water and crude methanol leaf extracts on HT-29 colon cancer cells.

Chapter 2

2. Literature review

Before the development of western medicine, plants and plant derivatives were used as herbal medicines for the treatment and prevention of diseases [45] and have over the years shown to play a vital role in preserving human lives [46]. The use of herbal plants as medicine stems from a tradition based on theories, beliefs, and experiences indigenous to different cultures used to maintain health, improve diagnosis and treat physical and mental illnesses [47]. Herbal medicines and CAMs are still used in many developing and developed countries [8] and are relied on as primary sources of medical treatment by more than 80% of the world's population [14].

Plants and plant derivatives have become important in the search for new, effective, and safe therapeutic agents for the treatment of a variety of conditions [48, 49, 50], such as obesity [51, 52], jaundice [53], liver disease [54, 55], malaria [56] and cancer [8, 57, 17]. About a third of drugs approved by the food and drug administration (FDA) have over the past 20 years been based on natural products or their derivatives [58, 59]. Moreover, about 50% of the approved medication in the last 30 years have a natural origin, either as semi-synthetic or mimicking natural compounds [60, 61]. Some examples of semi-synthetic drugs include the antibiotic penicillin from Penicillium moulds (*Penicillium chrysogenum and P. rubens*), the heart medication, digoxin from the foxglove plant Digitalis and the anticancer drug, paclitaxel, derived from the bark of *Taxus brevifolia* [62, 63, 64]. Natural products provide an important source of medicinal compounds as they serve as chemical scaffolds or templates for designing and synthesising products with pharmacological importance [60, 65, 66, 67].

2.1 Secondary metabolites

Plant secondary metabolites are responsible for the beneficial properties of medicinal plants and plant-derived products [68]. These are chemical compounds produced by plants as a defence mechanism against herbivores and microorganisms. Various secondary metabolites have been shown to have *in vivo* and *in vitro* antibacterial, antifungal and antiviral properties and as such serve as defence compounds against herbivores and microorganisms [70, 71]. Plant secondary metabolites are classified as phenolics, alkaloids, saponins and terpenes based on their chemical structures [69, 71].

2.1.1 Phenolics

Phenolics are the most common class of secondary metabolites found in plants [72, 73, 74]. They are characterised by the presence of at least one aromatic ring attached to one or more hydroxyl groups and are classified as flavonoids and non-flavonoids [42]. Phenolic compounds are synthesised via the shikimic acid and phenylpropanoid pathways [75]. The shikimic acid pathway is also responsible for the production of vitamins and amino acids such as phenylalanine, tyrosine and tryptophan, while the phenylpropanoid pathway is a rich source of plant metabolites and is a starting point for the production of flavonoids, coumarins and lignans [76, 77].

2.1.2 Flavonoids

Flavonoids are ubiquitous polyphenolic compounds found in plants forming the largest group of natural products and the most studied class of polyphenols [78, 79, 80, 81]. They are characterised by a flavan nucleus which consists of 15 carbon atoms arranged in three rings (C_6–C_3–C_6) [82, 83]. Flavonoids may be conjugated with other phenols, organic acids, amines, lipids and sugars [84]. Each of the structural units of flavonoids possesses distinctive chemical and biological properties that exhibit activities against stress-related diseases and cell death through modulation of the activity of several signalling mediators associated with the pathogenesis and progression of diseases [85, 86]. Furthermore, flavonoids can be divided into subgroups based on the carbon of the C ring on which the B ring is attached [87]. Flavonoids whose B ring is linked in position 3 of the C ring are called isoflavones, while those whose B ring is linked to position 4 are called neoflavonoids. Moreover, flavonoids whose B ring is linked in position 2 of the C ring are further subdivided based on the structural features of the C ring [87]. The principal players in this group include anthocyanins (e.g cyanidin), flavonols (e.g rutin), flavones (e.g luteolin) and flavanones (e.g myricetin) (Figure 2.1) [87, 88], which have all been shown to possess antioxidant and anticancer activities [89, 90, 91, 92, 93, 94, 95, 96].

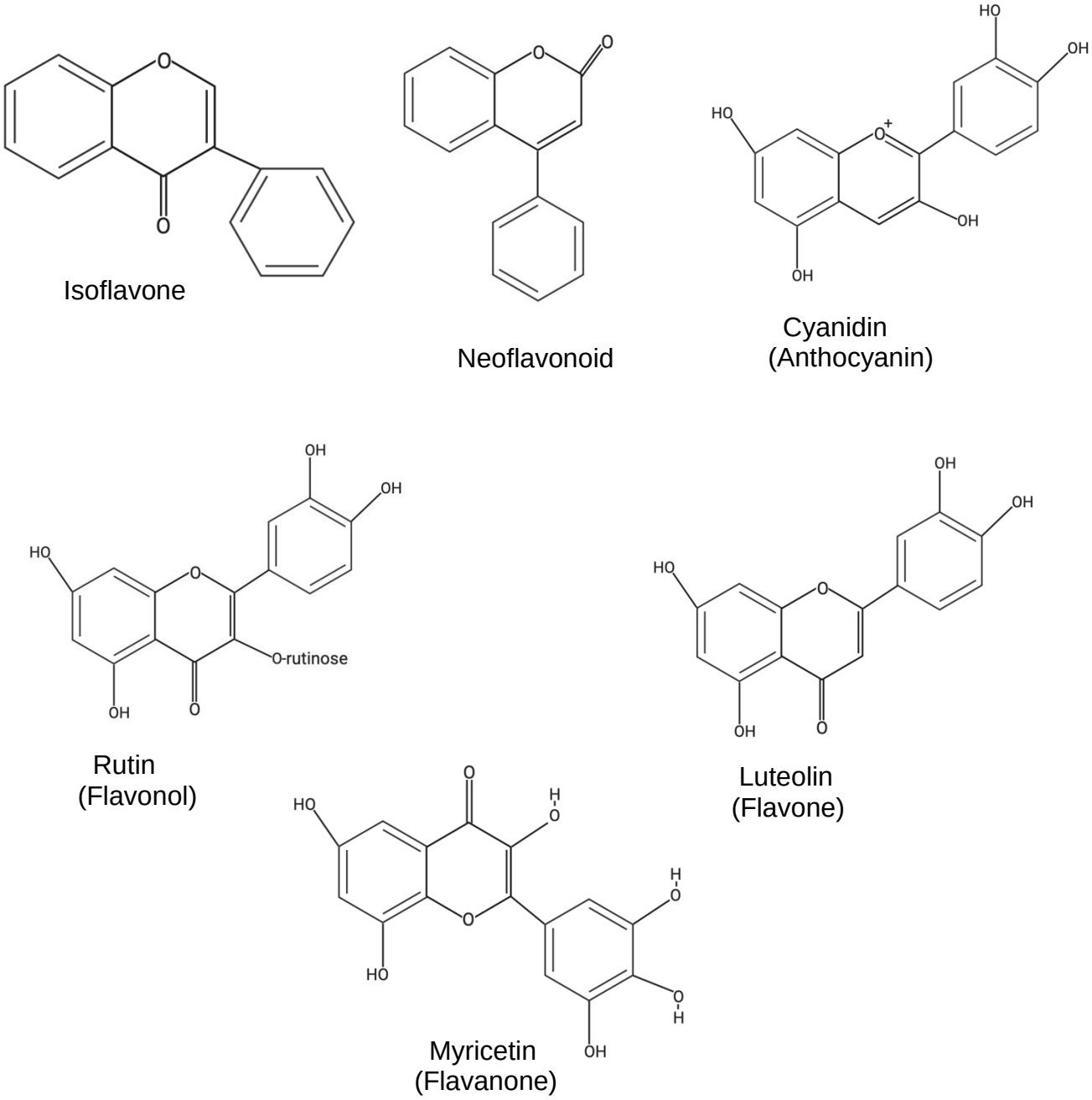

Figure 2.1: Classes and examples of flavonoids.

Flavonoids are characterised by a flavan nucleus arranged in three rings (C_6–C_3–C_6) which consists of 15 carbon atoms. They can be divided into subgroups based on the benzopyrone moiety position to the two aromatic rings A and B as; Isoflavones, Neoflavonoids, Anthocyanins, Flavonols, Flavones and Flavanones. Chemical structures drawn using BioRender.com

2.1.3 Non-flavonoids

Non-flavonoids have variable structures, yet are found commonly as a free form or conjugated hydroxybenzoic and hydroxycinnamic acids. They are classified into phenolic acids, tannins, stilbenes and lignans [42, 97]. Phenolic acids have one carboxylic acid group often found bound to a carbohydrate, existing either as a free aglycone or conjugated form [98, 99]. Tannins can be found in their hydrolysable or condensed form and have been shown to possess chemopreventive activities, exhibiting the regulation of apoptosis and autophagy [100, 101]. Stilbenes on the other hand are characterised by a 1,2-diphenylethylene nucleus and are known to prevent carcinogenesis by inhibiting inflammation, oxidative stress, suppressing proliferation of cancer cells and promoting cell death mechanisms [102]. Lignans have a steroid-analogous chemical structure and also exhibit biological properties such as antioxidant, anti-inflammatory and antitumour [103]. Examples of non-flavonoids include p-coumaric acid (phenolic acid), piceatannol (stilbenes) and Justicidin A (Lignans) (Figure 2.2).

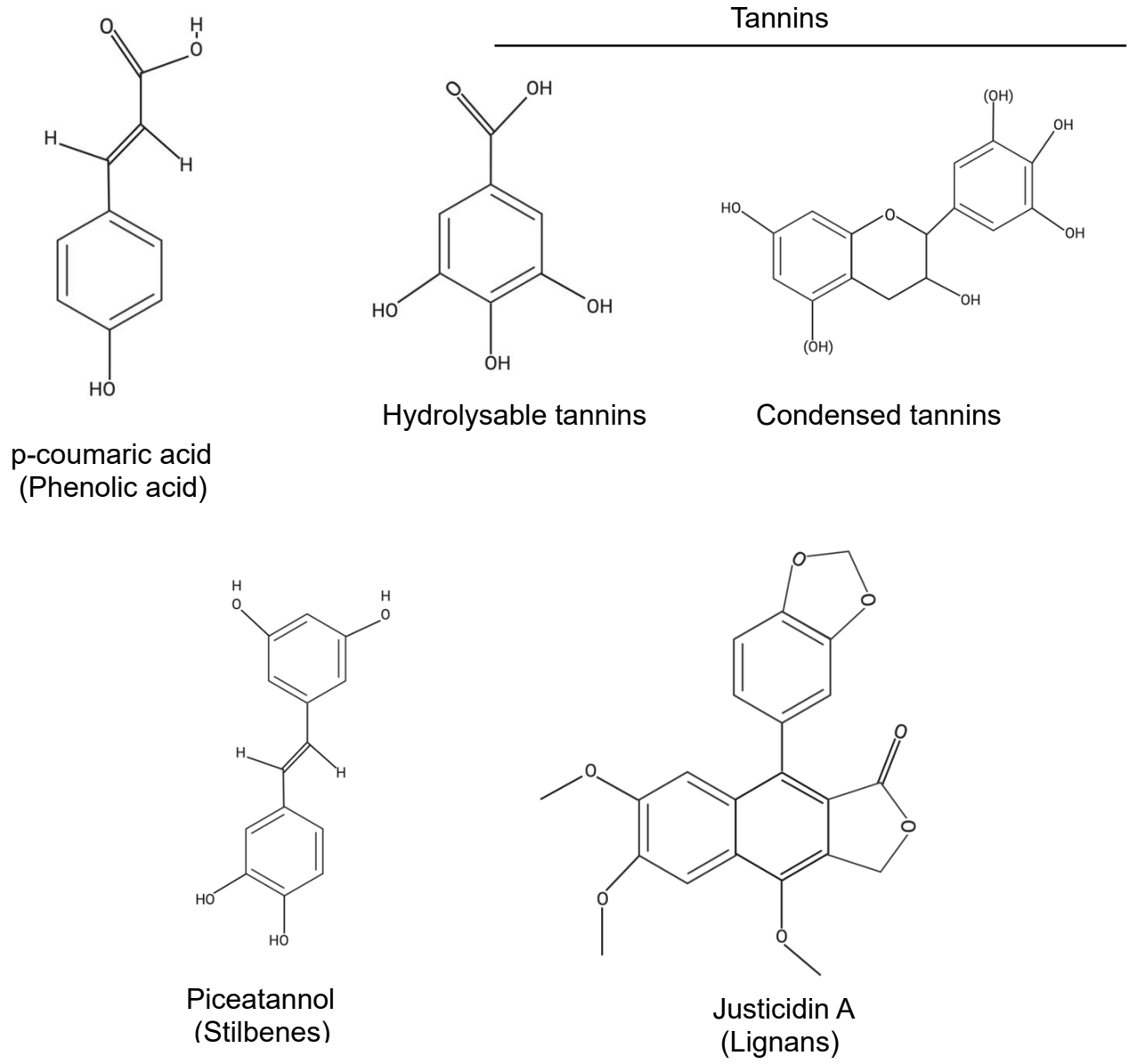

Figure 2.2: Non-flavonoid classes and examples.

Non-flavonoids are found commonly as a free form or conjugated hydroxybenzoic and hydroxycinnamic acids. They are classified into (i) phenolic acids, which have one carboxylic acid group often bound to a carbohydrate as a free aglycone or conjugated form, (ii) tannins, which are further classified into hydrolysable tannins and condensed tannins, (iii) stilbenes, which are characterised by a 1,2-diphenylethylene nucleus and (iv) lignans, which have a steroid-analogous chemical structure. Chemical structures drawn using BioRender.com

2.1.4 Alkaloids

Alkaloids are a class of naturally occurring organic substances with varying chemical structures [104]. They possess at least one basic nitrogen atom coupled with carbon, oxygen and a hydrogen element [105]. Alkaloids are classified based on their biosynthetic pathways, such as the amino acids that provide nitrogen atoms and part of their skeleton including terpenoids and purines [106]. The biological activities of alkaloids such as antitumour and anti-metastatic properties are greatly influenced by the presence of the nitrogen atom [107, 108, 109]. Examples of alkaloids used widely as chemotherapeutic agents include vincristine and camptothecin [110] (Figure 2.3).

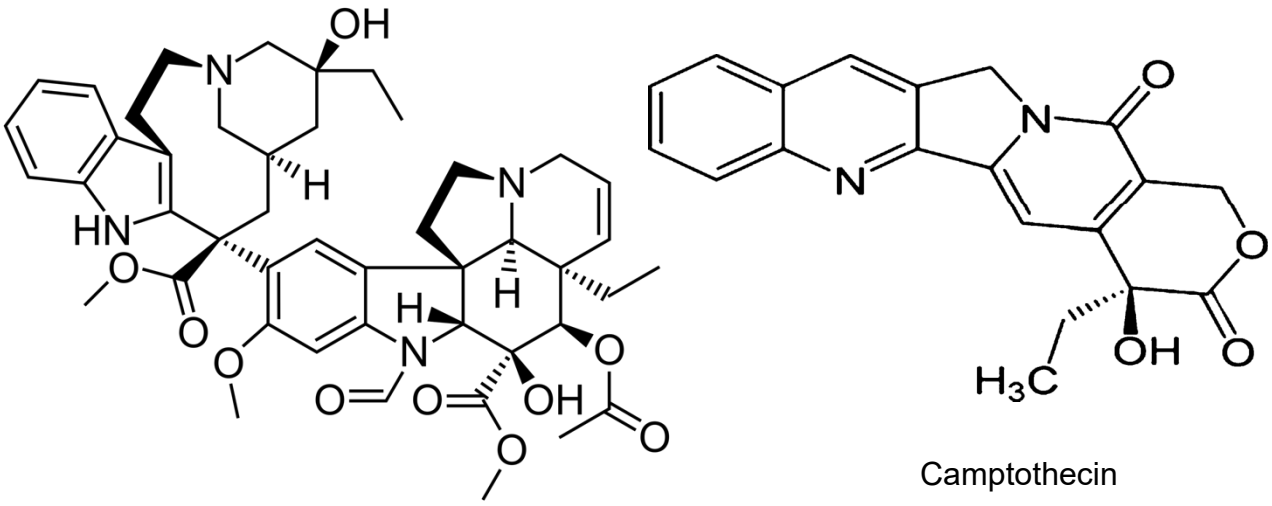

Figure 2.3: Examples of alkaloids used as chemotherapy agents.

Alkaloids possess at least one basic nitrogen coupled with a carbon, oxygen and hydrogen element and have varying chemical structures. They are classified based on their biosynthetic pathways. Chemical structures drawn using BioRender.com

2.1.5 Saponins

Saponins are plant-derived organic substances with an inflexible skeleton consisting of at least four hydrocarbon rings linked to oligosaccharide moieties of one or two groups [111, 112]. Traditionally, saponins are subdivided into triterpenoids and steroid glycosides [113] and are known to possess antioxidant, analgesic, antiviral, antifungal and hypoglycemia activities [114]. Examples include ursolic acid, lupeol (triterpenoids) and diosgenin (steroid glycosides) (Figure 2.4).

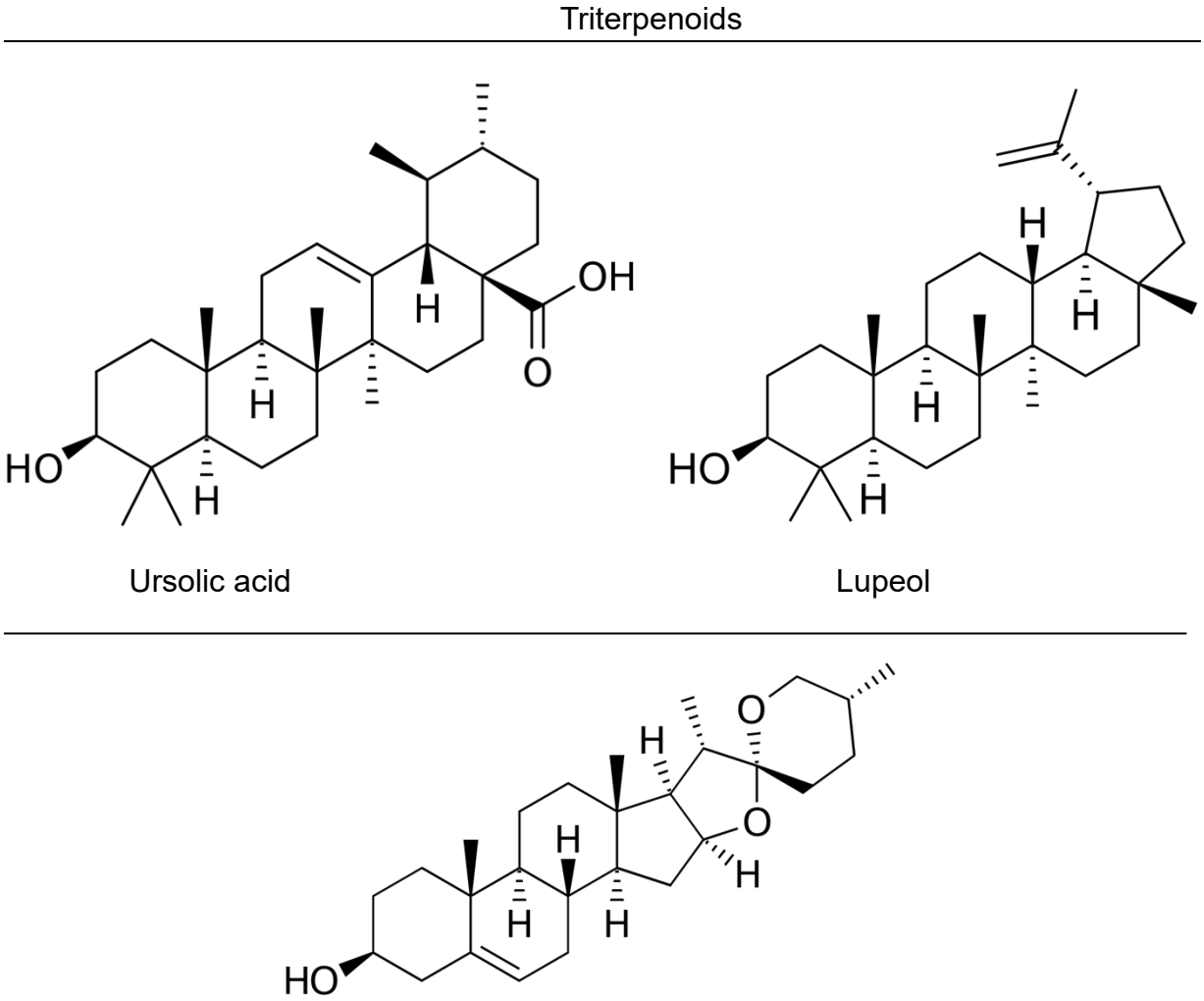

Figure 2.4: Saponins (triterpenoids and steroid glycosides) examples.

Saponins have an inflexible skeleton that consists of at least four hydrocarbon rings linked to oligosaccharide moieties of one or two groups. They are traditionally subdivided into triterpenoid and steroid glycosides. Chemical structures drawn using BioRender.com

2.1.6 Terpenes

Terpenes are built mainly from five-carbon isoprene units, and as a result, these compounds are categorised based on the number of their isoprene units as mono-, di-, tri-, tetra-, sesqui- and poly-terpenes (Figure 2.1.4A) [115]. They are classified as a group of phytochemicals, which are mainly produced by conifers amongst a host of other plants and insects. They are also considered as the largest class of phytochemicals [116], responsible for inducing apoptosis through the activity of proteasome inhibitors [117]. Examples include the monoterpene pulegone, diterpene retinol and the triterpene squalene (Figure 2.5).

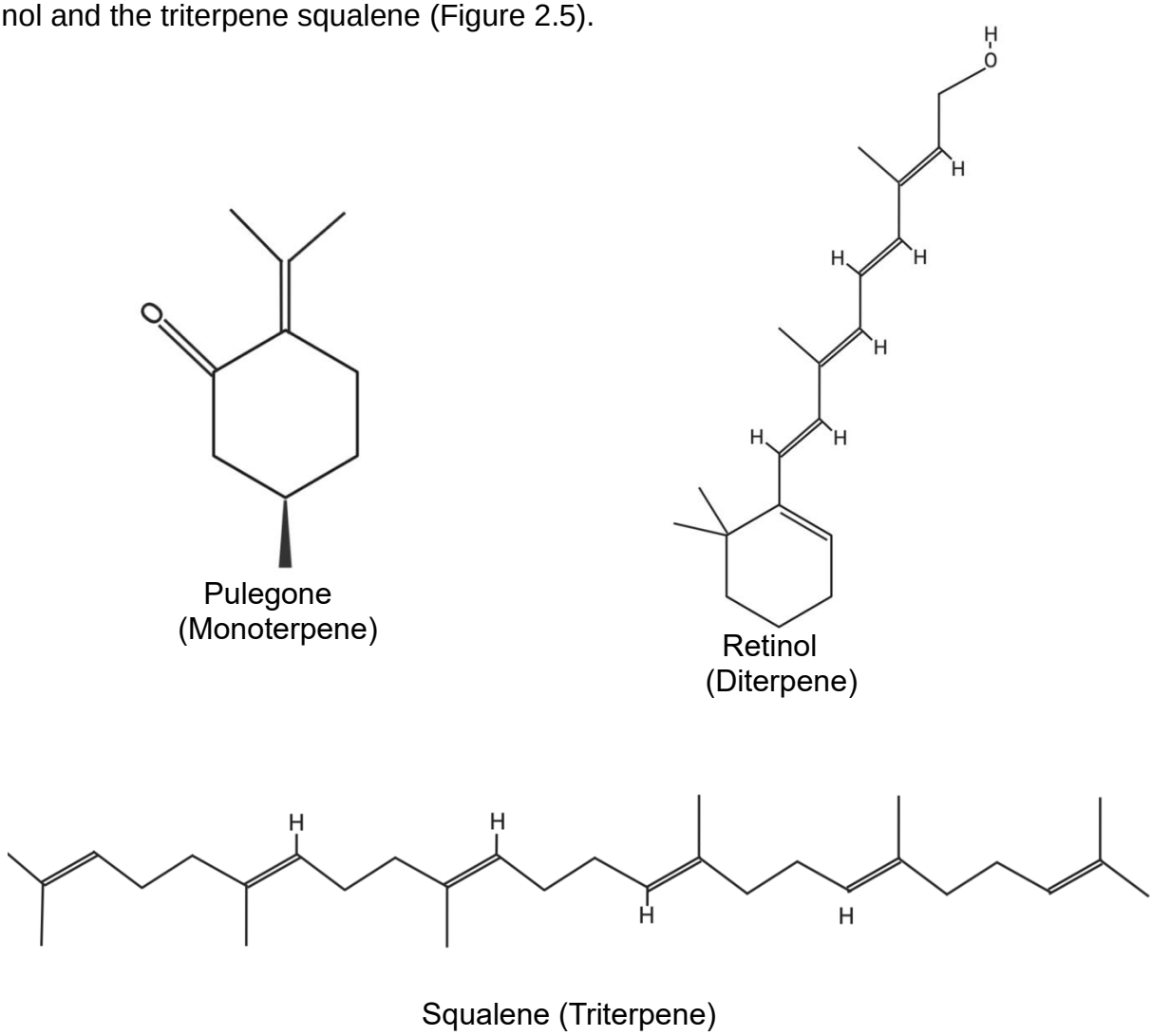

Figure 2.5: Categories of terpenes and examples:

Terpenes are built from five-carbon isoprene units and are categorised based on the number of their isoprene units as monoterpenes, diterpenes, triterpene and *etc*. Chemical structures drawn using BioRender.com

2.2 *Momordica* genus

The genus *Momordica*, from the family Cucurbitaceae, comprises 59 species, 47 of which are found in Africa and 12 in Asia and Australia [118]. Several species from this genus are consumed mainly in African and Asian countries as a vegetable and also used in indigenous medicine [42]. Plants from this family are known for their bitter taste attributed to the presence of alkaloids possessing a wide range of medicinal values [42,119]. This plant family is also known to contain cucurbitane-type triterpenoids and saponin glycosides, which are the major plant-derived chemical groups in the family recognised for their health-promoting effects in Type I and Type II diabetes [42].

Momordica charantia is the most-studied species of the *Momordica spp*. as a source of natural antioxidants [120] as it contains polyphenols, flavonoids and tannins [121] as well as glycosides, alkaloids and triterpenes that exhibit antitumour activities [122, 123]. Its fruits are used to treat diseases such as diabetes, pneumonia, kidney stones and piles in traditional Chinese herbal medicine [124]. *Momordica charantia* has also been shown to possess anti-hyperglycaemic and reno-protective effects [125]. Furthermore, *M. charantia* is thought to have health benefits as a functional food and value-added ingredient [120] and for that reason, its leaves and fruit are packaged and sold as capsules for consumers by companies like Wilson Drugs and Pharmaceuticals (P) Ltd (www.indiamart.com). Furthermore, *M. charantia* forms a very close clade with *Momordica balsamina* [126].

Momordica balsamina, commonly known as balsam apple is a tendril-bearing wild climber with leaves, fruits, seeds and bark (Figure 2.6) [127]. It is largely used as a vegetable in sub-Saharan Africa due to its nutritional quality and as a traditional medicine for the treatment of diabetes and malaria [128]. In northern Maputaland and South Africa, this species is used for the treatment of hypertension [129]. In Nigeria, the leaves are cooked for lactating mothers for purification of breast milk and regeneration of lost blood during labour [44]. Furthermore, in Mozambique, it is used to alleviate vomiting caused by bile and fever [130], and for the prevention and treatment of malaria in the Chipinge district of Zimbabwe [131]. A study by Ludidi *et al*. [125] showed that *M. balsamina* possesses anti-hyperglycaemic and reno-protective effects in STZ-induced diabetic rats and ameliorates kidney dysfunction.

M. balsamina is also a source of several cucurbitane-type triterpenoids that include balsaminapentaol, balsaminols A and B and cucurbalsaminols A and B, known to possess a variety of biological properties [42], such as hepatoprotective, cytotoxic, anti-inflammatory, cardiovascular, antidiabetic and antiparasitic effects [132]. Its leaves and fruit are a rich source of proteins, carbohydrates, vitamins and minerals [42]. In a study by Nagarani *et al*. [44], results for amino acid profiling of *M. balsamina* indicated the presence of essential and nonessential amino acids. Essential amino acids accounted for 41% of total amino acids analysed, while nonessential amino acids accounted for fifty-nine percent. Predominant amino acids in *M. balsamina* leaves were identified as leucine, phenylalanine and tyrosine, which are all present in amounts that meet recommendations set by the Food and Agriculture Organisation [44]. Leucine is an important supplement for the regulation of metabolic diseases such as diabetes mellitus as it is involved in the regulation of several cellular processes which includes tissue regeneration and metabolism thus influences signalling pathways involved in the regulation of metabolism [133]. Phenylalanine provides the carbon skeleton for the phenylpropanoid pathway that is responsible for the production of chemicals used for structure, defence and other cell and organism physiology [134]. It is also an important precursor of tyrosine [135], which in turn is a precursor of dopamine and norepinephrine known to have beneficial effects on psychological functioning [136]. *M. balsamina* leaves also contain minerals; potassium, sodium, calcium, magnesium, phosphorus, manganese, iron, copper and zinc, all of which are present in adequate amounts suitable for an adult human as prescribed by the world health organisation (WHO) [44].

Figure 2.6: *Momordica balsamina*.

Momordica balsamina is a tendril-bearing wild climber, commonly known as balsam apple. Its flowers are pale yellow with deep veins. The fruits are bright orange, round, warty and when ripe, burst apart to reveal many scarlet red seeds covered by a sticky coating.

2.3 Cancer

Cancer is a disease characterised by unrestrained cell proliferation resulting from genetic and/or epigenetic changes that control normal cell function such as cell growth, cell differentiation and apoptosis [137]. Cancer development occurs via a multi-step process of initiation, promotion and progression [138] (Figure 2.7). In the process of initiation, the three classes of genes that play a crucial role are proto-oncogenes, genes involved in the DNA repair mechanisms as well as tumour suppressor genes [139]. During initiation, the cell's genetic material changes either spontaneously or as a result of carcinogens [140]. These changes are characterised by altered gene expression which leads to uncontrolled proliferation of a single cell which eventually leads to the formation of a tumour [141, 142,140]. Moreover, the process of tumour promotion may also involve nongenotoxic carcinogens thought to exert their effects through signalling pathways that involve cell growth, cell differentiation and apoptosis [143]. The last step of cancer development, progression, is characterised by precise morphological, molecular and functional changes in tumour cells [144]. Tumour cells can either be benign, where the cells remain constricted to their original location or malignant, where they invade the surrounding normal tissue and spread to other organs in the body [145, 146]. These changes cause the tumour cells to become more aggressive, promote tumour invasion to distal organs and ultimately metastatic disease [147].

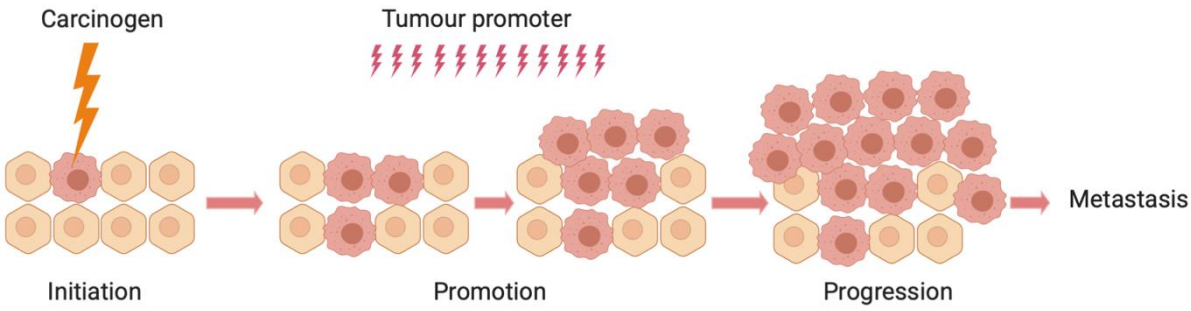

Figure 2.7: Stages of cancer development.

Cancer develops when a normal cell sustains genetic alterations that causes it to lose growth signals and begin to proliferate limitlessly forming tumours that either remain confined at the origin of development or invade nearby organs through the processes of metastasis.

Cancer metastasis is a process where cancer cells spread from their site of origin to neighbouring tissues and/or distal organs [148]. It comprises five stages of multiple distinctive, yet functionally interrelated steps known as metastasis cascade [149]. First, cell detachment occurs as a result of the growing tumour exerting pressure onto the extracellular matrix (ECM) which leads to the dissociation of cells at cytosolic and extracellular sites [150, 151]. The detached cells perforate the ECM and the basement membrane (BM) either by ECM degradation through mesenchymal cell invasion or use of mechanical force to create a path via amoeboid cell invasion [152, 153, 154, 155]. The invasive cells then enter a motility cycle and migrate within circulatory systems to a susceptible metastatic organ by polymerising new actin-rich filaments and extending protrusions that direct their movement [156, 157, 158]. At the secondary site, the cells interact with the ECM and adhere using cell adhesion molecules such as cadherins, integrins or lymphocyte homing receptors [159, 160]. Finally, the cells generate a new vascular network from pre-existing blood vessels for nutrient and oxygen supply as well as to facilitate the removal of waste products from the tumour to sustain their survival and ensure further proliferation (Figure 2.8) [161].

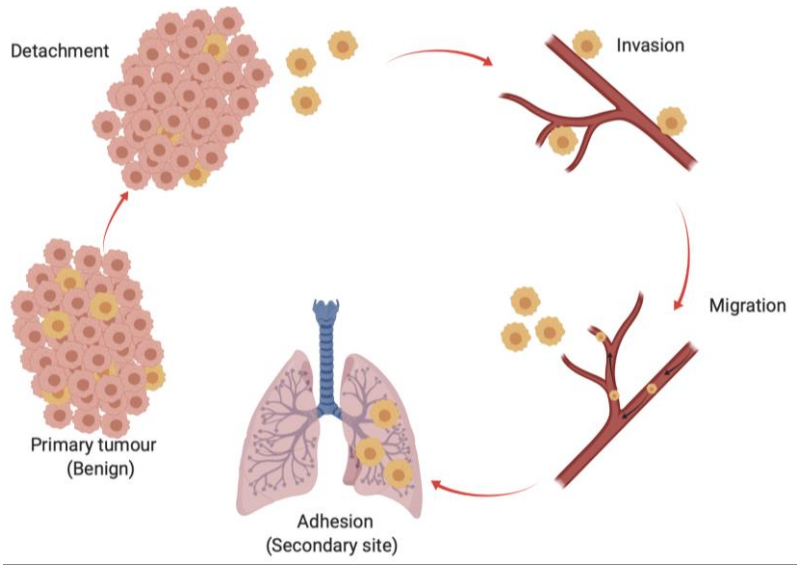

Figure 2.8: Metastatic cascade.

Metastasis is the process of cancer cells spreading from the primary site to distal organs. Metastatic cells from the primary tumour detach and invade the extracellular matrix as well as the basement membrane then enter circulatory systems and migrate to distal organs where they adhere and establish growth mechanisms to survive and proliferate further leading to the formation of a secondary tumour.

Hanahan and Weinberg [162, 163] described the cardinal abnormality in cells that have become cancerous as the persistent uncontrolled proliferation which arises from unresponsiveness to signals that govern cell homeostasis and proliferation of normal cells. They further outlined the changes in the physiology of the cells that direct malignant growth as; (i) self-sufficiency in growth signals, (ii) insensitivity to growth-inhibitory signals, (iii) evasion of programmed cell death, (iv) sustained angiogenesis, (v) reprogramming energy metabolism, (vi) evasion of immune response and (vii) limitless replicative potential.

With regards to self-sufficiency in growth signals, before normal cells can move from a state of dormancy to an active proliferation state, mitogenic growth signals (GS) are required. Transmembrane receptors transmit these signals into the cells, however, cancer cells produce their growth signals and are therefore no longer dependent on normal stimulation signals from the normal tissue microenvironment [162]. These cells then become insensitive to growth-inhibitory signals that confer normal cells with antiproliferative signals and thus proliferate uncontrollably and ultimately evade apoptosis [162]. Cancer cells further develop angiogenic ability which facilitates their size expansion [162, 164, 165, 166], and reprogramme their energy metabolism to fuel their growth and division and thus continue to replicate limitlessly, while evading immune response which would under normal circumstances cause the destruction of incipient neoplasms and nascent tumours [162].

2.4 Colon cancer

Colorectal cancer (CRC) is the 2nd leading cause of cancer-related deaths worldwide and in South Africa it accounted for an estimated 3 728 deaths and 7 354 new cases in 2020 [1, 167]. The small clump of cells that forms on the lining of the colon or rectum (polyp) in CRC has a slow progression and thereby makes CRC one of the most preventable cancers as the slow progression allows for the detecting and removing of the polyps before they become cancerous [168, 169].

Identified risk factors for the development of CRC include smoking, poor nutrition, unhealthy diet (e.g. overeating of fatty foods), physical inactivity, obesity, environmental factors, race, age, alcohol intake, low socioeconomic status, inflammatory bowel disease as well as a family history of colon cancer [170, 171, 172, 173,

[174, 175]. Cigarette smoke contains carcinogens such as benzopyrenes, whose activated form intercalates and damages DNA [176]. Cigarette smoking is also associated with the MSI-high, CIMP-positive, and *BRAF* mutation–positive colorectal cancer subtypes, thereby indicating that epigenetic modification may be functionally involved in smoking-related colorectal carcinogenesis [177]. Furthermore, diet and exercise have a direct effect on immune responsiveness, metabolic dysregulation, inflammation, and oxidative stress [178], [179], [180], [181]. Several epidemiologic and experimental investigations have linked the consumption of red and processed meat to the risk of colorectal neoplasia caused by the release of chemicals in the body which can inhibit the repair of genetic material [182]. Nutrients such as calcium, fiber and whole grain, however, have been associated with a lower risk of colorectal cancer [183]. Studies of mice have shown that a high-fat diet, as well as hormonal alterations related to obesity produce more intestinal stem cells which can lead benign and malignant tumours in the colon [184], [185]**.** Moreover, a number of known autosomal dominant inherited syndromes (familial adenomatous polyposis and hereditary nonpolyposis colorectal cancer (HNPCC)) are related to a high penetrant phenotype which gives individuals with a family history of colon cancer a 2-3 fold increased risk of getting colon cancer [186], [187], [188], [189], [190], [191], [192], [193].

Colorectal cancer may also be a result of the accumulation of genetic and epigenetic alterations [168], as nearly 80% of all CRC cases are related to the mutation of the tumour suppressor gene *adenomatous polyposis coli* (*APC*) [194]. Mechanisms of genomic instabilities attributed to the development of CRC are DNA microsatellite instability (MSI); chromosomal instability (CIN) and CpG island methylator phenotype (CIMP) [195].

2.4.1 DNA microsatellite instability

DNA microsatellite instability accounts for about 15% of all CRC cases [196]. This occurs when there is a mutation in the DNA mismatch repair genes [195]. Deactivation of these genes contributes to MSI tumourigenesis through the dissemination of genetic instability by reinstating errors in DNA replication, obstructing DNA damage responses and inhibiting the recombination of unidentical DNA sequences [197].

2.4.2 Chromosomal instability

Chromosome instability is responsible for about 85% of CRC sporadic tumours [198]. CIN are mutations in the *adenomatous polyposis coli* gene that result from various genomic abnormalities caused either by an imbalance in the number of chromosomes, loss of heterozygosity in some chromosomes as well as sub-chromosomal amplifications [195, 199,200,201]. This is followed by mutations that activate the Ki-ras2 *Kirsten rat sarcoma viral oncogene homolog* (*KRAS*) gene, an oncogene involved in the regulation of cell division and inactivation of the tumour suppressor protein p53 (*TP53*) [202, 203, 204].

2.4.3 CpG island methylator phenotype

CpG islands are short sequences in DNA where a cytosine nucleotide is followed by a guanine nucleotide found in the 5′ region of approximately half the number of genes in humans [205, 206, 207]. CIMP occurs due to the deactivation of tumour suppressor genes as a result of global genome hypermethylation associated with microsatellite instability and mutation of the proto-oncogene B-Raf (*BRAF*). B-Raf is responsible for the regulation of the MAPK/ERK pathway which transmits chemical signals from outside the cell into the nucleus thereby contributing to mechanisms of CRCs [208, 209, 210, 195, 211].

Colon cancer is classified from stages 0 to stage IV (Figure 2.4A) [212]. For stage 0 colon cancers, abnormal cells are found only within the wall or mucosa of the colon [213], while in stage I, the abnormal cells would have invaded the mucosa and submucosa but remain within the colon [214]. Stage II occurs when the abnormal cells have spread past the wall of the colon, however, have not as yet affected lymph nodes [215]. In stage III, the abnormal cells would have spread past the lining of the colon and affected the lymph nodes, yet are still found within the colon and have not spread to other organs of the body [216]. In stage IV, the cancer is metastatic wherein the abnormal cells would have now spread to other organs, via the blood and lymph nodes, such as the lungs and the liver [217].

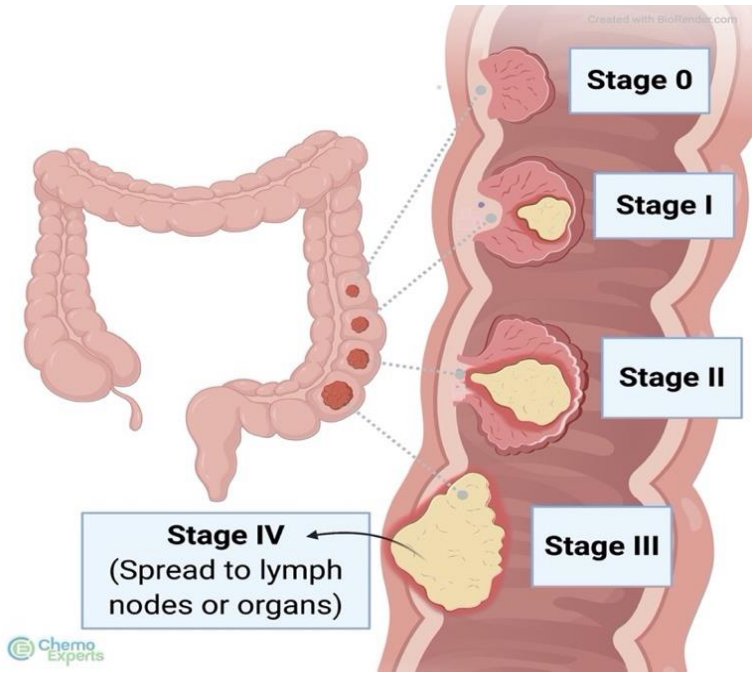

Figure 2.9: Primary stages of colon cancer.

Colon cancer is classified into five stages that involve development of abnormal cells in the colon mucosa, invasion of the mucosa and submucosa, spreading of the abnormal cells past the walls of the colon, spreading past the lining of the colon and entry into lymph nodes and spreading into distal organs via the blood and lymph nodes (https-//www.chemoexperts.com/colon-cancer.html).

The different stages of CRC require various treatment strategies that include surgery, chemotherapy, radiation and immunotherapy [218, 219]. When diagnosed early, surgical resection is the primary treatment for CRC. Although this improves CRC survival, CRC remains a major health problem due to the inhibition of neoadjuvant and cytotoxicity therapy in advanced stages as a result of tumour relapse and drug resistance [220, 221, 222]. Tumour relapse is associated with poorly differentiated histology, invasion of the perineural and lymphovascular, tumour penetration to the thyroxine (T4), raptured or clinically obstructed bowel as well as elevated preoperative plasma levels of the carcinoembryonic antigen (CEA) [223, 224, 225, 226].

Drug resistance is the main cause of treatment failure in cancer chemotherapy [227]. It is caused by factors such as genetic or epigenetic modifications intrinsic to the cell that are capable of inducing drug sensitivity alterations and increasing the drug's efflux out of the cell [228]. Drug resistance may also be acquired as a result of drug exposure,

chemical insults or cellular stress [229]. These changes lead to cancer cells receiving a decreased concentration of the drug, reduced uptake into the cell as well as alteration to enzymes involved in the drug's metabolism [230]. Furthermore, there may also be an upregulation, mutational activation or bypassing of downstream signalling molecules within specific pathways [231]. Tumour cells develop resistance by improving DNA repair mechanisms, acquisition of drug metabolising capability, activating drug transporters that efflux drugs, increasing gene amplification and changing survival or cell death pathways [232].

Current chemotherapy treatment for CRC involves single-agent therapy such as 5-FU or multi-agent therapy which makes use of more than one drug for example irinotecan, capecitabine and oxaliplatin [233]. 5-FU is a fluorinated pyrimidine analogue used to treat breast, head, gastrointestinal and neck cancers as well as a range of other solid tumours [234, 235]. It acts by blocking DNA synthesis as well as the synthesis of proteins and enzymes [236]. In mammalian cells, 5-FU prevents the replication and repair of DNA by inhibiting the production of deoxythymidine monophosphate (dTMP) [237, 236]. This occurs when 5-FU is converted to the metabolite 5-fluoro-2′-deoxyuridine-5′-monophosphate (FdUMP), which forms a complex with thymidylate synthase (TS), the only enzyme that generates a *de novo* precursor of DNA [238, 239, 240]. This complex ultimately inhibits the production of deoxythymidine monophosphate (dTMP) [241, 242]. When intravenously administered, about 85% of 5-FU is catabolised into inactive metabolites and only 3% of the original dose is responsible for the observed cytotoxic effects. 5-Fluorouracil catabolism occurs through the activity of the rate-limiting enzyme, dihydropyrimidine dehydrogenase (DPD) [243]. Furthermore, 5-FU is also metabolised to ribose and deoxyribose triphosphate metabolites which cause cell death when incorporated into RNA and DNA [239, 239].

Although 5-FU is one of the most frequently prescribed drugs and is used as a first-line chemotherapy treatment for various cancers over the past seventy years [244, 245], its response rate for advanced CRC treatment is less than 15% [246]. Furthermore, 5-FU is associated with severe toxicity of the gastrointestinal tract as well as haematological, neural, cardiac and dermatological reactions [247, 246]. Moreover, 5-FU has a short elimination half-life in plasma. To enhance its efficacy, it is usually administered in combination with other drugs or agents [248, 234]. The efficacy of multiple-

agent combinations such as oxaliplatin and fluorouracil have been analysed in an adjuvant setting and has shown greater efficacy than when fluoropyrimidine is used alone [249]. Although this combination was shown to be superior, oxaliplatin is overtime associated with neurotoxicity [249]. Some combinations tested *in vitro* and *in vivo* using animal models include 5-fluorouracil or resveratrol and curcumin [168], which are found in red grapes and turmeric, respectively [250]. These bioactive compounds derived from vegetables, fruits and medicinal plants are known as nutraceuticals [251] and have over the years shown potential for numerous chronic illnesses including colon cancer [218].

2.5 Eukaryotic cell division cycle

The activity and regulation of mitogenic signalling pathways that govern cell proliferation and cell division cycle progression is crucial in the development of tumours as they are capable of gaining self-sufficiency in growth signals [252, 253, 162]. The cell division cycle is divided into two major phases; interphase and mitosis. During the interphase, the cell grows in size and mass as it replicates its DNA, while during the mitotic phase, the cell's cytoplasmic content, as well as the replicated DNA, are separated and the cell undergoes division into two daughter cells (Figure 2.10) [254, 255].

The interphase is divided into three distinct phases; Gap 1 (G1) phase, DNA synthesis (S) phase and Gap 2 (G2) phase [256]. During the G1 phase, the cell is metabolically active, its size increases and it accumulates building blocks and energy required in the later stages of the cell cycle [257]. RNA and ribosomes are also synthesised during the G1 phase [256]. The G1 phase is then followed by the S phase [258], where the genetic material is amplified [259]. The centrosome, microtubule-organising structure that aids in the separation of the chromosomes during the M phase, also get duplicated during the S phase [225, 230]. During the G2 phase, the cell continues to grow and replenishes energy stores and synthesises proteins and organelles that are necessary for cell division as it prepares to enter mitosis [259].

In the M phase, the cell divides contents of the nucleus and cytoplasm to make two new daughter cells in a multistep process that can be sub-divided into five phases; prophase, prometaphase, metaphase, anaphase, and telophase and cytokinesis [256]. During the prophase, the cell undergoes chromatin condensation that continues until the metaphase. The prometaphase begins when the nuclear envelope dissociates into

small vesicles. These vesicles will then be divided among the two new daughter cells. Chromatin condensation continues during the metaphase and becomes coiled. The replicated chromosomes are then split and the sister chromatids separate during anaphase. Lastly, during telophase and cytokinesis, two daughter nuclei are formed and the nuclear envelope reforms around each nuclei producing two new daughter cells and the chromosomes decondense into their interphase state [261]. Following the completion of the cycle, the cell may not immediately enter the next round of cell division, but instead enter a resting phase, G0, known as quiescence [256]. During the G0 phase, the cell exists in a quiescent state and is neither actively dividing nor preparing to divide [262]. This state may be temporary or permanent for some cells [263].

The progression and transition from one phase to the next is under control of the expression and activity of some cyclin-dependent kinases, (CDKs) (CDK-1, CDK-2, CDK-4, CDK-6, CDK-8, CDK-12). CDKs form complexes with cyclins (cyclin A to E) [264, 265, 266, 267], leading to their enzymatic activity which is critical for the entry of cells into the cell cycle and progression thereof [268]. On the other hand, cell cycle checkpoints serve to ensure genomic stability through cell cycle arrest and repair or induction of apoptosis and therefore decide whether the cell proceeds to the next phase of the cell cycle or not [243, 267]. There are three primary checkpoints, namely; G1/S, G2/M and M [269]. At the G1/S checkpoint, the cell is assessed for the availability of nutrients and DNA synthesising enzymes [270]. This checkpoint, therefore, determines the transition of the cell from the G1 phase to the S phase [271, 272]. At the G2/M checkpoint, cells are assessed for DNA damage to prevent the entry of cells with damaged DNA into the mitotic phase [273]. At the M checkpoint, the integrity of the chromosomes is assessed to prevent premature separation of the chromosomes [274, 269]. Failure to repair the cell's genome, DNA replication and transcription is prevented and the cell undergoes necrosis or apoptosis [275].

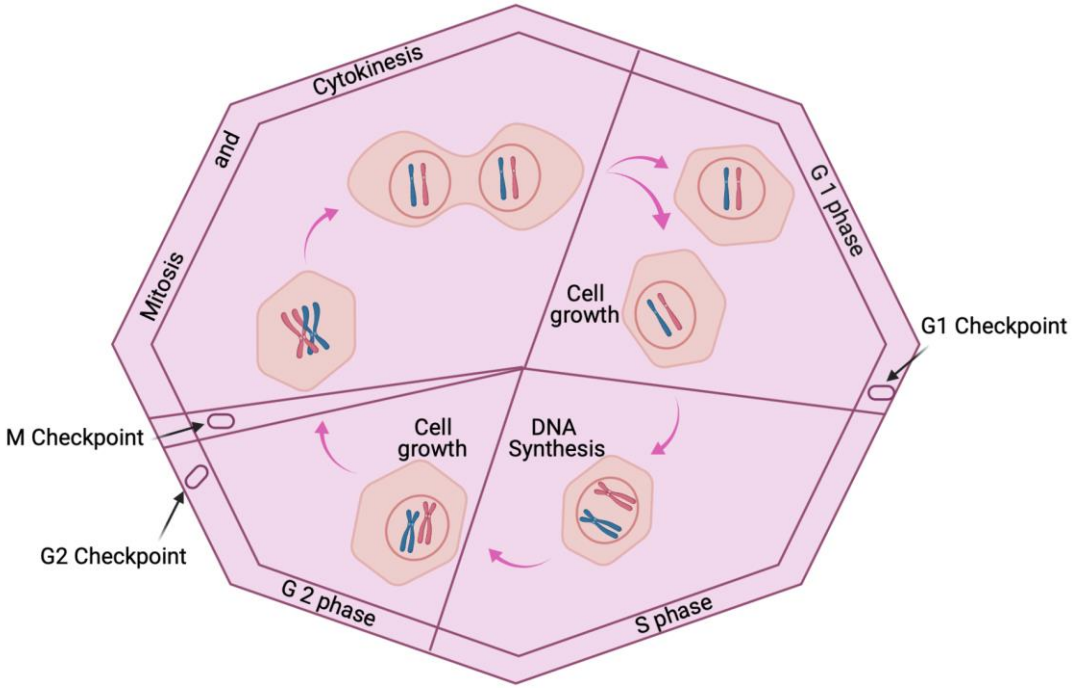

Figure 2.10: **The eukaryotic cell division cycle and checkpoints.**

The eukaryotic cell division cycle is divided into two major phase. The interphase, which is further sub-divided into G1, S, G2 and M phases, and Mitosis. Complex formation by CDKs and cyclins decide the fate of the cell at cell cycle checkpoints. Image generated using Biorender.com

2.6 Apoptosis

Apoptosis is a well-orchestrated series of cell suicide events that maintains cell populations in tissues by eliminating unwanted cells during development and ageing [276, 277]. Unlike necrosis, which is cell death that occurs in response to severe cell injury and cell energy depletion, apoptosis is induced by diverse pharmacological agents and physiological stimuli [278]. Necrosis is further characterised by cell lysis caused by the swelling of intracellular organelles [279], while apoptosis is characterised by distinct cell morphological features such as a decrease in cell volume, membrane blebbing, condensing of the chromatin, DNA fragmentation and formation of apoptotic bodies as well as the externalisation of phosphatidylserine [280, 281, 282, 283]. This leads to apoptotic cell engulfment by macrophages to prevent the release of intracellular contents and inflammation [284]. As such, apoptosis is a preferred mode of cell death and thus also plays a role in cancer prevention and treatment [285].

The activation of caspases is another specific feature of apoptosis [280]. Caspases are a group of enzymes that belong to a family of cysteine proteases which play a crucial role as mediators of apoptosis [280, 286]. There are three types of caspases; (i) apoptosis initiators, caspases -2, -8, -9 and -10; (ii) inflammatory mediators, which are caspases -1, -4, -5, -11 and -12; and (iii) apoptosis effectors, which are caspases -3, -6 and -7 [287]. Caspases can be activated either via the intrinsic (mitochondrial) pathway or the extrinsic (death receptor) pathway (Figure 2.11) [288].

2.6.1 Intrinsic apoptosis pathway

The intrinsic pathway is initiated within the cell as a result of internal stimuli and is regulated by the B-cell lymphoma 2 (Bcl-2) family of proteins [289]. This family is divided into three sub-groups: i) the anti-apoptotic group, which have four Bcl-2 homology domains (BH1, BH2, BH3 and BH4) and comprise of the B-cell lymphoma-2 (Bcl-2), B-cell lymphoma extra-large (Bcl-xL), Bcl-2-like protein 2 (Bcl-W), induced myeloid leukaemia cell differentiation protein (Mcl-1), Bcl-2 related protein A1 (Bcl2A1) and a Bcl-2-like protein similar in amino acid sequence to the Boo protein (Bcl-B); ii) pro-apoptotic proteins lacking the BH4 domain which consists of Bcl-2-associated protein X (Bax), Bcl-2 homologous antagonist killer (Bak) and Bcl-2-related ovarian killer (Bok); and iii) pro-apoptotic proteins with only the BH3 domain which consists of Bcl-2-interacting killer (Bik), Harakiri (Hrk), Bcl-2-like protein 11 (Bim), Bcl-2-associated death promoter (Bad), BH3 interacting-domain death agonist (Bid), p53 upregulated modulator of apoptosis (PUMA), Phorbol-12-myristate-13-acetate-induced protein 1 (NOXA) and Bcl-2 modifying factor (Bmf) [290, 291]. The Bcl-2 protein family members are located on the outer mitochondrial membrane as dimers responsible for membrane permeability via an ion channel or the creation of pores [292, 293, 294].

Anti-apoptotic proteins act by preventing pore formation on the outer mitochondrial membrane thus blocking the release of mitochondrial proteins into the cytosol. In contrast, pro-apoptotic proteins act by promoting pore formation on the outer mitochondrial membrane resulting in the release of mitochondrial proteins such as cytochrome c [295, 296], as well as high-temperature requirement protein A (HTRA2)/Omi, second mitochondria-derived activator of caspase/direct IAP binding protein with Low pI (SMAC/Diablo), endonuclease G and apoptosis-indicing factor (AIF), which may execute cell death through caspase-dependent or caspase-independent mechanisms

[297, 298, 299, 300]. The presence of cytochrome c in the cytosol disables the cell's production of energy and initiates a proteolytic cascade which deconstructs the cell [301]. This is done through the binding of cytochrome c to Apaf-1, a cytosolic protein, to facilitate the formation of an apoptosome for the recruitment and activation of the initiator caspase-9, which in turn activates the executioner caspases-3 or -7 [302].

2.6.2 Extrinsic apoptosis pathway

Apoptosis via the extrinsic pathway occurs independent of the mitochondria and is initiated by caspase-8 or -10 following external stimuli [303, 304, 305, 306]. The extrinsic pathway is initiated when a death ligand, fas-1 induced apoptosis signal ligand (FasL) or tumour necrosis factor-alpha ligand (TNF-α) binds to its death receptor, fas-1 induced apoptosis signal receptor (FasR) or tumour necrosis factor-alpha receptor (TNFR) [307]. Upon binding of FasL to FasR, there is an activation of the fas-associated death domain (FADD) which triggers the binding of TNF- α ligand to TNFR. The result of this binding leads to activation of TNFR1-associated death domain (TRADD) and receptor-interacting protein (FADD) recruitment [308, 309]. , [310, 311]. FADD then forms a death-inducing signalling complex (DISC) by associating with procaspase-8, resulting in its activation (caspase-8) which in turn activates caspase-3 [312, 308].

2.6.3 Execution of Apoptosis

The intrinsic and extrinsic pathways of apoptosis end at the point of execution [308]. Once activated, executioner caspases-3, -6 or -7 cleave various cellular components, such as the nuclear protein poly ADP ribose polymerase (PARP) which detects and initiates immediate cellular response to single-strand DNA breaks, and the cytoskeletal protein alpha fodrin [313, 312, 308]. This then leads to the morphological features associated with apoptosis [314]. Furthermore, the cytoskeleton is reorganised, the cell disintegrated into apoptotic bodies [315] and chromosomal DNA fragmented via cleavage of the inhibitor of caspase-activated deoxyribonuclease (ICAD) to CAD, causing chromatin condensation [316, 317, 318, 319].

The last component of apoptosis is the engulfment of apoptotic bodies by phagocytic cells [320]. This is facilitated by phagocytic phosphatidylserine recognition, which allows for the early uptake and disposal of apoptotic cells to prevent an inflammatory response [321].

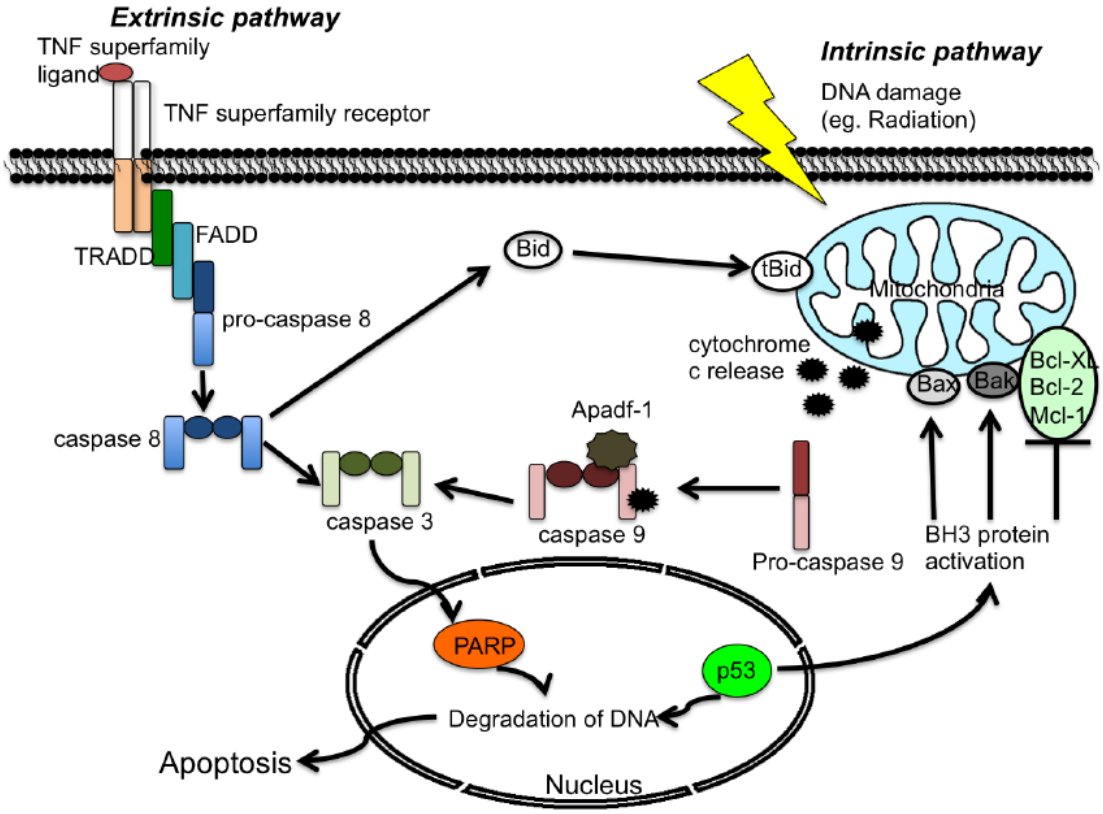

Figure 2.11: Apoptosis pathways.

Apoptosis is a naturally programmed form of cell suicide that may be triggered via the intrinsic or extrinsic pathway. The intrinsic pathway occurs when cytochrome c is released from the mitochondria. This release leads to the initiator caspase-9 being activated. The extrinsic pathway occurs when a death receptor bunds to a death ligand which results in the initiator caspase-8 being activated. Initiator caspase activation then leads to the execution of apoptosis through activation of the executioner caspases-3\-7.

2.7 Reactive oxygen species

Reactive oxygen species are highly reactive chemical molecules with a single unpaired electron that are, for instance, produced by the mitochondria of living cells as by-products of normal cellular oxidative processes [322, 323, 324]. They play a vital role in many physiological processes that include liver detoxification, production of prostaglandin, cell signaling processes and the intracellular killing of bacteria by neutrophil granulocytes [325], [326], [327], [328], [329]. ROS encompasses transient molecules and free radicals such as superoxide anion (O_2^-), hydrogen peroxide (H_2O_2) and hydroxyl radical ($^{\bullet}OH$) [330]. In the presence of an invading bacteria, phagocytic cells are activated and generate O_2^- which then attacks the bacteria as part of an inflammatory

response. Hydrogen peroxide selectively takes part in the generation of •OH [331], [332], [333]. In the body, the antioxidant enzyme catase breaks down H_2O_2 to yield water and dioxygen (O_2) [331], [334], [335]. Hydrogen peroxide can also be broken down into water and oxidized glutathione by glutathione peroxidase and other peroxides that are formed on lipids within the body [331], [335], [336], [337]. Other intracellular sources that generate ROS are xanthine, by the enzyme xanthine oxidase along with uric acid as waste products of purine metabolism [338], reactions involving cytochrome P450 enzymes [339], ascorbate [340], NAD(P)H oxidases [341], [342], the endoplasmic reticulum (ER) or by exposure to exogenous stress, chemotherapeutic agents and environmental insults [343]. These intracellular antioxidants prevent the uncontrolled formation of free radicals and activated oxygen species, or inhibit their reactions with biological structures [340].

Initially, ROS were thought to only be a toxic by-product of mitochondrial respiration. This is because excessive ROS production suppresses the body's natural response mechanism resulting in oxidative damage of DNA, lipids and proteins which subsequently promotes cancer development, among many other diseases [344, 345, 346]. Furthermore, ROS are often higher in colorectal cancer cells [347]. However through the years, functional roles for ROS have been revealed in cells, for instance (i) aiding immunity by oxidative bursts in phagocytes which subsequently eliminates pathogens [348], (ii) H_2O_2 regulating nuclear factor kappa B (NFκB) as well as (iii) regulating pathways of mitogen-activated protein kinase (MAPK) [349].

Processes initiated by an imbalance in ROS are commonly referred to as oxidative stress. Increased oxidative stress in the mitochondria is proportionally associated with apoptosis [350] which subsequently leads to the activation of pro-apoptotic proteins and release of cytochrome c [328, 351]. The pro-apoptosis activity of ROS can be inhibited by the anti-apoptotic proteins Bcl-2 and Bcl-xL by preventing pore formation on the outer membrane of the mitochondria preventing the release of cytochrome c. Moreover, Bcl-2 protein may increase the cell's resistance to ROS thereby preventing apoptosis [352, 353, 354, 355, 356, 357]. Bcl-2 increases cellular redox capacity and prevents cell death caused by H_2O_2 in a manner similar to glutathione peroxidase explained above [354], [358].

To achieve tumour cell apoptosis, chemotherapeutic strategies, such as the use of anthracyclines (e.g doxorubicin) or platinum coordination complexes (e.g cisplatin) and camptothecins (e.g irinotecan), mainly aim at the enhancement of intracellular

ROS levels, which induce irreparable damage to the target cells that ultimately leads to apoptosis [359, 360].

ROS initiated apoptosis can be via both the intrinsic and extrinsic signalling pathways [361]. ROS also regulates the activation of poly (ADP-ribose) polymerase (PARP-1), causing a reduction in β-nicotinamide adenine dinucleotide (NAD). This leads to the release of mitochondria apoptosis-inducing factor (AIF) [362], which is then transferred to the nucleus where it cleaves DNA resulting in apoptosis should the damage to DNA not be repaired[, 363].

2.8 Drug metabolism

Most drugs are metabolised for detoxification and elimination purposes as they are treated as xenobiotics in the body. This metabolism involves entry of the drug into cells (Phase 0), the introduction of a reactive group into xenobiotics (Phase I), conjugation of the modified compounds with polar moieties (Phase II) and further processing of the conjugated xenobiotics and their excretion (Phase III) [364]. Pharmacokinetic studies of most herbal medicines have shown that herbal medicines undergo Phase I and Phase II metabolism [365]. Cytochrome P450 (CYPs) are major drug metabolising enzymes present in all organisms [327, 328] and are responsible for over 80% of all phase I drug metabolism (Figure 2.12) [366]. The CYP family constitutes major enzymes capable of catalysing the oxidative biotransformation of most drugs [367], and are classified under two main classes concerning redox partners: Class I, known as the adrenal mitochondrial P450 systems obtains electrons from Nicotinamide adenine dinucleotide phosphate (NADPH) via adrenodoxin reductase and adrenodoxin; Class II, the liver microsomal P450s obtain electrons from NADPH via a flavin adenine dinucleotide (FAD) and flavin mononucleotide (FMN) containing P450 reductase [368].

A number of these enzymes are selectively expressed in tumours and play a significant role in the metabolism of several currently used cancer drugs and as such, provide a mechanism for drug resistance [369]. These include cytochrome P450s 1A2 (CYP1A2), 2A6 (CYP2A6), 2C8 (CYP2C8) and 2C9 (CYP2C9), mainly expressed in the liver (Figure 2.12) [369].

2.8.1 Cytochrome P450 (CYPs) enzymes

(i). CYP1A2

CYP1A2 is one of the three types of CYP1 enzymes produced by humans [370]. It makes up around 15% of the total hepatic CYPs and is expressed also in tissues outside the liver. Its expression is under the transcriptional regulation of the aryl hydrocarbon receptor (AhR), which mediates countless biological and toxicological actions of hydrophobic natural and synthetic chemicals [371, 370, 372]. It is also involved in the metabolism of many anti-inflammatory drugs such as nabumetone [373], analgesics, cardiovascular drugs (e.g. guanabenz) and procarcinogens [367, 374, 370, 375, 376]. Its substrates include etoposide, which is FDA-approved for the treatment of small-cell lung and testicular cancers [377]; flutamide, which is approved for prostate cancer treatment [378]; as well as the 5-Fluorouracil prodrug, Tegafur, which is used for the treatment of many cancers, including colon [379], stomach and breast [369] cancer. Moreover, CYP1A2 is implicated in numerous clinical herb-drug interactions [380, 381, 382] and plays a significant role in the metabolic clearance of about 5% of the drugs that are currently on the market [383].

(ii). CYP2A6

CYP2A6 belongs to the human CYP2A family along with two other genes namely; *CYP2A7* and *CYP2A13* [384]. It makes up about 4% of the total CYP450 content and is primarily expressed in hepatic cells, but may also be expressed in some specialised cells found outside of the liver [385, 386]. CYP2A6 is reported to metabolise 3% of pharmaceutical agents, including therapeutic drugs as well as procarcinogens and toxins [387, 366]. Its substrates include the anticoagulant coumarin and general anaesthetic halothane [369], disulfiram, which is used for the treatment of chronic alcoholism [388] and methoxyflurane, used for pain [389]. Furthermore, CYP2A6 is also involved in the metabolism of letrozole, an aromatase inhibitor used for the treatment of breast cancer, as well as Tegafur [369].

(iii). CYP2C8

CYP2C8 belongs to the 2C subfamily, which is the second most plentiful CYP following the CYP3A subfamily, constituting more than 20% of the total CYP content that exists in the human liver [390]. It is involved in the metabolism of about 5% of clinically used

antidiabetic and antimalarial drugs [369]. CYP2C8 substrates include paclitaxel, which is used for the treatment of many cancers; repaglinide, used to treat diabetes, chloroquine, used in malaria treatment; and dapsone, which is used for the treatment of arrhythmia [366, 369]. CYP2C8 also participates in the metabolism of endogenous compounds which include all-trans-retinoic acid given alongside cancer chemotherapy [390]. Furthermore, CYP2C8 is involved in the catalytic activation of Tegafur [391].

(iv). CYP2C9

CYP2C9, also belonging to the 2C subfamily, is a class II highly polymorphic CYP450 enzyme that is involved in the metabolism of many drugs and constitutes about 18% of the total liver microsome CYP450s [369, 392]. It is responsible for the metabolism of approximately 10% of all currently used drugs [366]. CYP2C9 is mainly expressed in the liver where it participates in the oxidation of endogenous and xenobiotic compounds [393, 392]. Its substrates include tamoxifen, used for the prevention and treatment of breast cancer [394], the widely used anticoagulant, warfarin [395] and idarubicin, used for the treatment of leukaemia [396]. Furthermore, CYP2C9 is also responsible for the metabolism of nonsteroidal anti-inflammatory drugs and hypoglycemic agents [394].

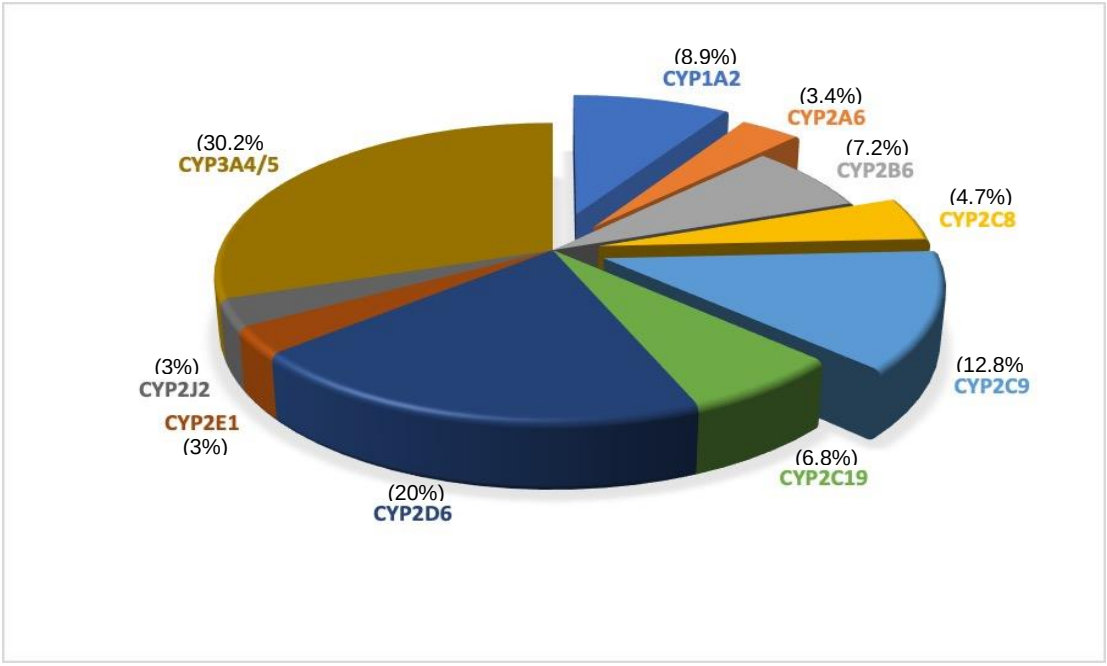

Figure 2.12: Summarised fraction of clinically used drugs metabolised by P450 isoforms.

Cytochromes P450 (CYP)enzymes are a major source of variability in drug pharmacokinetics and response. Of the 57 putatively functional human CYPs, only about a dozen enzymes, belonging to the CYP1, 2, and 3 families, are responsible for the biotransformation of most foreign substances including 70-80% of all drugs in clinical use (Zanger and Schwab, 2013).

2.8.2 Herb-drug interactions

Herbal medicines are generally regarded as safe because they are natural. However, their safety profiles in humans are usually based on anecdotal data, not on scientific assessment [365]. These medicines may potentiate the pharmacological and toxicological action of synthetic drugs [397, 398], potentiated by the fact that, while synthetic drugs contain a single active ingredient, herbal extracts and medicines often contain a mixture of pharmacologically active constituents, thereby increasing the likelihood of herb-drug interactions [399, 400]. These interactions can either increase or decrease the toxicological and pharmacological effects of the drug or herbal medicine [399, 398, 397, 401], through alteration in the absorption, distribution, metabolism and excretion patterns of the other drug [397, 402].

2.8.2.1 Absorption

The bioavailability of herbal medicines is greatly influenced by pre-systemic processes that reduce the concentration of herbal components before it reaches the systemic circulation. This includes the herbal medicine's solubility in the gastrointestinal fluid, degradation in the gastrointestinal tract, absorption through the intestinal mucosa and transportation within the body [403]. The drug transporter protein, P-glycoprotein (P-gp), greatly influences intestinal absorption of herbal medicines and many other drugs as it is expressed in high levels in the membranes of the small and large intestines where it participates in the efflux of xenobiotics [404, 405, 406]. Moreover, poor absorption of these herbal components, in particular flavonoids, results in low bioavailability and as such effects the pharmacokinetics of the bioactive constituents [403]. Some herb-drug interactions may improve the bioavailability of target compounds within the drug and/or lessen the side effects of the drug [407, 408].

2.8.2.2 Metabolism

The *in vivo* metabolism of herbal medicine components greatly depends on CYP450 metabolising enzymes as well as the drug transporter protein, P-gp [409]. Inhibition or induction of such metabolic enzymes by herbal medicines causes pharmacotoxicity that could ultimately result in treatment failure [397]. Intestinal metabolism involves the absorption of drugs from the intestinal lumen into the mesenteric capillaries where along the way, they are subjected to metabolic transformation [410 411]. This is done

mostly by the subfamily 3A of CYP450 enzymes which are the most abundant in the intestine [412], where CYP3A4, in particular, acts as a metabolic barrier during the uptake of herbal medicines [413]. In hepatic parenchymal cells, a similar process occurs where the drug is absorbed into the portal vein, passed through the liver to the heart and the rest of the body [414].

2.8.2.3 Distribution

The interaction of plasma proteins and pharmacodynamic properties of drugs govern a drug's distribution and thereby plays a vital role in its toxicity [415]. Many drugs are ineffective when bound to such proteins [416]. Herbal medicines contain various components whose pharmacological effects result from the binding of active compounds to proteins such as the plasma protein, human serum albumin (HSA), which can enhance the solubility of hydrophobic drugs and therefore regulate their delivery into cells [417].

2.8.2.4 Elimination

Following the processes of absorption, metabolism and distribution, herbal medicines are excreted either via the faecal or renal route, the latter being the predominant route. Compounds that can enter the bloodstream are transported to the liver for metabolising and biliary excretion [404, 418, 419, 420, 421]. Drugs excreted by the kidneys via the renal route can either be through passive (glomerular filtration) or active (tubular secretion) filtration [422].

2.8.3 Drug transporter P-glycoprotein

P-glycoprotein (P-gp), also known as a multidrug resistance protein 1 (*MDR1*), is a transmembrane glycoprotein, from the ATP-binding cassette (ABC) family of drug transporters. It is directly encoded by the human *ABCB1* gene that acts as a barrier, extruding toxins and xenobiotics from cells [423, 397, 424, 425, 426]. It is widely distributed in organisms and found in tumours and normal tissues, such as the liver, kidneys, small intestine, placental tissue and synovial tissue [425]. The P-gp family accounts for one of the well-known mechanisms of multiple drug resistance (MDR) to chemotherapeutic agents by cancerous cells. This is because it plays a significant role in the absorption, distribution and elimination of drugs and as such may decrease intracellular drug

availability thereby mediating resistance to a variety of pharmacological drugs, especially, anticancer drugs [427, 428, 429, 397, 430, 431]. P-gp is overexpressed in cancer cells as an adaptive method to reduce toxicity [432, 433]. To date, only a few of the developed P-gp inhibitors have made it past clinical trials due to non-specific toxicity [433], and as such, there is still a need to explore alternative P-gp inhibitors.

Several herbal medicines are made available at pharmacies and shops as either dried leaves for tea, powdered, as capsules or tablets, or in solution at the disposal of anyone mostly without a list of precautions. This is mainly because herbal medicines are not subject to review by the Food and Drug Administration (FDA), but can be seized and removed when the FDA is made aware of the problems. However, since these herbal supplements are taken unmonitored patients often do not disclose their intake to their physicians, the problems encountered are rarely documented or voiced out. An example of this herbal supplement is *Actaea racemosa* (Black cohosh). It is a shrub-like plant that grows in North America and is now packaged and sold in many outlets, even in South Africa. It is often used for menopausal disorders, uterine spasms and vaginitis. Black cohosh is alleged to be toxic to the liver and when used with prescription drugs, certain liver enzymes required for breaking down prescription drugs may cause it to accumulate in the body and thus lead to liver toxicity. Another readily available herbal supplement is *Hypericum perforatum* (St John's-wort). It is widely used to treat symptoms of depression and is reported to have many serious drug-interactions, yet is still sold in pharmacies and supermarkets (www.drugs.com). As such, because herbal active constituents may affect the pharmacokinetic profile and trigger unexpected and inappropriate effects [434], the use of medicinal plants as a collection of bioactive phytochemicals should be optimised [32]

2.9 Aim

The study aimed to characterise the crude water and crude methanol leaf extracts of *Momordica balsamina*, investigate their potential anticancer activity on HT-29 colon cancer cells and assess their effect on CYP450 enzymes which metabolise 5-Fluorouracil.

2.9.1 Hypothesis

Momordica balsamina crude water and crude methanol leaf extracts possess compounds with anticancer activities against HT-29 colon cancer cells. The extracts also have an additive effect on the efficacy of 5-Fluorouracil and do not interact with drug metabolising enzymes.

2.9.2 Null hypothesis

Momordica balsamina crude water and crude methanol leaf extracts do not possess compounds with anticancer activities against HT-29 colon cancer cells. The extracts also do not have an additive effect on the efficacy of 5-Fluorouracil and they interact with drug metabolising enzymes.

2.9.3 Objectives

I. To characterise the *M. balsamina* crude water and crude methanol leaf extracts using Thin-Layer Chromatography (TLC), standard phytoconstituent tests and Liquid Chromatography-Mass Spectrometry (LC-MS).
II. To assess the cytotoxicity of the extracts and 5-Fluorouracil on HT-29 colon cancer and C2C12 muscle cells using cell viability assays.
III. To assess the effect of the extracts on the efficacy of 5-Fluorouracil on HT-29 colon cancer cells using cell viability assays.
IV. To assess the genotoxicity of the extracts and 5-Fluorouracil on C2C12 muscle cells using the Muse™ Multi-Colour DNA Damage kit.
V. To assess ROS production in HT-29 cells following treatment with the extracts and 5-Fluorouracil using the DCFH-DA staining assay.
VI. To assess the potential pro-apoptotic activity of the extracts and 5-Fluorouracil on HT-29 colon cancer cells using the JC-1 staining assay, the acridine orange/propidium iodide (AO/PI) dual staining assay, the Annexin V/PI and Caspase-8 and Caspase-9 colourimetric assays.
VII. To assess the effect of the extracts and 5-Fluorouracil on the mechanism of apoptosis induction of HT-29 colon cancer cells using the human apoptosis antibody array kit.

VIII. To assess the potential of herb-drug interactions between the extracts and 5-Fluorouracil using Vivid® CYP450 Screening kits and the P-gp-Glo™ Assay Systems with P-glycoprotein.

Chapter 3

3. Methodology and analytical procedures

3.1 Plant collection and extraction

The *Momordica balsamina* plant, voucher specimen number UNIN121046, leaves were collected from Letsitele (23°57'51" S 30°22'39" E) in the Limpopo province, South Africa. The plant leaves were washed with distilled water, air-dried at room temperature and ground to powder using a commercial blender. The powdered leaves were then extracted by boiling (125 g/L) in distilled water using a method described by Azwanida [435], or macerating in methanol (Rochelle Chemicals, SA) at 70ºC using a method described by Cheng *et al*. [436]. Following extraction, the extracts were filtered using a filter paper with a pore size of 12-15 µm (Munktell, UK). The water extract was then freeze-dried using a freeze-dryer (Labconco, Labotec, Cape Town) and the methanol extract dried using an industrial fan. The water extract was then stored as a powder in the dark, at room temperature and the methanol extract weighed and dissolved in 100% dimethyl sulfoxide (DMSO) (Sigma-Aldrich, St. Louis, USA) to give a stock solution of 100 mg/ml which was then stored at -20ºC.

3.2 Screening and chemical characterisation of the extracts

3.2.1 TLC fingerprint

The phytochemical fingerprint of the *M. balsamina* H_2O and MeOH extracts was analysed by thin-layer chromatography (TLC) using a method described by Kotzé and Eloff [437]. The extracted compounds were separated on aluminium-backed silica gel 60 F_{254} plates (MilliporeSigma, cat# 10554, Burlington, USA). A volume of 5 µl of the extracts at a concentration of 20 mg/ml was spotted onto the TLC plates. The plates were developed in closed tanks saturated with mobile phases of varying polarities in descending order, namely; butanol: acetic acid: water (4:1:5) [BAW]; chloroform: ethyl acetate: formic acid (5:4:1) [CEF] and benzene: ethyl acetate: ammonium hydroxide (90:10:1) [BEA]. The plates were then viewed and photographed under UV light at 365 nm and sprayed with vanillin-sulphuric acid (0.1 g vanillin in 28 ml methanol: 1 ml sulphuric acid) for visualisation.

3.2.2 Presence of phytochemicals

The type of phytochemicals present in the *M. balsamina* MeOH and H_2O extracts were determined qualitatively using standard phytochemical tests as described in Table 3.1 according to methods described by Harbone [438] and Kokate [439]. Comparative analysis between the H_2O and MeOH extracts was done qualitatively by observing colour intensity and annotating + for moderate and ++ for intense colouration or change.

Table 3.1: Test for the presence of phytochemicals.

Phytoconstituents	Test	Observation
Tannins	2 ml extract[#] + 2 ml H_2O + 2-3 drops $FeCl_3$ (5%)	Green precipitate
Coumarins	2 ml extract[#] + 3 ml NaOH (10%)	Yellow colouration
Phenols	2 ml extract[#] 2 ml of 2% $FeCl_3$	Blue/black colouration
Flavonoids	1 ml extract[#] + 1 ml $Pb(OAc)_4$ (10%)	Yellow colouration
Carbohydrates	2 ml extract[#] + 10 ml H_2O + 2 drops Ethanolic α-naphthol (20%) + 2 ml H_2SO_4 (conc.)	Reddish-violet ring at the junction
Saponins	5 ml extract[#] + 5 ml H_2O + heat	Froth appears
Triterpenoids	2 ml extract[#] + 2 ml $(CH_3CO)_2O$ + 2-3 drops H_2SO_4 (conc.)	Reddish-violet colouration

[#]Extract concentration (10 µg/ml)

3.2.3 Ferric ion reducing power

The ferric ion reducing the power of the MeOH and H_2O extracts of the *M. balsamina* leaves was determined using a method by Benzie and Strain [440]. The MeOH and H_2O extracts were prepared in methanol and distilled water, respectively, at a concentration of 10 µg/ml. Ascorbic acid (Sigma-Aldrich, cat# A92902, St. Louis, USA) was used as a reference standard. A volume of 100 µl of the extracts or ascorbic acid was added to 250 µl of 0.2 M phosphate-buffered saline (PBS) (Lonza, cat# BE17-516F, Basel, Switzerland) at pH 7.4, 250 µl of 1% potassium ferricyanide and incubated for 20 minutes at 50 ºC. Following incubation, 250 µl of 10% (w/v) trichloroacetic acid was added to each sample, the mixtures centrifuged at 1100 g for 10 minutes and the supernatant (250 µl) mixed with equal parts of distilled water. Ferric chloride (50 µl of 0.1%) was then added to the supernatant-distilled water mixture and the absorbance of the samples measured using a microtiter plate reader (GloMax®-Multi+Detection system, Promega, Madison, USA) at a wavelength of 600 nm. Data were presented

as EC_{50} reducing power calculated using linear regression from a quercetin standard curve.

3.2.4 Liquid chromatography-mass spectrometry

3.2.4.1 Sample preparation

The *M. balsamina* extracts were obtained by extraction as described in section 3.1. The powdered H_2O extract was dissolved in 10 ml of deionised water obtained using a Milli-Q water purification system (Millipore, Milford, USA) and the MeOH extract in 10 ml of methanol. The samples were then diluted 1:1 (v:v) in deionised water and filtered through a 0.22 µm polyethersulfone filter unit (Millipore, cat#SLGPO33RS Watford, UK) before being subjected to analysis by liquid chromatography-mass spectrometry (LC-MS).

3.2.4.2 LC-MS conditions

Samples were separated by reverse-phase liquid chromatography (RP-LC) performed on an InfinityLab Poroshell 120 SB-C18 column (4.6 x 100 mm, 2.7 µm) using mobile phases water (A) and acetonitrile (B). The solvent gradient used was 1 – 95% B from 0 to 20 minutes, 95% B from 20.01 to 25 minutes, 95 – 1% B from 25.01 to 30 minutes with a flow rate of 0.4 ml/min. MS analysis was accomplished using the 1260 Infinity II liquid chromatographic system coupled to a single quadrupole Infinity Lab LC/MSD (Agilent Technologies, Santa Clara, USA) system equipped with a jet stream electrospray ionisation source. Data acquisition and processing were performed using the OpenLab CDS software (Chemstation). Compounds within the extracts were detected using the scan mode in the positive ionisation mode with a fragmentation voltage of 200 V. Furthermore, nitrogen was used as the desolvation gas at a flow rate of 5 L/min at 300ºC and sheath gas at a flow rate of 12 L/min at 360ºC.

3.3 Study model

The HT-29 colon cancer cell line is a human colorectal adenocarcinoma cell line with epithelial morphology used extensively to study the biology of human colon cancers [441]. The HT-29 are able to differentiate and simulate characteristics of mature intestinal cells and thus are a good model for *in vitro* studies of absorption, transport and secretion by intestinal cells. Under standard cell culture conditions (when grown

in DMEM), the cells grow as a non-polarised, undifferentiated multilayer [442]. Moreover, these cells are sensitive to chemotherapeutic drugs such as 5-fluorouracil and oxaliplatin [443].

3.4 Cell culture and maintenance

Human HT-29 colon cancer cells (ATCC® HTB-38™) and mouse (*Mus musculus*) C2C12 cells (ATCC® CRL-1772™) were purchased from the American Type Culture Collection (Manassas, VA, USA). The C2C12 muscle cells were used as a model for normal cells as they are highly proliferative, easy to culture and have good basic metabolic panel responsiveness (BMP), which provides information on the body's metabolism [444]. The cells were grown in 75 cm^3 flasks in Dulbecco's Modified Eagle's Medium (DMEM) (HyClone Laboratories, cat# SH30285.03, South Logan, USA), supplemented with 10% (v/v) heat-inactivated foetal bovine serum (FBS) (Gibco, cat# 10500064, Life Technologies, Carlsbad, USA). Cells were grown in a tissue culture incubator at 37ºC in humidified air containing 5% CO_2. The C2C12 cells were sub-cultured every second day at a ratio of 1:8, while the HT-29 cells were sub-cultured every fourth day at a ratio of 1:8 and refreshed every second day in a level 2 biosafety cabinet (Labtech™, Ortenberg, Germany). Passage numbers were recorded with each sub-culture and restricted to under 30 passages to avoid phenotypic drift caused by sub-culturing. To retrieve cells from the culture flask surface, all media was aspirated and the cells were washed with 8 ml of 1x Dulbecco's phosphate-buffered saline (DPBS) (Gibco, cat# 14040133, Life Technologies, Carlsbad, USA). Following the aspiration of DPBS, 2 ml of 1x trypsin (Gibco, cat# 25200072, Life Technologies, Carlsbad, USA) was added to the flask and incubated in the tissue culture incubator for 5 – 7 min. To stop trypsinisation, 8 ml of supplemented DMEM was added to the flask and the cells resuspended by pipetting to ensure all cells have detached from the culture surface. The cells were then centrifuged at 800 rpm for 5 min and resuspended in 8 ml of supplemented DMEM. The cell suspension was then either transferred to a new flask or counted and seeded for experiments.

3.5 Cell counting and seeding

For cell counting, the cell suspension was stained with 0.4% (w/v) trypan blue (Invitrogen, cat# T10282, Carlsbad, USA) in DPBS at a 1:1 ratio (v:v), by adding equal

volumes (10 µl) of the cell suspension and trypan blue. The solution was gently mixed by pipetting and 10 µl of the mixture transferred to the counting chamber of a Neubauer haemocytometer. Live and dead cells were counted at 10x magnification using an inverted phase-contrast microscope (Olympus CKX31, Tokyo, Japan). Cell concentration was calculated using equation 1. C2C12 cells were seeded at a density of 1.5 x 10^5 cells per cm^2 and HT-29 cells at a density of 3.0 x 10^4 cells per cm^2. Upon seeding, the cells were allowed to attach and grow for 48 hours (C2C12) or 72 hours (HT-29) before commencing the respective experiments.

$$\#\ of\ cells\ per\ ml = average\ of\ cells\ counted\ per\ mm^2\ x\ 2\ x\ 10\ 000 \quad (1)$$

3.6 Treatment preparation and cell treatment conditions

For cytotoxicity and genotoxicity assays, the *M. balsamina* water extract (H_2O) stock solution of 100 mg/ml was prepared by dissolving the dried extract (stored at RT) in cell culture media which was further diluted to make up concentrations ranging from 250 – 2000 µg/ml. The MeOH extract concentrations were prepared by diluting the stock solution (100 mg/ml, in 100% DMSO, stored at -20ºC) in cell culture media to make up concentrations between 50 – 300 µg/ml. A 5-Fluorouracil (5-FU) (Sigma, cat# F6627-1G, Sigma-Aldrich, St. Louis, USA) stock solution of 50 mg/ml was prepared in 100% DMSO, aliquoted and kept at 4°C until use. The 5-FU stock solution was further diluted with cell culture media to make up concentrations of 0.001 – 100 µg/ml. Curcumin (Sigma, cat# C1386-5G, Sigma-Aldrich, St. Louis, USA) at 200 µM was prepared from a stock solution (1000 µM) in cell culture media and served as a positive control. The DMSO (vehicle control) final concentration in all treatments was 0.5%. Furthermore, for reactive oxygen species, apoptosis detection and cell cycle distribution assays, the cells were treated with a low concentration and either the IC_{50} or a higher concentration determined from the MTT assay results (250 and 2000 µg/ml of the H_2O extract, 100 and 267 µg/ml of the MeOH extract, 10 and 100 µg/ml of 5-FU) and 200 µM of curcumin for 24 hours. For protein expression analysis, the cells were treated with 267 µg/ml of the MeOH extract, 100 µg/ml of 5-FU and 200 µM of curcumin for 24 hours. All treatments were filter sterilised using a 0.22 µm polyethersulfone filter unit before treating the cells.

3.7 Cytotoxicity assay

The effect of the *M. balsamina* H_2O, MeOH extracts or 5-FU on the viability of HT-29 colon cancer and C2C12 muscle cells was evaluated using the 3-(4,5-dimethylthiazol-2-yl)-2,5-diphenyltetrazolium (MTT) (Sigma, cat# M2003-1G, Sigma-Aldrich, St. Louis, USA) assay, as described by Mosmann [445], with slight modifications. The MTT assay is based on the reduction of the yellow tetrazolium dye, MTT, blue/purple water-insoluble formazan crystals by the action of nicotinamide adenine dinucleotide phosphate (NADPH)-dependent cellular oxidoreductase enzyme [446]. Cells were seeded as described in section 3.5 in 96-well plates and allowed to attach. The cells were treated as described in section 3.6 for 24 and 72 hours. Following treatment, the cell culture media was removed, 100 µl of 1 mg/ml of MTT in 1x DPBS was added and the cells incubated in a tissue culture incubator for 30 minutes. The MTT solution was then removed and 200 µl of DMSO added to dissolve the formazan crystals. The absorbance was measured at a wavelength of 570 nm using the SpectraMax i3x (Molecular Devices, LLC, Sunnyvale, CA, USA). Data were expressed as percentage viability calculated using equation (2).

$$\%\ Viability = \frac{Absorbance\ of\ treated\ cells}{Absorbance\ of\ vehicle\ control\ treated\ cells} \times 100 \quad (2)$$

For the testing of potential interactions between *M balsamina* extracts and 5-FU, the cells were treated with the vehicle control as well as varying concentrations of the extracts and/or IC_{50} of 5-FU and the MeOH extract. To test for the H_2O extract and 5-FU, the cells were treated with 250 – 2000 µg/ml of the H_2O extract together with the 5-FU IC_{50} obtained from the MTT assay at 72 hours of treatment (3.2 µg/ml). For the MeOH extract and 5-FU, cells were treated with 0.001 – 100 µg/ml of 5-FU and the MeOH IC_{50} (267 µg/ml) for 24 hours. The same treatments were also applied for 72 hours, except for the concentration of the MeOH extract, which was the IC_{50} (151 µg/ml) obtained from the MTT assay at 72 hours of treatment. MTT analysis was done as above and the data expressed as percentage viability calculated using equation 2.

3.8 Genotoxicity assay

To assess the genotoxicity of the *M. balsamina* MeOH extract or 5-FU on C2C12 cells, the Muse™ Multi-Colour DNA Damage kit (MilliporeSigma, cat# MCH200107, Burlington, USA) was used, following the manufacturer's description. The kit uses two directly conjugated antibodies; a phospho-specific ATM (Ser1981)-PE and a phospho-specific Histone H2A.X PE_Cy5 to measure the extent of DNA damage in treated and control cells. This allows for simultaneous detection of the phosphorylation state of ATM and Histone H2A.X, thereby assessing the DNA damage signalling pathway. Briefly, cells were seeded at 1.0 x 10^5 cells/well in a 24-well plate and allowed to attach. The cells were treated with 0.5% DMSO or 267 µg/ml of the MeOH extract, 100 µg/ml of 5-FU and 200 µM of curcumin for 24 hours. Following treatment, the spent media was collected and the cells were harvested by trypsinisation. Briefly, the cells were washed with warm 1x DPBS and incubated with 300 µl of trypsin in a tissue culture incubator for 5 min. The cells were then centrifuged at 800 rpm for 5 min before being washed with 1x DPBS and the pellet resuspended in 500 µl of 1x assay buffer. Equal parts of the fixation buffer were then added to the cell suspension and the samples were incubated on ice for 5 min. The cells were then centrifuged at 300 g for 5 min and 1 ml of ice-cold permeabilisation buffer added to the pellet and incubated on ice for another 5 min. The cells were centrifuged as above and resuspended in 450 µl of 1x assay buffer. A volume of 90 µl was then transferred to a new microcentrifuge tube, 10 µl of the antibody cocktail was added to the cells and incubated for 30 min in the dark, at room temperature. The cells were centrifuged and washed with 1x assay buffer as above. The cell pellet was then resuspended in 200 µl of 1x assay buffer and the samples analysed using the BD Accuri™ C6 flow cytometer (BD Biosciences, Johannesburg, South Africa). Cell samples were initially stained with each fluorophore separately to determine the required colour compensation and for setting the quadrant gate to select for positive events. Fluorescence spill over in FL2 was corrected by subtracting 1.79% of FL3 while FL3 was corrected by subtracting 27.9% of FL2. Data were presented as percentage expression of H2A.X, H2A.X/ATM and ATM.

3.9 DCFH-DA reactive oxygen species assay

The effect of the *M. balsamina* H_2O, MeOH extracts, and 5-FU on the generation of intracellular reactive oxygen species (ROS) in HT-29 cells was measured using 2',7'-

dichlorodihydrofluorescein diacetate (DCFH-DA) (Sigma, cat# D6883, Sigma-Aldrich, St. Louis, USA) using a method described by Wu and Yotnda [447], with slight modifications. The assay uses DCFH-DA, a fluorogenic dye, which is non-fluorescent, that is deacetylated by the cellular hydrolase enzymes (esterase) once diffused into cells. Inside the cells, DCFH-DA is oxidised into 2',7'-dichlorodihydrofluorescein (DCF), which is fluorescent, in the presence of ROS [447]. Cells were seeded as described in section 0, allowed to attach and treated as described in section 3.6 for 24 hours. Following incubation, the treatment media was discarded and the cells washed with 1x DPBS and further incubated with 10 µM of DCFH-DA solution in 1x DPBS at 37°C in the dark for 30 min in a tissue culture incubator. The fluorescence signal was detected following trypsinisation of the cells using the BD Accuri™ C6 flow cytometer, using the FL1 detector. Data were presented as percentage of DCF positive cells separated by a marker between the negative and positive populations.

3.10 Apoptotic assays

3.10.1 Mitochondrial membrane potential

The effect of the *M. balsamina* H_2O, MeOH extracts and of 5-FU on the mitochondrial membrane potential of HT-29 cells was assessed using 5,5′,6,6′-tetrachloro-1,1′,3,3′-tetraethylbenzimi-dazolylcarbocyanine iodide (JC-1) (Sigma, cat# T4069-5MG, Steinheim, Germany), following a method by Sivandzade *et al*. [448], with modifications. The assay is used to measure the cell's mitochondrial membrane potential. The JC-1 dye selectively enters the mitochondria and changes fluorescence from red to green as the cell's membrane potential decreases, fluorescing orange when the cell's mitochondria are healthy and green when the cell is in distress [449]. Cells were seeded in 24-well plates as described in section 0 and allowed to attach. The cells were then treated as described in section 3.6 for 24 hours. Following treatment, the supernatant was removed and the cells were washed with warm 1x DPBS and incubated with 500 µl of 2 µM JC-1 solution made by reconstituting 2.7 µl of the stock solution in 100 µl of 100% DMSO and 1x DPBS was added to make a final volume of 10 ml. The cells were incubated for 30 min in a tissue culture incubator, whereafter the supernatant was then replaced with warm 1x DPBS and the samples viewed and captured under an inverted fluorescent microscope (Nikon Eclipse Ti/S Fluorescence Microscope (Nikon, Minato City, Tokyo, Japan)) with 10x magnification using a tri-bandpass filter. Images from 3

independent experiments were analysed and the intensity of the red fluorescence was quantified using the ImageJ (32 bit) software application [450], version 1.52a. The procedure used for quantitation is outlined in Annexure A. Briefly, the RGB images were split into single channels and the red channel used to create a binary image. The binary image was then used for background subtraction and measuring the intensity of the fluorescence. Data were presented as representative images from three experiments and as a percentage of mitochondrial depolarisation.

3.10.2 Nuclear morphology analysis

Nuclear morphology associated with apoptosis in treated and control HT-29 cells were assessed using the acridine orange/propidium iodide (AO/PI) (AO; Sigma, cat# A6014, Sigma-Aldrich, St. Louis, USA) (PI; Invitrogen, cat# p3566, Life Technologies, Carlsbad, USA), dual staining assay as described by Hussain *et al*. [451], with slight modifications. Acridine orange is a DNA intercalating dye that can permeate live and apoptotic cells to stain the nucleus and generate green fluorescence. In contrast, PI can only permeate cells with poor cell membrane integrity, staining all dead nucleated cells to generate red fluorescence [452, 453]. The nuclear of apoptotic cells will thus stain orange due to the combination of the AO and PI. Cells were seeded and treated as described in section 3.10. Following treatment, the supernatant was removed and the cells were washed twice with 1x DPBS and stained with 30 µg/ml of AO for 15 min in the dark, at room temperature. The cells were washed as before and counterstained with 30 µg/ml of PI for 15 min in the dark, at room temperature. Following incubation, the images of 3 independent experiments were captured using an inverted fluorescent microscope with a 10x magnification using a tri-band pass filter. The excitation/emission profile for AO is 460/650 nm and 525/595 nm for PI. Data were presented as representative images from 3 independent experiments and the number of green and red fluorescent cells counted using the ImageJ (32 bit) software application [450], version 1.52a. The procedure used for quantitation is outlined in Annexure B. Briefly, the RGB images were split into single channels and the green and red channels converted to 8-bit type and the relative size of the cells calibrated using the scale bar and set to 100 µm. Cells of interest were then counted and quantified and data were presented representative images from one experiment and as a percentage of red fluorescent cells.

3.10.3 Quantitation of apoptosis

To determine the quantity of apoptotic HT-29 cells following treatment, the annexin-V/PI assay was used, following the manufacturer's description (Invitrogen, cat# A13199, Carlsbad, USA), with slight modifications. The assay is based on the binding of annexin-V to phosphatidylserine (PS) which becomes externalised in cells undergoing apoptosis. Propidium iodide (PI) stains the nuclei of cells with poor or compromised cell membrane function and thus distinguishes late apoptotic or dead cells from early apoptotic cells [454]. Briefly, cells were seeded and treated as described in section 3.10. for 24 hours. Following treatment, the cells were harvested by trypsinisation. Briefly, the supernatant was collected and the cells washed in 1x DPBS and incubated with trypsin for 5 – 10 min in a tissue culture incubator. The collected supernatant and dislodged cells were centrifuged at 800 rpm for 5 min and the pellet resuspended in 100 µl annexin-binding buffer (1x DPBS containing 133 mg/ml $CaCl_2$ and 10 mM HEPES, pH 7.4). Thereafter, 5 µl of the annexin-V conjugate as well as 0.60 µl of PI (25 µg/ml) were added to the cells and incubated in the dark at room temperature for 15 min. Following incubation, 400 µl of the annexin-binding buffer was added to each sample prior to analysis by flow cytometry using the BD Accuri™ C6 flow cytometer using the "BD Pharmingen Annexin-V FITC" template and detector FL1 and FL3. To correct for autofluorescence, all the cell samples were also acquired unstained. Cells were also stained separately with each fluorophore to determine colour compensation and set the quadrant gate (Annexure C). Fluorescence spill over in FL3 was corrected by subtracting 1.6% of FL1, while FL1 was corrected by subtracting 0.28% of FL3. Data were expressed as the percentage of early apoptotic cells (Annexin-V+ and PI-), late apoptotic cells (Annexin-V+ and PI+), and dead/necrotic cells (PI+ and Annexin-V-).

3.10.4 Determination of Caspase-8 and -9 activity

To determine the effect of the *M. balsamina* MeOH extract or 5-FU on caspase-8/-9 activity, the Caspase-8 and Caspase-9 colourimetric assay kits were used, following the manufacturer's description (R&D Systems, cat# K119-100 and cat# K113-100, Minneapolis, USA). The assay uses a peptide coupled to a coloured reporter system to evaluate the activity of caspases in cell lysates. Briefly, cells (5×10^5 cells/well) were seeded in 6-well plates, allowed to attach and treated with 267 µg/ml of the MeOH

extract, 100 µg/ml of 5-Fluorouracil, 200 µM of curcumin and the vehicle control for 24 hours. Following treatment, the supernatant was collected and the cells harvested by trypsinisation. The cells were centrifuged at 250 g for 10 min, 25 µl of cold lysis buffer added and incubated on ice for 10 min. The lysate was centrifuged at 10 000 g for 1 min and the supernatant transferred to a new tube and kept on ice. The protein concentration was then determined following the manufacturer's description, using the Pierce™ BCA Protein Assay kit (ThermoFisher Scientific, cat# 23225, Waltham, USA). Briefly, the bicinchoninic acid assay (BCA) working reagent was prepared by adding 50 parts of solution A to 1 part of solution B, as per instructions. A volume of 10 µl of bovine serum albumin (BSA) standards (between 2 µg/ml and 0.125 µg/ml) and experimental samples were pipetted in triplicate into a 96-well flat-bottom assay plate. Two hundred microlitres of the working reagent were added to each well containing the standards as well as the experimental samples. The plate was placed onto a plate shaker and mixed for ten seconds, followed by incubation at 37°C for thirty minutes before the absorbances of the samples were measured at OD (570 nm) using a plate reader, GloMax®-Multi+Detection. The absorbance readings from the BSA standards were used to calculate concentrations of the experimental samples by extrapolation from the standard curve. For the caspase activity assay, 50 µl of protein diluted to 200 µg/ml were transferred to a flat-bottom 96-well plate. A volume of 50 µl of the 2x reaction buffer 8/9 was added to each sample as well as 5 µl of Caspase-8 or Caspase-9 colourimetric substrates. The samples were then incubated at 37°C for 2 hours and the plate read at a wavelength of 405 nm using a microtiter plate reader, GloMax®-Multi+Detection system. Data were expressed as fold change of the caspases as a function of the DMSO-treated control cells.

3.10.5 Protein expression profile analysis

The effect of the MeOH extract or 5-FU on the expression levels of apoptosis regulatory proteins was assessed using the human apoptosis antibody array kit, following the manufacturer's protocol (R&D Systems, cat# ARY009, Minneapolis, USA). This is a membrane-based sandwich immunoassay that makes use of capture antibodies that are spotted in duplicate on nitrocellulose membranes allowing the binding of numerous specific target proteins [455]. Cells (7 x 10^6 cells/flask) were seeded in 75 cm^3 flasks, allowed to attach and treated as described in section 3.6 for 24 hours.

The cells were harvested by scraping in lysis buffer [10 mM Tris, pH 7.4, 100 mM NaCl, 1 mM EDTA, 1 mM EGTA, 1 mM NaF, 20 mM $Na_4P_2O_7$ 2 mM Na_3VO_4, 1% Triton X-100, 10% glycerol, 0.1% SDS, 0.5% deoxycholate] (Invitrogen, cat# FNN0011, Carlsbad, USA). Following cell harvesting, a stainless steel bead (Qiagen™, Hilden, Germany) was added to each 2 ml centrifuge tubes containing the cell suspension. The samples were then homogenised using a TissueLyser (Qiagen™, Hilden, Germany) at 25 Hertz for 60 seconds. This was repeated 5 times with sixty-second intervals on ice. The homogenised suspension was then centrifuged at 15000 g for 15 minutes at 4 °C and the supernatant containing total cellular protein carefully removed and transferred to a 2 ml Eppendorf tube. Total protein was then quantified using the BCA as described in section 3.10.4. The membrane arrays were blocked for 30 minutes using the array buffer 1 and 400 µg of the protein were added to the respective array membranes. Array membranes were then incubated at 4°C overnight on a rocking platform shaker, followed by washing 3 times with the 1x wash buffer for 10 minutes on a rocking platform shaker. The detection antibody cocktail (15 µl) was diluted in 1.5 ml of the 1x array buffer 2/3 prepared by diluting 2.0 ml of the 5x array buffer 2 concentrate into 8.0 ml of array buffer 3 and added to the membranes which were further incubated for one hour on a rocking platform shaker. The membranes were washed as above, whereafter the diluted streptavidin-HRP (1:2000) was added to the membranes followed by a 30 minute incubation at room temperature, on a rocking platform shaker. Lastly, the membranes were washed as above and a chemiluminescent-reagent mix (1:1 of chemi reagent 1 and 2) added for the development of the spots. The spots were then visualised and captured using the ChemiDoc MP system (Bio-Rad, Hercules, USA), and data were presented as fold of protein expression/activation as a function of the control cells treated with 0.5% DMSO.

3.11 Cell cycle analysis

To assess the effect of the *M. balsamina* MeOH extract or 5-FU on the cell division cycle of HT-29 cells, flow cytometry was used, following a description by Agarwal *et al*. [324], with slight modifications. The assay assesses the distribution of cells in three major phases of the cell cycle by use of the fluorescent DNA-binding dye, PI [456]. Cells were seeded and treated with the MeOH extract and 5-FU as described in section 3.10

for 24 hours. Following treatment, the supernatant was collected and the cells harvested by trypsinisation. The combined supernatant and cell pellet were then washed with ice-cold 1x DPBS by centrifugation at 300 g for 5 min and fixed overnight in 70% ethanol at 4°C. The cells were then washed and incubated with a mixture of 100 µg/ml RNase A (Qiagen, cat# 19101, Hilden, Germany) and 50 µg/ml PI in 1 ml 1x DPBS at room temperature, in the dark for 30 min. The stained cells were subjected to analysis by flow cytometry using the BD Accuri™ C6 flow cytometer, using the "BD Cycletest" template. The analysis was performed using the FlowJo analysis software application, version 10.6.2 (https://www.flowjo.com) and the procedure outlined in Annexure D. Data were presented as percentage of cells in each cell cycle phase.

3.12 Assessment of the activity of drug metabolising enzymes

The effect of the *M. balsamina* H_2O , MeOH extracts or 5-FU on CYP1A2 (cat# P2863), CYP2A6 (cat# PV6140), CYP2C8 (cat# P2861) and CYP2C9 (cat# P2860), was assessed using the Vivid® CYP450 screening kits, following the manufacturer's description (Thermo Fisher Scientific, Waltham, USA). The assay enables measurement of the interactions between drug candidates and cytochrome P450 enzymes by use of a "mix-and-read" fluorescent assay. The specific CYP450 enzymes were chosen from those listed by the DrugBank (drugbank.com) [457] as those for which 5-FU prodrugs serve as a substrate (CYP1A2, CYP2A6 and CYP2C8) or are inhibited by 5-FU (CYP2C9) since it was used as a reference compound in this study. Briefly, test compounds and P450 inhibitors were prepared at a 2.5x concentration in either methanol or DMSO. For the H_2O and MeOH extracts, concentrations ranged from 40 – 200 µg/ml, while those of 5-FU ranged between 0.8 to 80 µg/ml. Forty microliters of the test compounds were added in duplicate to a black clear bottomed 96-well plate. A Master Pre-Mix (50 µl) containing P450 Baculosomes® Plus Reagent and Vivid® Regeneration System in 1x Vivid® CYP450 Reaction Buffer was added to the wells. The plate was incubated at room temperature for 10 minutes to allow the test compounds to interact with the P450 baculosomes in the absence of enzyme turnover. The background fluorescence was then measured using the SpectraMax i3x before adding 10 µl of a 10x mixture of the Vivid® substrate and Vivid® $NADP^+$ to each well. The fluorescence was measured in kinetic mode for 30 min at 2 min intervals using the SpectraMax i3x. The inhibitors, their concentrations and wavelengths used are

summarised in Table 3.2. Fluorescence intensity was measured over time to illustrate enzyme activity. Reaction rates were obtained by calculating the change in fluorescence per unit time (slope of the curves) and data calculated as percentage inhibition as a function of the inhibitor using equation (3).

$$\%\ Inhibition = 1 - \left(\frac{rate\ observed\ for\ test\ compound - rate\ observed\ for\ inhibitor}{rate\ observed\ for\ solvent\ control - rate\ observed\ for\ inhibitor}\right) x\ 100$$

(3

Table 3.2: Reaction set-up for Vivid® screening assays

Enzyme	Vivid® Substrate	Solvent	Buffer	Inhibitor	Concentration	Excitation/emission (nm)
CYP1A2	EOMCC	DMSO	I (1x)	α-naphthoflavone	10 µM	415/460
CYP2A6	CC	Methanol	II (0.5x)	Tranylcypromine	100 µM	415/460
CYP2C8	DBOMF	DMSO	II (1x)	Montelukast	10 µM	490/520
CYP2C9	BOMCC	DMSO	II (1x)	Sulfaphenazole	50 µM	415/460

EOMCC = 7-ethyloxymethyloxy-3-cyanocoumarin
CC = 3-cyanocoumarin
DBOMF = dibenzoxymethylfluorescein
BOMCC = 7-benzyloxymethyloxy-3-cyanocoumarin

3.13 Assessment of the activity of the drug transporter P-glycoprotein

To assess the influence of the *M. balsamina* H_2O , MeOH extracts or 5-FU on multidrug resistance, the activity of the drug transporter protein, P-glycoprotein, was determined using the P-gp-Glo™ Assay Systems with P-glycoprotein, following the manufacturer's description (Promega, cat# V3591, Madison, USA). The assay relies on the ATP-dependence of the light-generating reaction of firefly luciferase which allows detection of ATP consumption by a decrease in luminescence. In an opaque 96-well plate, 20 µl of the following samples and controls were added to individual wells in duplicate, (i) P-gp-Glo™ assay buffer as a control, (ii) 0.25 mM sodium orthovanadate (Na_3VO_4) as a selective inhibitor of P-gp, (iii) 0.5 mM Verapamil as a stimulator for P-gp ATPase activity and (iv) 2.5x concentrated test compounds with concentrations ranging from 0.02 to 200 µg/ml for the H_2O and MeOH extracts, and 0.008 to 32 µg/ml for 5-FU. Diluted P-gp membranes (20 µl) were added to each well and the plate incubated at 37°C for 5 minutes. To initiate the reaction, 10 µl of 25 mM MgATP was added to all

wells, mixed briefly by gently tapping the plate and incubated at 37°C for a further 40 minutes. The reaction was stopped by adding 50 µl of ATP detection reagent (ATP detection buffer + ATP detection substrate) to all the wells. The reaction mixture was mixed briefly by gently tapping the sides of the plate and incubated at room temperature for 20 minutes. Luminescence was measured using the SpectraMax i3x. Data were presented as a change in luminescence, representing ATPase activity, obtained using the following calculations:

1. The ΔRLU_{basal}, which reflects basal P-gp ATPase activity, was calculated by calculating the difference between the average luminescent signals from Na_3VO_4- treated control (RLU_{Na3VO4}) and untreated control (RLU_{NT})

   $\Delta RLU_{basal} = RLU_{Na3VO4} – RLU_{NT}$. (equation 4?)
2. Difference between the average luminescent signals from Na_3VO_4-treated control (RLU_{Na3VO4}) and test compound-treated samples (RLU_{TC}) to determine ΔRLU_{TC} as follows:
   - $\Delta RLU_{TC} = RLU_{Na3VO4} – RLU_{TC}$.

   (ΔRLU_{TC} reflects P-gp ATPase activity in the presence of a test compound).

3.14 Statistical analysis

For all experiments, unless specified, data were generated from 3 independent experiments and expressed as mean ± S.E.M. Statistically significant differences between untreated or DMSO-treated controls and treatments were determined using GraphPad Prism version 8.4.3. (GraphPad Software Inc., La Jolla, USA) software by one-way ANOVA with a Dunnett's *post hoc* test. Differences between the mean of the untreated or DMSO-treated control and treated cells were considered significant at $p \leq 0.05$ (*), $p \leq 0.01$ (**), $p \leq 0.001$ (***) and $p \leq 0.0001$ (****). IC_{50} values were calculated using the GraphPad Prism version 8.4.3. (GraphPad Software Inc., La Jolla, USA) software by plotting activity against log concentration of the compounds in a line graph. A Non-linear regression (curve fit) and dose response-inhibition was selected and the variable slope (four parameters) used to analyse the plot. An IC_{50} value was determined for each independent repeat to calculate averages and S.E.Ms.

Chapter 4

4. Results

4.1 Plant characterisation

4.1.1 Thin-layer chromatography fingerprinting

Under UV light, TLC plates developed in butanol: acetic acid: water (4:1:5) [BAW] showed that the *M. balsamina* water (H_2O) extract contained more polar compounds when compared to the methanolic (MeOH) extract as most of the compounds of the H_2O extract were found to have lower retention factors thus migrated furthest from the solvent front. Vanillin sulphuric acid sprayed plates developed in BAW also showed more polar compounds in the H_2O extract when compared to the MeOH extract. Plates developed in chloroform: ethyl acetate: formic acid (5:4:1) [CEF] showed that the H_2O extract contained additional polar compounds that were lacking in the MeOH extract under UV light. The vanillin-sulphuric acid sprayed plates developed in CEF showed that the H_2O and MeOH extracts had similar compounds, although, the MeOH extract had more compounds than the H_2O extract. Furthermore, plates developed in the least polar mobile phase, benzene: ethyl acetate: ammonium hydroxide (90:10:1) [BEA] only showed the presence of compounds within the MeOH extract and not the H_2O extract after viewing under UV light and spraying with vanillin-sulphuric acid (Figure 4.1).

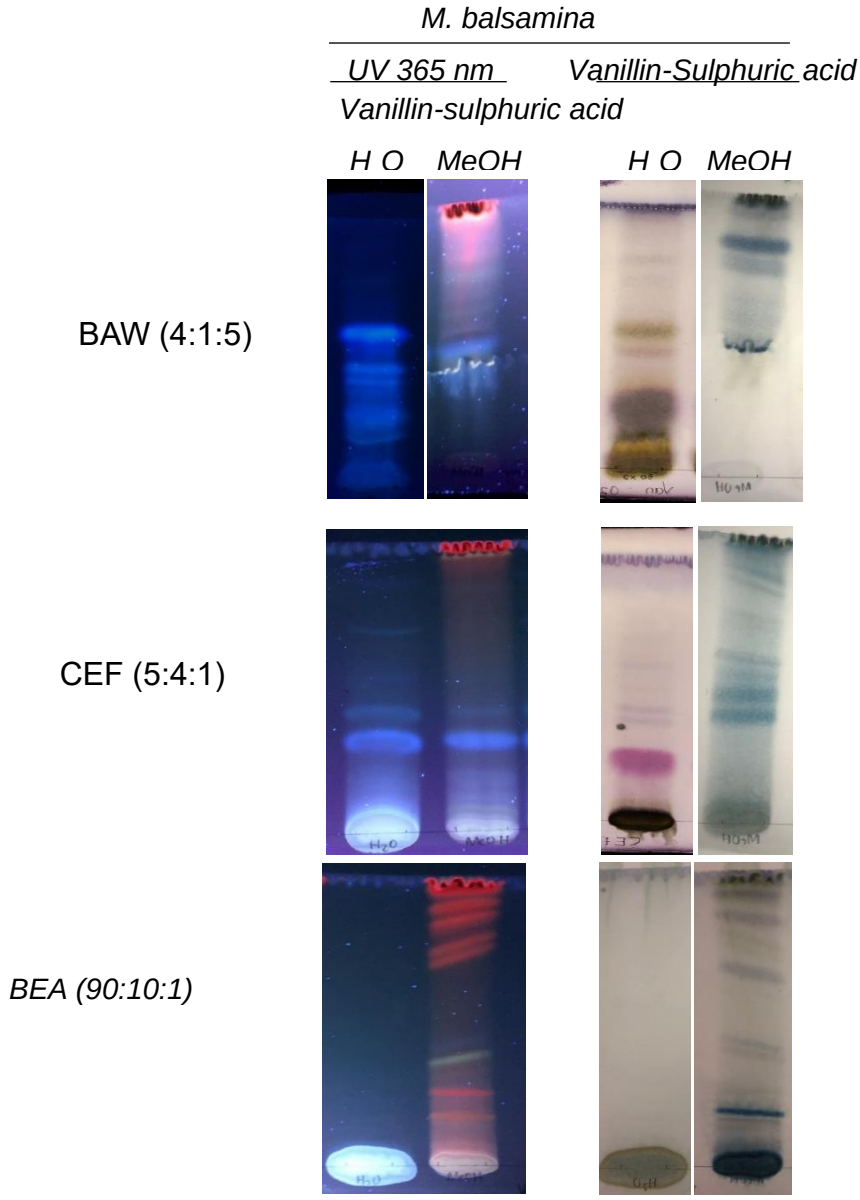

Figure 4.1: Chromatograms of the crude water (H_2O) and crude methanol (MeOH) extracts of *M. balsamina* leaves.

The extracts were spotted on TLC plates and developed in three eluent systems; Butanol: Acetic acid: Water (4:1:5) [BAW]; Chloroform: Ethyl acetate: Formic acid (5:4:1) [CEF] and Benzene: Ethyl Acetate: Ammonium hydroxide (90:10:1) [BEA], in a closed eluent saturated tank. The plates were then photographed under UV light at 365 nm and sprayed with vanillin-sulphuric acid for visualisation.

4.1.2 Phytoconstituents

Qualitative analysis of the type of phytochemicals present in the H_2O and MeOH extracts of *M. balsamina* leaves revealed the presence of tannins, coumarins, phenols, flavonoids, carbohydrates, saponins and triterpenoids (Table 4.1). Coumarins and flavonoids were found to be most abundant in the MeOH extract, while phenols were most abundant in the H_2O extract.

Table 4.1: Presence and/or absence of some secondary metabolites in the *M. balsamina* crude H_2O and MeOH extracts.

Phytoconstituents	Presence (+) or absence (-)	
	MeOH	H_2O
Tannins	+	+
Coumarins	++	+
Phenols	+	++
Flavonoids	++	+
Carbohydrates	+	+
Triterpenoids	+	+

++ Abundant

4.1.3 Quantitative ferric reducing antioxidant power

The EC_{50} values for the ferric reducing power of the H_2O and MeOH extracts of the *M. balsamina* leaves were calculated using linear regression from a quercetin standard curve. The results showed that the H_2O extract had the least antioxidant power as it had the highest EC_{50} value of 1.33 ± 0.29 mg/ml, while the MeOH had more antioxidant potential with the least EC_{50} value of 0.85 ± 0.08 mg/ml. These EC_{50} values were higher than that of ascorbic acid (0.48 ± 0.28 mg/ml), which was used as a reference standard.

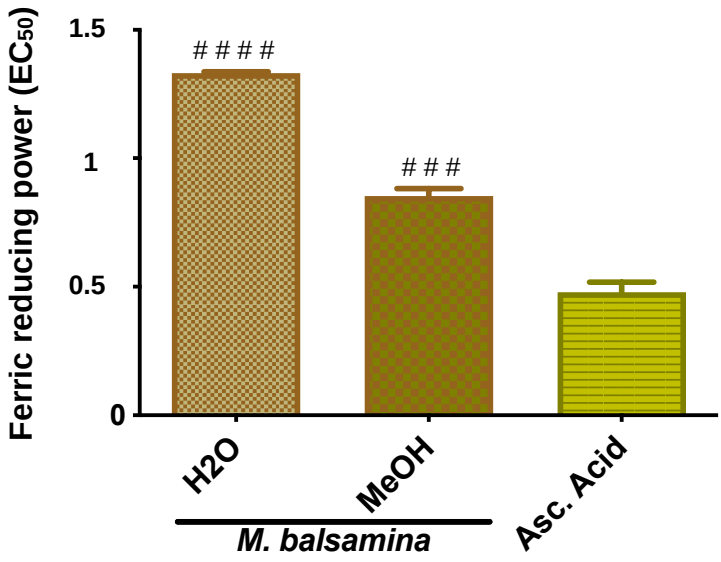

Figure 4.2: Ferric reducing antioxidant power of the *M. balsamina* crude water (H_2O) and crude methanol (MeOH) extracts.

The extracts and ascorbic acid were mixed with phosphate buffer, potassium ferricyanide, trichloroacetic acid, distilled water and ferric chloride solution with cycles of incubation. Ascorbic acid was used as a standard for comparison to the extracts. Data represents S.E.M of three independent experiments performed in triplicate. # # # $p \leq 0.001$ and # # # # $p \leq 0.0001$ indicate significant differences to the ascorbic acid control.

4.1.4 Liquid chromatography-mass spectrometry

The base peak ion chromatograms obtained for the H_2O and MeOH extracts are presented in Figure 4.3 A and B, respectively. Molecular species in methanol extracts of *M. balsamina* were previously identified in a study by Venter *et al*. (2021) [458]. These included flavonol glycosides, cucurbitane-type triterpenoid aglycones and cucurbitane-type glycosides. A comparison of the relative quantity of these previously identified compounds found in the MeOH and H_2O extracts was conducted. Table 4.2 shows that the flavonol glycosides rutin, nicotiflorin and Isorhamnetin 3-O-rutinoside were only found in the MeOH extract. Cucurbitane-type triterpenoid aglycones balsaminol D and F were more abundant in the MeOH extract than the H_2O extract by 73 and 85%, respectively. Balsaminol E on the other hand was only found in the MeOH extract (Table 4.3). Cucurbitane-type glycosides balsaminoside B and C were also found only in the MeOH extract as ammonia $[M+NH_4]^+$ adducts, while the sodium $[M+Na]^+$ adduct was found predominantly in the MeOH extract, i.e. it was 79% less abundant in the H_2O extract. On the other hand, the potassium $[M+K]^+$ adducts of balsaminoside B and C were found to be only 30% more abundant in the MeOH extract than the H_2O extract (Table 4.4)

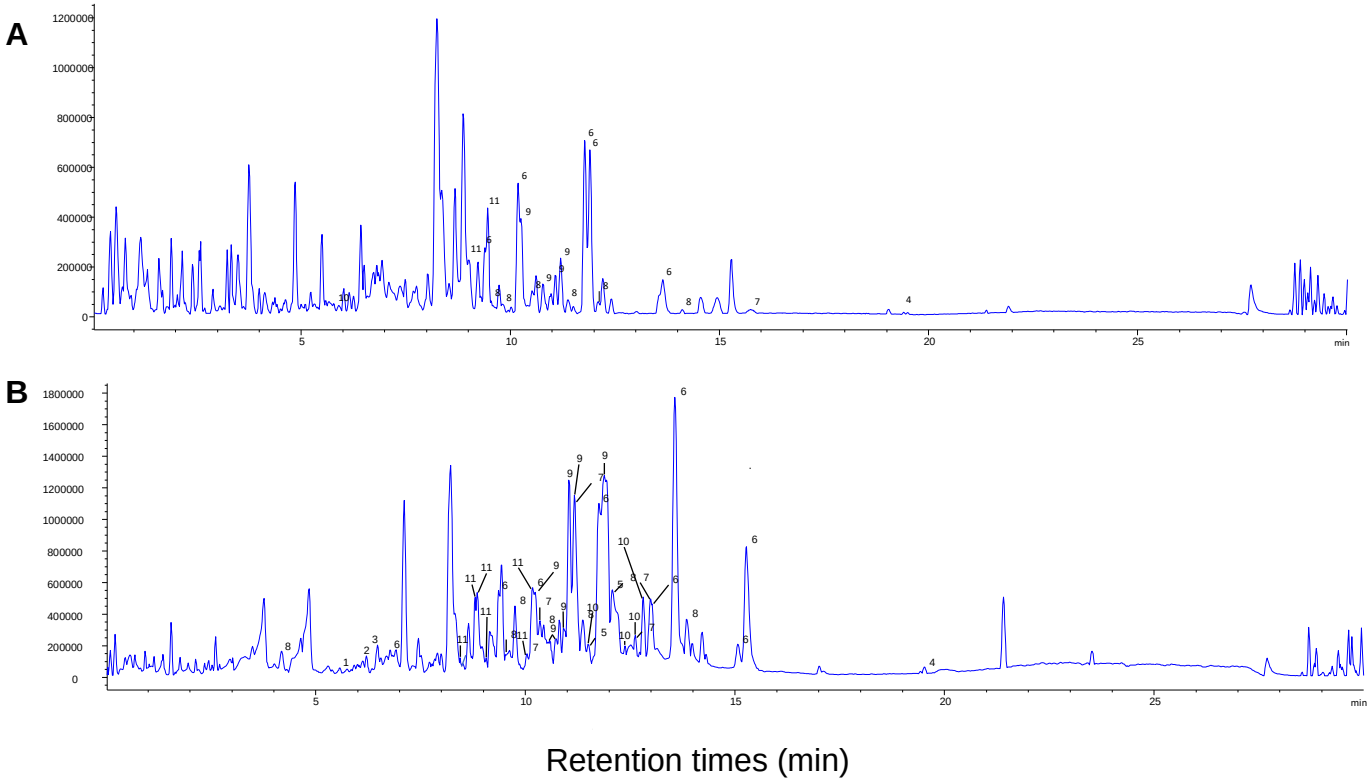

Figure 4.3: Base peak ion chromatograms obtained for the LC/MS analysis of the *M. balsamina* crude H_2O (A) and crude MeOH (B) leaf extracts.

Table 4.2: Identified flavonol glycosides in the H_2O and MeOH extracts of *M. balsamina* using LC/MS

Compound name (no)	Molecular formula	$[M+H]^+$	MeOH extract		H_2O extract	
			Retention time (min)	(%)	Retention time (min)	(%)
Quercetin 3-O-rutinoside (Rutin) (**1**)	$C_{27}H_{30}O_{16}$	611.2	5.54	100	-	0
Kaempferol 3-O-rutinoside (Nicotiflorin) (**2**)	$C_{27}H_{31}O_{15}$	595.2	6.00	100	-	0
Isorhamnetin 3-O-rutinoside (**3**)	$C_{28}H_{33}O_{16}$	625.2	6.12	100	-	0

Table 4.3: Identified cucurbitane-type triterpenoid aglycones in the H_2O and MeOH extracts of *M. balsamina* using LC/MS

Compound no. (Name)	Molecular formula	$[M+H-H_2O]^+$	MeOH extract		H_2O	
			Retention time(s) (min)	(%)	Retention time (min)	(%)
Balsaminol D (**4**)	$C_{27}H_{42}O_4$	413.3010	19.52	100	19.50	27
Balsaminol E, Karavilagenin E (**5**)	$C_{30}H_{48}O_3$	439.3555	11.50, 12.00	100	-	0
Balsaminagenin C, Balsaminol F (**6**)	$C_{30}H_{50}O_3$	*441.3719	7.99, 9.36, 10.16, 11.79, 12.99, 13.57, 15.07, 15.27	100	9.38, 10.18, 11.78, 11.90, 13.59	15
Balsaminagenin A, Cucurbalsaminol A, Balsaminol A (**7**)	$C_{30}H_{50}O_4$	457.3670	10.04, 10.35, 11.21, 12.65, 12.98	100	10.13, 10.40, 15.86	5
Compound **8**	$C_{31}H_{50}O_4$	486.3709	4.08, 9.51, 9.78, 10.49, 11.35, 12.07, 13.85	100	9.54, 9.82, 10.52, 11.37, 12.10, 13.36, 13.88, 14.16	<1

* Predominate ionic species detected for compound **6** is *m/z* 423 $[M+H-2H_2O]^+$

Table 4.4: Identified cucurbitane-type triterpenoids glycosides in the H_2O and MeOH extracts of *M. balsamina* using LC/MS

Compound no. (Name)	Molecular formula	$[M+NH_4]^+$	MeOH extract		H_2O extract		$[M+Na]^+$	MeOH extract		H_2O extract		$[M+K]^+$	MeOH extract		H_2O extract	
			Retention time (min)	%	Retention time (min)	%		Retention time (min)	%	Retention time (min)	%		Retention time (min)	%	Retention time (min)	%
Compound **9** (Balsaminoside B and C)	$C_{36}H_{60}O_8$	638.4632	15.19	100	-	0	643.4183	10.25, 10.62, 10.75, 10.89, 11.05, 11.17, 11.88	100	10.28, 10.79, 11.08, 11.20, 11.78, 11.90	21	659.3943	9.62,10.81, 11.91, 13.99	100	8.99, 9.28, 9.59, 9.90, 10.07, 10.16, 10.29, 10.50, 10.85, 11.20, 11.78, 11.91	16
Compound **10** (Balsaminoside A and Kuguaglycoside A)	$C_{37}H_{62}O_8$	652.4774	-	0	-	0	657.4243	11.44, 12.40, 12.62, 12.81	100	5,989, 10,508, 10,713, 11,198	<1	673.4089	11.44, 12.62, 12.81, 14.50, 14.70	100	10.92, 12.05	9
Compound **11** (Momordicoside D)	$C_{42}H_{70}O_{13}$	800.5133	-	0	-	0	805.4694	8.46, 8.78, 8.88, 9.07, 10.02, 10.17,	100	9.10, 9.46, 10.19	61	821.4448	7.73, 7.91, 8.13, 8.53, 8.94, 9.40, 9.49, 9.60, 9.80, 10.18	100	7.77, 7.95, 8.56, 8.83, 8.98, 9.43, 9.81, 10.19, 18.98	70

4.2 Anticancer activity

4.2.1 Cytotoxicity on HT-29 and C2C12 cells

The MTT assay showed that there was no significant reduction in the viability of HT-29 cells treated with the H_2O extract at 24 and 72 hours of treatment. On the other hand, treatment with the MeOH extract at 24 hours resulted in a significant ($p \leq 0.0001$) reduction in HT-29 cell viability from concentrations of 200 µg/ml and an IC_{50} of 267.4 ± 7.4 µg/ml. At 72 hours, the MeOH extract further significantly reduced HT-29 cell viability at concentrations from 50 µg/ml with an IC_{50} of 151.1 ± 5.3 µg/ml. Treatment with 5-FU resulted in a significant reduction in cell viability only at 72 hours of treatment at concentrations from 0.1 µg/ml with an IC_{50} of 3.2 ± 0.3 µg/ml (Figure 4.4). Furthermore, at 24 hours (Figure 4.5A) and 72 (Figure 4.5C), when the cells were treated with the H_2O extract at concentrations ranging from 250 to 2000 µg/ml combined with the 5-FU IC_{50} (3.2 µg/ml) obtained from the 72h treatment of HT-29 cells, there was no significant change in cell viability observed when compared to the cells treated with only 3.2 µg/ml of 5-FU. The 5-FU-MeOH extract treatment at concentrations ranging from 0.001 to 100 µg/ml of 5-FU combined with the MeOH extract IC_{50} (267.4 µg/ml) obtained from the 24 hours treatment of the HT-29 cells, only showed a significant ($p \leq 0.0001$) increase in cell viability at 100 µg/ml at 24 hours (Figure 4.5B) of treatment when compared to the cells treated with only 267 µg/ml of the MeOH extract. At 72 hours (Figure 4.5D), however, there was no significant change in cell viability when compared to the cells treated with only the MeOH extract IC_{50} (151.1 µg/ml) obtained from the 72 hours treatment of HT-29 cells (Figure 4.5). Moreover, treatment of the C2C12 cells with the H_2O extract showed a significant reduction in cell viability with concentrations from 1000 µg/ml at 24 hours of treatment ($p \leq 0.0001$) and 500 µg/ml a 72 hours of treatment ($p \leq 0.01$), although the cells still maintained viability of above 80%. The MeOH extract led to a significant ($p \leq 0.05$) decrease in cell viability only at 300 µg/ml at 24 hours of treatment and at concentrations from 100 µg/ml at 72 hours ($p \leq 0.001$). Treatment with 5-FU showed a significant ($p \leq 0.0001$) reduction in thel viability of C2C12 muscle cells with concentrations from 1 µg/ml at 24 hours of treatment and 0.01 µg/ml at 72 hours of treatment ($p \leq 0.01$) (Figure 4.6) Moreover, the IC_{50} of the MeOH extract on HT-29 cells was shown to be far less toxic to the C2C12 cells when compared to the HT-29 cells as the cells maintained viability of above 70%.

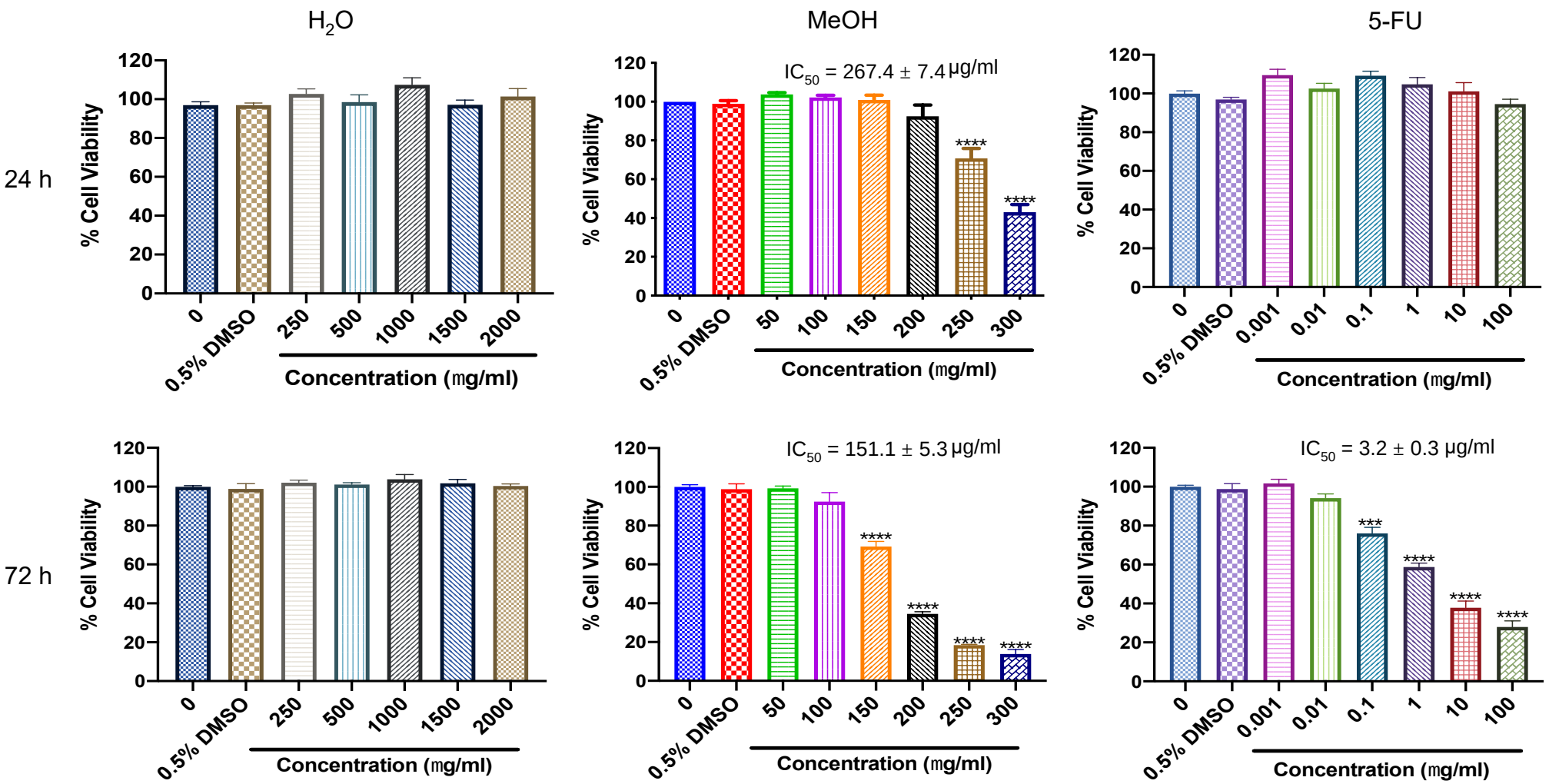

Figure 4.4*:* Effect of the *M. balsamina* extracts or 5-Fluorouracil on the viability of HT-29 colon cancer cells.

Cells were treated with various concentrations of the extracts, 5-Fluorouracil or 0.5% DMSO as the vehicle control for 24 and 72 hours. Effect on cell via viability was determined using the MTT assay. Each data point represents the mean ± S.E.M of three independent experiments, performed in sextuplicate. *** $p \leq 0.001$ and **** $p \leq 0.0001$ indicate significant differences to the DMSO control cells .

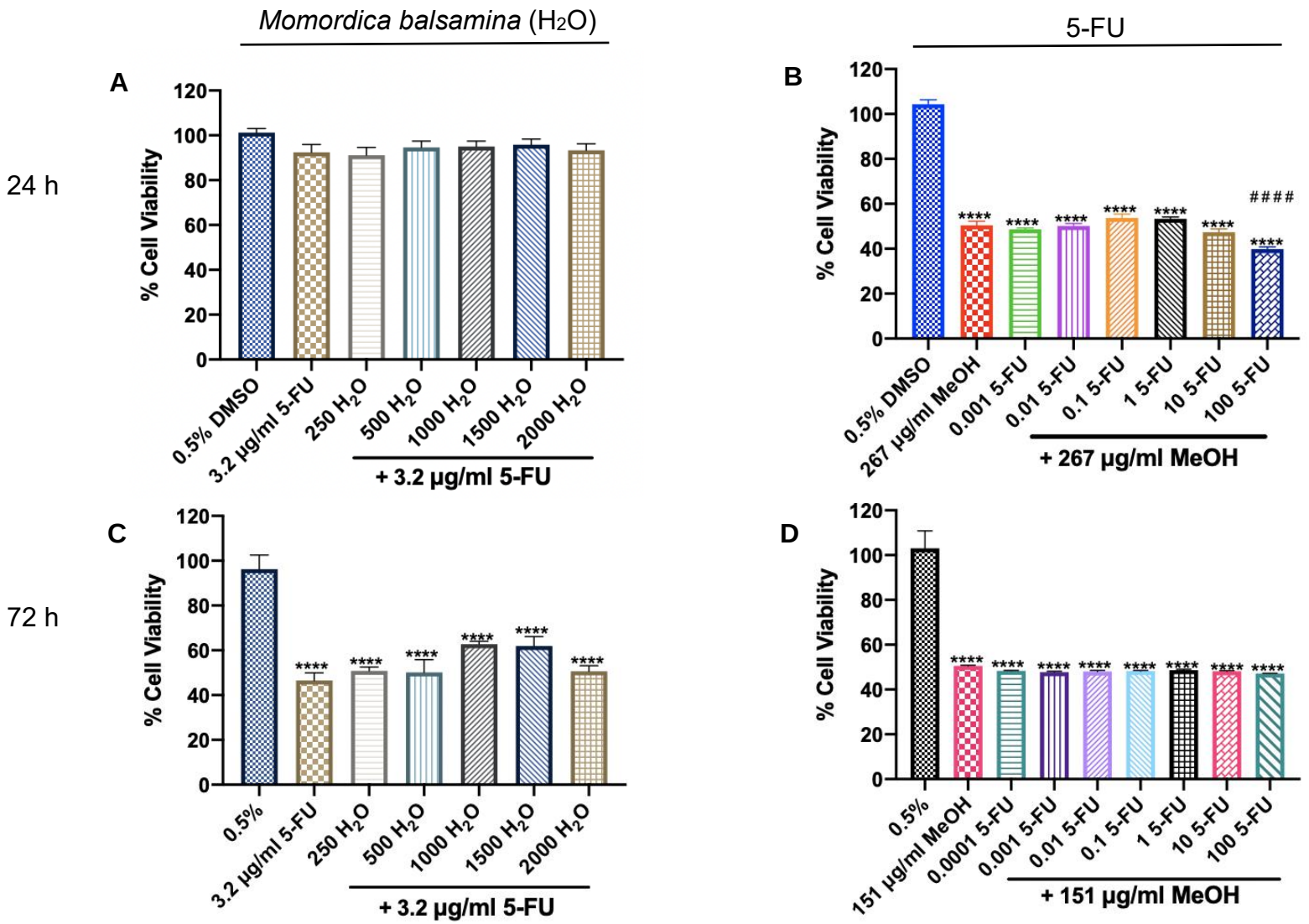

Figure 4.5: Effect of the *M. balsamina* extracts on the efficacy of 5-Fluorouracil on the viability of HT-29 colon cancer cells.

Cells were treated with 0.5% DMSO as the vehicle control or 250 – 2000 µg/ml of the H_2O extract and 3.2 µg/ml of 5-FU (A and C) or 0.001 – 100 µg/ml of 5-FU and 267 µg/ml (B) or 151 µg/ml of the MeOH extract (D) for 24 and 72 hours. Effect on cell viability was determined using the MTT assay. Each data point represents the S.E.M of two independent experiments, performed with six replicates. **** $p \leq 0.0001$ indicates a significant difference to the DMSO control cells, # # # # $p \leq 0.0001$ indicates a significant difference to the 267 µg/ml MeOH treated cells.

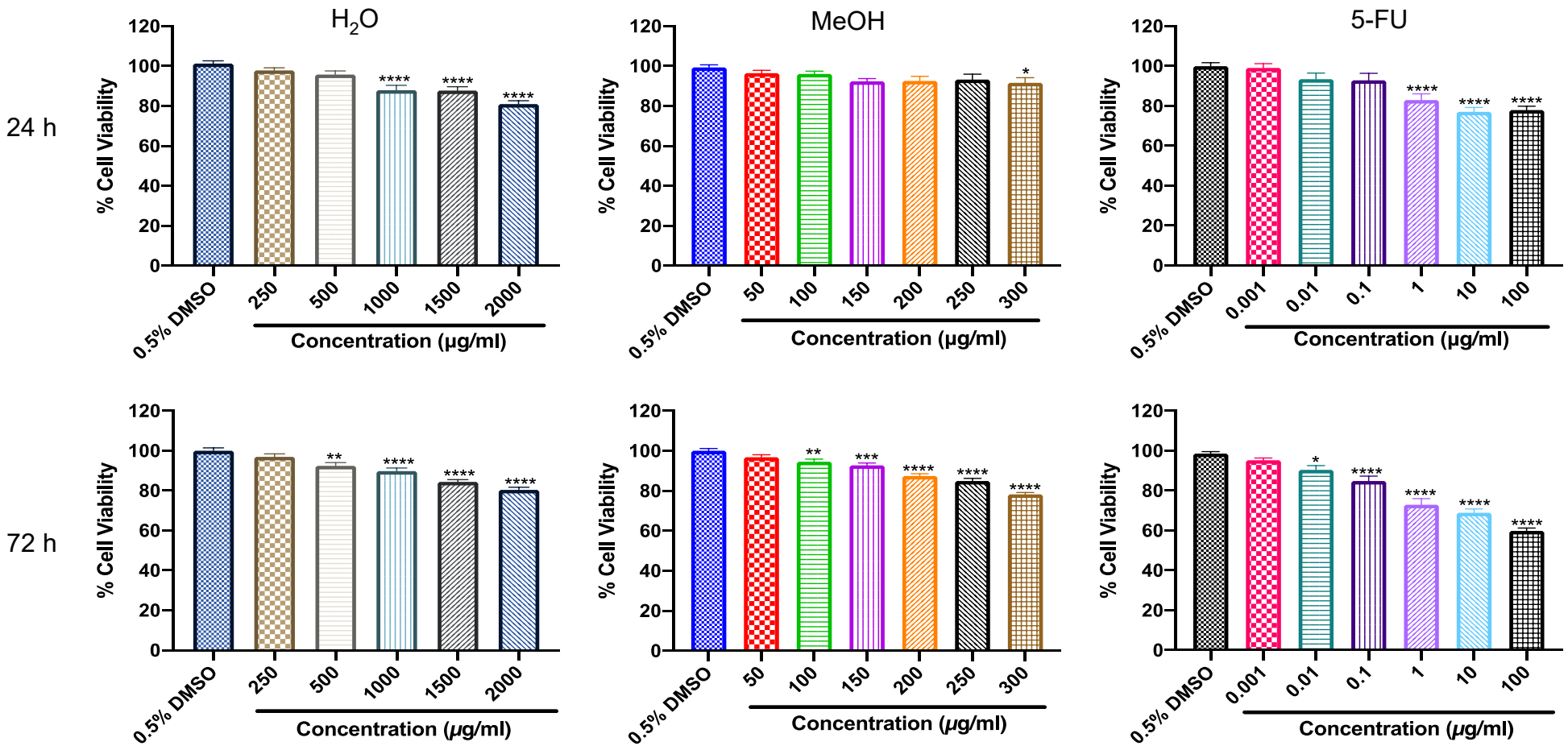

Figure 4.6: Effect of the *M. balsamina* extracts or 5-Fluorouracil on the viability of C2C12 muscle cells.

Cells were treated with various concentrations of the extracts, or 5-Fluorouracil or 0.5% DMSO as the vehicle control for 24 and 72 hours. Effect on cell viability was determined using the MTT assay. Each data point represents the mean ± S.E.M of three independent experiments with 6 replicates each. *p ≤ 0.05, ** p ≤ 0.01, *** p ≤ 0.001 and **** p ≤ 0.0001 indicate significant differences to the control cells treated with 0.5% DMSO.

4.2.2 Genotoxicity on C2C12 cells

HT-29 cells treated with the IC_{50} (267 µg/ml) of the MeOH extract served as a positive control. The results showed that there was little to no change in the activation of H2A histone family member X (H2A.X) or H2A.X-ataxia telangiectasia mutated kinase (ATM) in C2C12 muscle cells treated with the MeOH extract or 5-FU. Furthermore, ATM activity was slightly increased with the MeOH extract treatment as well as 5-FU, however, this increase was not significant. In contrast, treatment with 200 µM of curcumin as well as HT-29 cells treated with 267 µg/ml of the MeOH extract showed a significant ($p \leq 0.01$) increase in ATM expression. Treatment with curcumin further showed a significant ($p \leq 0.01$) increase in H2A.X/ATM activation in the HT-29 cells (Figure 4.7).

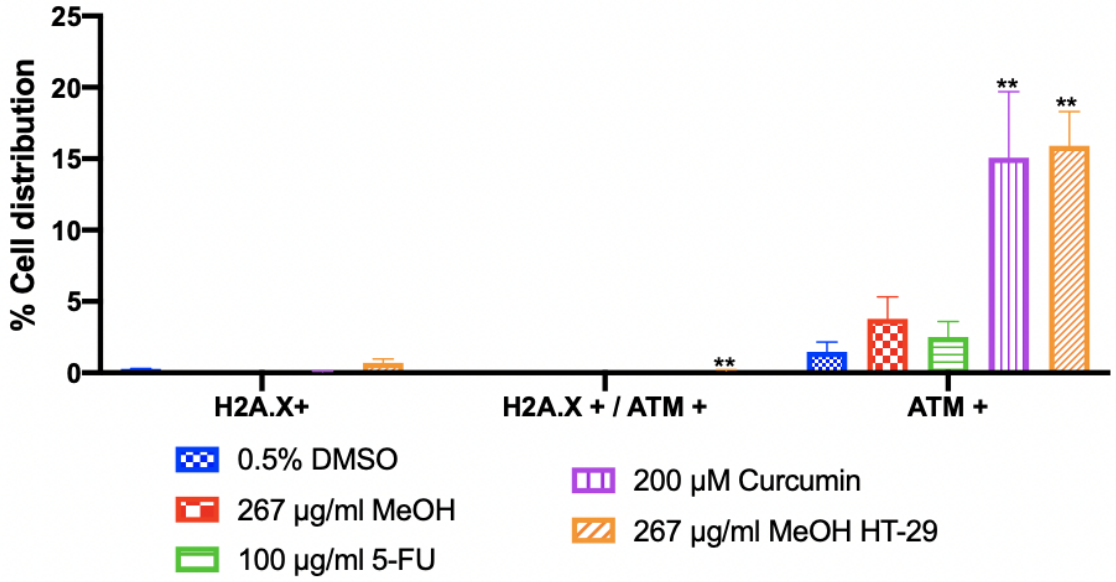

Figure 4.7: Effect of the *M. balsamina* methanol extract or 5-Fluorouracil on C2C12 muscle cell genotoxicity.

Cells were treated with 267 µg/ml of the MeOH extract or 100 µg/ml of 5-Fluorouracil or 0.5% DMSO as the vehicle control for 24 hours. Effect on genotoxicity was determined using the Muse™ Multi-Colour DNA Damage Kit. Each data point represents the mean ± S.E.M of two independent experiments, performed in duplicate. ** $p \leq 0.01$ indicates a significant difference to the vehicle control cells.

4.2.3 Oxidative stress

4.2.3.1 Intracellular reactive oxygen species

The 2',7' dichlorodihydrofluorescein diacetate (DCFH-DA) assay showed that treatment with 100 µg/ml of the MeOH extract resulted in the lowest intracellular ROS levels when compared to the other treatments. A significant increase, however, was observed in cells treated with 267 µg/ml of the MeOH extract ($p \leq 0.0001$), 5-FU ($p \leq 0.0001$) and 200 µM of curcumin ($p \leq 0.01$). The MeOH extract at 267 µg/ml induced the highest level of oxidative stress, which was 8% higher than the 10 µg/ml 5-FU treatment (Figure 4.8B). Representative histograms are shown in Figure 4.8A.

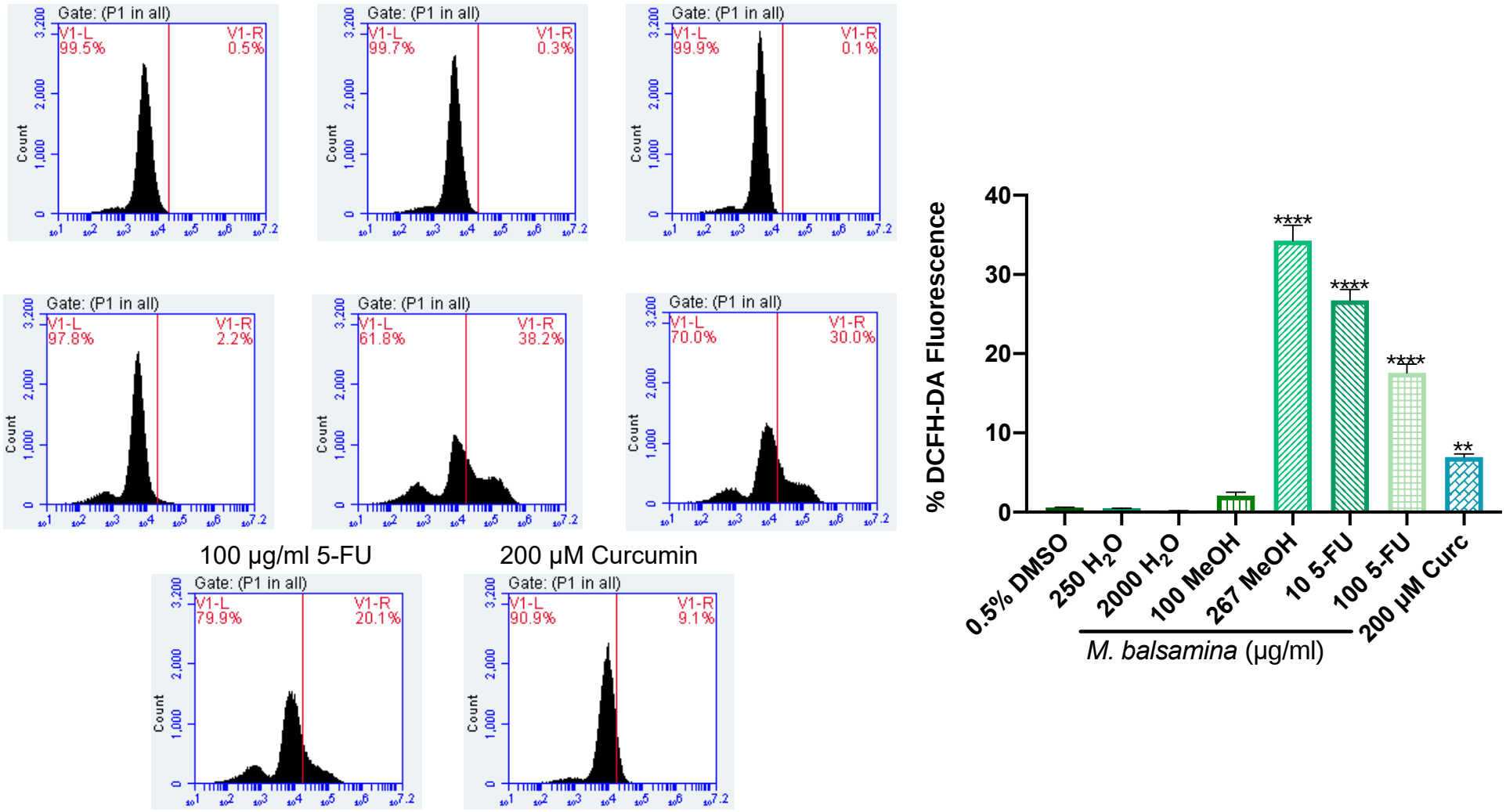

Figure 4.8: Effect of the *M. balsamina* extracts or 5-Fluorouracil on intracellular ROS levels in HT-29 colon cancer cells.

Cells were treated with various concentrations of the extracts, 5-Fluorouracil or 0.5% DMSO as the vehicle control for 24 hours. Effect on intracellular ROS levels was determined using H_2DCFDA. Each histogram is a representative of three independent experimental repeats, performed in duplicate (A). Each data point represents the mean ± S.E.M of three independent experiments, performed in duplicate (B). ** $p \leq 0.01$, and **** $p \leq 0.0001$ indicate significant differences to the vehicle control cells.

3.2.3.2 ROS regulating proteins

The expression of heme-oxygenase 1 (HO-1) protein was significantly upregulated following treatment with 267 µg/ml of the MeOH extract ($p \leq 0.01$) and 200 µM of curcumin ($p \leq 0.05$). The HO-1 levels increased by 48% in the MeOH extract-treated cells and 38% in the 5-FU treatment when compared to control cells treated with 0.5% DMSO. Furthermore, paraoxonase 2 (PON2) protein expression level was significantly downregulated by 30% following treatment with the MeOH extract ($p \leq 0.01$), by 24% and 42% following treatment with 5-FU ($p \leq 0.05$) and 200 µM of curcumin ($p \leq 0.0001$), respectively, when compared to the DMSO-treated control cells. On the other hand, Catalase protein expression levels were only significantly ($p \leq 0.0001$) upregulated upon treatment with 200 µM of curcumin, while treatment with the MeOH extract resulted in a slight, but non-significant downregulation of Catalase protein expression. Conversely, treatment with 5-FU resulted in a slight, non-significant upregulation of Catalase protein expression (Figure 4.9).

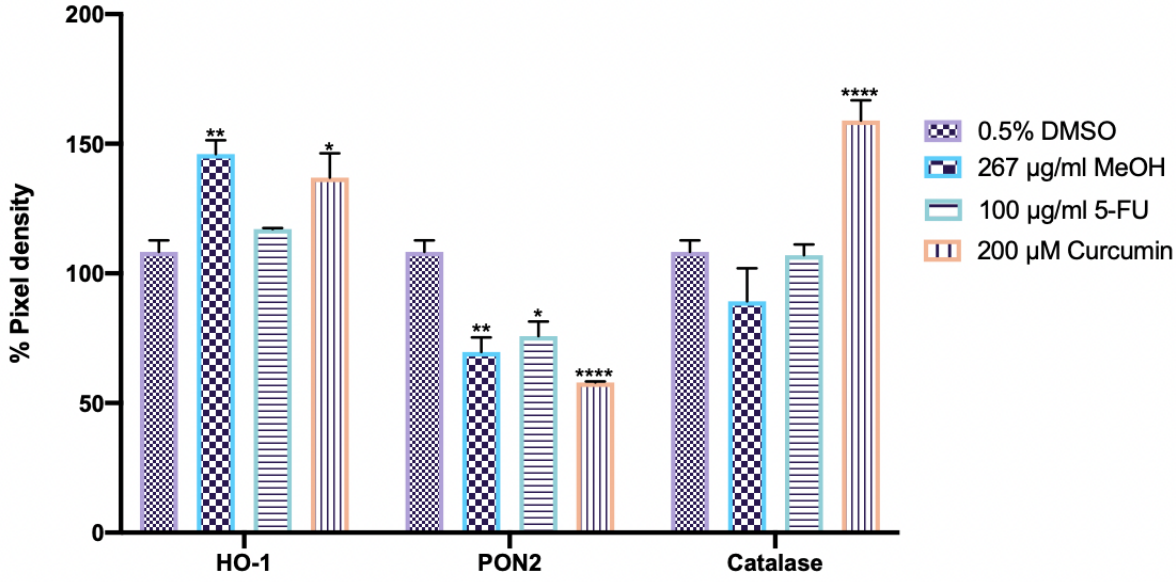

Figure 4.9: Effect of the *M. balsamina* methanol extract or 5-Fluorouracil on ROS regulating proteins.

HT-29 cells were treated with 267 µg/ml of the methanol extract,100 µg/ml of 5-Fluorouracil or 0.5% DMSO as the vehicle control for 24 hours. Effect on ROS regulating proteins was determined using the proteome profiler array. Each data point represents the mean ± S.E.M of three independent experiments, performed in duplicate. *$p \leq 0.05$, ** $p \leq 0.01$ and **** $p \leq 0.0001$ indicate significant differences to the vehicle control cells.

4.2.4 Effect of *M. balsamina* extracts or 5-FU on apoptosis of HT-29 cells

4.2.4.1 Mitochondrial membrane potential

The 5,5′,6,6′-tetrachloro-1,1′,3,3′-tetraethylbenzimidazolylcarbocyanine iodide (JC-1) staining assay showed that the cells maintained a high mitochondrial membrane potential upon treatment with the H_2O extract, 100 µg/ml of the MeOH extract and 100 µg/ml of 5-FU. However, treatment with 267 µg/ml of the MeOH extract, 10 µg/ml of 5-FU and 200 µM of curcumin resulted in a reduction in the mitochondrial membrane potential of the cells, which was evident by the increase in green fluorescence when compared to the DMSO-treated control cells (Figure 4.10A). Intensity analysis of the red fluorescence depicting healthy mitochondria was shown to decrease significantly in cells treated with 267 µg/ml of the MeOH extract ($p \leq 0.0001$), 10 µg/ml of 5-FU ($p \leq 0.05$) and 200 µM of curcumin ($p \leq 0.001$) (Figure 4.10B).

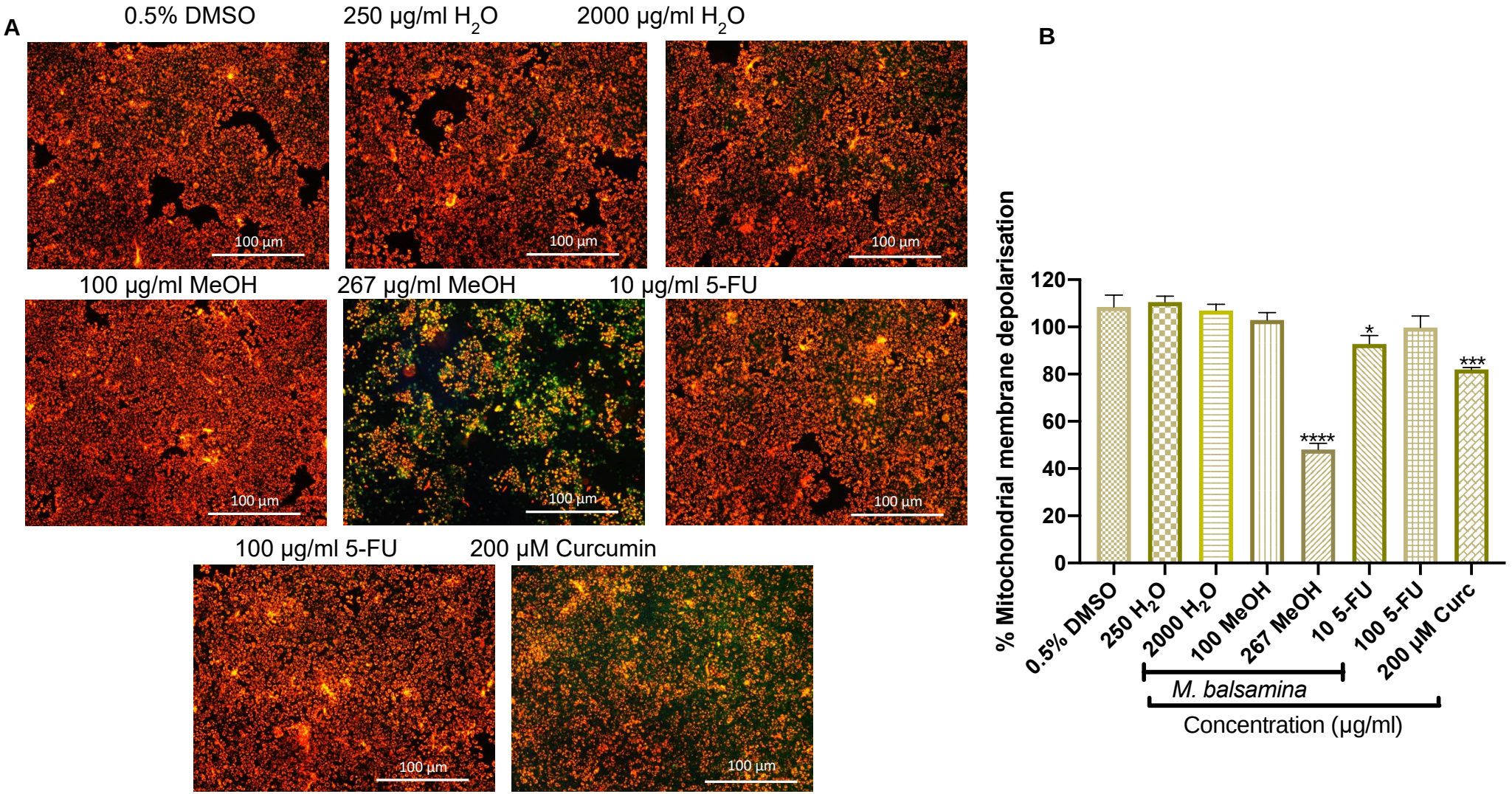

Figure 4.10: Effect of the *M. balsamina* extracts or 5-Fluorouracil on mitochondrial function of HT-29 colon cancer cells.

Cells were treated with various concentrations of the extracts, 5-Fluorouracil or 0.5% DMSO as the vehicle control for 24 hours. Effect of on mitochondrial function was determined using JC-1. Cells were viewed and photographed under a fluorescent microscope (10X). Each image is a representative of three independent experimental repeats (A). Each data point represents the mean ± S.E.M of three independent experimental repeats, performed in duplicate (B). * $p \leq 0.05$, *** $p \leq 0.001$ and **** $p \leq 0.0001$ indicate significant differences to the vehicle control cells.

4.2.4.2 Effect of *M. balsamina* extracts or 5-FU on nuclear morphology of HT-29 cells

Nuclear morphological changes in cells treated with the *M. balsamina* H_2O, MeOH extracts or 5-FU-treated HT-29 cells were assessed using the acridine orange and propidium iodide (AO/PI) dual staining assay. The results showed an increase in orange/red fluorescence in MeOH extract, 5-FU or curcumin-treated cells when compared to the control cells treated with 0.5% DMSO (Figure 4.11A). Moreover, chromatin condensation was observed to a greater degree in the 267 µg/ml MeOH extract-treated cells seen by the bright green fluorescence as a result of AO intercalating the compact or condensed chromatin (Figure 4.11A). The orange/red fluorescent cell count showed a significant increase in cells treated with 100 µg/ml ($p \leq 0.001$) and 267 µg/ml ($p \leq 0.0001$) of the MeOH extract, 10 µg/ml ($p \leq 0.001$) and 100 µg/ml ($p \leq 0.0001$) of 5-FU as well as 200 µM of curcumin ($p \leq 0.001$). Treatments with the higher doses of 267 µg/ml of the MeOH extract and100 µg/ml of 5-FU were the more effective, showing an increase of 19% and 16%, respectively, of the orange/red fluorescent cells, when compared to the DMSO-treated control cells (Figure 4.11B).

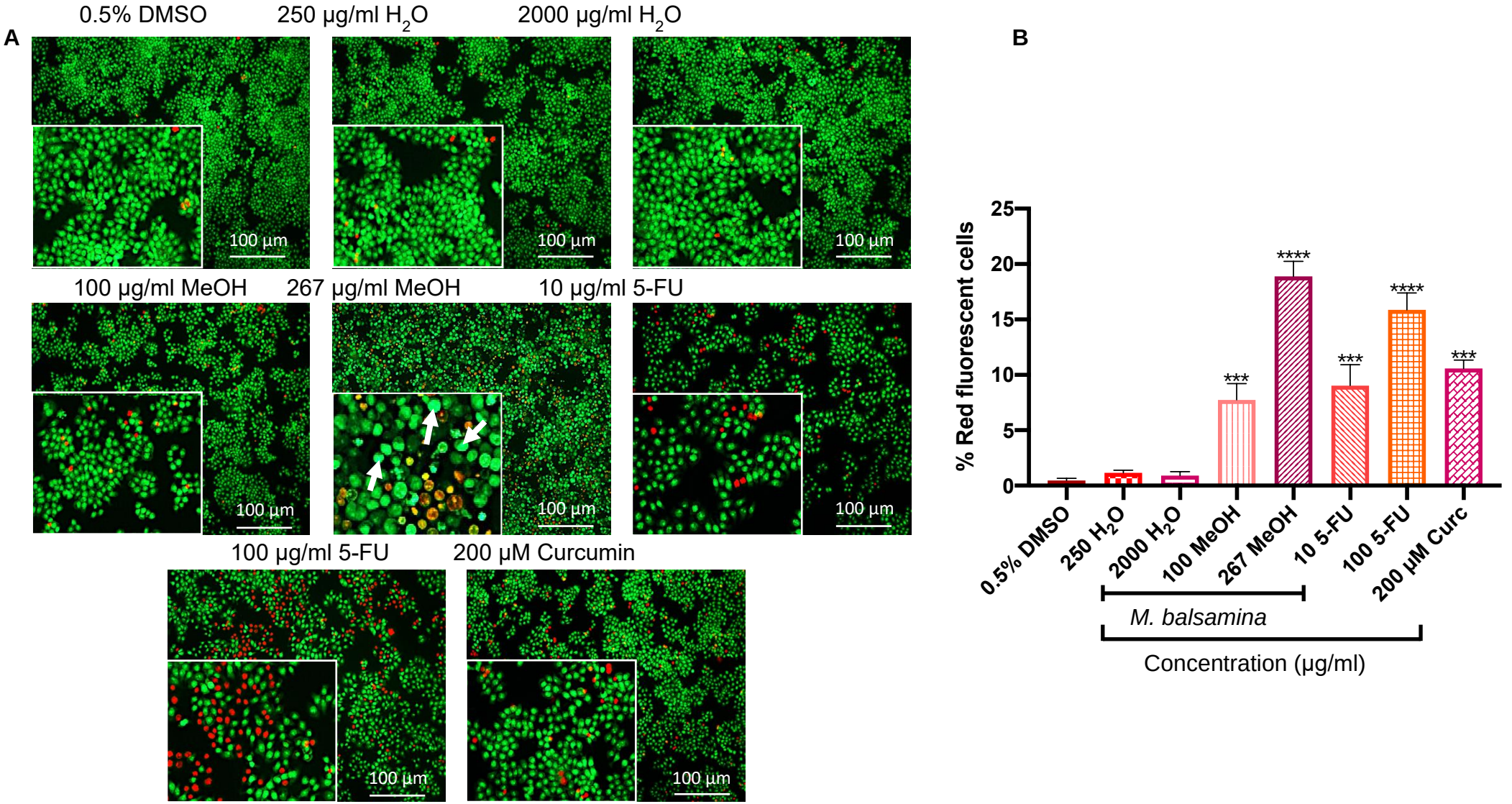

Figure 4.11: Effect of the *M. balsamina* extracts or 5-Fluorouracil on nuclear morphology of HT-29 colon cancer cells.

Cells were treated with various concentrations of the extracts, 5-Fluorouracil or 0.5% DMSO as the vehicle control for 24 hours. Effect of the extract on cell nucleic content was determined using acridine orange and propidium iodide. Each image is a representative of three independent experimental repeats (A). Cells were viewed and photographed under a fluorescent microscope (10X). Each data point represents the mean ± S.E.M of three independent experimental repeats, performed in duplicate. ** $p \leq 0.01$, *** $p \leq 0.001$ and **** $p \leq 0.0001$ indicate significant differences to the vehicle control (B).

4.2.4.3 Assessment and quantification of apoptosis in HT-29 cells

A significant increase in cells stained only with annexin-V (quadrant 3; Apoptotic; Annexin-V^+, PI^-), depicting early apoptosis was observed with 267 µg/ml of the MeOH extract treatment ($p \leq 0.01$). However, treatment with the H_2O extract, the lower concentration (100 µg/ml) of the MeOH extract and 5-FU showed no significant change in the percentage of cells undergoing early stages of apoptosis when compared to the control cells treated with 0.5% DMSO. Treatment with 267 µg/ml of the MeOH extract further showed a significant ($p \leq 0.0001$) increase in cells stained positive for both annexin-V and PI (quadrant 4; Dead; Annexin-V^+ and PI^+), depicting late stages of apoptosis. Treatment with curcumin, on the other hand, showed no significant change in cell population across all quadrants when compared to the DMSO-treated control cells (Figure 4.12A and B).

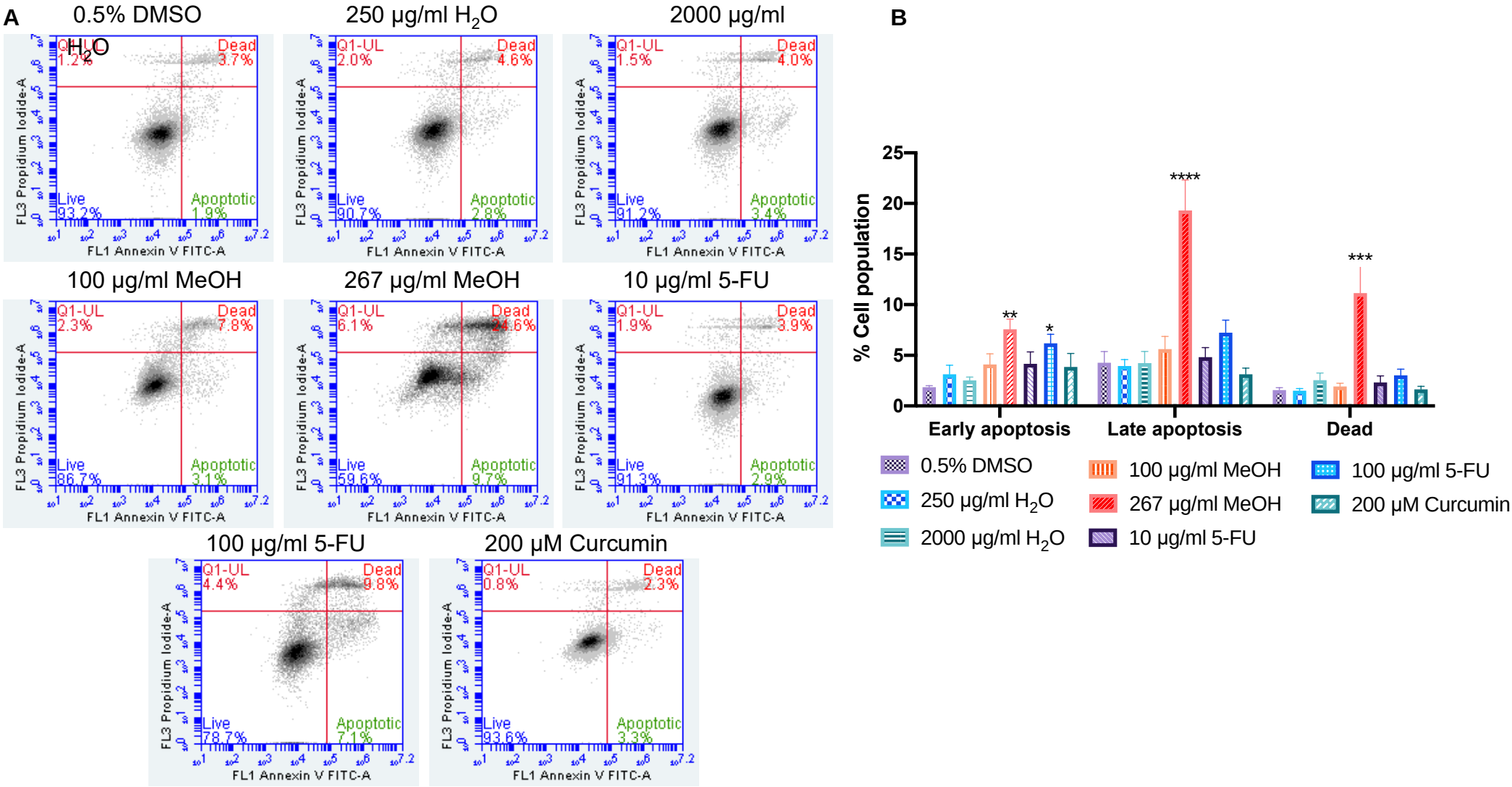

Figure 4.12: Assessment and quantitation of apoptosis in *M. balsamina* extracts or 5-Fluorouracil-treated HT-29 colon cancer cell.

Cells were treated with various concentrations of the extracts, 5-Fluorouracil or 0.5% DMSO as the vehicle control for 24 hours. Assessment and quantitation of apoptosis was determined by flow cytometry using Annexin-V/PI. Each image is a representative of three experimental repeats (A). Each data point represents the mean ± S.E.M of three independent experiments, performed in duplicate (B). *p ≤ 0.05, **p ≤ 0.01, **** p ≤ 0.0001 indicate significant differences to the vehicle control cells.

4.2.4.4 Caspase-3 protein expression and activation in HT-29 cells

There was little to no change observed in the expression level of pro-caspase-3 in all treatments as well as the cleaved caspase-3 of cells treated with 100 µg/ml of 5-FU or 200 µM of curcumin when compared to the control cells treated with 0.5% DMSO. However, treatment with 267 µg/ml of the MeOH extract showed a significant ($p \leq 0.001$) upregulation in the expression level of the active caspase-3, (cleaved caspase-3). The expression of the cleaved caspase-3 in MeOH extract-treated cells was increased by 85% when compared to the DMSO-treated control cells (Figure 4.13).

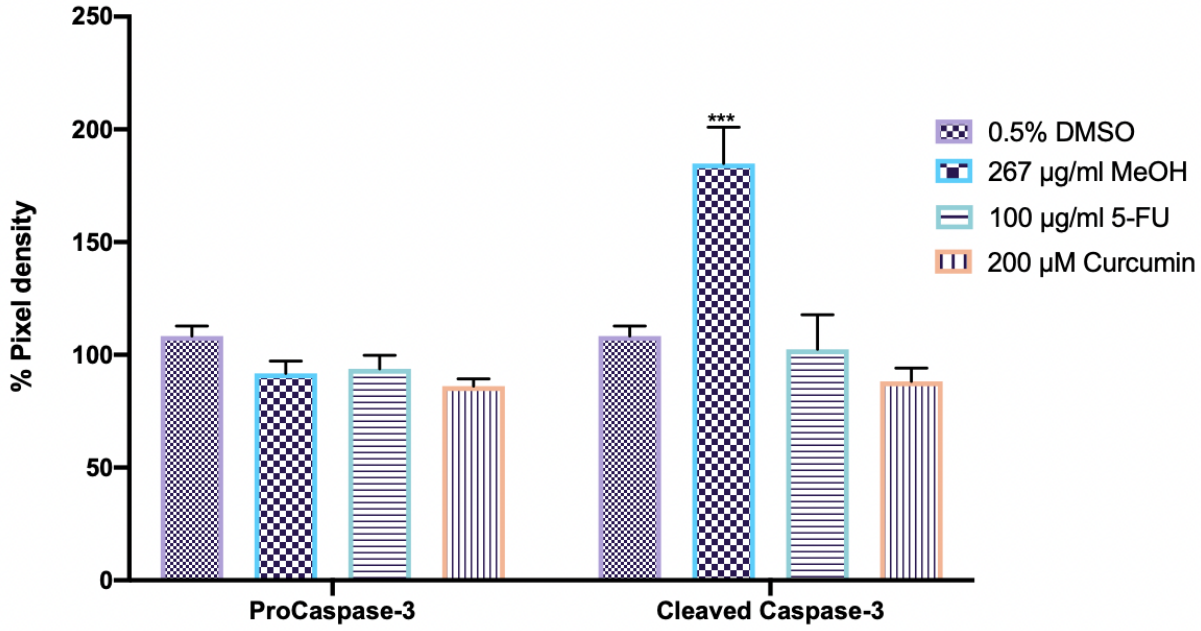

Figure 4.13: Effect of the *M. balsamina* methanol extract or 5-Fluorouracil on caspase-3 expression and cleavage.

Cells were treated with 267 µg/ml of the methanol extract, 100 µg/ml of 5-Fluorouracil or 0.5% DMSO as the vehicle control for 24 hours. Effect on caspase-3 expression was determined using the proteome profiler array. Each data point represents the mean ± S.E.M of three independent experiments, performed in duplicate. *** $p \leq 0.001$ indicates a significant difference to the vehicle control.

4.2.4.5 Activation of apoptosis initiator caspases -8 and -9 in HT-29 cells

Assessment of the activity of the initiator caspases, caspase-8 and -9, showed a significant ($p \leq 0.01$) upregulation of caspase-8 and -9 activity in cells treated with 267 µg/ml of the MeOH extract. This increase was 2.2 fold higher for the activity of caspase-8 and 2.3 fold higher for caspase-9 when compared to the control cells treated with 0.5% DMSO. In 5-FU and curcumin-treated cells, no significant change in caspase-8 or caspase-9 activity was observed when compared to the DMSO-treated control cells (Figure 4.14).

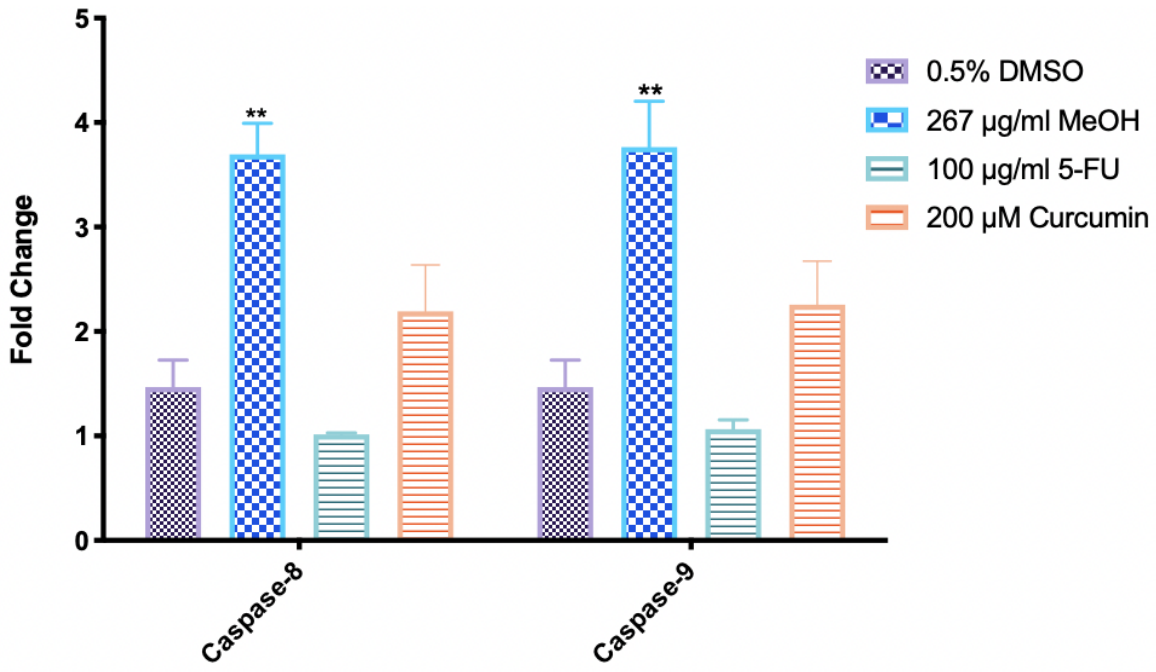

Figure 4.14: Effect of the *M. balsamina* methanol extract or 5-Fluorouracil on the activity of apoptosis initiator caspases-8 and -9.

Cells were treated with 267 µg/ml of the methanol extract, 100 µg/ml of 5-Fluorouracil or 0.5% DMSO as the vehicle control for 24 hours. Assessment of caspase activity was determined spectrophotometrically using the caspase-8 and caspase-9 activity colorimetric assay kits. Each data point represents the mean ± S.E.M of three independent experiments, performed in duplicate. *$p \leq 0.05$ and **** $p \leq 0.0001$ indicate significant differences to the vehicle control cells.

4.2.4.6 Bcl-2 family of proteins expression in HT-29 cells

Treatment with 267 µg/ml of the MeOH extract resulted in a significant downregulation of both pro-apoptosis Bad ($p \leq 0.001$), Bax ($p \leq 0.0001$) and anti-apoptosis and Bcl-2 ($p \leq 0.01$), Bcl-x ($p \leq 0.0001$) proteins. Treatment with 100 µg/ml of 5-FU only led to a significant ($p \leq 0.01$) downregulation of Bax expression. Curcumin significantly downregulated the expression levels of Bad ($p \leq 0.01$), Bax ($p \leq 0.0001$), Bcl-2 ($p \leq 0.01$) and Bcl-x ($p \leq 0.0001$) proteins. Interestingly, the ratio of Bax to Bcl-2 was reduced with all the treatments, suggesting that the anti-apoptotic protein, Bcl-2, showed slightly higher expression levels than the pro-apoptotic protein Bax (Table 4.5).

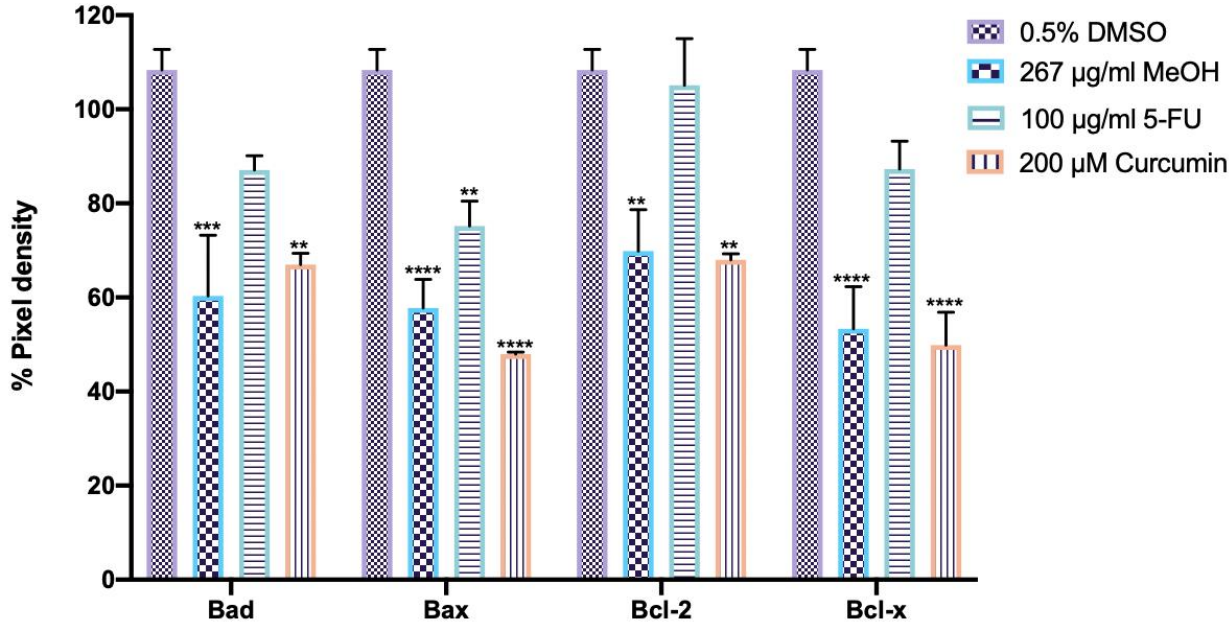

Figure 4.15: Effect of the *M. balsamina* methanol extract or 5-Fluorouracil on the expression levels of Bcl-2 family of proteins.

Cells were treated with 267 µg/ml of the methanol extract, 100 µg/ml of 5-Fluorouracil or 0.5% DMSO as the vehicle control for 24 hours. Effect on expression levels of Bcl-2 family of proteins was determined using the proteome profiler array. Each data point represents the mean ± S.E.M of three independent experiments, performed in duplicate. *** $p \leq 0.01$, *** $p \leq 0.001$ and **** $p \leq 0.0001$ indicate significant differences to the vehicle control cells.

Table 4.5: Ratio of Bax/Bcl-2 protein

	0.5% DMSO	267 µg/ml MeOH	100 µg/ml 5-FU	200 µM curcumin
Bax/Bcl-2	1	0.69 ± 0.09 **	0.72 ± 0.10 **	0.68 ± 0.05 **

4.2.4.7 Release of mitochondrial proteins in HT-29 cells

The presence of mitochondrial proteins in the cytosol of cells treated with the *M. balsamina* MeOH extract or 5-FU was assessed using the proteome profiler array kit. The results showed that treatment with 267 µg/ml of the MeOH extract resulted in a significant decrease in the amount of cytochrome c ($p \leq 0.01$), HTRA2/Omi and SMAC/Diablo ($p \leq 0.0001$). Treatment with 100 µg/ml of 5-FU also showed a significant decrease in the amount of cytochrome c ($p \leq 0.001$), HTRA2/Omi ($p \leq 0.0001$) and SMAC/Diablo ($p \leq 0.0001$) present in the cytosol, while treatment with curcumin resulted in a significant decrease in cytosolic HTRA2/Omi ($p \leq 0.05$) and cytosolic cytochrome c and SMAC/Diablo ($p \leq 0.0001$) (Figure 4.16).

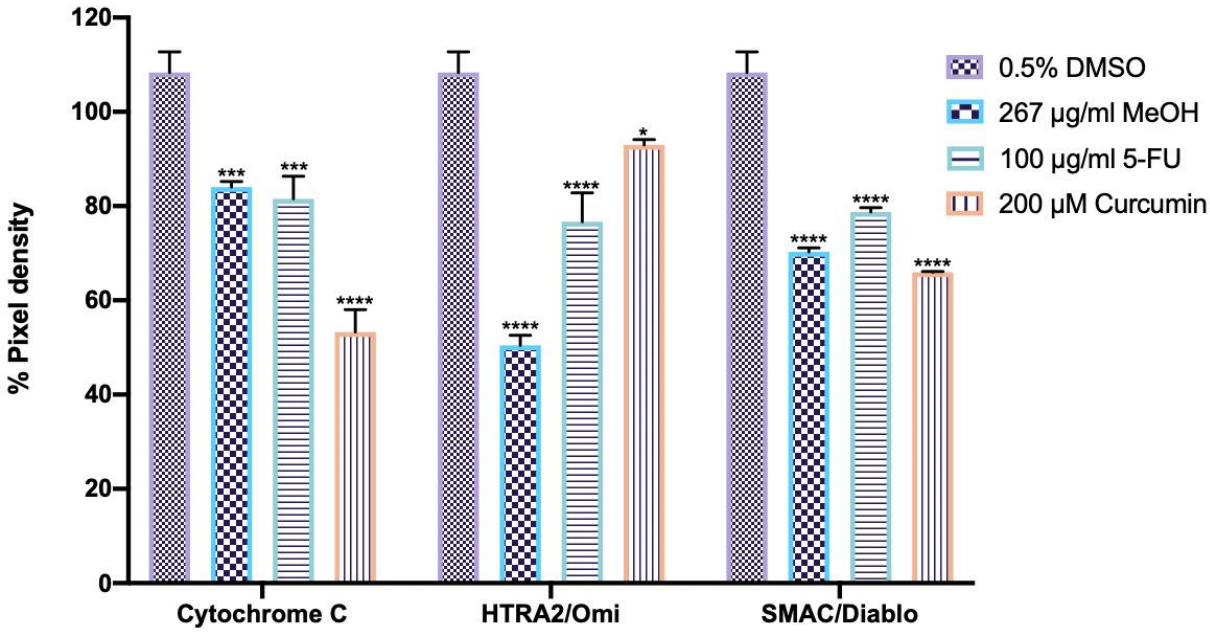

Figure 4.16: Effect of the *M. balsamina* methanol extract or 5-Fluorouracil on the release of mitochondrial proteins into the cytosol.

Cells were treated with 267 µg/ml of the methanol extract, 100 µg/ml of 5-Fluorouracil or 0.5% DMSO as the vehicle control for 24 hours. The amount of mitochondrial proteins in the cytosol was determined using the proteome profiler array. Each data point represents the mean ± S.E.M of three independent experiments, performed in duplicate. * $p \leq 0.05$, ** $p \leq 0.01$, *** $p \leq 0.001$ and **** $p \leq 0.0001$ indicate significant differences to the vehicle control cells.

4.2.4.8 Expression of Bcl-2 protein inhibitors in HT-29 cells

Treatment with 267 µg/ml of the MeOH extract or 100 µg/ml of 5-FU tended to downregulation the expression of the Bcl-2 inhibitor, Hypoxia-inducible factor 1-alpha (HIF-1α). Treatment with 200 µM of curcumin significantly ($p \leq 0.01$) downregulated the expression of HIF-1α. The expression level of the influencer of HIF-1α response, heme-oxygenase-2 (HO-2) was significantly ($p \leq 0.01$) downregulated in cells treated with 5-FU, while the MeOH extract treatment resulted in its upregulation, however, not significant. Furthermore, treatment with curcumin downregulated the expression of HO-2, however, also not significantly (Figure 4.17).

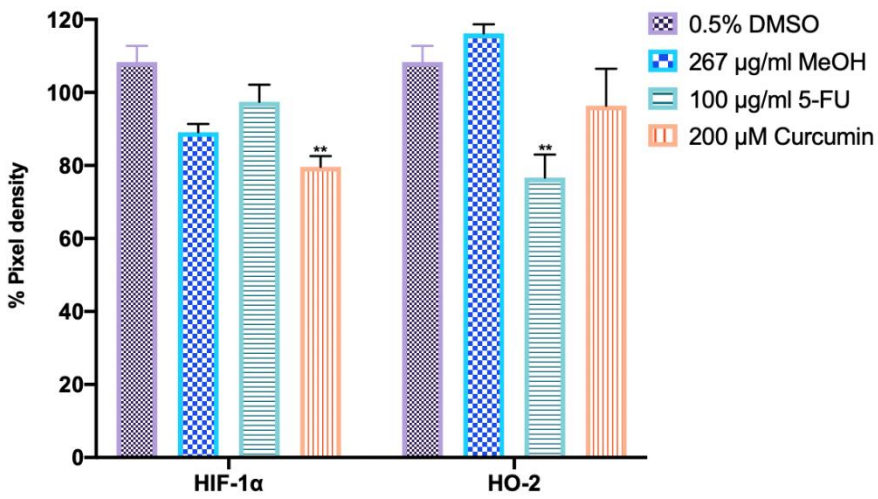

Figure 4.17: Effect of the *M. balsamina* methanol extract or 5-Fluorouracil on Bcl-2 protein inhibitors.

Cells were treated with 267 µg/ml of the methanol extract, 100 µg/ml of 5-Fluorouracil or 0.5% DMSO as the vehicle control for 24 hours. Effect on Bcl-2 protein inhibitors was determined using the proteome profiler array. Each data point represents the mean ± S.E.M of three independent experiments, performed in duplicate. ** $p \leq 0.01$ indicates a significant difference to the vehicle control cells.

Assessment of the protein expression levels of apoptosis extracellular membrane receptors and death domains revealed that treatment with 267 µg/ml of the MeOH extract significantly downregulated the expression levels of Fas ($p \leq 0.0001$), TRAIL R1 ($p \leq 0.0001$), TNF RI ($p \leq 0.0001$) and FADD ($p \leq 0.0001$). However, the expression level of TRAIL R2 was significantly upregulated in cells treated with the MeOH extract ($p \leq 0.0001$). Treatment with 100 µg/ml of 5-FU showed little to no change in the expression level of Fas, TRAIL RI and a significant decrease in FADD ($p \leq 0.05$) and TNF RI ($p \leq 0.0001$) expression. Curcumin significantly downregulated the expression of Fas ($p \leq 0.001$), TNF RI ($p \leq 0.0001$) and FADD ($p \leq 0.001$). TRAIL RI and TRAIL R2 expression levels were also downregulated with curcumin treatment, however, this downregulation was not significant (Figure 4.18).

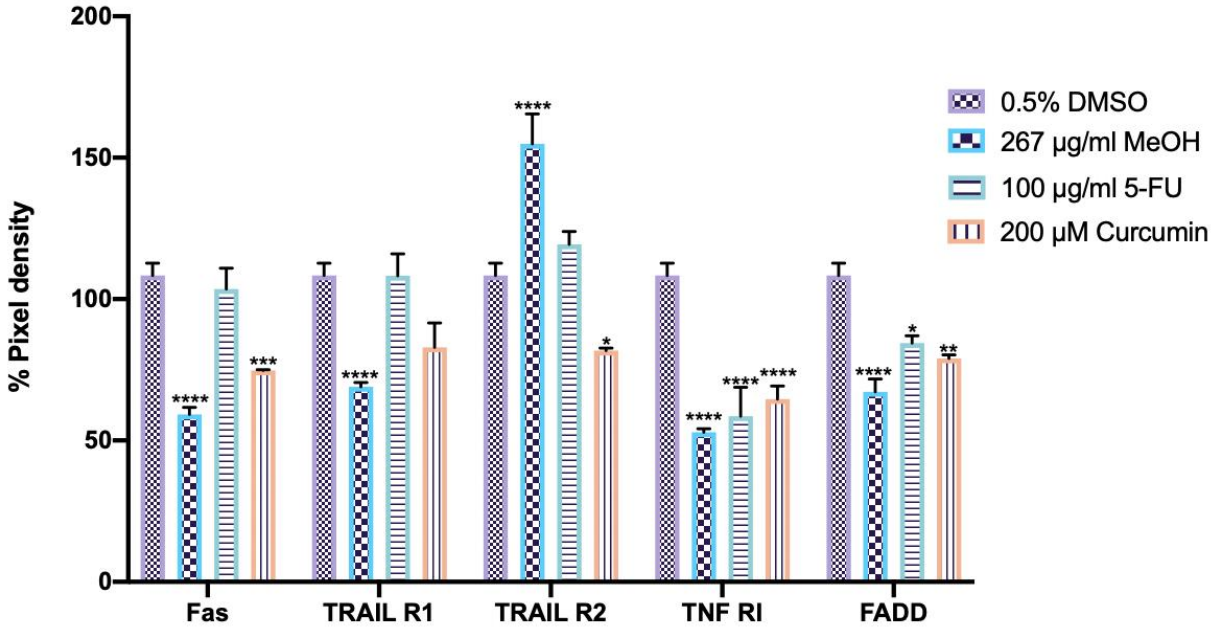

Figure 4.18: **Effect of the *M. balsamina* methanol extract or 5-Fluorouracil on the protein expression levels of apoptosis receptors and death domains.**

Cells were treated with 267 µg/ml of the methanol extract, 100 µg/ml of 5-Fluorouracil or 0.5% DMSO as the vehicle control for 24 hours. Effect on the protein expression levels of apoptosis receptors and death domains was determined using the proteome profiler array. Each data point represents the mean ± S.E.M of three independent experiments, performed in duplicate. * $p \leq 0.05$, ** $p \leq 0.01$, *** $p \leq 0.001$ and **** $p \leq 0.0001$ indicate significant differences to the vehicle control cells.

The protein expression level of apoptosis inhibitor, cIAP-1, was significantly downregulated upon treatment with 267 µg/ml of the MeOH extract ($p \leq 0.05$), 100 µg/ml of 5-FU ($p \leq 0.01$) and 200 µM of curcumin ($p \leq 0.05$). Treatment with 267 µg/ml of the MeOH extract further significantly downregulated the expression levels of Survivin ($p \leq 0.0001$) and XIAP ($p \leq 0.01$). Livin expression level in MeOH-extract treated cells was also downregulated, however, not significantly. Furthermore, the MeOH extract slightly upregulated the expression levels of cIAP-2 and Clusterin. Treatment with 5-FU resulted in the significant ($p \leq 0.05$) downregulation of cIAP-2 and Livin expression levels. The expression of Clusterin and Survivin were also downregulated upon treatment with 5-FU, however not significantly. On the other hand, treatment with curcumin resulted in the significant downregulation of cIAP-1 ($p \leq 0.05$), cIAP-2 ($p \leq 0.05$), Clusterin ($p \leq 0.001$), Survivin ($p \leq 0.0001$), Livin ($p \leq 0.0001$) expression levels, as well as XIAP, although not significantly (Figure 4.19).

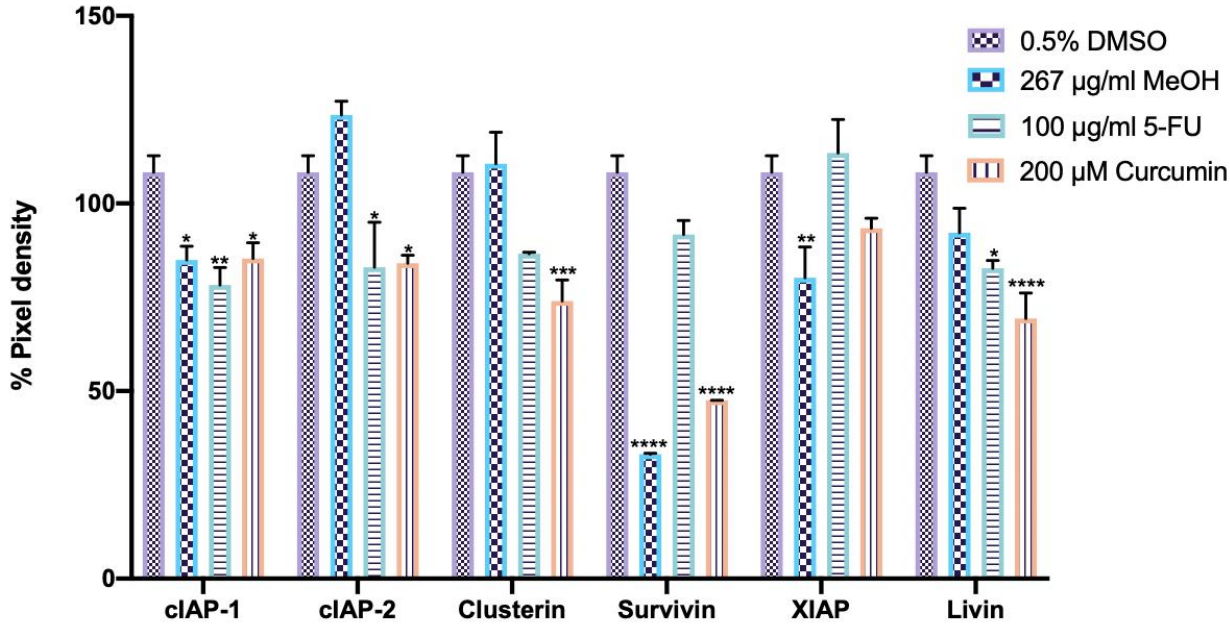

Figure 4.19: Effect of the *M. balsamina* methanol extract or 5-Fluorouracil on the protein expression levels of apoptosis inhibitors.

Cells were treated with 267 µg/ml of the methanol extract, 100 µg/ml of 5-Fluorouracil or 0.5% DMSO as the vehicle control for 24 hours. Effect on the protein expression levels of apoptosis inhibitors was determined using the proteome profiler array. Each data point represents the mean ± S.E.M of three independent experiments, performed in duplicate. * $p \leq 0.05$, ** $p \leq 0.01$, *** $p \leq 0.001$ and **** $p \leq 0.0001$ indicate significant differences to the vehicle control cells.

4.2.4.11 Cell cycle analysis of HT-29 cells

Assessment of the cell cycle of the *M. balsamina* MeOH extract-treated HT-29 cells showed a significant ($p \leq 0.05$) decrease (by 9.2%) in the distribution of cells in the G0/G1 phase and a subsequent significant ($p \leq 0.01$) increase (by 5.3%) in the S phase with at 100 µg/ml. The 267 µg/ml MeOH extract treatment only showed a significant ($p \leq 0.01$) decrease (by 10%) in the G2/M phase (Figure 4.20). Treatment with 10 µg/ml of 5-FU also only showed a significant ($p \leq 0.001$) decrease (by 12.4%) in the G2/M phase, while at 100 µg/ml, there was a significant ($p \leq 0.01$) increase (by 10%) in the S phase and a subsequent significant ($p \leq 0.0001$)decrease (by 16%) in the G2/M phase (Figure 4.21). Moreover, treatment with curcumin showed a significant ($p \leq 0.0001$) decrease (by 20.3%) in the distribution of cells in the G0/G1 phase with a subsequent significant ($p \leq 0.0001$) increase (by 26.9%) in the S phase and a significant ($p \leq 0.0001$) decrease (by 14.4%) in the G2/M phase.

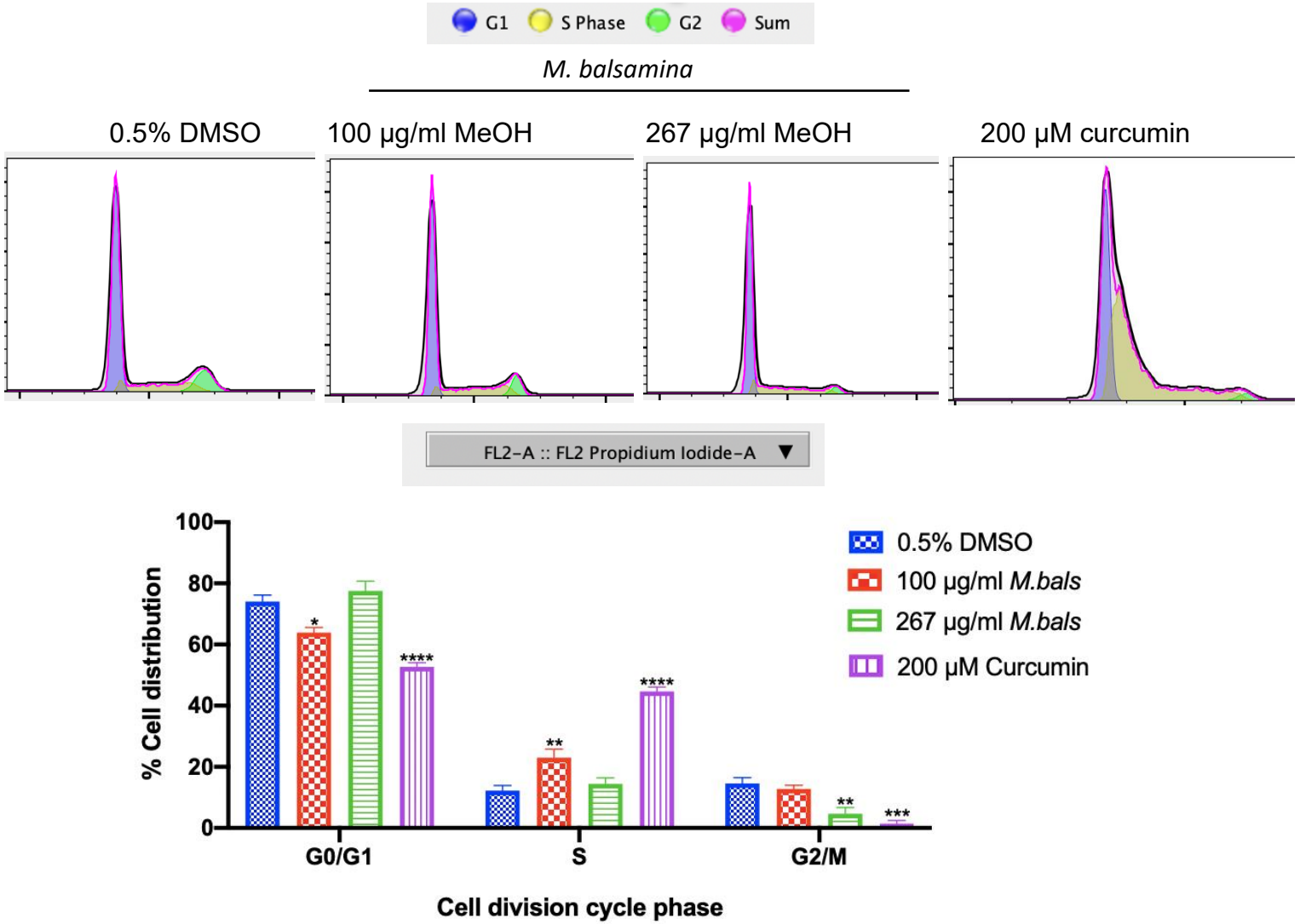

Figure 4.20: Cell cycle distribution of the *M. balsamina* methanol extract treated HT-29 colon cancer cells.

Cells were treated with 100 or 267 µg/ml of the methanol extract or 0.5% DMSO as the vehicle control for 24 hours. Assessment of the cell cycle distribution was determined by flow cytometry using PI. Each data point represents the mean ± S.E.M of three independent experiments, performed in duplicate. * $p \leq 0.05$, ** $p \leq 0.01$, *** $p \leq 0.001$ and **** $p \leq 0.0001$ indicate significant differences to the vehicle control cells.

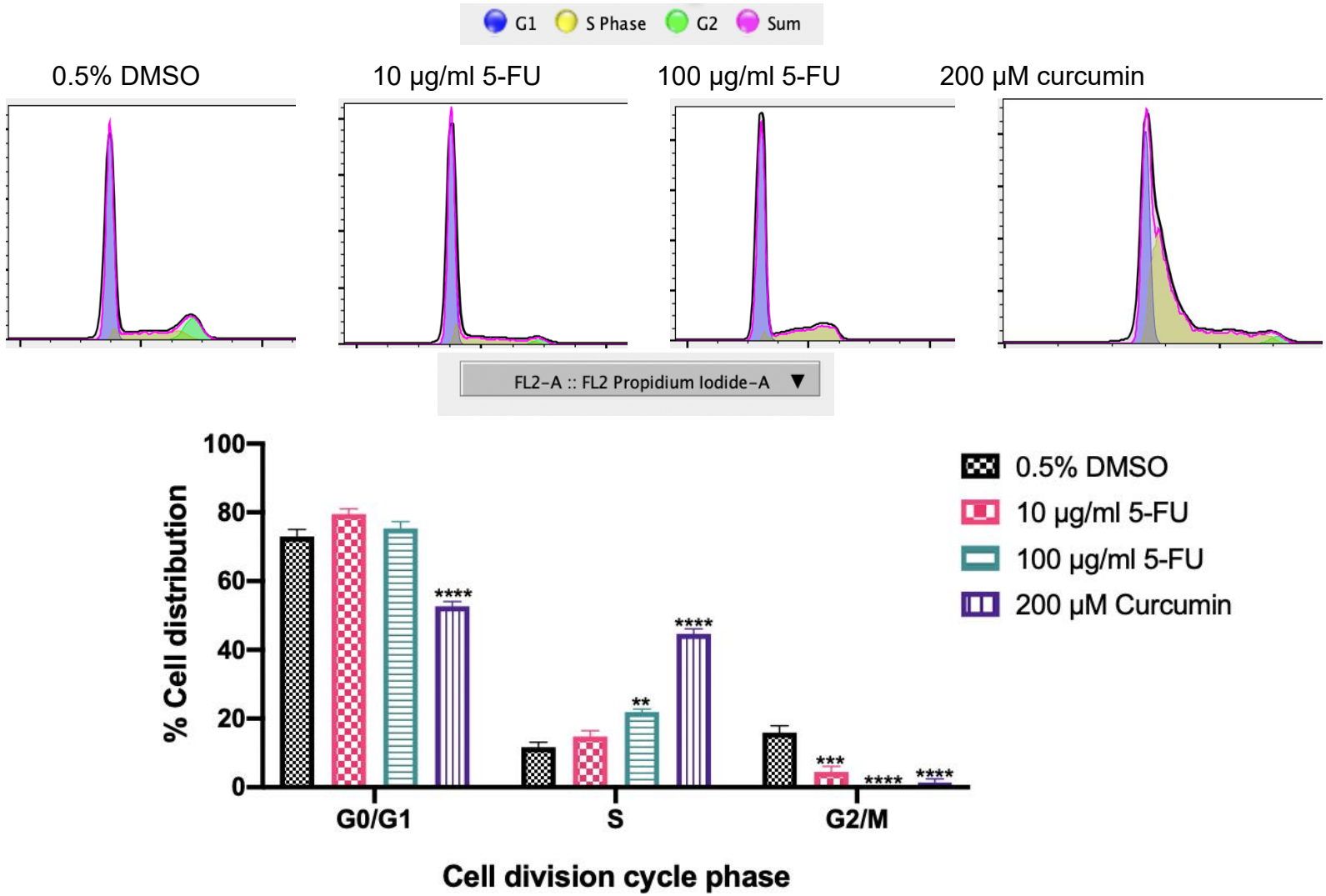

Figure 4.21: Cell cycle distribution of the 5-Fluorouracil treated HT-29 colon cancer cells.

Cells were treated with 10 or 100 µg/ml of 5-Fluorouracil or 0.5% DMSO as the vehicle control for 24 hours. Assessment of the cell cycle distribution was determined by flow cytometry using PI. Each data point represents the mean ± S.E.M of three independent experiments, performed in duplicate. ** $p \leq 0.01$, *** $p \leq 0.001$ and **** $p \leq 0.0001$ indicate significant differences to the vehicle control cells.

4.2.4.12 Cell cycle regulatory and checkpoint proteins in HT-29 cells

Analysis of the expression of cell cycle regulatory and checkpoint proteins in HT-29 cells showed that treatment with 267 µg/ml of the MeOH extract resulted in a significant ($p \leq 0.05$) downregulation of Claspin (by 34%) and a significant upregulation of p21 ($p \leq 0.0001$; by 80%). Treatment with the MeOH extract further resulted in a non-significant upregulation of p27 (by 47%) expression level. Treatment with 100 µg/ml of 5-FU resulted in an upregulation in the expression level of Claspin (by 40%), however, not significant. 5-FU treatment also resulted in a non-significant decrease in expression levels of p21 (down by 23%) and p27 (by 10%). On the other hand, treatment with curcumin resulted in the downregulation of Claspin ($p \leq 0.01$; by 36%), p21 ($p \leq 0.01$; by 37%) and p27 (by 26%). Moreover, phospho-Rad17 expression level was slightly upregulated with the MeOH extract (up by 9%) treatment and showed a non-significant downregulation with 5-FU (by 16%) and curcumin (by 20%) treatments (Figure 4.22).

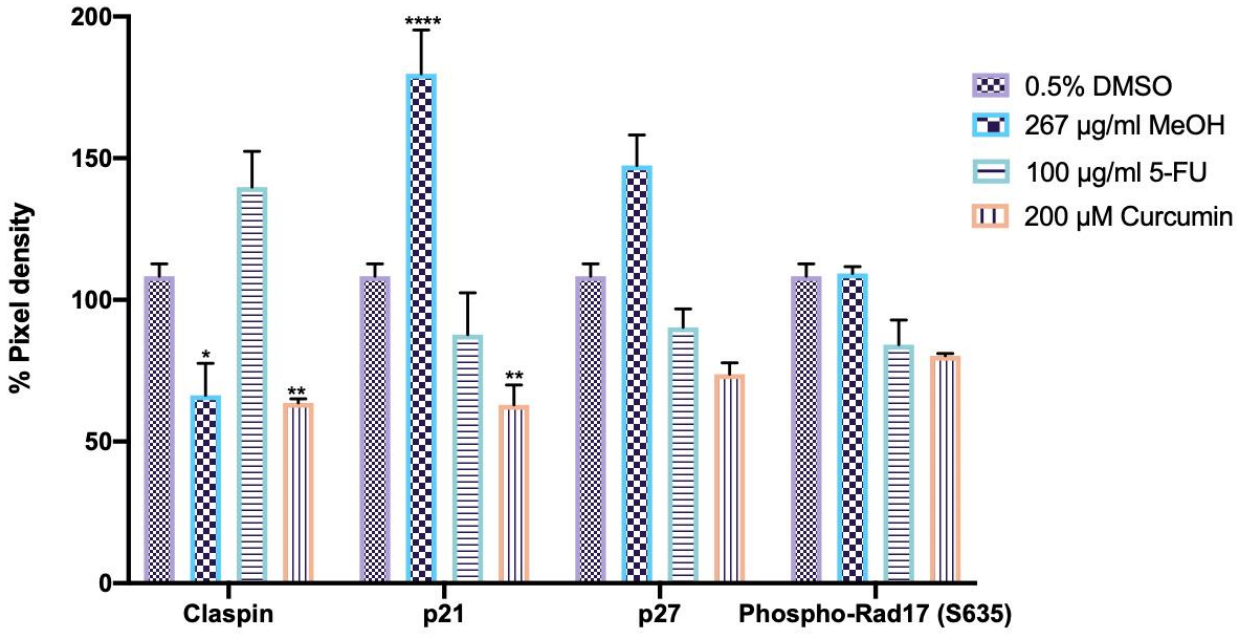

Figure 4.22: Effect of the *M. balsamina* methanol extract or 5-Fluorouracil on the expression levels of the cell cycle regulatory and checkpoint proteins.

Cells were treated with 267 µg/ml of the methanol extract, 100 µg/ml of 5-Fluorouracil or 0.5% DMSO as the vehicle control for 24 hours. Effect on expression levels of cell cycle distribution and checkpoint proteins was determined using the proteome profiler array. Each data point represents the mean ± S.E.M of three independent experiments, performed in duplicate. * $p \leq 0.05$, ** $p \leq 0.01$ and **** $p \leq 0.0001$ indicate significant differences to the vehicle control cells.

4.2.4.13 Assessment of p53 phosphorylation in HT-29 cells

The determination of the phosphorylation of p53 serine residue 15 (S15) in HT-29 cells treated with 267 µg/ml of the MeOH extract showed non-significant phosphorylation (increased by 40%). Treatment with 267 µg/ml of the MeOH extract further downregulated the phosphorylation of S46 (by 25%) and S392 (by 19%), however, this was not statistically significant. Treatment with 100 µg/ml of 5-FU resulted in a significant ($p \leq 0.0001$; by 200%) phosphorylation of S15, little to no change in S46 (by 4%) and a slight downregulation in S392 (by 13%) phosphorylation levels. On the other hand, treatment with curcumin showed a slight upregulation in the phosphorylation of S15 (by 16%) and a slight downregulation in S46 (by 26%) and S392 (by 30%) phosphorylation levels (Figure 4.23).

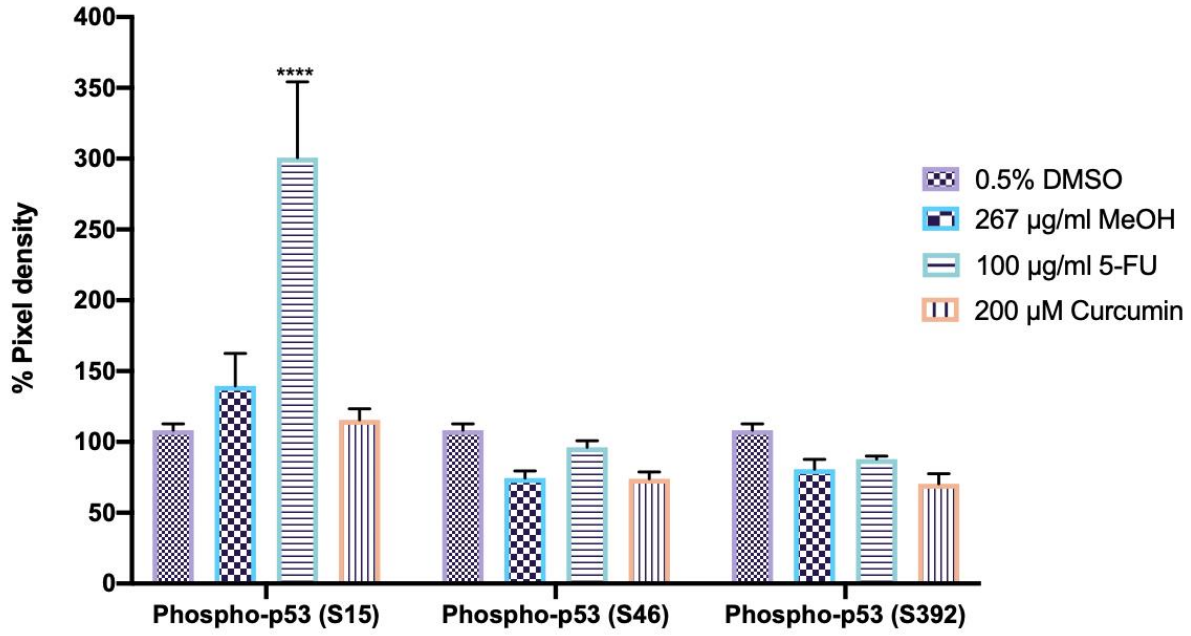

Figure 4.23: Effect of the *M. balsamina* methanol extract or 5-Fluorouracil on the phosphorylation levels of p53.

Cells were treated with 267 µg/ml of the methanol extract, 100 µg/ml of 5-Fluorouracil or 0.5% DMSO as the vehicle control for 24 hours. Effect on the phosphorylation of p53 was determined using the proteome profiler array. Each data point represents the mean ± S.E.M of three independent experiments, performed in duplicate. **** $p \leq 0.0001$ indicates a significant difference to the vehicle control cells.

4.2.4.14 Heat shock proteins

Treatment with 267 µg/ml of the MeOH extract had no effect on the expression level of HSP27, HSP70 and HSP60 proteins when compared to the control cells treated with 0.5% DMSO. Treatment with 100 µg/ml of 5-FU had no effect on HSP27 protein expression level, but resulted in a significant downregulation in expression levels of HSP60 ($p \leq 0.01$; by 12%) and HSP70 ($p \leq 0.001$; by 15%). Furthermore, treatment with curcumin resulted in a significant downregulation of HSP27 ($p \leq 0.01$; by 10%), HSP60 ($p \leq 0.01$; by 14%) and HSP70 ($p \leq 0.01$; by 12%) proteins (Figure 4.24).

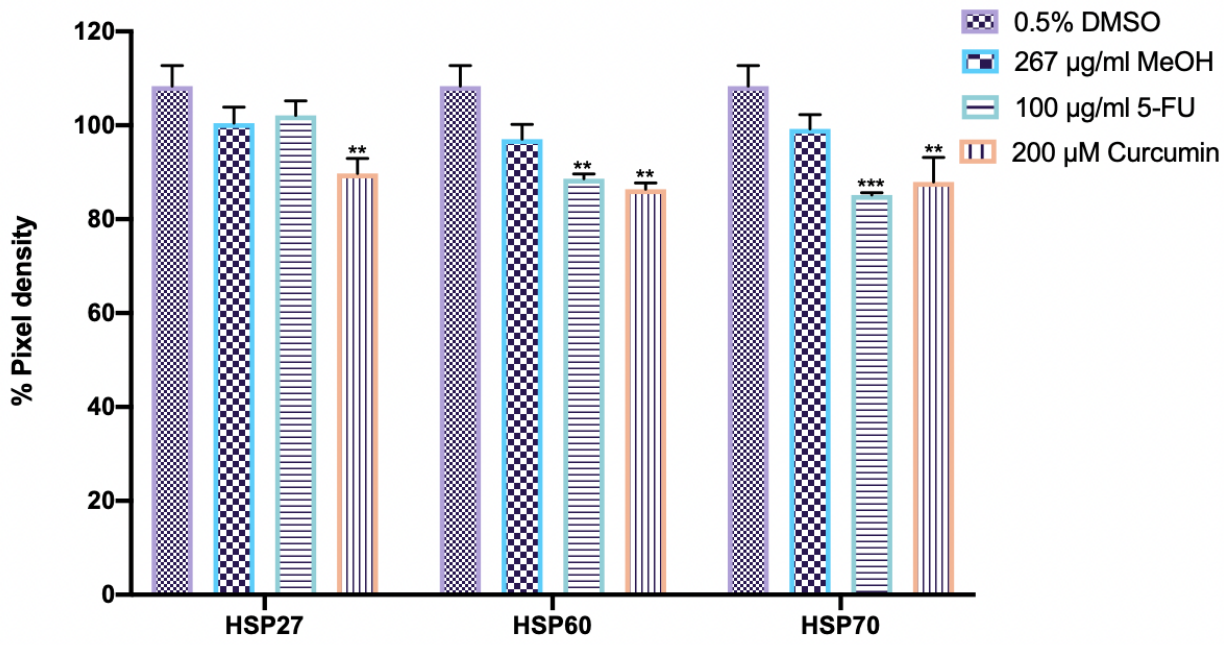

Figure 4.24: Effect of the *M. balsamina* methanol extract or 5-Fluorouracil on the expression levels of heat shock proteins.

Cells were treated with 267 µg/ml of the methanol extract, 100 µg/ml of 5-Fluorouracil or 0.5% DMSO as the vehicle control for 24 hours. Effect on expression levels of heat shock proteins was determined using the proteome profiler array. Each data point represents the mean ± S.E.M of three independent experiments, performed in duplicate. ** $p \leq 0.01$ and *** $p \leq 0.001$ indicate significant differences to the vehicle control cells.

4.3 Determination of herb-drug interactions

4.3.1 *Momordica balsamina* extracts or 5-FU effect on the activity of drug metabolising enzymes

Treatment with the H_2O extract significantly inhibited the activity of CYP1A2 at 200 µg/ml ($p \leq 0.01$) (Figure 4.25). CYP1A2 activity was maintained on average 80% or more with all treatment concentrations and no IC_{50} could be established for the concentrations tested. The MeOH extract resulted in significant inhibition of CYP1A2 from concentrations of 120 µg/ml and above showing a concentration-dependent response, i.e. an increase in the inhibition of enzyme activity with increasing extract concentration, resulting in an IC_{50} of 154.6 ± 3.3 µg/ml. On the other hand, 5-FU only showed no significant inhibition of CYP1A2 activity at all tested concentrations and no IC_{50} could be established (Figure 4.25).

CYP2A6 (Figure 4.26) activity was significantly inhibited with 160 µg/ml ($p \leq 0.05$) and 200 µg/ml ($p \leq 0.01$) of the H_2O extract, with a remaining enzyme activity of 87% and 84%, respectively. However, no IC_{50} could be established for the concentrations tested. The MeOH extract showed a significant ($p \leq 0.0001$) inhibition of CYP2A6 activity at concentrations of 40 µg/ml and above, resulting in an IC_{50} of 93.2 ± 6.8 µg/ml. Both the H_2O and MeOH extracts showed a concentration-dependent response with CYP2A6 activity. Furthermore, 5-FU resulted in a significant ($p \leq 0.05$) inhibition of CYP2A6 activity at 80 µg/ml, but with a remaining enzyme activity of 78% and a concentration-dependent response with no established IC_{50} for the concentrations tested.

The activity of CYP2C8 showed no significant inhibition at all tested concentrations of the H_2O extract, with remaining activity of more than 79% across all concentrations. The MeOH extract resulted in significant inhibition of CYP2C8 activity at concentrations of 10 µg/ml ($p \leq 0.001$) and above ($p \leq 0.0001$), resulting in an IC_{50} of 14.1 ± 1.6 µg/ml and concentration-dependent response. On the other hand, no significant change in the activity of CYP2C8 was observed with 5-FU treatment and all 5-FU concentrations had a remaining enzyme activity of more than 80% (Figure 4.27).

The activity of CYP2C9 showed no significant inhibition with the H_2O extract at all tested concentrations and had a remaining enzyme activity of over 85%. Although there was a concentration-dependent response, there was no IC_{50} established. The MeOH extract showed significant inhibition of CYP2C9 activity at concentrations of 10 µg/ml ($p \leq 0.01$) and above ($p \leq 0.0001$), with a concentration-dependent response and an IC_{50} of 26.3 ± 1.6 µg/ml. Furthermore, treatment with 5-FU resulted in no significant inhibition of CYP2C9 activity and remaining enzyme activity of above 70% across all the tested concentrations. There was also no IC_{50} established with the concentration, even though treatment showed a concentration-dependent response (Figure 4.28).

CYP1A2 activity

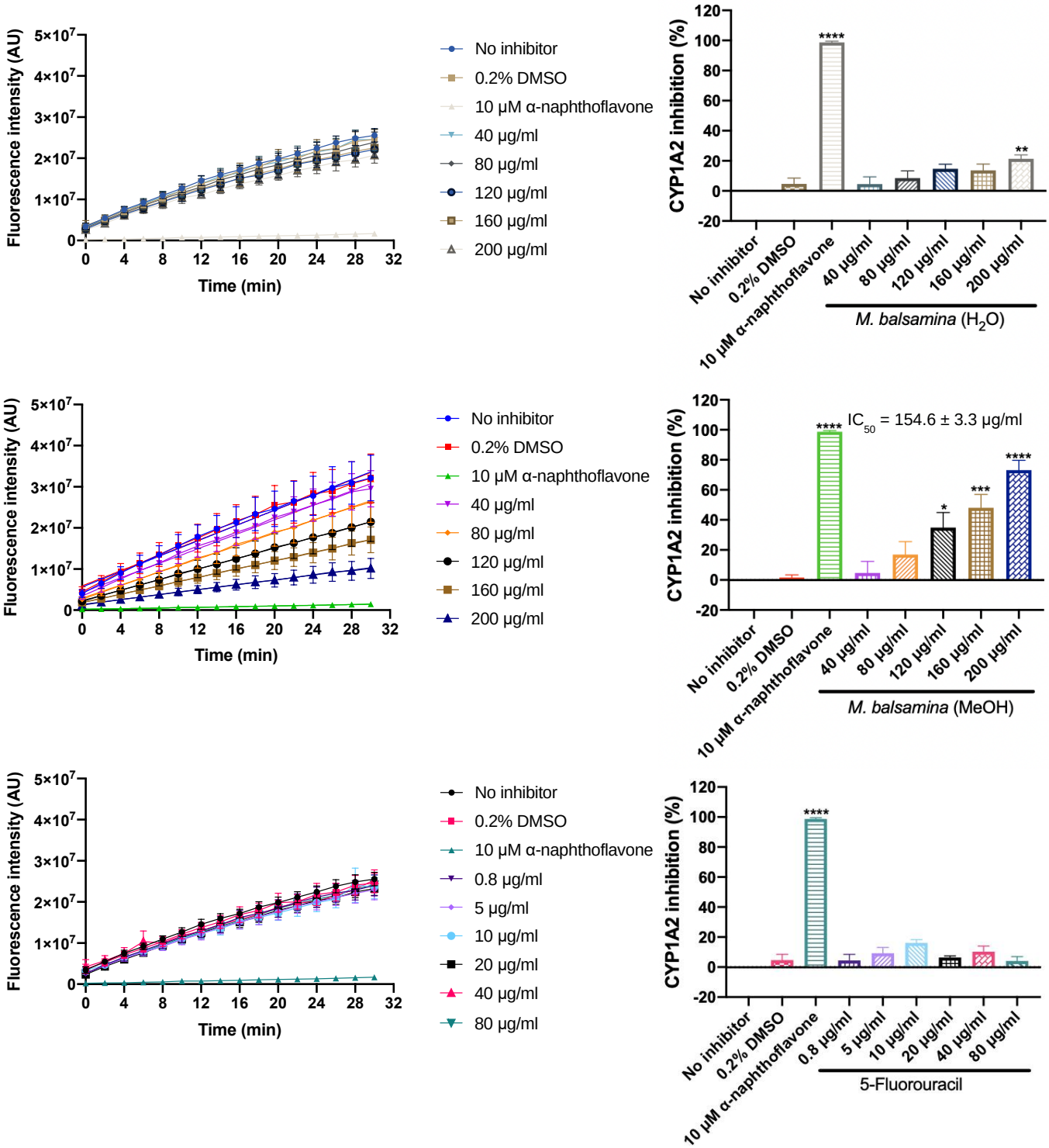

Figure 4.25: Effect of the *M. balsamina* H_2O, MeOH extracts or 5-FU on activity of CYP1A2.

CYP1A2 activity was assessed by spectrophotometry using the Vivid® CYP450 Screening Kits. Tested extract concentrations ranged from 40 to 200 µg/ml for the H_2O or MeOH extract or 0.8 to 80 µg/ml for 5-FU. DMSO at 0.2% served as a vehicle control and 10 µM of α-napthoflavone as a positive inhibitor. Each data point represents the mean ± S.E.M of three independent experiments, performed in duplicate. * $p \leq 0.05$, ** $p \leq 0.01$, *** $p \leq 0.001$ and **** $p \leq 0.0001$ indicate significant differences to the 0.2% DMSO control.

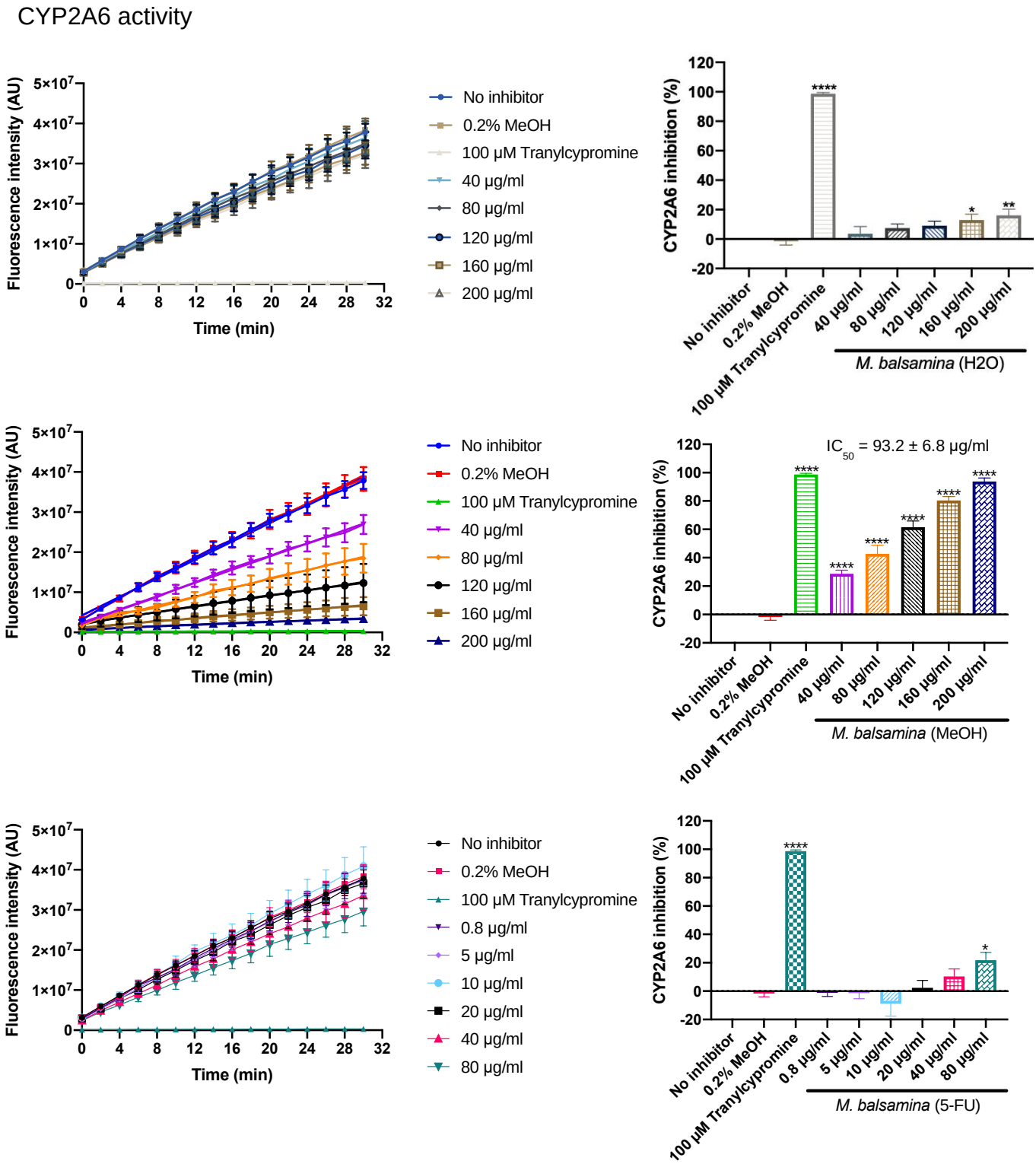

Figure 4.26: Effect of the *M. balsamina* H_2O, MeOH extracts or 5-FU on activity of CYP2A6.

CYP2A6 activity was assessed by spectrophotometry using the Vivid® CYP450 Screening Kits. Tested extract concentrations ranged from 40 to 200 µg/ml for the H_2O or MeOH extract or 0.8 to 80 µg/ml for 5-FU. Methanol at 0.2% served as a vehicle control and 100 µM of tranylcypromine as a positive inhibitor. Each data point represents the mean ± S.E.M of three independent experiments, performed in duplicate. * $p \leq 0.05$, ** $p \leq 0.01$ and **** $p \leq 0.0001$ indicate significant differences to the 0.2% MeOH control.

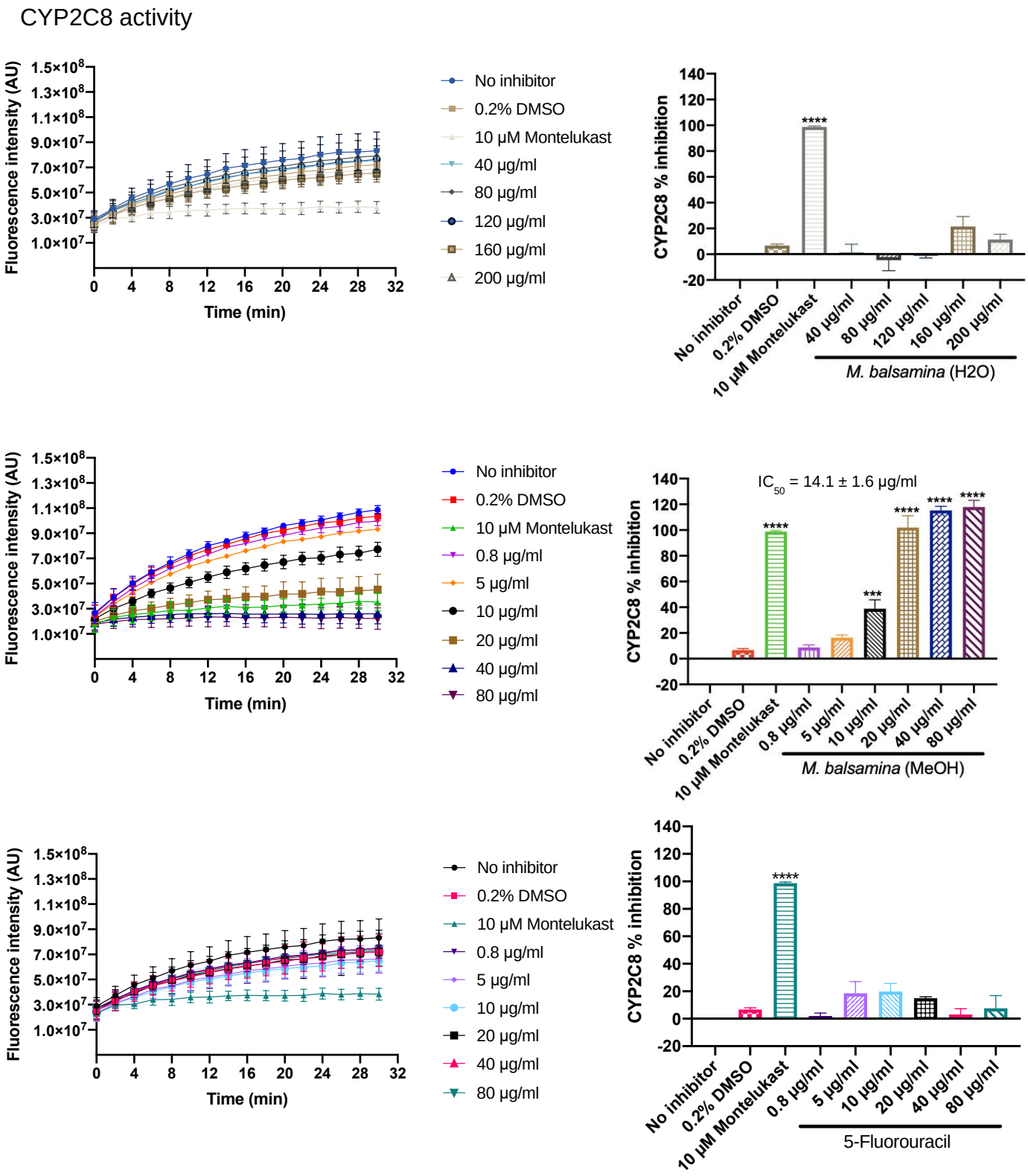

Figure 4.27: Effect of the *M. balsamina* H_2O, MeOH extracts or 5-FU on activity of CYP2C8.

CYP2C8 activity was assessed by spectrophotometry using the Vivid® CYP450 Screening Kits. Tested extract concentrations ranged from 40 to 200 µg/ml for the H_2O or MeOH extract or 0.8 to 80 µg/ml for 5-FU. DMSO at 0.2% served as a vehicle control and 10 µM of montelukast as a positive inhibitor. Each data point represents the mean ± S.E.M of three independent experiments, performed in duplicate. *** $p \leq 0.001$ and **** $p \leq 0.0001$ indicate significant differences to the 0.2% DMSO control.

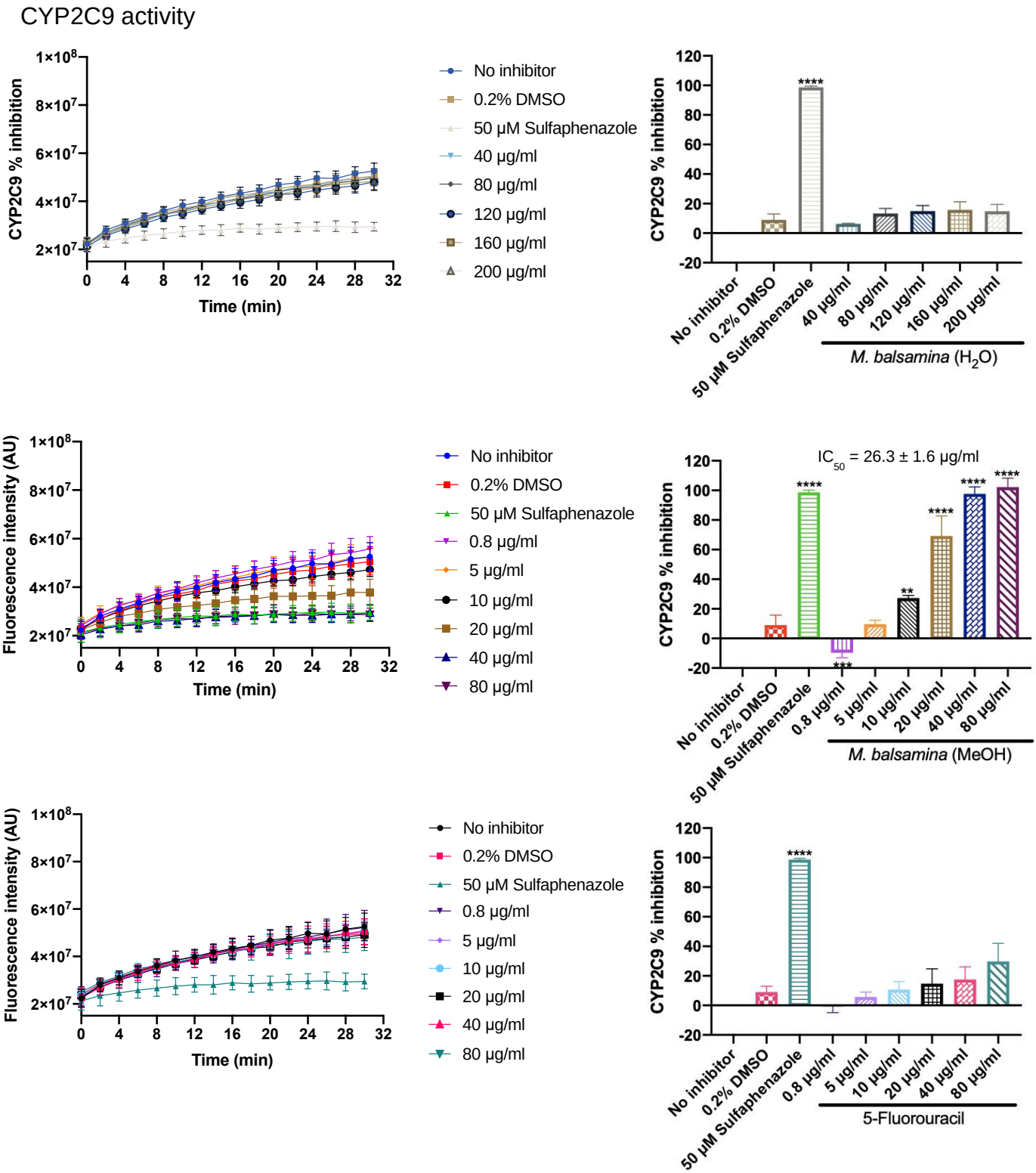

Figure 4.28: Effect of the *M. balsamina* H_2O, MeOH extracts or 5-FU on activity of CYP2C9.

CYP2C9 activity was assessed by spectrophotometry using the Vivid® CYP450 Screening Kits. Tested extract concentrations ranged from 40 to 200 µg/ml for the H_2O or MeOH extract or 0.8 to 80 µg/ml for 5-FU. DMSO at 0.2% served as a vehicle control and 50 µM of sulfaphenazole as a positive inhibitor. Each data point represents the mean ± S.E.M of three independent experiments, performed in duplicate. * $p \leq 0.05$, ** $p \leq 0.01$, *** $p \leq 0.001$ and **** $p \leq 0.0001$ indicate significant differences to the 0.2% DMSO control.

4.3.2 *Momordica balsamina* extracts or 5-FU effect on the activity of drug transporter P-glycoprotein

Treatment with the H_2O extract of *M. balsamina* resulted in significantly increased P-gp ATPase activity, at concentrations of 0.02 ($p \leq 0.05$), 0.2 µg/ml ($p \leq 0.01$), 2 µg/ml ($p \leq 0.01$), 20 µg/ml ($p \leq 0.0001$) and 200 µg/ml ($p \leq 0.05$) (Figure 4.29). Treatment with the MeOH extract resulted in decreased P-gp ATPase activity at concentrations from 0.2 µg/ml, with 20 µg/ml being significantly ($p \leq 0.01$) decreased. Furthermore, treatment with 5-FU also resulted in significantly increased P-gp ATPase activity, at concentrations of 0.008 µg/ml ($p \leq 0.01$), 0.8 µg/ml ($p \leq 0.001$), 8 µg/ml ($p \leq 0.05$), 16 µg/ml ($p \leq 0.05$) and 32 µg/ml ($p \leq 0.010$) (Figure 4.29).

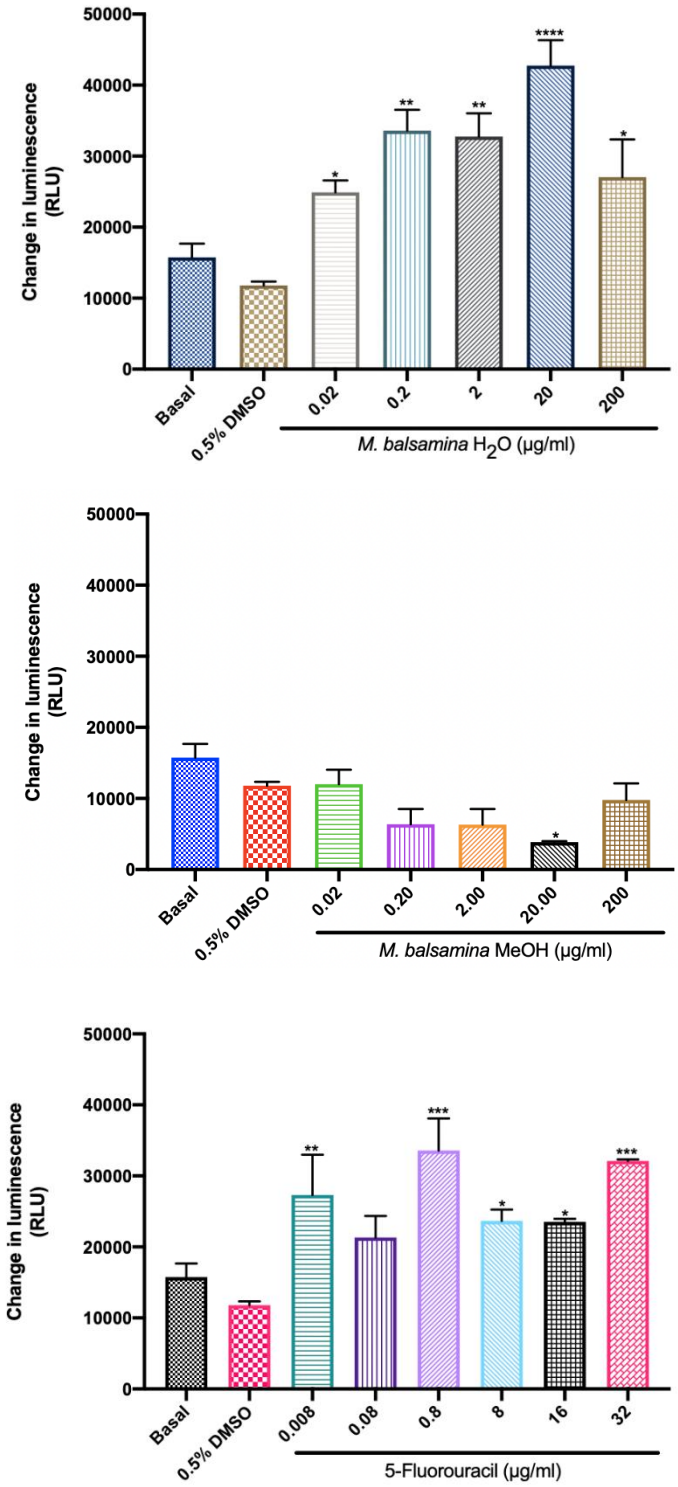

Figure 4.29: Effect of the *M. balsamina* H_2O, MeOH extracts or 5-FU on ATPase activity of the drug transporter, P-glycoprotein.

P-gp activity was assessed by chemiluminescence using the P-gp-GloTM Assay Systems with P-glycoprotein. Tested concentrations ranged from 0.02 to 200 µg/ml for the H_2O or MeOH extract or 0.008 to 32 µg/ml for 5-FU. DMSO at 0.5% served as a vehicle control. Each data point represents the mean ± S.E.M of three independent experiments, performed in duplicate. * $p \leq 0.05$, ** $p \leq 0.01$ and*** $p \leq 0.001$ indicate significant differences to the basal activity.

Chapter 5

5. Discussion

Colorectal cancer (CRC) is the fifth leading cause of cancer-related deaths in South Africa [459]. Despite great treatment improvements, CRC remains one of the leading causes of cancer mortality and morbidity worldwide, due to high relapse rates [419, 420]. 5-Fluorouracil (5-FU) has had the largest impact on CRC chemotherapy treatment [462, 463, 464]. However, the frequent occurrence of tumour resistance to 5-FU therapy [237] necessitates the need to develop and improve new chemotherapeutic treatment regimens and perhaps combinatory treatment regimens that would increase the activity of 5-FU and overcome clinical resistance [464].

For centuries, herbal medicines have been relied on for the treatment and prevention of many chronic illnesses and are still often used as an alternative and complementary approach to achieve better therapeutic options and overcome disadvantages resulting from synthetic drug use [465]. *M. balsamina* is regarded as a miracle herb mainly due to its nutritional and medicinal properties [466]. Leaf extracts of *M. balsamina* have been shown to possess bioactive compounds with antidiabetic [467], antimalarial [468], and anticancer [469] properties. In this study, the crude water and crude methanol leaf extracts of *M. balsamina* were characterised and investigated for their potential anticancer activity *in vitro*, in HT-29 colon cancer cells. This study further assessed the effect of the extracts on the activity of drug metabolising enzymes relevant for 5-FU.

Plants produce a variety of secondary metabolites that are non-nutritive, but serve protective functions in the plant and may possess health beneficial effects when consumed by humans [470]. Examples of these include phenolic acids, flavonoids, and isoflavones [471]. Phytochemical fingerprinting of the *M. balsamina* H_2O and MeOH extracts by thin-layer chromatography (TLC) revealed that the MeOH extract contained a more complex mixture of compounds than the H_2O extract. This suggests that the MeOH extract may contain more biologically active compounds than the H_2O extract. Compounds within the MeOH extract were shown to resolve better in the mobile phase with intermediate polarity (CEF) as well as the non-polar mobile phase (BEA). This is because the MeOH extract contained the least polar compounds when

compared to the H_2O extract, which resolved better in the most polar mobile phase (BAW) as well as the mobile phase with intermediate polarity than the non-polar mobile phase (***Figure 4.1***). This phenomenon was also reported by Masoko *et al*. [472]. Moreover, the vanillin-sulphuric acid spray is known to detect triterpenoids, flavonoids and glycosides [473] therefore, it can be said that the MeOH extract may contain an abundance of these compound classes than the H_2O extract.

Although TLC was able to illustrate the phytochemical profiles of the *M. balsamina* extracts, this method cannot with 100% certainty identify which specific compounds or compound classes were present in each extract. For this reason, chemical tests were conducted to screen for selected phytochemical classes within the extracts. The tests revealed the presence of phytochemicals that have been typically found in the *Momordica* species and reported in the literature [470, 474]. Tannins, carbohydrates, and triterpenoids were found to be equally distributed in both extracts. Coumarins and flavonoids were found to be more abundant in the MeOH extract than the H_2O extract (***Table 4.1***). The presence and distribution of these compounds as well as the antioxidant capacity (***Figure 4.2***) in each extract may be the basis for the pharmacological effects acclaimed in the *Momordica balsamina* plant.

A recent study aimed to provide detailed identification of compounds that are present in the methanol extracts of *M. balsamina* led to the identification of eleven molecular species. The study used reversed-phase liquid chromatography (RP-LC) coupled with ion mobility (IM) and high-resolution mass spectrometry (HRMS) operating in the positive ion mode. The molecular species identified included three flavonol glycosides (***Table 4.2***), five cucurbitane-type triterpenoid aglycones (***Table 4.3***) and three glycosidic cucurbitane-type triterpenoids (***Table 4.4***) [458]. In this study, 11 molecular species were detected in the MeOH extract and 7 in the H_2O extract (***Figure 4.3***). A comparison of the H_2O and the MeOH extracts, regarding the abundance of flavonol glycosides, cucurbitane-type triterpenoid aglycones and glycosidic cucurbitane-type triterpenoids found that the MeOH extract showed a higher abundance of flavonol glycosides (**Table 4.2**), cucurbitane-type triterpenoid aglycones (**Table 4.3**), and glycosidic cucurbitane-type triterpenoids (**Table 4.4**). Furthermore, since flavonoids, saponins and triterpenoids have a wide range of biological activities, which include antioxidative [475, 476], antiproliferative and anticancer properties [477, 478, 479, 480], this may

suggest that the *M. balsamina* H_2O and MeOH extracts may possess antioxidative, antiproliferative and anticancer activities, especially the MeOH extract as it had an abundance of the compound classes.

Ideally, an anticancer agent should specifically target cancer cells without damaging normal cells by inhibiting the growth, viability and proliferation of the cancer cells and inducing apoptosis [440, 441]. When assessing the effect of the *M. balsamina* H_2O or MeOH extracts as well as 5-FU, it was found that the water extract was slightly cytotoxic to the C2C12 cells used in this study as a model for normal cells as there was a 20% decrease in cell viability at 24 and 72 hours of treatment, respectively. Furthermore, the H_2O extract was not cytotoxic to the HT-29 colon cancer cells. However, a study by Thiagarajan *et* al. (2019) [483] tested the crude water leaf extract of *M. charantia*, which is closely related to *M. balsamina*, against A549 lung cancer cells and found that the extract inhibited cell viability with an IC_{50} of 32.5 ± 0.18 µg/ml after 24 hours of treatment. This may imply that the *M. balsamina* H_2O extract used in this study is far less toxic than the *M. charantia* H_2O extract or that the A549 lung cancer cells are more sensitive than the HT-29 cells. Treatment with 5-FU showed significant toxicity in both cell lines at 72 hours of treatment. The IC_{50} of 5-FU was consistent with those reported by Wiebke et al. [442] (1.69 µg/ml) and Varghese et al. [443] (3.09 µg/ml) at 72 hours. Moreover, several other studies reported IC_{50} for 5-FU treatment in HT-29 cells as 11.25 µM after five days of treatment [444], 11.5 µg/ml [445] and 8.7 µM (≈1.13 µg/ml) [446] at 48 hours. Combinatory treatment with 5-FU and the MeOH extract showed that the MeOH extract has no additive effects to the cytotoxicity exhibited by 5-FU treatment (***Figure 4.5***). The MeOH extract selectively inhibited the viability of HT-29 colon cancer cells with an IC_{50} of 267.4 ± 7.4 µg/ml at 24 hours of treatment (***Figure 4.4***), without affecting the viability of C2C12 muscle cells *(**Figure 4.6**)*. A study by Ofuegbe *et al*. (2017) [484] using the methanolic leaf extract of *M. charantia* showed that the extract also exhibits selective cytotoxicity against HT-29 colon cancer cells without affecting normal cells, with a 77.1% decrease in cell viability after 24 hours of treatment with 400 µg/ml.

The MeOH extract contains a variety of different compound classes such as flavonol glycosides, cucurbitane-type triterpenoid aglycones and glycosidic cucurbitane-type triterpenoids. Pure compounds such as the flavonol glycosides Quercetin 3-O-

rutinoside (Rutin), Kaempferol 3-O-rutinoside (Nicotiflorin) and Isorhamnetin 3-O-rutinoside (Narcissin) from these classes have been shown to have significant cytotoxic effects. Rutin has shown anticancer properties in several cell lines such as 786-O cancer cells [90], LAN-5 neuroblastoma cells [91], breast cancer MDA-MB-231 cells [485] and SW480 colon cancer cells *in vitro* [486]. Nicotiflorin, has been reported to reduce the risk of cancer [487, 488, 489, 490, 491, 492]; and Isorhamnetin 3-O-rutinoside (Narcissin) is capable of inhibiting the proliferation of tumour cells, induce tumour cell apoptosis and regulate tumour suppressor and proto-oncogenes, signalling pathways [493]. Narcissin inhibited the growth of several cancer cell lines such as human cervical [494, 495], lung [496, 497, 498], colon [499, 500], breast [501, 502, 503], pancreatic [504], nasopharyngeal [505], liver [506] and gastric cancer cells [507]. Furthermore, cucurbitane-type triterpenoids previously isolated from various parts of *Momordica charantia* [508, 509, 510], have been shown and confirmed in several studies to have antidiabetic [511, 512, 513], antioxidant [513, 514], antitumuor [515, 516, 517], antiobesity [518, 519] and antiviral [520, 511, 512, 513] properties. The antitumour activity was by inhibition of migration and invasion of cells [516] as well as the induction of cell cycle arrest at G1 and apoptosis [517]. Considering that the MeOH extract displayed significantly higher toxicity in the cancer cells, the MeOH extract of *M. balsamina* may be a potential for further exploration as an anticancer agent. The H_2O extract although not cytotoxic to the HT-29 colon cancer cells, possesses a variety of minerals and amino acids attributed to the species [44], it would be interesting to analyse the extract further to ascertain whether the mineral and amino acid content are high enough to develop as a potential beneficial herbal supplement and be used as part of a healthy diet.

When investigating new compounds for potential anticancer activity, it is important to establish whether the extracts have potential genotoxic properties, since genotoxicity could contribute to carcinogenicity [521]. Many plants synthesise substances that protect them against infections, insects and herbivores [522], which when present in herbal medicines, may exhibit genotoxicity [523, 524, 525, 526]. As such, assessing the potential genotoxicity of herbal medicines is vital since mutations that lead to an increased risk of cancer and many other diseases are a result of damage to the genetic material. In response to DNA damage, ataxia-telangiectasia mutated (ATM) kinase is activated [527]. ATM acts upstream p53 and controls the DNA damage response (DDR) pathway which is responsible for resolving DNA double-stranded breaks [528]. The H2A histone

family member X (H2A.X) also plays a crucial part in the repair of double-stranded DNA breaks [529]. Its phosphorylated form, gamma H2AX (γH2AX) functions as a marker for double-stranded DNA breaks [530]. Findings in this study showed that the MeOH extract did not exhibit genotoxicity in C2C12 cells as made evident by no apparent ATM and/or H2A.X activation when compared to the cells treated with 200 µM of curcumin as well as the HT-29 cells treated with 267 µg/ml of the MeOH extract (***Figure 4.7***), thereby further suggesting that the MeOH extract was selectively cytotoxic and genotoxic to only the cancer cells. It would be important to confirm the lack of genotoxic potential with additional assays in the future.

Reactive oxygen species (ROS) are active metabolic by-products capable of causing either beneficial or deleterious effects [531]. Reactive oxygen species are necessary molecules in the regulation of biological and physiological processes such as cell differentiation and proliferation [532, 533]. An imbalance in the body between free radicals and antioxidants leads to oxidative stress, which may induce damage to cells and macromolecules such as lipids, proteins and DNA [534, 535, 536]. Some plant phytochemicals exhibit pro-oxidant activity and may contribute to apoptosis of cancer cells as a result of ROS-induced DNA damage, thereby constituting the desired effect in cancer therapy [537, 538]. Furthermore, agents capable of inducing heme oxygenase-1 (HO-1), a stress-induced protein that protects cells from oxidative injury, can either directly or indirectly promote ROS generation [539, 540]. Heme oxygenase-1 is also known to induce anti-inflammatory, anti-apoptosis, antioxidant and drug resistance properties [541]. An increase in HO-1 expression is associated with an increase in the removal of ROS and therefore, its upregulation can combat stressful events and further contributes to apoptosis inhibition, inflammation and cell proliferation [542, 543]. Paraoxonase-2 (PON2) is an enzyme that is also capable of protecting cells from oxidative stress by exerting antioxidant functions that lessen cellular oxidation damage, thereby influencing redox signalling and promoting survival of cells [544, 545]. When overexpressed, PON2 reduces the generation of intracellular ROS and when deficient, increases its generation [546]**.** When assessing intracellular ROS in HT-29 cells, it was found that the treatment with 267 µg/ml of the MeOH extract, 10 and 100 µg/ml of 5-FU and 200 µM of curcumin significantly increased ROS production when compared to the control cells (***Figure 4.8***), despite the significant upregulation in HO-1 expression in cells treated with 267 µg/ml of the MeOH extract and 200 µM of

curcumin (***Figure 4.9***). Even though HO-1 expression increases due to increased oxidative stress [547, 548], the increase may not have been sufficient to remove ROS or the enzyme activity may have been inhibited. Although there are studies that report a significant upregulation of HO-1 by 5-FU due to oxidative stress, this was shown in mice *in vivo* rather than in cells *in vitro* [549, 550]. The upregulation of HO-1 by curcumin was consistent with several studies that showed that curcumin is an inducer of HO-1 [551] in mice [552], Huh7.5-HCV [553] and mesangial cells [554]. Furthermore, the significant decrease in PON2 expression levels may further support ROS generation and/or may have prevented ROS removal in the cells treated with the MeOH extract (***Figure 4.9***).

ROS generation by natural products disrupts the mitochondrial membrane and therefore interferes with the electron transport chain. This leads to a reduction in the mitochondrial membrane potential, which is considered as one of the early events of apoptosis [555, 556] and is responsible for the loss of cell viability [557]. The changes in mitochondrial membrane potential and condensing of the chromatin [558], allows for detection by several dyes such as the JC-1, which selectively enters the mitochondria of the cell and changes fluorescence from red to green as the membrane potential decreases [449], and nuclear DNA-binding dyes such as acridine orange (AO), used to assess chromatin integrity where the intercalating dye, AO, will fluoresce more brightly in cells undergoing apoptosis due to condensation of the chromatin [452]. On the other hand, propidium iodide (PI) stains the chromatin of necrotic cells as well as apoptotic cells that have lost cell membrane function, a feature of cells in the late stages of apoptosis [454]. The induction of apoptosis in cells treated with 267 µg/ml of the MeOH extract was evident by the observed decrease in mitochondrial membrane potential (***Figure 4.10***), as well as changes in the nuclear morphology and loss of cell membrane integrity (***Figure 4.11***).

Another characteristic of cells that are undergoing apoptosis is the change in the asymmetry of phosphatidylserine (PS). Phosphatidylserine in normal healthy cells is found within the inner layer of the cell membrane (cytoplasmic surface) but gets translocated to the outer layer of cells undergoing apoptosis [8]. The translocated PS is recognised by phagocytes for removal [284]. Phosphatidylserine translocation also serves as a marker for apoptosis as it has a high affinity to Annexin-V, a 35-36 kDa human vascular anticoagulant, which allows for the detection of apoptotic cells [559]. In

this study, an increase in the percentage of MeOH-treated HT-29 cells stained with Annexin-V or Annexin-V/PI was observed (***Figure 4.12***). This further confirmed the pro-apoptotic activity of the MeOH extract in HT-29 cells.

Cellular and nuclear morphological changes in apoptotic cells are initiated by biochemical changes such as caspase activation [560]. Once activated, there is a cascade of events that ultimately lead to apoptosis where initiator caspases such as caspase-8 and -9, responsible for initiating the extrinsic and intrinsic pathways, respectively, activate the executioner caspase, caspase-3 or -7 [561, 562, 299, 563]. The activation of the executioner caspase then results in cytoskeletal reorganisation and disintegration of the cell into apoptotic bodies [563, 315]. The active form of caspase-3, cleaved caspase-3, was upregulated upon treatment with 267 µg/ml of the MeOH extract (***Figure 4.13***), validating the occurrence of apoptosis in MeOH-treated HT-29 cells. Moreover, caspase-3 activation could be attributed to the activation of both initiator caspase-8 and -9 as suggested by the significant ($p \leq 0.0001$) increase in their activity when compared to the untreated cells (***Figure 4.14***).

In the intrinsic pathway of apoptosis, the pro-apoptotic and anti-apoptotic members of the Bcl-2 family of proteins form dimers to either promote or prevent apoptosis [564, 565]. The ratio of pro-apoptotic proteins to anti-apoptotic proteins determines whether a cell undergoes apoptosis or not [566]. The pro-apoptotic members Bcl-2-associated X protein (Bax) and Bcl-2 associated agonist of cell death (Bad) cause mitochondrial dysfunction and induce the release of cytochrome c into the cytosol. In the cytosol, cytochrome c interacts with the apoptotic protease activating factor 1 (Apaf-1) to initiate the activation of a caspase cascade [567, 568]. The anti-apoptotic member B-cell lymphoma 2 (Bcl-2) preserves the integrity of the outer mitochondrial membrane and suppresses the release of cytochrome c thereby inhibiting apoptosis [567]. Furthermore, Bad can selectively form dimers with the anti-apoptotic proteins, thereby displacing Bax so it is free to initiate the permeabilisation of the outer mitochondrial membrane which leads to the release of mitochondrial proteins such as cytochrome c [569, 570]**.** Treatment with the MeOH extract downregulated the expression levels of both pro-apoptotic and anti-apoptotic proteins when compared to the control (***Figure 4.15***). However, the absolute quantity may be of less importance rather than the overall balance between pro-apoptotic and anti-apoptotic proteins for apoptosis to occur [294,

[289]. In this study, the expression of the Bax protein was lower compared to the expression of the Bcl-2 protein in HT-29 cells treated with 267 µg/ml of the MeOH extract. Bad, which is capable of binding anti-apoptotic proteins displacing Bax to initiate permeabilisation of the outer mitochondrial membrane for release of cytochrome c was also expressed. Thus, the presence, although downregulated, of cytochrome c and other mitochondrial proteins in the cytosol could be attributed to Bad displacing Bax from the anti-apoptotic proteins allowing Bax to form pores on the outer mitochondrial membrane.

Cytochrome c, as well as other mitochondrial proteins such as high-temperature requirement protein A (HTRA2)/Omi and second mitochondria-derived activator of caspase/direct IAP Binding protein with Low pI (SMAC/Diablo), are released into the cytosol and trigger activation of caspase-9 which in turn activates caspase-3 thereby inducing apoptosis [298, 299]. HTRA2/Omi contributes to apoptosis via a caspase-dependent as well as a caspase-independent pathway, while SMAC/Diablo is responsible for interacting and antagonising inhibitors of apoptosis proteins (IAPs) to allow activation of caspases and execution of apoptosis [300, 571, 572, 573]. HTRA2/Omi and SMAC/Diablo were detected in lower amounts as compared to the DMSO control cells following treatment with the MeOH extract or 5-FU (***Figure 4.16***). However, an increase in caspase-9 (***Figure 4.14***) and -3 (***Figure 4.13***) activity upon treatment with the MeOH extract was observed. This suggests that, even though the amount of cytochrome c and other mitochondrial proteins that promote apoptosis was low, overall, they were sufficient to trigger a caspase cascade in the treated cells as seen by the increase in caspase-9 and -3 activity.

The extrinsic pathway of apoptosis is triggered by the binding of a death ligand such as FasL or TNF-*α* to death receptors FasR or TNFR1, respectively [574]. Once FasL binds to FasR or TNF-*α* to TNFR1, cytoplasmic adaptor proteins with corresponding death domains, Fas-associating protein with death domain (FADD) or TNFR1-associated death domain protein (TRADD) are recruited and bind with the receptors. The death domain FADD recruits the receptor-interacting protein (RIP) and associates it with procaspase-8, the initiator caspase of the extrinsic pathway, to form a death-inducing signalling complex (DISC). The DISC then activates procaspase-8 which in turn triggers apoptosis by activating caspase-3 [575, 311, 312]. In this study, although the

expression levels of FasL, TRAIL R1 and TNF RI proteins were downregulated upon treatment with the MeOH extract, there was a significant upregulation of the receptor TRAIL R2, whose corresponding death domain, FADD, was downregulated (***Figure 4.18***). Whether TRAIL R2 expression could have been sufficient for the formation of DISC remains speculative, however, caspase-8 was found to be activated (***Figure 4.14***), suggesting that the extrinsic pathway of apoptosis was to some degree also activated.

The increase in caspase-9 and -8 activities upon treatment with the MeOH extract, suggests that the extract triggered both the intrinsic and extrinsic pathways of apoptosis. The simultaneous activation of the extrinsic and intrinsic pathway is reported to involve the cleavage of the BH3 interacting-domain death agonist (BID) protein by the extrinsic pathway initiator caspase-8 [537]. The BH3 interacting-domain death agonist is a member of the BH3 only domain subgroup of the Bcl-2 family which once activated, activates the pro-apoptotic protein Bax which then complexes with the anti-apoptotic protein, Bak to form a channel in the outer mitochondrial membrane. This increases the permeability of the outer mitochondrial membrane and releases cytochrome c and other pro-apoptotic molecules which then activate caspase-9, thus triggering the intrinsic pathway of apoptosis [538, 539]. Moreover, the MeOH extract is in its crude form and thus contains a mixture of phytochemicals, therefore, this may lead to the phytochemicals targeting numerous proteins leading to the activation of various pathways and possibly the activation of both the intrinsic and extrinsic pathways of apoptosis.

Apoptosis can be inhibited by inhibitors of apoptosis (IAPs) which prevent caspase activation and thereby ensure cell survival [576]. These IAPs regulate the activity of the initiator caspase-9, responsible for the intrinsic pathway of apoptosis and effector caspase-3 [577, 578]. cIAP-1/2 deficiency leads to apoptotic cell death by the formation of a pro-apoptotic complex and activation of caspase-8 [579]. Expression of Clusterin is known to sensitise cancer cells to apoptosis mediated by chemotherapeutic drugs through Bax activation interference [580]. Among all IAPs, XIAP is the one that directly inactivates active catalytic sites of caspase-3 and activation of caspase-9 [581, 582]. Furthermore, Survivin is proposed to exert its anti-apoptotic activity by jointly blocking the activation of caspase-9 with XIAP [583]. However, XIAP activity is inhibited by the

IAP-antagonist SMAC/Diablo [584, 585, 586]. Treatment with the MeOH extract significantly ($p \leq 0.01$) upregulated the expression level of cIAP-2. This finding, therefore, also contributes to the induction of apoptosis via the intrinsic pathway in cells treated with the MeOH extract since cIAP-2 is responsible for inhibiting the activity of the extrinsic pathway of apoptosis initiator caspase, caspase-8, but does not affect apoptosis initiator caspase of the intrinsic pathway, caspase-9. Interestingly, the activity of caspase 8 was increased as much as the caspase 9 activity, while there was little evidence from the protein expression studies to indicate how this activation occurred. Moreover, the MeOH treatment significantly downregulated expression levels of Survivin and XIAP (***Figure 4.19***) thus allowing activation of the executioner caspase, caspase-3 (***Figure 4.13***).

Following cellular stress, such as DNA damage, p53, a tumour suppressor protein is upregulated and/or phosphorylated at multiple serine residues [587, 588]. Upregulation of the p53 protein results in the transcription of CDK inhibitors, such as p21 and p27, which leads to cell division cycle arrest [589, 590, 591, 592, 593]. Moreover, direct activation of p27, a CDK inhibitor with tumour suppressor potential, was found to induce cell cycle arrest in a study by Yadav *et al*. [594, 595]. This arrest leads to the repair of the damage or induction of apoptosis in cases where it is irreparable [596, 597]. A study by Zhu *et al*. [598] found that molecules that upregulated p21 expression could also induce S-phase arrest. In our study, the MeOH extract and 5-FU-treated cells underwent S phase arrest as seen by the significant increase in cells distributed in the S phase when treated with 100 µg/ml of the MeOH extract (***Figure 4.20***) and 100 µg/ml of 5-FU (***Figure 4.21***). The observed S phase arrest in MeOH-treated cells could be a result of DNA damage induced by the extract. Phosphorylation of p53 is reported to modify its biochemical function as a transcription factor [599, 600, 601, 602]. Phosphorylation at S15 triggers events of phosphorylation to other serine residues, such as serine 46 (S46) when the damage to DNA is intense enough, which further contributes to the induction and activation of p53 [603, 604]. Furthermore, serine 392 (S392), which regulates mitochondrial translocation of p53 to induce transcription-independent apoptosis may also get phosphorylated upon DNA damage [605]. The increase in S15 phosphorylation was witnessed in the cells treated with the MeOH extract and 5-FU (***Figure 4.23***), and therefore, suggests that the observed cell cycle arrest could have been mediated by p53 through p21 and p27 in extract-treated cells (***Figure 4.22***). A study by Semple *et*

al. [606] found that when the expression level of Claspin, which is known as a key player in the DNA damage repair pathway [607], is downregulated by short interfering RNA, there is an increase in the induction of apoptosis in both the presence and absence of DNA damage. The downregulation in Claspin expression levels in MeOH extract-treated cells (***Figure 4.22***) further supports the observed increase in apoptotic cells with the MeOH extract treatment (***Figure 4.12***).

In response to stress conditions, heat shock proteins (HSPs) are produced to make cells resistant to stress-induced damage [608]. When overexpressed, Hsp27 increases cell resistance to apoptotic stimuli by directly binding to cytochrome c and inhibiting it from binding to Apaf-1 [609, 610, 611, 612]. Under normal conditions, Hsp60 forms a complex with the pro-apoptotic protein, Bax. However, under hypoxic conditions, Hsp60 dissociates from Bax, leaving it to translocate to the mitochondria and mediate apoptosis [613]. Furthermore, Hsp70 is suspected to have direct interaction with Apaf-1 wherein it prevents the formation of the apoptosome and thus inhibits apoptosis [614, 615]. However, in this study, the levels of HSPs in MeOH-treated HT-29 cells were not regulated in a biologically significant way and could therefore not have exerted any significant pro- or anti-apoptotic effects (***Figure 4.24***). Moreover, treatment of HT-29 cells with 5-FU resulted in a significant decrease in expression levels of Hsp60 and Hsp70 (***Figure 4.24***) and thus may be the influence in the degree of apoptosis witnessed in 5-FU treated cells.

Although the use of chronic medication and herbal medicines is common, little is known about how the interaction of the herbal medicine and drug can affect the pharmacological or toxicological effects of the drug [14, 402]. Drug metabolising enzymes are responsible for the detoxification of foreign chemicals and degradation of drugs in the body [616, 617]. These include cytochrome P450s which are mainly found in the liver where they play a vital role in metabolising drugs and xenobiotics through their induction and inhibition [618, 619]. Co-administration of enzyme-inducing herbal medicines with prescription drugs may result in sub-therapeutic plasma levels of the drug and therefore result in therapeutic failure [397]. In contrast, enzyme-inhibiting herbal medicines can also compete with prescription drugs for binding sites and as such, alter the therapeutic effects of the drug which can then result in elevated serum levels of the drugs and thus severe toxicity [397, 620]. Furthermore, if a drug depends only on one

CYP450 enzyme for its metabolism or has a narrow safety range, it is most likely to cause unfavourable effects if a CYP450 enzyme inhibitor is added to the therapy [621, 622]. Of more than thirty CYP450 enzymes that exist, 5-Fluorouracil is associated with twelve. Four of which were selected for this study based on information retrieved from drugbank.com [457]. Orally administered prodrugs of 5-Fluorouracil are substrates for CYPs 1A2 [623, 624], 2A6 [623, 624] and CYP2C8 [623] which facilitate the conversion of 5-FU. On the other hand, 5-FU inhibits the activity of CYP2C9 [234, 625]. 5-FU is further converted to fluorouridine triphosphate (FUTP), fluorodeoxyuridine triphosphate (FdUTP) and fluorodeoxyuridine monophosphate (FdUMP). FUTP is incorporated into RNA instead of uridine triphosphate (UTP) and causes alterations in RNA processing and function, while FdUTP is incorporated into DNA instead of deoxythymidine triphosphate (dTTP) and causes DNA damage. FdUMP inhibits the activity of thymidylate synthase (TS) in the ternary complex which also causes DNA damage [626].

In this study, 5-FU showed weak or no inhibition of CYPs 1A2 (***Figure 4.26***), 2A6 (***Figure 4.27***) and 2C8 (***Figure 4.28***), presumably because they are responsible for converting prodrugs to 5-FU. However, the inhibition of CYP2C9 (***Figure 4.29***) concurred with the literature [234, 625]. Inhibition of CYPs 1A2 (***Figure 4.26***), 2A6 (***Figure 4.27***), and 2C8 (***Figure 4.28***) by the MeOH extract would suggest that 5-FU will not be converted to its active metabolites and would therefore suggest the potential to interfere with the activation of orally administered 5-FU prodrugs thus affecting efficacy. Moreover, since more than 80% of clinically used drugs are metabolised by these CYPs, the MeOH extract of *M. balsamina* may therefore present a significant risk for herb-drug interactions when used concurrently with pharmaceuticals with potential for toxicity and treatment failure. On the other hand, the H_2O extract was shown to have minimal inhibition of the tested CYPs (1A2, ***Figure 4.26***, 2A6, ***Figure 4.27***, 2C8, ***Figure 4.28***, and 2C9 ***Figure 4.29***) but displayed no anti-apoptotic or cytotoxic effects. Although the biological activity of the H_2O extract was also minimal, its medicinal and nutritional content [128, 466], attributed to the plant species contributes to its potential use as a nutraceutical.

Many forms of chemotherapy fail due to multidrug resistance (MDR) associated with the overexpression of ATP-binding cassette (ABC) transporters [627, 628, 629]. The drug efflux transporter, P-glycoprotein (P-gp), which belongs to the ABC transporter family

contributes to MDR by conferring cancer cells the potential to withstand doses of cytotoxic drugs that would under normal circumstances be lethal to the cancer cells [630, 631]. Inhibitors of P-gp have been shown to increase chemotherapeutic-induced mortality due to MDR tumours [629]. All tested concentrations of 5-FU (0.008 – 32 µg/ml) and the H_2O extract (0.02 – 200 µg/ml) used in this study were shown to stimulate P-gp ATPase activity, thereby suggesting that these treatments would not be able to reverse MDR. However, with the MeOH extract, the P-gp ATPase activity was significantly inhibited with 0.2, 2 and 20 µg/ml thereby suggesting that the MeOH extract may have the potential to reverse the effects of P-gp MDR by inhibiting its activity (***Figure 4.30***), confirming results from a study by Ramalhete *et al*. [632, 633] which showed that several cucurbitanes obtained from *M. balsamina* methanol extract of the aerial parts had MDR reversing activity.

Conclusion

This study hypothesised that *Momordica balsamina* crude water and crude methanol leaf extracts possess compounds with anticancer activities against HT-29 colon cancer cells and may have an additive effect on the efficacy of 5-Fluorouracil due to its mineral and nutritional content.

The MeOH extract selectively induced toxicity and genotoxicity to cancer cells and further exhibited anticancer activities against HT-29 colon cancer cells by induction of apoptosis and cell cycle arrest. The extract however did not have additive effects on the efficacy of 5-Fluorouracil and its inhibition of drug metabolising enzymes that are needed for conversion of 5-FU from its orally administered prodrugs, however, may present a potential problem. The extract further decreased the ATPase activity of the drug transporter P-gp, thereby suggesting it may have the potential to reverse P-gp multidrug resistance (MDR), however, this again will need to be carefully assessed against its CYP inhibitory function. Moreover, given that more than 80% of the clinically used drugs are metabolised by CYPs inhibited by this extract, its use may potentiate toxicity and result in treatment failure when used concurrently with other drugs. Therefore, its potential interactions with commonly used chronic medication need further exploration.

These pro-apoptotic and MDR reversal activities can likely be attributed to the abundance of flavonol glycosides, cucurbitane-type triterpenoid aglycones and cucurbitane-type glycosides. Moving forward, it may be beneficial to isolate and purify these compounds to further investigate the pro-apoptotic mechanisms and provide a more comprehensive perspective. Thus potentially improving the pro-apoptotic activity of the MeOH extract.

Chapter 6

6. References

1. 1. Sung, H., Ferlay, J., Siegel, R.L., Laversanne, M., Soerjomataram, I., Jemal, A. & Bray, F. Global cancer statistics 2020: GLOBOCAN estimates of incidence and mortality worldwide for 36 cancers in 185 countries. *CA: A Cancer Journal for Clinicians* (2021).
2. World Health Organisation. Cancer 2018. https://www.who.int/news-room/fact-sheets/detail/cancer (2018).
3. Herbst, C., Miot, J. K., Moch, S. L. & Ruff, P. Access to colorectal cancer (CRC) chemotherapy and the associated costs in a South African public healthcare patient cohort. *Journal of Cancer Policy* **15**, 18–24 (2018).
4. Siddiqui, M. & Rajkumar, S. V. The high cost of cancer drugs and what we can do about it. *Mayo Clinic proceedings* **87**, 935–943 (2012).
5. Desai, A.G., Qazi, G.N., Ganju, R.K., El-Tamer, M., Singh, J., Saxena, A.K., Bedi, Y.S., Taneja, S.C. & Bhat, H. K. Medicinal plants and cancer chemoprevention. *Current Drug Metabolism* **9**, 581–591 (2008).
6. Afzal, O., Lieber, M., Dottino, P. & Beddoe, A. M. Cervical cancer screening in rural South Africa among HIV-infected migrant farm workers and sex workers. *Gynecologic Oncology Reports* **20**, 18–21 (2017).
7. Manil, L., Mahieu, P. & Couvreur, P. Acute Renal Toxicity of Doxorubicin (Adriamycin)-Loaded Cyanoacrylate Nanoparticles. *Pharmaceutical Research* **12**, 85–87 (1995).
8. Greenwell, M. & Rahman, P. K. S. M. Medicinal Plants: Their Use in Anticancer Treatment. *International Journal of Pharmaceutical Sciences & Research* **6**, 4103–4112 (2015).
9. Rahman, M.M., Masum, G.Z.H., Sharkar, P. & Sima, S. N. Medicinal plant usage by traditional medical practitioners of rural villages in Chuadanga district, Bangladesh. *International Journal of Biodiversity Science, Ecosystem Services & Management* **9**, 330–338 (2013).
10. Maroyi, A. Traditional use of medicinal plants in south-central Zimbabwe: review and perspectives. *Journal of Ethnobiology & Ethnomedicine* **9**, 31 (2013).

11. Cunningham, A. B., An investigational report of Natural resources, University in Natal/Kwazulu. Pietermaritzburg, Institute of Natural Resources, University of Natal (1988).
12. Astin, J. A. Why Patients Use Alternative MedicineResults of a National Study. *The Journal of the American Medical Association* **279**, 1548–1553 (1998).
13. Ziel, H. K. Complementary alternative medicine boon or boondoggle? *Skeptic* **7**, 86 (1999).
14. Ekor, M. The growing use of herbal medicines: issues relating to adverse reactions and challenges in monitoring safety. *Frontiers in Pharmacology* **4,** 177 (2014).
15. Rafieian-Kopaei, M. Medicinal plants and the human needs. *Journal of HerbMed Pharmacology* **1** (2012).
16. Committee, I. B. Report of the IBC on traditional medicine systems and their ethical implications. Submitted at the 19th Session of IBC, held at UNESCO Headquarters, Paris on, 11. (2013).
17. Iqbal, J., Abbasi, B. A., Mahmood, T., Kanwal, S., Ali, B., Shah, S. A. & Khalil, A. T. Plant-derived anticancer agents: A green anticancer approach. *Asian Pacific Journal of Tropical Biomedicine* **7**, 1129–1150 (2017).
18. Prakash, D., Gupta, C. and Sharma, G. Importance of phytochemicals in nutraceuticals. *Journal of Chinese Medicine Research & Development* **1**, 70–78 (2012).
19. Rock, C. L., Doyle, C., Demark-Wahnefried, W., Meyerhardt, J., Courneya, K. S., Schwartz, A. L., Bandera, E. V, Hamilton, K. K., Grant, B., McCullough, M., Byers, T. & Gansler, T. Nutrition and physical activity guidelines for cancer survivors. *CA: A Cancer Journal for Clinicians* **62**, 242–274 (2012).
20. Martínez, M. E., Jacobs, E. T., Baron, J. A., Marshall, J. R. & Byers, T. Dietary supplements and cancer prevention: balancing potential benefits against proven harms. *Journal of the National Cancer Institute* **104**, 732–739 (2012).
21. Lippman, S. M., Klein, E. A., Goodman, P. J., Lucia, M. S., Thompson, I. M., Ford, L. G., Parnes, H. L., Minasian, L. M., Gaziano, J. M., Hartline, J. A., Parsons, J. K., Bearden 3rd, J. D., Crawford, E. D., Goodman, G. E., Claudio, J., Winquist, E., Cook, E. D., Karp, D. D., Walther, P., Lieber, M. M., Kristal, A. R., Darke, A. K., Arnold, K. B., Ganz, P. A., Santella, R. M., Albanes, D., Taylor, P. R., Probstfield, J. L., Jagpal, T. J., Crowley, J. J., Meyskens Jr, F. L., Baker, L. H. &

Coltman Jr, C. A. Effect of selenium and vitamin E on risk of prostate cancer and other cancers: the Selenium and Vitamin E Cancer Prevention Trial (SELECT). *The Journal of the American Medical Association* **301**, 39–51 (2009).

22. Omenn, G. S., Goodman, G. E., Thornquist, M. D., Balmes, J., Cullen, M. R., Glass, A., Keogh, J. P., Meyskens, F. L., Valanis, B., Williams, J. H., Barnhart, S. & Hammar, S. Effects of a Combination of Beta Carotene and Vitamin A on Lung Cancer and Cardiovascular Disease. *New England Journal of Medicine* **334**, 1150–1155 (1996).
23. Duffield-Lillico, A. J., Reid, M. E., Turnbull, B. W., Combs, G. F., Slate, E. H., Fischbach, L. A., Marshall, J. R. & Clark, L. C. Baseline Characteristics and the Effect of Selenium Supplementation on Cancer Incidence in a Randomized Clinical Trial. *Cancer Epidemiology Biomarkers & Prevention* **11**, 630 LP–639 (2002).
24. Klein, E. A., Thompson Jr, I. M., Tangen, C. M., Crowley, J. J., Lucia, M. S., Goodman, P. J., Minasian, L. M., Ford, L. G., Parnes, H. L., Gaziano, J. M., Karp, D. D., Lieber, M. M., Walther, P. J., Klotz, L., Parsons, J. K., Chin, J. L., Darke, A. K., Lippman, S. M., Goodman, G. E., Meyskens Jr, F. L. & Baker, L. H. Vitamin E and the risk of prostate cancer: the Selenium and Vitamin E Cancer Prevention Trial (SELECT). *The Journal of the American Medical Association* **306**, 1549–1556 (2011).
25. Lawenda, B. D., Kelly, K. M., Ladas, E. J., Sagar, S. M., Vickers, A. & Blumberg, J. B. Should Supplemental Antioxidant Administration Be Avoided During Chemotherapy and Radiation Therapy? *Journal of the National Cancer Institute* **100**, 773–783 (2008).
26. Bahmani, M., Shirzad, H., Shahinfard, N., Sheivandi, L. & Rafieian-Kopaei, M. Cancer Phytotherapy: Recent Views on the Role of Antioxidant and Angiogenesis Activities. *Journal of Evidence-based Complementary & Alternative Medicine* **22**, 299–309 (2017).
27. Sewell, R. D. E. & Rafieian-Kopaei, M. The history and ups and downs of herbal medicines usage. *Journal of Herbal Medicine & Pharmacology* **3**, 1–3 (2014).
28. VandeCreek, L., Rogers, E. & Lester, J. Use of alternative therapies among breast cancer outpatients compared with the general population. *Alternative Therapies in Health & Medicine* **5**, 71–76 (1999).
29. Ghosh, D. Seed to Patient in Clinically Proven Natural Medicines*. in

Nutraceuticals; Efficacy, Saftey and Toxicity (ed. Gupta, R. C. B. T.-N.) 925–931 (Academic Press, 2016). doi:https://doi.org/10.1016/B978-0-12-802147-7.00064-4.

30. Harvie, M. Nutritional Supplements and Cancer: Potential Benefits and Proven Harms. *American Society of Clinical Oncology Educational Book* e478–e486 (2014) doi:10.14694/EdBook_AM.2014.34.e478.
31. Fatima, N. & Nayeem, N. Toxic effects as a result of herbal medicine intake. *In Toxicology* (ed. Larramendy, M. L.) DOI: 10.5772/64468 (2016).
32. Bahmani, F., Esmaeili, S., Bashash, D., Dehghan-Nayeri, N., Mashati, P. & Gharehbaghian, A. Centaurea albonitens extract enhances the therapeutic effects of Vincristine in leukemic cells by inducing apoptosis. *Biomedicine & Pharmacotherapy* **99**, 598–607 (2018).
33. Bent, S. Herbal medicine in the United States: review of efficacy, safety, and regulation: grand rounds at University of California, San Francisco Medical Center. *Journal of General Internal Medicine* **23**, 854–859 (2008).
34. Singh, D., Gupta, R. & Saraf, S. A. Herbs–Are they Safe Enough? An Overview. *Critical Reviews in Food Science & Nutrition* **52**, 876–898 (2012).
35. Cupp, M. J. Herbal remedies: adverse effects and drug interactions. *American Family Physician* **59**, 1239 (1999).
36. Lee, A., Chui, P. T., Aun, C. S. T., Gin, T. & Lau, A. S. C. Possible Interaction Between Sevoflurane and Aloe vera. *Annals of Pharmacotherapy* **38**, 1651–1654 (2004).
37. Holman, C. P., & Bell, A. F. A trial of evening primrose oil in the treatment of chronic schizophrenia. *Journal of Orthomolecular Psychiatry* **12**, 302–304 (1983).
38. Aslam, M. & Stockley, I. H. Interaction between curry ingredient (karela) and drug (chlorpropamide). *The Lancet* **313**, 607 (1979).
39. Bilgi, N., Bell, K., Ananthakrishnan, A. N. & Atallah, E. Imatinib and Panax Ginseng: A Potential Interaction Resulting in Liver Toxicity. *Annals of Pharmacotherapy* **44**, 926–928 (2010).
40. Gutsch, J. On the state of therapy of chronic myeloid leukemia in adults with the mistletoe preparation Helixor. *Ärztezeitschrift für Naturheilverfahren* **23**, 523–544 (1982).
41. Chakraborty, P. Herbal genomics as tools for dissecting new metabolic pathways of unexplored medicinal plants and drug discovery. *Biochimie Open* **6**, 9–16

(2018).

42. Nagarani, G., Abirami, A. & Siddhuraju, P. Food prospects and nutraceutical attributes of Momordica species: A potential tropical bioresources – A review. *Food Science & Human Wellness* **3**, 117–126 (2014).
43. Basch, E., Gabardi, S. & Ulbricht, C. Bitter melon (*Momordica charantia*): a review of efficacy and safety. *American Journal of Health System Pharmacy* **60**, 356–359 (2003).
44. Hassan, L. G. & Umar, K. J. Nutritional Value of Balsam Apple (*Momordica balsamina* L.) Leaves. *Pakistan Journal of Nutrition* **5**, 522–529 (2006).
45. Zhou, J., Wu, J., Wu, C.-Y., Long, F., Shen, H., Zhang, W. & Li, S.-L. Herb-drug interaction: A case study of effects and involved mechanisms of cisplatin on the pharmacokinetics of ginsenoside Rb1 in tumor-bearing mice. *Biomedicine & Pharmacotherapy* **110**, 95–104 (2019).
46. Sofowora, A., Ogunbodede, E. & Onayade, A. The role and place of medicinal plants in the strategies for disease prevention. *African Journal of Traditional, Complementary, & Alternative Medicines* **10**, 210–229 (2013).
47. Mahomoodally, M. F. Traditional Medicines in Africa: An Appraisal of Ten Potent African Medicinal Plants. *Evidence-Based Complementary & Alternative Medicine* **2013**, 617459 (2013).
48. Nagarani, G., Abirami, A. & Siddhuraju, P. A comparative study on antioxidant potentials, inhibitory activities against key enzymes related to metabolic syndrome, and anti-inflammatory activity of leaf extract from different Momordica species. *Food Science & Human Wellness* **3**, 36–46 (2014).
49. Butler, M. S. Natural products to drugs: natural product derived compounds in clinical trials. *Natural Product Reports* **22**, 62–195 (2005).
50. Monciardini, P., Iorio, M., Maffioli, S., Sosio, M. and Donadio, S. Discovering new bioactive molecules from microbial sources. *Microbial Biotechnology* **7**, 209–220 (2014).
51. Latha, B., Reddy, I. R., Shaik, M. & Vijaya, T. Medicinal plants and their derivatives as potential source in treatment of obesity. *Asian Journal of Experimental Biological Sciences* **1**, 719–727 (2010).
52. Kumar, P. & Bhandari, U. Common medicinal plants with antiobesity potential: A special emphasis on fenugreek. *Ancient Science of Life* **35**, 58–63 (2015).
53. Singh, S.S., Pandey, S.C., Srivastava, S., Gupta, V.S., Patro, B. & Ghosh, A. C.

Chemistry and medicinal properties of Tinospora cordifolia (Guduchi). *Indian Journal of Pharmacology* **35**, 83–91 (2003).

54. Ferenci, P., Dragosics, B., Dittrich, H., Frank, H., Benda, L., Lochs, H., Meryn, S., Base, W. & Schneider, B. Randomized controlled trial of silymarin treatment in patients with cirrhosis of the liver. *Journal of Hepatology* **9**, 105–113 (1989).
55. Magliulo, E., Gagliardi, B. & Fiori, G. P. [Results of a double blind study on the effect of silymarin in the treatment of acute viral hepatitis, carried out at two medical centres (author's transl)]. *Medizinische Klinik* **73**, 1060–1065 (1978).
56. Boye, G.L. & Ampofo, O. Proceedings of the First International Symposium on Cryptolepine. (1983).
57. Kuruppu, A. I., Paranagama, P. & Goonasekara, C. L. Medicinal plants commonly used against cancer in traditional medicine formulae in Sri Lanka. *Saudi Pharmaceutical Journal* **27**, 565–573 (2019).
58. Newman, D.J. & Cragg, G. M. Natural products as sources of new drugs over the 30 years from 1981 to 2010. *Journal of Natural Products* **75**, 311–335 (2012).
59. Carter, G. T. Natural products and Pharma 2011: Strategic changes spur new opportunities. *Natural Product Reports* **28**, 1783–1789 (2011).
60. Veeresham, C. Natural products derived from plants as a source of drugs. *Journal of Advanced Pharmaceutical Technology & Research* **3**, 200–201 (2012).
61. Gurnani, N., Mehta, D., Gupta, M. & Mehta, B. K. Natural Products: source of potential drugs. *African Journal of Basic and Applied Sciences* **6**, 171–186 (2014).
62. Oshiro, B. T. The Semisynthetic Penicillins. *Primary Care Update for OB/GYNS* **6**, 56–60 (1999).
63. Patel, S. Plant-derived cardiac glycosides: Role in heart ailments and cancer management. *Biomedicine & Pharmacotherapy* **84**, 1036–1041 (2016).
64. Lahlou, M. 'The Success of Natural Products in Drug Discovery,'. *Pharmacology & Pharmacy* **4**, 17–31 (2013).
65. Akbulut, Y., Gaunt, H.J., Muraki, K., Ludlow, M.J., Amer, M.S., Bruns, A., Vasudev, N.S., Radtke, L., Willot, M., Hahn, S. & Seitz, T. (−)-Englerin A is a potent and selective activator of TRPC4 and TRPC5 calcium channels. *Angewandte Chemie International Edition* **54**, 3787–3791 (2015).
66. Ludlow, M.J., Gaunt, H.J., Rubaiy, H.N., Musialowski, K.E., Blythe, N.M., Vasudev, N.S., Muraki, K. and Beech, D. J. (−)-Englerin A-evoked cytotoxicity is mediated by Na+ influx and counteracted by Na+/K+-ATPase. *Journal of*

Biological Chemistry **292**, 723–731 (2017).

67. Muraki, K., Ohnishi, K., Takezawa, A., Suzuki, H., Hatano, N., Muraki, Y., Hamzah, N., Foster, R., Waldmann, H., Nussbaumer, P. & Christmann, M. Na+ entry through heteromeric TRPC4/C1 channels mediates (−) Englerin A-induced cytotoxicity in synovial sarcoma cells. *Scientific Reports* **7**, 1–12 (2017).
68. Carabajal, M. P. A., Isla, M. I. & Zampini, I. C. Evaluation of antioxidant and antimutagenic activity of herbal teas from native plants used in traditional medicine in Argentina. *South African Journal of Botany* **110**, 258–265 (2017).
69. Hussein, R. A. Plants Secondary Metabolites: The Key Drivers of the Pharmacological Actions of Medicinal Plants. **1**, 13 (2019).
70. Wink, M. Plant Secondary Metabolites Modulate Insect Behavior-Steps Toward Addiction? *Frontiers in Physiology* **9**, 364 (2018).
71. Younas, M., Hano, C., Giglioli-Guivarc'h, N. & Abbasi, B. H. Mechanistic evaluation of phytochemicals in breast cancer remedy: current understanding and future perspectives. *The Royal Society of Chemistry Advances* **8**, 29714–29744 (2018).
72. Harborne, J.B., Baxter, H. & Moss, G.R. *Phytochemical Dictionary: A Handbook of Bioactive Compounds from Plants.* (ed. Harbone, J.B, H, M. G) 360-518 (Taylor & Francis, 1999).
73. Vuolo, M. M., Lima, V. S. & Maróstica Junior, M. R. Phenolic Compounds: Structure, Classification, and Antioxidant Power. in *Bioactive compounds* (ed. Campos, M. R. S.) 33–50 (Woodhead Publishing, 2019). doi:https://doi.org/10.1016/B978-0-12-814774-0.00002-5.
74. Minatel, I. O. Phenolic Compounds: Functional Properties, Impact of Processing and Bioavailability. in *Phenolic compounds* (ed. Borges, C. V.) 1–24 (IntechOpen, 2017). doi:10.5772/66368.
75. Laura, A., Moreno-Escamilla, J.O., Rodrigo-García, J. &Alvarez-Parrilla, E. Phenolic Compounds. in *Postharvest physiology and biochemistry of fruits and vegetables* (ed. Yahia, E. M. B. T.) 253–271 (Woodhead Publishing, 2019). doi:https://doi.org/10.1016/B978-0-12-813278-4.00012-9.
76. Boerjan, W., Ralph, J. & Baucher, M. Lignin biosynthesis. *Annual Review of Plant Biology* **54**, 519–546 (2003).
77. Fraser, C. M. & Chapple, C. The phenylpropanoid pathway in Arabidopsis. *The Arabidopsis Book* **9**, e0152–e0152 (2011).

78. Giada, M. de L. R. Food Phenolic Compounds: Main Classes, Sources and Their Antioxidant Power. in *Oxidative Stress and Chronic Degenerative Diseases* (ed. Morales-González, J. A.) 87–112 (IntechOpen, 2013). doi:10.5772/51687.
79. Mahomoodally, M. F., Gurib-Fakim, A. & Subratty, A. H. Antimicrobial Activities and Phytochemical Profiles of Endemic Medicinal Plants of Mauritius. *Pharmaceutical Biology* **43**, 237–242 (2005).
80. Jan, S. & Abbas, N. Chemistry of Himalayan Phytochemicals. in *Himalayan Phytochemicals* (eds. Jan, S. & Abbas, N. B. T.-H. P.) 121–166 (Elsevier, 2018). doi:https://doi.org/10.1016/B978-0-08-102227-6.00004-8.
81. Drynan, J. W., Clifford, M. N., Obuchowicz, J. & Kuhnert, N. The chemistry of low molecular weight black tea polyphenols. *Natural Product Reports* **27**, 417–462 (2010).
82. Babu, P. V. A. & Liu, D. Flavonoids and Cardiovascular Health. in *Complementary and Alternative Therapies and the Aging Population* (ed. Watson, R. R. B. T.-C. and A. T. and the A. P.) 371–392 (Elsevier, 2009). doi:10.1016/B978-0-12-374228-5.00018-4.
83. Higuchi, M. Antioxidant Properties of Wheat Bran against Oxidative Stress. in *Wheat and Rice in Disease Prevention and Health* (eds. Watson, R. R., Preedy, V. R. & Zibadi, S. B. T.-W. and R. in D. P. and H.) 181–199 (Academic Press, 2014). doi:https://doi.org/10.1016/B978-0-12-401716-0.00015-5.
84. Figueira, I., Menezes, R., Macedo, D., Costa, I. & Dos Santos, C. N. Polyphenols Beyond Barriers: A Glimpse into the Brain. *Current Neuropharmacology* **15**, 562–594 (2017).
85. Nabavi, S. F., Sureda, A., Dehpour, A. R., Shirooie, S., Silva, A. S., Devi, K. P., Ahmed, T., Ishaq, N., Hashim, R., Sobarzo-Sánchez, E., Daglia, M., Braidy, N., Volpicella, M., Vacca, R. A. & Nabavi, S. M. Regulation of autophagy by polyphenols: Paving the road for treatment of neurodegeneration. *Biotechnology Advances* **36**, 1768–1778 (2018).
86. Kimura, Y., Ito, H., Ohnishi, R. & Hatano, T. Inhibitory effects of polyphenols on human cytochrome P450 3A4 and 2C9 activity. *Food & Chemical Toxicology* **48**, 429–435 (2010).
87. Panche, A. N., Diwan, A. D. & Chandra, S. R. Flavonoids: An overview. *Journal of Nutritional Science* **5**, e47–e47 (2016).
88. Lila, M. A. Anthocyanins and Human Health: An *In Vitro* Investigative Approach.

Journal of Biomedicine & Biotechnology **2004**, 306–313 (2004).

89. Ma, X. & Ning, S. Cyanidin-3-glucoside attenuates the angiogenesis of breast cancer via inhibiting STAT3/VEGF pathway. *Phytotherapy Research* **33**, 81–89 (2019).
90. Caparica, R., Júlio, A., Araújo, M. E. M., Baby, A. R., Fonte, P., Costa, J. G. & Santos de Almeida, T. Anticancer Activity of Rutin and Its Combination with Ionic Liquids on Renal Cells. *Biomolecules* **10**, 233 (2020).
91. Chen, H., Miao, Q., Geng, M., Liu, J., Hu, Y., Tian, L., Pan, J. & Yang, Y. Anti-Tumor Effect of Rutin on Human Neuroblastoma Cell Lines through Inducing G2/M Cell Cycle Arrest and Promoting Apoptosis. *The Scientific World Journal* **2013**, 269165 (2013).
92. Perk, A. A., Shatynska-Mytsyk, I., Gerçek, Y. C., Boztaş, K., Yazgan, M., Fayyaz, S. & Farooqi, A. A. Rutin mediated targeting of signaling machinery in cancer cells. *Cancer Cell International* **14**, 124 (2014).
93. Seelinger, G., Merfort, I., Wölfle, U. & Schempp, C. M. Anti-carcinogenic effects of the flavonoid luteolin. *Molecules* **13**, 2628–2651 (2008).
94. Imran, M., Rauf, A., Abu-Izneid, T., Nadeem, M., Shariati, M. A., Khan, I. A., Imran, A., Orhan, I. E., Rizwan, M., Atif, M., Gondal, T. A. & Mubarak, M. S. Luteolin, a flavonoid, as an anticancer agent: A review. *Biomedicine & Pharmacotherapy* **112**, 108612 (2019).
95. Jiang, M., Zhu, M., Wang, L. & Yu, S. Anti-tumor effects and associated molecular mechanisms of myricetin. *Biomedicine & Pharmacotherapy* **120**, 109506 (2019).
96. Afroze, N., Pramodh, S., Hussain, A., Waleed, M. & Vakharia, K. A review on myricetin as a potential therapeutic candidate for cancer prevention. *Biotechnology* **10**, 211 (2020).
97. Dei Cas, M. & Ghidoni, R. Cancer Prevention and Therapy with Polyphenols: Sphingolipid-Mediated Mechanisms. *Nutrients* **10**, 940 (2018).
98. Wang, J., Li, G., Lu, H., Zheng, Z., Huang, Y. & Su, W. Taxol from Tubercularia sp. strain TF5, an endophytic fungus of Taxus mairei. *Federation of European Microbiological Sciences Microbiology Letters* **193**, 249–253 (2000).
99. Ma, G., Yang, J., Zhang, L. & Song, C. Effective antitumor activity of paclitaxel-loaded poly (ε-caprolactone)/pluronic F68 nanoparticles after intratumoral delivery into the murine breast cancer model. *Anti-Cancer Drugs* **21**, (2010).
100. Sun, L., Zhou, W., Zhang, H., Guo, Q., Yang, W., Li, B., Sun, Z., Gao, S. & Cui,

R. Modulation of Multiple Signaling Pathways of the Plant-Derived Natural Products in Cancer. Frontiers in Oncology 9, 1153 (2019).

101. Molyneux, R. J., Lee, S. T., Gardner, D. R., Panter, K. E. & James, L. F. Phytochemicals: The good, the bad and the ugly? *Phytochemistry* **68**, 2973–2985 (2007).
102. Sirerol, J. A., Rodríguez, M. L., Mena, S., Asensi, M. A., Estrela, J. M. & Ortega, A. L. Role of Natural Stilbenes in the Prevention of Cancer. *Oxidative Medicine & Cellular Longevity* **2016**, 3128951 (2016).
103. Ionkova, I. Anticancer lignans-from discovery to biotechnology. *Mini Reviews in Medicinal Chemistry* **11**, 843-856. (2011).
104. Dostál, J. Two faces of alkaloids. *Journal of Chemical Education* **77**, 993 (2000).
105. Hussain, G., Rasul, A., Anwar, H., Aziz, N., Razzaq, A., Wei, W., Ali, M., Li, J. & Li, X. Role of Plant Derived Alkaloids and Their Mechanism in Neurodegenerative Disorders. *International Journal of Biological Sciences* **14**, 341–357 (2018).
106. Aniszewski, T. Alkaloids: chemistry, biology, ecology, and applications. *Elsevier* (2015).
107. Habli, Z., Toumieh, G., Fatfat, M., Rahal, O. N. & Gali-Muhtasib, H. Emerging Cytotoxic Alkaloids in the Battle against Cancer: Overview of Molecular Mechanisms. *Molecules* **22**, 250 (2017).
108. Lu, J.-J., Bao, J.-L., Chen, X.-P., Huang, M. & Wang, Y.-T. Alkaloids Isolated from Natural Herbs as the Anticancer Agents. *Evidence-Based Complementary & Alternative Medicine* **2012**, 485042 (2012).
109. Zhai, H., Hu, S., Liu, T., Wang, F., Wang, X., Wu, G., Zhang, Y., Sui, M., Liu, H. & Jiang, L. Nitidine chloride inhibits proliferation and induces apoptosis in colorectal cancer cells by suppressing the ERK signaling pathway. *Molecular Medicine Reports* **13**, 2536–2542 (2016).
110. Moudi, M., Go, R., Yien, C. Y. S. & Nazre, M. Vinca alkaloids. *International Journal of Preventive Medicine* **4**, 1231–1235 (2013).
111. Sparg, S. G., Light, M. E. & van Staden, J. Biological activities and distribution of plant saponins. *Journal of Ethnopharmacology* **94**, 219–243 (2004).
112. Mohan, V. R., Tresina, P. S. & Daffodil, E. D. Antinutritional Factors in Legume Seeds: Characteristics and Determination. in *Food Science* (eds. Caballero, B.,

Finglas, P. M. & Toldrá, F. B. T.-E. of F. and H.) 211–220 (Academic Press, 2016). doi:https://doi.org/10.1016/B978-0-12-384947-2.00036-2.

113. Vincken, J.-P., Heng, L., de Groot, A. & Gruppen, H. Saponins, classification and occurrence in the plant kingdom. *Phytochemistry* **68**, 275–297 (2007).

114. Desai, S.D., Desai, D.G. & Kaur, H. Saponins and their biological activities. *Pharma Times* **41**, 13–16 (2009).

115. Yang, H. & Dou, Q. P. Targeting apoptosis pathway with natural terpenoids: implications for treatment of breast and prostate cancer. *Current Drug Targets* **11**, 733–744 (2010).

116. González-Vallinas, M., González-Castejón, M., Rodríguez-Casado, A. & Ramírez de Molina, A. Dietary phytochemicals in cancer prevention and therapy: a complementary approach with promising perspectives. *Nutrition Reviews* **71**, 585–599 (2013).

117. Mahizan, N. A., Yang, S.-K., Moo, C.-L., Song, A. A.-L., Chong, C.-M., Chong, C.-W., Abushelaibi, A., Lim, S.-H. E. & Lai, K.-S. Terpene Derivatives as a Potential Agent against Antimicrobial Resistance (AMR) Pathogens. *Molecules* **24**, 2631 (2019).

118. Schaefer, H. & Renner, S. S. A three-genome phylogeny of Momordica (Cucurbitaceae) suggests seven returns from dioecy to monoecy and recent long-distance dispersal to Asia. *Molecular Phylogenetics & Evolution* **54**, 553–560 (2010).

119. Khoza, B. S., Dubery, I. A., Byth-Illing, H. A., Steenkamp, P. A., Chimuka, L. & Madala, N. E. Optimization of Pressurized Hot Water Extraction of Flavonoids from *Momordica foetida* Using UHPLC-qTOF-MS and Multivariate Chemometric Approaches. *Food Analytical Methods* **9**, 1480–1489 (2016).

120. Kubola, J. & Siriamornpun, S. Phenolic contents and antioxidant activities of bitter gourd (*Momordica charantia* L.) leaf, stem and fruit fraction extracts *in vitro*. *Food Chemistry* **110**, 881–890 (2008).

121. Lubinska-Szczygeł, M., Różańska, A., Namieśnik, J., Dymerski, T., Szterk, A., Luksirikul, P., Vearasilp, S., Katrich, E. & Gorinstein, S. Influence of steam cooking on pro-health properties of Small and Large variety of *Momordica charantia*. *Food Control* **100**, 335–349 (2019).

122. Grover, J. K. & Yadav, S. P. Pharmacological actions and potential uses of *Momordica charantia*: a review. *Journal of Ethnopharmacology* **93**, 123–132

(2004).

123. Joseph, B. & Jini, D. Antidiabetic effects of *Momordica charantia* (bitter melon) and its medicinal potency. *Asian Pacific Journal of Tropical Disease* **3**, 93–102 (2013).

124. Cao, X., Sun, Y., Lin, Y., Pan, Y., Farooq, U., Xiang, L. & Qi, J. Antiaging of Cucurbitane Glycosides from Fruits of *Momordica charantia* L. *Oxidative Medicine & Cellular Longevity* **2018**, 1538632 (2018).

125. Ludidi, A., Baloyi, M. C., Khathi, A., Sibiya, N. H. & Ngubane, P. S. The effects of *Momordica balsamina* methanolic extract on haematological function in streptozotocin-induced diabetic rats: Effects on selected markers. *Biomedicine & Pharmacotherapy* **116**, 108925 (2019).

126. Madala, N. E., Piater, L., Dubery, I. & Steenkamp, P. Distribution patterns of flavonoids from three *Momordica* species by ultra-high performance liquid chromatography quadrupole time of flight mass spectrometry: a metabolomic profiling approach. *Revista Brasileira de Farmacognosia* **26**, 507–513 (2016).

127. Thakur, G. S., Bag, M., Sanodiya, B. S., Bhadouriya, P., Debnath, M., Prasad, G. B. K. S. & Bisen, P. S. *Momordica balsamina*: a medicinal and neutraceutical plant for health care management. *Current Pharmaceutical Biotechnology* **10**, 667–682 (2009).

128. Ramalhete, C., Mansoor, T. A., Mulhovo, S., Molnár, J. & Ferreira, M.-J. U. Cucurbitane-Type Triterpenoids from the African Plant *Momordica balsamina*. *Journal of Natural Products* **72**, 2009–2013 (2009).

129. de Wet, H., Ramulondi, M. & Ngcobo, Z. N. The use of indigenous medicine for the treatment of hypertension by a rural community in northern Maputaland, South Africa. *South African Journal of Botany* **103**, 78–88 (2016).

130. Bandeira, S. O., Gaspar, F. & Pagula, F. P. African ethnobotany and healthcare: emphasis on mozambique. *Pharmaceutical biology* **39** Suppl 1, 70–73 (2001).

131. Ngarivhume, T., van't Klooster, C. I. E. A., de Jong, J. T. V. M. & Van der Westhuizen, J. H. Medicinal plants used by traditional healers for the treatment of malaria in the Chipinge district in Zimbabwe. *Journal of Ethnopharmacology* **159**, 224–237 (2015).

132. Chen, Q. & Li, E. T. S. Reduced adiposity in bitter melon (*Momordica charantia*) fed rats is associated with lower tissue triglyceride and higher plasma

catecholamines. *British Journal of Nutrition* **93**, 747–754 (2005).

133. Pedroso, J. A. B., Zampieri, T. T. & Donato Jr, J. Reviewing the Effects of L-Leucine Supplementation in the Regulation of Food Intake, Energy Balance, and Glucose Homeostasis. *Nutrients* **7**, 3914–3937 (2015).
134. Perkowski, M. C. & Warpeha, K. M. Phenylalanine roles in the seed-to-seedling stage: Not just an amino acid. *Plant Science* **289**, 110223 (2019).
135. Kohlmeier, M. Phenylalanine. in *Food Science and Technology* (ed. Kohlmeier, M. B. T.-N. M.) 314–321 (Academic Press, 2003). doi:https://doi.org/10.1016/B978-012417762-8.50051-X.
136. Hase, A., Jung, S. E. & aan het Rot, M. Behavioral and cognitive effects of tyrosine intake in healthy human adults. *Pharmacology Biochemistry & Behavior* **133**, 1–6 (2015).
137. Dasari, S., Wudayagiri, R. & Valluru, L. Cervical cancer: Biomarkers for diagnosis and treatment. *Clinica Chimica Acta* **445**, 7–11 (2015).
138. Robert, A. G. & Thomas, L, V. An evolutionary model of carcinogenesis. *Cancer Research* - **63**, 19, 6212–6220 (2003).
139. Tysnes, B. B. & Bjerkvig, R. Cancer initiation and progression: Involvement of stem cells and the microenvironment. *Biochimica et Biophysica Acta - Reviews on Cancer* **1775**, 283–297 (2007).
140. Cooper, G. M. The Development and Causes of Cancer. in *The Cell: A Molecular Approach.* (Sunderland (MA): Sinauer Associates, 2000).
141. Rundhaug, J. E. & Fischer, S. M. Cellular and Molecular Mechanisms of Tumor Promotion. in *Comprehensive Toxicology* (ed. McQueen, C. A. B. T.-C. T. (Second E.) 311–333 (Elsevier, 2010). doi:https://doi.org/10.1016/B978-0-08-046884-6.01416-0.
142. Abel, E. L. & DiGiovanni, J. Environmental Carcinogenesis. in *The molecular basis of cancer* (eds. Mendelsohn, J., Gray, J. W., Howley, P. M., Israel, M. A. & Thompson, C. B. B. T.-T. M. B. of C. (Fourth E.) 103-128.e2 (W.B. Saunders, 2015). doi:https://doi.org/10.1016/B978-1-4557-4066-6.00007-X.
143. Klaunig, J.E. Mutagenesis, Carinogenesis. in Biomedical sciences. (Elsevier, 2014). doi:https://doi.org/10.1016/B978-0-12-801238-3.00207-5.
144. Conti, C. J. Mechanisms of Tumor Progression. Chapter fourteen - in *Comprehensive Toxicology* (ed. McQueen, A. B. T.-C. T (Second E.) 335–347 (Elsevier, 2010). doi:https://doi.org/10.1016/B978-0-08-046884-6.01417-2.

145. Lodish, H., Berk, A., Zipursky, S. L., Matsudaira, P., Baltimore, D. & Darnell, J. Tumor cells and the onset of cancer. in *Molecular Cell Biology*. (Fourth E.) (W.H. Freeman) Available from: https://www.ncbi.nlm.nih.gov/books/NBK21475/ (2000).
146. Anusha, S., Mohan, C. D., Ananda, H., Baburajeev, C. P., Rangappa, S., Mathai, J., Fuchs, J. E., Li, F., Shanmugam, M. K., Bender, A., Sethi, G., Basappa & Rangappa, K. S. Adamantyl-tethered-biphenylic compounds induce apoptosis in cancer cells by targeting Bcl homologs. *Bioorganic & Medicinal Chemistry Letters* **26**, 1056–1060 (2016).
147. Rutkowski, M. R., Svoronos, N., Perales-Puchalt, A. & Conejo-Garcia, J. R. Chapter seven - The Tumor Macroenvironment: Cancer-Promoting Networks Beyond Tumor Beds. in *Immunotherapy of Cancer* (eds. Wang, X.-Y. & Fisher, P. B. B. T.-A. in C. R.) **128** 235–262 (Academic Press, 2015).
148. Seyfried, T. N. & Huysentruyt, L. C. On the origin of cancer metastasis. *Critical Reviews in Oncogenesis* **18**, 43–73 (2013).
149. Alizadeh, A. M., Shiri, S. & Farsinejad, S. Metastasis review: from bench to bedside. *Tumor Biology* **35**, 8483–8523 (2014).
150. Bhattacharya, R., Panda, C. K., Nandi, S. & Mukhopadhyay, A. An insight into metastasis: Random or evolving paradigms? *Pathology - Research & Practice* **214**, 1064–1073 (2018).
151. Kirfel, G., Rigort, A., Borm, B. & Herzog, V. Cell migration: mechanisms of rear detachment and the formation of migration tracks. *European Journal of Cell Biology* **83**, 717–724 (2004).
152. Gupta, G. P. & Massagué, J. Cancer Metastasis: Building a Framework. *Cell* **127**, 679–695 (2006).
153. Nguyen, D. X., Bos, P. D. & Massagué, J. Metastasis: from dissemination to organ-specific colonization. *Nature Reviews Cancer* **9**, 274–284 (2009).
154. Pepper, M. S., Tille, J.-C., Nisato, R. & Skobe, M. Lymphangiogenesis and tumor metastasis. *Cell & Tissue Research* **314**, 167–177 (2003).
155. Sahai, E. Mechanisms of cancer cell invasion. *Current Opinion in Genetics & Development* **15**, 87–96 (2005).
156. Aceto, N., Bardia, A., Miyamoto, D. T., Donaldson, M. C., Wittner, B. S., Spencer, J. A., Yu, M., Pely, A., Engstrom, A., Zhu, H., Brannigan, B. W., Kapur, R., Stott, S. L., Shioda, T., Ramaswamy, S., Ting, D. T., Lin, C. P., Toner, M.,

Haber, D. A. & Maheswaran, S. Circulating tumor cell clusters are oligoclonal precursors of breast cancer metastasis. *Cell* **158**, 1110–1122 (2014).

157. Cho, E. H., Wendel, M., Luttgen, M., Yoshioka, C., Marrinucci, D., Lazar, D., Schram, E., Nieva, J., Bazhenova, L., Morgan, A., Ko, A. H., Korn, W. M., Kolatkar, A., Bethel, K. & Kuhn, P. Characterization of circulating tumor cell aggregates identified in patients with epithelial tumors. *Physical Biology* **9**, 16001 (2012).
158. Hanna, S. & El-Sibai, M. Signaling networks of Rho GTPases in cell motility. *Cellular Signalling* **25**, 1955–1961 (2013).
159. Vlahakis, A. & Debnath, J. The Interconnections between Autophagy and Integrin-Mediated Cell Adhesion. *Journal of Molecular Biology* **429**, 515–530 (2017).
160. Guan, X. Cancer metastases: challenges and opportunities. *Acta Pharmaceutica Sinica B* **5**, 402–418 (2015).
161. Liekens, S., De Clercq, E. & Neyts, J. Angiogenesis: regulators and clinical applications. *Biochemical Pharmacology* **61**, 253–270 (2001).
162. Hanahan, D. & Weinberg, R. A. The hallmarks of cancer. *Cell* **100**, 57–70 (2000).
163. Hanahan, D. & Weinberg, R. A. Hallmarks of cancer: the next generation. *Cell* **144**, 646–674 (2011).
164. Bouck, N., Stellmach, V. & Hsu, S. C. How Tumors Become Angiogenic. in (eds. Vande Wude, G. F. & Klein, G. B. T.-A. in C. R.) **69**, 135–174 (Academic Press, 1996).
165. Hanahan, D. & Folkman, J. Patterns and emerging mechanisms of the angiogenic switch during tumorigenesis. *Cell* **86**, 353–364 (1996).
166. Folkman, J. Tumor angiogenesis. in *Cancer Medicine* (ed. J.F. Holland, R.C. Bast, D.L. Morton, E. Frei, D.W. Kufe, and R. R. W.) 181–204 (Baltimore, MD: Williams and Wilkins, 1997).
167. Ferlay, J., Ervik, M., Lam, F., Colombet, M., Mery, L., Piñeros, M., Znaor, A. & Soerjomataram, I.B.F. Global Cancer Observatory: Cancer Today. Lyon, France: International Agency for Research on Cancer. https://gco.iarc.fr/today (2020).
168. Selvam, C., Prabu, S. L., Jordan, B. C., Purushothaman, Y., Umamaheswari, A., Hosseini Zare, M. S. & Thilagavathi, R. Molecular mechanisms of curcumin and its analogs in colon cancer prevention and treatment. *Life Sciences* **239**,

117032 (2019).

169. Grady, W. M. & Markowitz, S. D. The molecular pathogenesis of colorectal cancer and its potential application to colorectal cancer screening. *Digestive Diseases & Sciences* **60**, 762–772 (2015).

170. Tao, J., Li, Y., Li, S. & Li, H.-B. Plant foods for the prevention and management of colon cancer. *Journal of Functional Foods* **42**, 95–110 (2018).

171. Doubeni, C. A., Laiyemo, A. O., Major, J. M., Schootman, M., Lian, M., Park, Y., Graubard, B. I., Hollenbeck, A. R. & Sinha, R. Socioeconomic status and the risk of colorectal cancer: an analysis of more than a half million adults in the National Institutes of Health-AARP Diet and Health Study. *Cancer* **118**, 3636–3644 (2012).

172. Willett, W. C. Diet and Cancer: An Evolving Picture. *The Journal of the American Medical Association* **293**, 233–234 (2005).

173. Doubeni, C. A., Major, J. M., Laiyemo, A. O., Schootman, M., Zauber, A. G., Hollenbeck, A. R., Sinha, R. & Allison, J. Contribution of behavioral risk factors and obesity to socioeconomic differences in colorectal cancer incidence. *Journal of the National Cancer Institute* **104**, 1353–1362 (2012).

174. Haggar, F. A. & Boushey, R. P. Colorectal cancer epidemiology: incidence, mortality, survival, and risk factors. *Clinics in Colon & Rectal Surgery* **22**, 191–197 (2009).

175. Amersi, F., Agustin, M. & Ko, C. Y. Colorectal cancer: epidemiology, risk factors, and health services. *Clinics in Colon & Rectal Surgery* **18**, 133–140 (2005).

176. Cook, J. L. Tobacco smoke: chemical carcinogenesis and genetic lesions. *The Ochsner Journal* **1**, 130–135 (1999).

177. Limsui, D., Vierkant, R. A., Tillmans, L. S., Wang, A. H., Weisenberger, D. J., Laird, P. W., Lynch, C. F., Anderson, K. E., French, A. J., Haile, R. W., Harnack, L. J., Potter, J. D., Slager, S. L., Smyrk, T. C., Thibodeau, S. N., Cerhan, J. R. & Limburg, P. J. Cigarette smoking and colorectal cancer risk by molecularly defined subtypes. *Journal of the National Cancer Institute* **102**, 1012–1022 (2010).

178. Childs, C. E., Calder, P. C. & Miles, E. A. Diet and Immune Function. *Nutrients* **11**, 1933 (2019).

179. Wu, D., Lewis, E. D., Pae, M. & Meydani, S. N. Nutritional Modulation of

Immune Function: Analysis of Evidence, Mechanisms, and Clinical Relevance. *Frontiers in Immunology* **9**, 3160 (2019).

180. Friedenreich, C. M., Shaw, E., Neilson, H. K. & Brenner, D. R. Epidemiology and biology of physical activity and cancer recurrence. *Journal of Molecular Medicine* **95**, 1029–1041 (2017).
181. Na, H.K. & Oliynyk, S. Effects of physical activity on cancer prevention. *Annals of the New York Academy of Sciences* **1229**, 176–183 (2011).
182. Smolińska, K. & Paluszkiewicz, P. Risk of colorectal cancer in relation to frequency and total amount of red meat consumption. Systematic review and meta-analysis. *Archives of Medical Science* **6**, 605–610 (2010).
183. Song, M., Garrett, W. S. & Chan, A. T. Nutrients, foods, and colorectal cancer prevention. *Gastroenterology* **148**, 1244–60.e16 (2015).
184. Pourvali, K. & Monji, H. Obesity and intestinal stem cell susceptibility to carcinogenesis. *Nutrition & Metabolism* **18**, 37 (2021).
185. Newmark, H. L., Yang, K., Lipkin, M., Kopelovich, L., Liu, Y., Fan, K. & Shinozaki, H. A Western-style diet induces benign and malignant neoplasms in the colon of normal C57Bl/6 mice. *Carcinogenesis* **22**, 1871–1875 (2001).
186. Johns, L. E. & Houlston, R. S. A systematic review and meta-analysis of familial colorectal cancer risk. *The American Journal of Gastroenterology* **96**, 2992–3003 (2001).
187. Slattery, M. L. & Kerber, R. A. Family History of Cancer and Colon Cancer Risk: the Utah Population Database. *Journal of the National Cancer Institute* **86**, 1618–1626 (1994).
188. Negri, E., Braga, C., La Vecchia, C., Franceschi, S., Filiberti, R., Montella, M., Falcini, F., Conti, E. & Talamini, R. Family history of cancer and risk of colorectal cancer in Italy. *British Journal of Cancer* **77**, 174–179 (1998).
189. Hemminki, K. & Li, X. Familial colorectal adenocarcinoma from the Swedish family-cancer database. *International Journal of Cancer* **94**, 743–748 (2001).
190. Lynch, H. T. & de la Chapelle, A. Genetic susceptibility to non-polyposis colorectal cancer. *Journal of Medical Genetics* **36**, 801 LP – 818 (1999).
191. Rodriguez-Bigas, M. A., Boland, C. R., Hamilton, S. R., Henson, D. E., Srivastava, S., Jass, J. R., Khan, P. M., Lynch, H., Smyrk, T., Perucho, M. & Sobin, L. A National Cancer Institute Workshop on Hereditary Nonpolyposis Colorectal Cancer Syndrome: Meeting Highlights and Bethesda Guidelines.

Journal of the National Cancer Institute **89**, 1758–1762 (1997).

192. Burt Randall W., M. D., DiSario James A., M. D. & Cannon-Albright Lisa, P. Genetics of colon cancer: Impact of Inheritance on Colon Cancer Risk. *Annual Review of Medicine* **46**, 371–379 (1995).
193. Diergaarde, B., Braam, H., Vasen, H. F., Nagengast, F. M., van Muijen, G. N. P., Kok, F. J. & Kampman, E. Environmental Factors and Colorectal Tumor Risk in Individuals With Hereditary Nonpolyposis Colorectal Cancer. *Clinical Gastroenterology & Hepatology* **5**, 736-742.e1 (2007).
194. Villalobos, C., Hernández-Morales, M., Gutiérrez, L. G. & Núñez, L. TRPC1 and ORAI1 channels in colon cancer. *Cell Calcium* **81**, 59–66 (2019).
195. Worthley, D. L. & Leggett, B. A. Colorectal cancer: molecular features and clinical opportunities. *The Clinical Biochemist Reviews* **31**, 31–38 (2010).
196. East, J. E., Saunders, B. P. & Jass, J. R. Sporadic and Syndromic Hyperplastic Polyps and Serrated Adenomas of the Colon: Classification, Molecular Genetics, Natural History, and Clinical Management. *Gastroenterology Clinics of North America* **37**, 25–46 (2008).
197. Boland, C. R. & Goel, A. Microsatellite instability in colorectal cancer. *Gastroenterology* **138**, 2073–2087.e3 (2010).
198. Smith, G, Carey, FA, Beattie, J, Wilkie, MJV, Lightfoot, TJ, Coxhead, J, Garner, RC, Steele, RJC & Wolf, C. ‘Mutations in APC, Kirsten-ras, and p53—alternative genetic pathways to colorectal cancer’,. in *National Academy of Sciences of the United States of America* 9433–9438 (2002).
199. Grady, W. M. Genomic instability and colon cancer. *Cancer & Metastasis Reviews* **23**, 11–27 (2004).
200. Rajagopalan, H. & Lengauer, C. Aneuploidy and cancer. *Nature* **432**, 338–341 (2004).
201. Rowan, A., Halford, S., Gaasenbeek, M., Kemp, Z., Sieber, O., Volikos, E., Douglas, E., Fiegler, H., Carter, N., Talbot, I., Silver, A. & Tomlinson, I. Refining Molecular Analysis in the Pathways of Colorectal Carcinogenesis. *Clinical Gastroenterology & Hepatology* **3**, 1115–1123 (2005).
202. Jančík, S., Drábek, J., Radzioch, D. & Hajdúch, M. Clinical Relevance of KRAS in Human Cancers. *Journal of Biomedicine & Biotechnology* **2010**, 150960 (2010).
203. Aubrey, B. J., Strasser, A. & Kelly, G. L. Tumor-Suppressor Functions of the

TP53 Pathway. *Cold Spring Harbor Perspectives in Medicine* **6**, a026062 (2016).

204. Fearon, E. R. & Vogelstein, B. A genetic model for colorectal tumorigenesis. *Cell* **61**, 759–767 (1990).

205. Jabbari, K. & Bernardi, G. Cytosine methylation and CpG, TpG (CpA) and TpA frequencies. *Gene* **333**, 143–149 (2004).

206. Bird, A. P. CpG-rich islands and the function of DNA methylation. *Nature* **321**, 209–213 (1986).

207. Lao, V. V. & Grady, W. M. Epigenetics and colorectal cancer. *Nature Reviews Gastroenterology & Hepatology* **8**, 686–700 (2011).

208. Ogino, S. & Goel, A. Molecular classification and correlates in colorectal cancer. *The Journal of Molecular Diagnostics* **10**, 13–27 (2008).

209. Grady, W. M. & Carethers, J. M. Genomic and epigenetic instability in colorectal cancer pathogenesis. *Gastroenterology* **135**, 1079–1099 (2008).

210. Cantwell-Dorris, E. R., O'Leary, J. J. & Sheils, O. M. BRAFV600E: Implications for Carcinogenesis and Molecular Therapy. *Molecular Cancer Therapeutics* **10**, 385 LP – 394 (2011).

211. Weisenberger, D. J., Siegmund, K. D., Campan, M., Young, J., Long, T. I., Faasse, M. A., Kang, G. H., Widschwendter, M., Weener, D., Buchanan, D., Koh, H., Simms, L., Barker, M., Leggett, B., Levine, J., Kim, M., French, A. J., Thibodeau, S. N., Jass, J., Haile, R. & Laird, P. W. CpG island methylator phenotype underlies sporadic microsatellite instability and is tightly associated with BRAF mutation in colorectal cancer. *Nature Genetics* **38**, 787–793 (2006).

212. Arena, E. A. & Bilchik, A. J. What is the optimal means of staging colon cancer? *Advances in Surgery* **47**, 199–211 (2013).

213. Ulanja, M. B., Rishi, M., Beutler, B. D., Sharma, M., Patterson, D. R., Gullapalli, N. & Ambika, S. Colon Cancer Sidedness, Presentation, and Survival at Different Stages. *Journal of Oncology* **2019**, 4315032 (2019).

214. Freeman, H. J. Early stage colon cancer. *World Journal of Gastroenterology* **19**, 8468–8473 (2013).

215. Varghese, A. Chemotherapy for Stage II Colon Cancer. *Clinics in Colon & Rectal Surgery* **28**, 256–261 (2015).

216. McCollum, A. D. Stage III colon cancer at Baylor University Medical Center at Dallas and the Baylor Sammons Cancer Center: experience from 2000 to 2004. *Proceedings (Baylor University. Medical Center)* **19**, 320–322 (2006).

217. Feo, L., Polcino, M. & Nash, G. M. Resection of the Primary Tumor in Stage IV Colorectal Cancer: When Is It Necessary? *The Surgical Clinics of North America* **97**, 657–669 (2017).
218. Kuppusamy, P., Yusoff, M. M., Maniam, G. P., Ichwan, S. J. A., Soundharrajan, I. & Govindan, N. Nutraceuticals as potential therapeutic agents for colon cancer: a review. *Acta Pharmaceutica Sinica B* **4**, 173–181 (2014).
219. Mishra, J., Drummond, J., Quazi, S. H., Karanki, S. S., Shaw, J. J., Chen, B. & Kumar, N. Prospective of colon cancer treatments and scope for combinatorial approach to enhanced cancer cell apoptosis. *Critical Reviews in Oncology/Hematology* **86**, 232–250 (2013).
220. Mehta, A. & Patel, B. M. Therapeutic opportunities in colon cancer: Focus on phosphodiesterase inhibitors. *Life Sciences* **230**, 150–161 (2019).
221. Ye, C., Xu, M., Lin, M., Zhang, Y., Zheng, X., Sun, Y., Deng, Y., Pan, J., Xu, Z., Lu, X. & Chi, P. Overexpression of FZD7 is associated with poor survival in patients with colon cancer. *Pathology - Research & Practice* **215**, 152478 (2019).
222. Xie, Q., Liu, Y. & Li, X. The interaction mechanism between autophagy and apoptosis in colon cancer. *Translational Oncology* **13**, 100871 (2020).
223. Wanebo, H. J., Rao, B., Pinsky, C. M., Hoffman, R. G., Stearns, M., Schwartz, M. K. & Oettgen, H. F. Preoperative Carcinoembryonic Antigen Level as a Prognostic Indicator in Colorectal Cancer. *New England Journal of Medicine* **299**, 448–451 (1978).
224. Wolmark, N., Fisher, B., Wieand, H. S., Henry, R. S., Lerner, H., Legault-Poisson, S., Deckers, P. J., Dimitrov, N., Gordon, P. H., Jochimsen, P. & al., et. The prognostic significance of preoperative carcinoembryonic antigen levels in colorectal cancer. Results from NSABP (National Surgical Adjuvant Breast and Bowel Project) clinical trials. *Annals of Surgery* **199**, 375–382 (1984).
225. Moertel, C.G., Fleming, T.R., Macdonald, J.S., Haller, D.G., Laurie, J.A., Tangen, C.M., Ungerleider, J.S., Emerson, W.A., Tormey, D.C. & Glick, J. H. Intergroup study of fluorouracil plus levamisole as adjuvant therapy for stage II/Dukes' B2 colon cancer. *Journal of Clinical Oncology* **13**, 2936–2943. (1995).
226. Krasna, M.J., Flancbaum, L., Cody, R.P., Shneibaum, S. & Ari, G. B. Vascular and neural invasion in colorectal carcinoma. Incidence and prognostic significance. *Cancer* **61**, 1018–1023 (1988).
227. Li, R. W. & Sperling, A. K. Drug Resistance. in *Brenner's Encyclopedia of*

Genetics (eds. Maloy, S. & Hughes, K. B. T.-B. E. of G. (Second E.) 418–420 (Academic Press, 2013). doi:https://doi.org/10.1016/B978-0-12-374984-0.00449-6.

228. Gottesman, M. M., Fojo, T. & Bates, S. E. Multidrug resistance in cancer: role of ATP–dependent transporters. *Nature Reviews Cancer* **2**, 48–58 (2002).

229. Singh, A. & Amiji, M. M. Combinatorial Approach in Rationale Design of Polymeric Nanomedicines for Cancer. in *Biomedical Applications of Functionalized Nanomaterials* (eds. Sarmento, B. & das Neves, J. B. T.-B. A. of F. N.) 371–398 (Elsevier, 2018). doi:https://doi.org/10.1016/B978-0-323-50878-0.00013-6.

230. Longley, D.B. & Johnston, P. G. Molecular mechanisms of drug resistance. *The Journal of Pathology: A Journal of the Pathological Society of Great Britain & Ireland* **205**, 275–292 (2005).

231. Tejpar, S., Prenen, H. & Mazzone, M. Overcoming resistance to antiangiogenic therapies. *The Oncologist* **17**, 1039 (2012).

232. Iyer, A. K., Singh, A., Ganta, S. & Amiji, M. M. Role of integrated cancer nanomedicine in overcoming drug resistance. *Advanced Drug Delivery Reviews* **65**, 1784–1802 (2013).

233. Xie, Y.-H., Chen, Y.-X. & Fang, J.-Y. Comprehensive review of targeted therapy for colorectal cancer. *Signal Transduction & Targeted Therapy* **5**, 22 (2020).

234. Gunes, A., Coskun, U., Boruban, C., Gunel, N., Babaoglu, M. O., Sencan, O., Bozkurt, A., Rane, A., Hassan, M., Zengil, H. & Yasar, U. Inhibitory effect of 5-fluorouracil on cytochrome P450 2C9 activity in cancer patients. *Basic & Clinical Pharmacology & Toxicology* **98**, 197–200 (2006).

235. Miyazaki, S., Satoh, H., Ikenishi, M., Sakurai, M., Ueda, M., Kawahara, K., Ueda, R., Ohtori, T., Matsuyama, K., Miki, A., Hori, S., Fukui, E., Nakatsuka, E. & Sawada, Y. Pharmacokinetic model analysis of interaction between phenytoin and capecitabine. *International Journal of Clinical Pharmacology & Therapeutics* **54**, 657–665 (2016).

236. Meunier, L. & Larrey, D. Chemotherapy-associated steatohepatitis. *Annals of Hepatology* (2020) doi:https://doi.org/10.1016/j.aohep.2019.11.012.

237. Zhang, N., Yin, Y., Xu, S.-J. & Chen, W.-S. 5-Fluorouracil: mechanisms of resistance and reversal strategies. *Molecules* **13**, 1551–1569 (2008).

238. Kwok, K. K., Vincent, E. C. & Gibson, J. N. Antineoplastic Drugs. in

Pharmacology & Therapeutics for Dentistry (eds. Dowd, F. J., Johnson, B. S. & Mariotti, A. J. B. T.-P. and T. for D. (Seventh E.) 530–562 (Mosby, 2017). doi:https://doi.org/10.1016/B978-0-323-39307-2.00036-9.

239. Latchman, J., Guastella, A. & Tofthagen, C. 5-Fluorouracil toxicity and dihydropyrimidine dehydrogenase enzyme: implications for practice. *Clinical Journal of Oncology Nursing* **18**, 581–585 (2014).
240. Kholodar, S. A., Ghosh, A. K., Świderek, K., Moliner, V. & Kohen, A. Parallel reaction pathways and noncovalent intermediates in thymidylate synthase revealed by experimental and computational tools. *Proceedings of the National Academy of Sciences* **115**, 10311 LP – 10314 (2018).
241. Parker, W. B. & Cheng, Y. C. Metabolism and mechanism of action of 5-fluorouracil. *Pharmacology & Therapeutics* **48**, 381–395 (1990).
242. Longley, D. B., Latif, T., Boyer, J., Allen, W. L., Maxwell, P. J. & Johnston, P. G. The interaction of thymidylate synthase expression with p53-regulated signaling pathways in tumor cells. *Seminars in Oncology* **30**, 3–9 (2003).
243. Saif, M. W., Syrigos, K. N. & Katirtzoglou, N. A. S-1: a promising new oral fluoropyrimidine derivative. *Expert Opinion on Investigational Drugs* **18**, 335–348 (2009).
244. Koriem, K. M. M. Protective effect of natural products and hormones in colon cancer using metabolome: A physiological overview. *Asian Pacific Journal of Tropical Biomedicine* **7**, 957–966 (2017).
245. Henricks, L. M., Opdam, F. L., Beijnen, J. H., Cats, A. & Schellens, J. H. M. DPYD genotype-guided dose individualization to improve patient safety of fluoropyrimidine therapy: call for a drug label update. *Annals of Oncology* **28**, 2915–2922 (2017).
246. Chandran, S. P., Natarajan, S. B., Chandraseharan, S. & Mohd Shahimi, M. S. B. Nano drug delivery strategy of 5-fluorouracil for the treatment of colorectal cancer. *Journal of Cancer Research & Practice* **4**, 45–48 (2017).
247. Flis, S. Inhibitory Effects of 5-Fluorouracil and Oxaliplatin on Human Colorectal Cancer Cell Survival Are Synergistically Enhanced by Sulindac Sulfide. *Anticancer Research* **442**, 435–441 (2009).
248. Khoo, E., O'Neill, S., Brown, E., Wigmore, S. J. & Harrison, E. M. Systematic review of systemic adjuvant, neoadjuvant and perioperative chemotherapy for resectable colorectal-liver metastases. *Hepato-Pancreato-Biliary* **18**, 485–493

(2016).

249. Gelibter, A. J., Caponnetto, S., Urbano, F., Emiliani, A., Scagnoli, S., Sirgiovanni, G., Napoli, V. M. & Cortesi, E. Adjuvant chemotherapy in resected colon cancer: When, how and how long? *Surgical Oncology* **30**, 100–107 (2019).

250. Hewlings, S. J. & Kalman, D. S. Curcumin: A Review of Its Effects on Human Health. *Foods* **6**, 92 (2017).

251. Dudeja, P. & Gupta, R. K. Nutraceuticals. in *Food Safety in the 21st Century* (eds. Gupta, R. K., Dudeja & Singh Minhas, B. T.-F. S. in the 21st C.) 491–496 (Academic Press, 2017). doi:https://doi.org/10.1016/B978-0-12-801773-9.00040-6.

252. Besson, A. and Yong, V. W. Mitogenic signaling and the relationship to cell cycle regulation in astrocytomas. *Journal of Neuro-Oncology* **51**, 245–264 (2001).

253. Duronio, R. J. & Xiong, Y. Signaling pathways that control cell proliferation. *Cold Spring Harbor Perspectives in Biology* **5**, a008904–a008904 (2013).

254. Guertin, D. A. & Sabatini, D. M. Cell Growth. in *The Molecular Basis of Cancer* (eds. Mendelsohn, J., Gray, J. W., Howley, P. M., Israel, M. A. & Thompson, C. B. B. T.-T. M. B. of C. (Fourth E.) 179-190.e1 (W.B. Saunders, 2015). doi:https://doi.org/10.1016/B978-1-4557-4066-6.00012-3.

255. Cooper, G. M. The Eukaryotic Cell Cycle. in *The Cell: A Molecular Approach.* (Sunderland (MA): Sinauer Associates, 2000).

256. Fang, H.S., Lang, M.F. & Sun, J. New Methods for Cell Cycle Analysis. *Chinese Journal of Analytical Chemistry* **47**, 1293–1301 (2019).

257. Kalucka, J., Missiaen, R., Georgiadou, M., Schoors, S., Lange, C., De Bock, K., Dewerchin, M. & Carmeliet, P. Metabolic control of the cell cycle. *Cell cycle* **14**, 3379

258. Alam, M. S., Hossain, M. A., Algoul, S., Majumader, M. A. A., Al-Mamun, M. A., Sexton, G. & Phillips, R. Multi-objective multi-drug scheduling schemes for cell cycle specific cancer treatment. *Computers & Chemical Engineering* **58**, 14–32 (2013).

259. T-Johari, S. A. T., Hashim, F., Ismail, W. I. & Ali, A. M. Combinatorial Cytotoxic Effects of Gelam Honey and 5-Fluorouracil against Human Adenocarcinoma Colon Cancer HT-29 Cells *In Vitro*. *International Journal of Cell Biology* **2019**, 3059687 (2019).

260. Darling, S., Fielding, A. B., Sabat-Pośpiech, D., Prior, I. A. & Coulson, J. M.

Regulation of the cell cycle and centrosome biology by deubiquitylases. *Biochemical Society Transactions* **45**, 1125–1136 (2017).

261. O'Connor, C. Cell Division: Stages of Mitosis. *Nature Education* **1**, 188 (2008).
262. Lodish, H., Berk, A., Zipursky, S. L., Matsudaira, P., Baltimore, D. & Darnell, J. The Life Cycle of Cells. in *Molecular Cell Biology.* (Fourth E.) (W.H. Freeman) Available from: https://www.ncbi.nlm.nih.gov/books/NBK21475/ (2000).
263. Chao, H. X., Poovey, C. E., Privette, A. A., Grant, G. D., Chao, H. Y., Cook, J. G. & Purvis, J. E. Orchestration of DNA Damage Checkpoint Dynamics across the Human Cell Cycle. *Cell Systems* **5**, 445-459 .e5 (2017).
264. Balounová, K., Soták, M., Ergang, P., Vodička, M., Vagnerová, K. & Pácha, J. Effects of aging and tumorigenesis on coupling between the circadian clock and cell cycle in colonic mucosa. *Mechanisms of Ageing & Development* **190**, 111317 (2020).
265. Ahmad, I., Fakhri, S., Khan, H., Jeandet, P., Aschner, M. & Yu, Z.-L. Targeting cell cycle by β-carboline alkaloids *in vitro*: Novel therapeutic prospects for the treatment of cancer. *Chemico-Biological Interactions* **109229** (2020) doi:https://doi.org/10.1016/j.cbi.2020.109229.
266. Khan, A., Singh, P. & Srivastava, A. Iron: Key player in cancer and cell cycle? *Journal of Trace Elements in Medicine & Biology* **62**, 126582 (2020).
267. Barnum, K. J. & O'Connell, M. J. Cell cycle regulation by checkpoints. *Methods in Molecular Biology* **1170**, 29–40 (2014).
268. Martínez-Alonso, D. & Malumbres, M. Mammalian cell cycle cyclins. *Seminars in Cell & Developmental Biology* (2020) doi:https://doi.org/10.1016/j.semcdb. 2020.03.009.
269. Visconti, R., Della Monica, R. & Grieco, D. Cell cycle checkpoint in cancer: a therapeutically targetable double-edged sword. *Journal of Experimental & Clinical Cancer Research* **35**, 153 (2016).
270. Bertoli, C., Skotheim, J. M. & de Bruin, R. A. M. Control of cell cycle transcription during G1 and S phases. *Nature reviews. Molecular Cell Biology* **14**, 518–528 (2013).
271. Ding, L., Cao, J., Lin, W., Chen, H., Xiong, X., Ao, H., Yu, M., Lin, J. & Cui, Q. The Roles of Cyclin-Dependent Kinases in Cell-Cycle Progression and Therapeutic Strategies in Human Breast Cancer. *International Journal of Molecular Sciences* **21**, 1960 (2020).

272. Li, J. & Stanger, B. Z. Cell Cycle Regulation Meets Tumor Immunosuppression. *Trends in Immunology* (2020) doi:https://doi.org/10.1016/j.it.2020.07.010.
273. Betharia, S., Farris, F. F., Corcoran, G. B. & Ray, S. D. Mechanisms of Toxicity. in *Encyclopedia of Toxicology* (ed. Wexler, P. B. T.-E. of T. (Third E.) 165–175 (Academic Press, 2014). doi:https://doi.org/10.1016/B978-0-12-386454-3.00329-8.
274. Liu, S.-T. & Zhang, H. The mitotic checkpoint complex (MCC): looking back and forth after 15 years. *AIMS Molecular Science* **3**, 597–634 (2016).
275. Nowsheen, S. & Yang, E. S. The intersection between DNA damage response and cell death pathways. *Experimental Oncology* **34**, 243–254 (2012).
276. Green, D. R. *Means to an End: Apoptosis and Other Cell Death Mechanisms*. (Cold Spring Harbor Laboratory Press, 2011).
277. Norbury, C. J. & Hickson, I. D. Cellular Responses to DNA Damage. *Annual Review of Pharmacology & Toxicology* **41**, 367–401 (2001).
278. Kerr, J. F., Wyllie, A. H. & Currie, A. R. Apoptosis: a basic biological phenomenon with wide-ranging implications in tissue kinetics. *British Journal of Cancer* **26**, 239–257 (1972).
279. Kamiński, M., Karbowski, M., Miyazaki, Y., Kędzior, J., Spodnik, J.H., Gil, A., Woźniak, M. & Wakabayashi, T. Co-existence of apoptotic and necrotic features within one single cell as a result of menadione treatment. *Folia Morphologica* **61**, 217–220 (2002).
280. Kroemer, G., El-Deiry, W. S., Golstein, P., Peter, M. E., Vaux, D., Vandenabeele, P., Zhivotovsky, B., Blagosklonny, M. V, Malorni, W., Knight, R. A., Piacentini, M., Nagata, S. & Melino, G. Classification of cell death: recommendations of the Nomenclature Committee on Cell Death. *Cell Death & Differentiation* **12**, 1463–1467 (2005).
281. Sorenson, C. M. Life, death and kidneys: regulation of renal programmed cell death. *Current Opinion in Nephrology & Hypertension* **7**, (1998).
282. Savill, J. Apoptosis and the kidney. *Journal of the American Society of Nephrology* **5**, 12–21 (1994).
283. Hammerman, M. R. Renal programmed cell death and the treatment of renal disease. *Current Opinion in Nephrology & Hypertension* **7**, (1998).
284. Lockshin, R. A. Early work on apoptosis, an interview with Richard Lockshin. *Cell Death & Differentiation* **15**, 1091–1095 (2008).

285. Lopez, J. & Tait, S. W. G. Mitochondrial apoptosis: killing cancer using the enemy within. *British Journal of Cancer* **112**, 957–962 (2015).
286. Green, D. R. Apoptotic Pathways: The Roads to Ruin. *Cell* **94**, 695–698 (1998).
287. Eldadah, B. A. & Faden, A. I. Caspase Pathways, Neuronal Apoptosis, and CNS Injury. *Journal of Neurotrauma* **17**, 811–829 (2000).
288. O'Brien, M. A. & Kirby, R. Apoptosis: A review of pro-apoptotic and anti-apoptotic pathways and dysregulation in disease. *Journal of Veterinary Emergency &d Critical Care* **18**, 572–585 (2008).
289. Shamas-Din, A., Kale, J., Leber, B. & Andrews, D. W. Mechanisms of action of Bcl-2 family proteins. *Cold Spring Harbor Perspectives in Biology* **5**, a008714–a008714 (2013).
290. Taylor, R. C., Cullen, S. P. & Martin, S. J. Apoptosis: controlled demolition at the cellular level. *Nature Reviews Molecular Cell Biology* **9**, 231 (2008).
291. Ke, N., Godzik, A. & Reed, J. C. Bcl-B, a Novel Bcl-2 Family Member That Differentially Binds and Regulates Bax and Bak. *Journal of Biological Chemistry* **276**, 12481–12484 (2001).
292. Minn, A. J., Vélez, P., Schendel, S. L., Liang, H., Muchmore, S. W., Fesik, S. W., Fill, M. & Thompson, C. B. Bcl-xL forms an ion channel in synthetic lipid membranes. *Nature* **385**, 353–357 (1997).
293. Karp, G. *Cell and molecular biology: concepts and experiments.* (John Wiley & Sons., 2009).
294. Tsujimoto, Y., Finger, L. R., Yunis, J., Nowell, P. C. & Croce, C. M. Cloning of the chromosome breakpoint of neoplastic B cells with the t(14;18) chromosome translocation. *Science* **226**, 1097 LP – 1099 (1984).
295. Reed, J. C. October. Bcl-2 family proteins: regulators of apoptosis and chemoresistance in hematologic malignancies. *In Seminars in Hematology* **34**, 9–19 (1997).
296. Loreto, C., La Rocca, G., Anzalone, R., Caltabiano, R., Vespasiani, G., Castorina, S., Ralph, D. J., Cellek, S., Musumeci, G., Giunta, S., Djinovic, R., Basic, D. & Sansalone, S. The Role of Intrinsic Pathway in Apoptosis Activation and Progression in Peyronie's Disease. *BioMed Research International* **2014**, 616149 (2014).
297. Walia, R., Madaan, R., Chaudhary, K., Mehta, B. & Bala, R. Molecular pathways of apoptotic cell death. in *Clinical Perspectives and Targeted Therapies*

in Apoptosis (eds. Sodhi, R. K. & Madan, J. B. T.-C. P. and T. T. in A.) 79–109 (Academic Press, 2021). doi:https://doi.org/10.1016/B978-0-12-815762-6.00003-2.

298. Poot, M. & Pierce, R. H. Detection of changes in mitochondrial function during apoptosis by simultaneous staining with multiple fluorescent dyes and correlated multiparameter flow cytometry. *Cytometry* **35**, 311–317 (1999).
299. Adrain, C., Creagh, E. M. & Martin, S. J. Apoptosis-associated release of Smac/DIABLO from mitochondria requires active caspases and is blocked by Bcl-2. *The European Molecular Biology Organization Journal* **20**, 6627–6636 (2001).
300. Vande Walle, L., Lamkanfi, M. & Vandenabeele, P. The mitochondrial serine protease HtrA2/Omi: an overview. *Cell Death & Differentiation* **15**, 453–460 (2008).
301. Liu, X., Kim, C. N., Yang, J., Jemmerson, R. & Wang, X. Induction of Apoptotic Program in Cell-Free Extracts: Requirement for dATP and Cytochrome c. *Cell* **86**, 147–157 (1996).
302. Nakayama, K., Nakayama, K., Negishi, I., Kuida, K., Sawa, H. & Loh, D. Y. Targeted disruption of Bcl-2 alpha beta in mice: occurrence of gray hair, polycystic kidney disease, and lymphocytopenia. *Proceedings of the National Academy of Sciences of the United States of America* **91**, 3700–3704 (1994).
303. Nuñez, G., Benedict, M. A., Hu, Y. & Inohara, N. Caspases: the proteases of the apoptotic pathway. *Oncogene* **17**, 3237–3245 (1998).
304. Van Opdenbosch, N. & Lamkanfi, M. Caspases in Cell Death, Inflammation, and Disease. *Immunity* **50**, 1352–1364 (2019).
305. Chowdhury, I., Tharakan, B. & Bhat, G. K. Caspases — An update. Comparative Biochemistry and Physiology Part B*: Biochemistry & Molecular Biology* **151**, 10–27 (2008).
306. Fan, T. J., Han, L. H., Cong, R.-S. & Liang, J. Caspase Family Proteases and Apoptosis. *Acta Biochimica et Biophysica Sinica* **37**, 719–727 (2005).
307. Hengartner, M. O. Apoptosis: Corralling the Corpses. *Cell* **104**, 325–328 (2001).
308. Elmore, S. Apoptosis: a review of programmed cell death. *Toxicologic Pathology* **35**, 495–516 (2007).
309. Reed, J. C. Mechanisms of apoptosis. *The American Journal of Pathology* **157**, 1415–1430 (2000).

310. Kang, T.-B., Ben-Moshe, T., Varfolomeev, E. E., Pewzner-Jung, Y., Yogev, N., Jurewicz, A., Waisman, A., Brenner, O., Haffner, R., Gustafsson, E., Ramakrishnan, P., Lapidot, T. & Wallach, D. Caspase-8 Serves Both Apoptotic and Nonapoptotic Role
311. Wajant, H. The Fas signaling pathway: more than a paradigm. *Science* **296**, 1635–1636 (2002).
312. Kischkel, F. C., Hellbardt, S., Behrmann, I., Germer, M., Pawlita, M., Krammer, P. H. & Peter, M. E. Cytotoxicity-dependent APO-1 (Fas/CD95)-associated proteins form a death-inducing signaling complex (DISC) with the receptor. *The European Molecular Biology Organization Journal* **14**, 5579–5588 (1995).
313. Slee, E. A., Adrain, C. & Martin, S. J. Executioner Caspase-3, -6, and -7 Perform Distinct, Non-redundant Roles during the Demolition Phase of Apoptosis*. *Journal of Biological Chemistry* **276**, 7320–7326 (2001).
314. Ashkenazi, A. & Dixit, V. M. Death Receptors: Signaling and Modulation. *Science* **281**, 1305 LP – 1308 (1998).
315. Sakahira, H., Enari, M. & Nagata, S. Cleavage of CAD inhibitor in CAD activation and DNA degradation during apoptosis. *Nature* **391**, 96–99 (1998).
316. Green, D. R. Apoptotic Pathways: Paper Wraps Stone Blunts Scissors. *Cell* **102**, 1–4 (2000).
317. Salvesen, G. S. & Dixit, V. M. Caspases: Intracellular Signaling by Proteolysis. *Cell* **91**, 443–446 (1997).
318. Fraser, A. & Evan, G. A License to Kill. *Cell* **85**, 781–784 (1996).
319. Ghobrial, I. M., Witzig, T. E. & Adjei, A. A. Targeting Apoptosis Pathways in Cancer Therapy. *CA: A Cancer Journal for Clinicians* **55**, 178–194 (2005).
320. Arandjelovic, S. & Ravichandran, K. S. Phagocytosis of apoptotic cells in homeostasis. *Nature Immunology* **16**, 907–917 (2015).
321. Martinvalet, D., Zhu, P. & Lieberman, J. Granzyme A Induces Caspase-Independent Mitochondrial Damage, a Required First Step for Apoptosis. *Immunity* **22**, 355–370 (2005).
322. Perry, J. J. P., Shin, D. S., Getzoff, E. D. & Tainer, J. A. The structural biochemistry of the superoxide dismutases. *Biochimica et Biophysica Acta - Proteins & Proteomics* **1804**, 245–262 (2010).
323. Liou, G.-Y. & Storz, P. Reactive oxygen species in cancer. *Free Radical Research* **44**, 479–496 (2010).

324. Agarwal, A., Kasinathan, A., Ganesan, R., Balasubramanian, A., Bhaskaran, J., Suresh, S., Srinivasan, R., Aravind, K. B. & Sivalingam, N. Curcumin induces apoptosis and cell cycle arrest via the activation of reactive oxygen species–independent mitochondrial apoptotic pathway in Smad4 and p53 mutated colon adenocarcinoma HT29 cells. *Nutrition Research* **51**, 67–81 (2018).

325. Anas, A. A., Wiersinga, W. J., de Vos, A. F. & van der Poll, T. Recent insights into the pathogenesis of bacterial sepsis. *The Netherlands Journal of Medicine* **68**, 147–152 (2010).

326. Sohal, R. S., Mockett, R. J. & Orr, W. C. Mechanisms of aging: an appraisal of the oxidative stress hypothesis 1, 2. *Free Radical Biology & Medicine* **33**, 575–586 (2002).

327. Webster, N. R. & Nunn, J. F. Molecular structure of free radicals and their importance in biological reactions. *British Journal of Anaesthesia* **60**, 98–108 (1988).

328. Cadenas, E. Mitochondrial free radical production and cell signaling. *Molecular Aspects of Medicine* **25**, 17–26 (2004).

329. Pacher, P., Beckman, J. S. & Liaudet, L. Nitric oxide and peroxynitrite in health and disease. *Physiological Reviews* **87**, 315–424 (2007).

330. Aguiar, P. H. N., Furtado, C., Repolês, B. M., Ribeiro, G. A., Mendes, I. C., Peloso, E. F., Gadelha, F. R., Macedo, A. M., Franco, G. R., Pena, S. D. J., Teixeira, S. M. R., Vieira, L. Q., Guarneri, A. A., Andrade, L. O. & Machado, C. R. Oxidative stress and DNA lesions: the role of 8-oxoguanine lesions in Trypanosoma cruzi cell viability. *PLoS Neglected Tropical Diseases* **7**, e2279–e2279 (2013).

331. D'Autréaux, B. & Toledano, M. B. ROS as signalling molecules: mechanisms that generate specificity in ROS homeostasis. *Nature Reviews Molecular Cell Biology* **8**, 813–824 (2007).

332. Pryor, W. A., Houk, K. N., Foote, C. S., Fukuto, J. M., Ignarro, L. J., Squadrito, G. L. & Davies, K. J. A. Free radical biology and medicine: it's a gas, man! *American Journal of Physiology-Regulatory, Integrative & Comparative Physiology* **291**, R491–R511 (2006).

333. Valko, M. & Cronin, H. M. & M. T. D. Metals, Toxicity and Oxidative Stress. *Current Medicinal Chemistry* **12**, 1161–1208 (2005).

334. Yu, B. P. Cellular defenses against damage from reactive oxygen species.

Physiological Reviews **74**, 139–162 (1994).

335. Matés, J. M. & Sánchez-Jiménez, F. Antioxidant enzymes and their implications in pathophysiologic processes. *Frontiers in Bioscience : A Journal & Virtual library* **4**, D339–345 (1999).

336. Schrader, M. & Fahimi, H. D. Mammalian peroxisomes and reactive oxygen species. *Histochemistry & Cell Biology* **122**, 383–393 (2004).

337. Fransen, M., Nordgren, M., Wang, B. & Apanasets, O. Role of peroxisomes in ROS/RNS-metabolism: implications for human disease. *Biochimica et Biophysica Acta-Molecular Basis of Disease* **1822**, 1363–1373 (2012).

338. Matesanz, N., Lafuente, N., Azcutia, V., Martín, D., Cuadrado, A., Nevado, J., Rodríguez-Mañas, L., Sánchez-Ferrer, C. F. & Peiró, C. Xanthine oxidase-derived extracellular superoxide anions stimulate activator protein 1 activity and hypertrophy in human vascular smooth muscle via c-Jun N-terminal kinase and p38 mitogen-activated protein kinases. *Journal of Hypertension* **25**, 609–618 (2007).

339. Zangar, R. C., Davydov, D. R. & Verma, S. Mechanisms that regulate production of reactive oxygen species by cytochrome P450. *Toxicology & Applied Pharmacology* **199**, 316–331 (2004).

340. Chaudière, J. & Ferrari-Iliou, R. Intracellular Antioxidants: from Chemical to Biochemical Mechanisms. *Food and Chemical Toxicology* **37**, 949–962 (1999).

341. Li, W. G., Miller Jr, F. J., Zhang, H. J., Spitz, D. R., Oberley, L. W. & Weintraub, N. L. H(2)O(2)-induced O(2) production by a non-phagocytic NAD(P)H oxidase causes oxidant injury. *The Journal of Biological Chemistry* **276**, 29251–29256 (2001).

342. Meitzler, J. L., Antony, S., Wu, Y., Juhasz, A., Liu, H., Jiang, G., Lu, J., Roy, K. & Doroshow, J. H. NADPH oxidases: a perspective on reactive oxygen species production in tumor biology. *Antioxidants & Redox Signaling* **20**, 2873–2889 (2014).

343. Ziech, D., Franco, R., Pappa, A. & Panayiotidis, M. I. Reactive Oxygen Species (ROS)–Induced genetic and epigenetic alterations in human carcinogenesis. *Mutation Research/Fundamental & Molecular Mechanisms of Mutagenesis* **711**, 167–173 (2011).

344. Nilsson, R. & Liu, N.-A. Nuclear DNA damages generated by reactive oxygen molecules (ROS) under oxidative stress and their relevance to human cancers,

including ionizing radiation-induced neoplasia part I: Physical, chemical and molecular biology aspects. *Radiation Medicine & Protection* **1**, 140–152 (2020).

345. Cairns, R.A., Harris, I.S. & Mak, T. W. Regulation of cancer cell metabolism. *Nature Reviews Cancer* **11**, 85–95 (2011).

346. Takahashi, A., Ohtani, N., Yamakoshi, K., Iida, S., Tahara, H., Nakayama, K., Nakayama, K. I., Ide, T., Saya, H. & Hara, E. Mitogenic signalling and the p16INK4a–Rb pathway cooperate to enforce irreversible cellular senescence. *Nature Cell Biology* **8**, 1291–1297 (2006).

347. Lin, S., Li, Y., Zamyatnin Jr., A. A., Werner, J. & Bazhin, A. V. Reactive oxygen species and colorectal cancer. *Journal of Cellular Physiology* **233**, 5119–5132 (2018).

348. Dahlgren, C. & Karlsson, A. Respiratory burst in human neutrophils. *Journal of Immunological Methods* **232**, 3–14 (1999).

349. Zhang, J., Wang, X., Vikash, V., Ye, Q., Wu, D., Liu, Y. & Dong, W. ROS and ROS-Mediated Cellular Signaling. *Oxidative Medicine & Cellular Longevity* **2016**, 4350965 (2016).

350. Redza-Dutordoir, M. & Averill-Bates, D. A. Activation of apoptosis signalling pathways by reactive oxygen species. *Biochimica et Biophysica Acta - Molecular Cell Research* **1863**, 2977–2992 (2016).

351. Simon, H.-U., Haj-Yehia, A. & Levi-Schaffer, F. Role of reactive oxygen species (ROS) in apoptosis induction. *Apoptosis* **5**, 415–418 (2000).

352. Kharbanda, S., Pandey, P., Schofield, L., Israels, S., Roncinske, R., Yoshida, K., Bharti, A., Yuan, Z.-M., Saxena, S., Weichselbaum, R., Nalin, C. & Kufe, D. Role for Bcl-xL as an inhibitor of cytosolic cytochrome C accumulation in DNA damage-induced apoptosis. *Proceedings of the National Academy of Sciences* **94**, 6939 LP–6942 (1997).

353. Kluck, R. M., Bossy-Wetzel, E., Green, D. R. & Newmeyer, D. D. The Release of Cytochrome c from Mitochondria: A Primary Site for Bcl-2 Regulation of Apoptosis. *Science* **275**, 1132 LP–1136 (1997).

354. Hockenbery, D. M., Oltvai, Z. N., Yin, X.-M., Milliman, C. L. & Korsmeyer, S. J. Bcl-2 functions in an antioxidant pathway to prevent apoptosis. *Cell* **75**, 241–251 (1993).

355. Kane, D. J., Sarafian, T. A., Anton, R., Hahn, H., Gralla, E. B., Valentine, J. S., Ord, T. & Bredesen, D. E. Bcl-2 inhibition of neural death: decreased generation

of reactive oxygen species. *Science* **262**, 1274 LP–1277 (1993).

356. Gottlieb, E., Vander Heiden, M. G. & Thompson, C. B. Bcl-x(L) prevents the initial decrease in mitochondrial membrane potential and subsequent reactive oxygen species production during tumor necrosis factor alpha-induced apoptosis. *Molecular & Cellular Biology* **20**, 5680–5689 (2000).
357. Li, P.-F., Dietz, R. & von Harsdorf, R. p53 regulates mitochondrial membrane potential through reactive oxygen species and induces cytochrome c-independent apoptosis blocked by Bcl-2. *The European Molecular Biology Organization Journal* **18**, 6027–6036 (1999).
358. Hochman, A., Sternin, H., Gorodin, S., Korsmeyer, S., Ziv, I., Melamed, E. & Offen, D. Enhanced Oxidative Stress and Altered Antioxidants in Brains of Bcl-2-Deficient Mice. *Journal of Neurochemistry* **71**, 741–748 (1998).
359. Block, K. I., Koch, A. C., Mead, M. N., Tothy, P. K., Newman, R. A. & Gyllenhaal, C. Impact of antioxidant supplementation on chemotherapeutic toxicity: A systematic review of the evidence from randomized controlled trials. *International Journal of Cancer* **123**, 1227–1239 (2008).
360. Trachootham, D., Alexandre, J. & Huang, P. Targeting cancer cells by ROS-mediated mechanisms: a radical therapeutic approach? *Nature Reviews Drug Discovery* **8**, 579–591 (2009).
361. NavaneethaKrishnan, S., Rosales, J. L. & Lee, K.-Y. ROS-Mediated Cancer Cell Killing through Dietary Phytochemicals. *Oxidative Medicine & Cellular Longevity* **2019**, 9051542 (2019).
362. Sosna, J., Voigt, S., Mathieu, S., Lange, A., Thon, L., Davarnia, P., Herdegen, T., Linkermann, A., Rittger, A., Chan, F. K.-M., Kabelitz, D., Schütze, S. & Adam, D. TNF-induced necroptosis and PARP-1-mediated necrosis represent distinct routes to programmed necrotic cell death. *Cellular & Molecular Life Sciences* **71**, 331–348 (2014).
363. Hongmei, Z. Extrinsic and intrinsic apoptosis signal pathway review. *Apoptosis & Medicine*, 3–22 (2012).
364. Stanley, L. A. Drug Metabolism. in *Pharmacognosy* (eds. Badal, S. & Delgoda, R. B. T.-P.) 527–545 (Academic Press, 2017). doi:https://doi.org/10.1016/B978-0-12-802104-0.00027-5.
365. Zhou, S.F., Xue, C.C., Yu, X.Q. & Wang, G. Metabolic activation of herbal and dietary constituents and its clinical and toxicological implications: an update.

Current Drug Metabolism **8**, 526–553 (2007).

366. Ingelman-Sundberg, M., Sim, S. C., Gomez, A. & Rodriguez-Antona, C. Influence of cytochrome P450 polymorphisms on drug therapies: Pharmacogenetic, pharmacoepigenetic and clinical aspects. *Pharmacology & Therapeutics* **116**, 496–526 (2007).
367. Zanger, U. M. & Schwab, M. Cytochrome P450 enzymes in drug metabolism: Regulation of gene expression, enzyme activities, and impact of genetic variation. *Pharmacology & Therapeutics* **138**, 103–141 (2013).
368. Hannemann, F., Bichet, A., Ewen, K. M. & Bernhardt, R. Cytochrome P450 systems—biological variations of electron transport chains. *Biochimica et Biophysica Acta - General Subjects* **1770**, 330–344 (2007).
369. Rodriguez-Antona, C. & Ingelman-Sundberg, M. Cytochrome P450 pharmacogenetics and cancer. *Oncogene* **25**, 1679–1691 (2006).
370. Ding, X. & Kaminsky, L. S. Human Extrahepatic Cytochromes P450: Function in Xenobiotic Metabolism and Tissue-Selective Chemical Toxicity in the Respiratory and Gastrointestinal Tracts. *Annual Review of Pharmacology & Toxicology* **43**, 149–173 (2003).
371. Martignoni, M., Groothuis, G. M. M. & de Kanter, R. Species differences between mouse, rat, dog, monkey and human CYP-mediated drug metabolism, inhibition and induction. *Expert Opinion on Drug Metabolism & Toxicology* **2**, 875–894 (2006).
372. Bagchi, M., Zafra, S. & Bagchi, D. DNA Damage, Gene Expression, and Carcinogenesis by Organophosphates and Carbamates. in *Toxicology of Organophosphate & Carbamate Compounds* (ed. Gupta, R. C. B. T.-T. of O. & C. C.) 533–548 (Academic Press, 2006). doi:https://doi.org/10.1016/B978-012088523-7/50038-7.
373. Turpeinen, M., Hofmann, U., Klein, K., Mürdter, T., Schwab, M. & Zanger, U. M. A Predominate Role of CYP1A2 for the Metabolism of Nabumetone to the Active Metabolite, 6-Methoxy-2-naphthylacetic Acid, in Human Liver Microsomes. *Drug Metabolism and Disposition* **37**, 1017 LP – 1024 (2009).
374. Corral, P. A., Botello, J. F. & Xing, C. Design, synthesis, and enzymatic characterization of quinazoline-based CYP1A2 inhibitors. *Bioorganic & Medicinal Chemistry Letters* **30**, 126719 (2020).
375. Hecht, S. S. Biochemistry, Biology, and Carcinogenicity of Tobacco-Specific N-

Nitrosamines. *Chemical Research in Toxicology* **11**, 559–603 (1998).

376. Eichelbaum, M. & Gross, A. S. The genetic polymorphism of debrisoquine/sparteine metabolism — Clinical aspects. *Pharmacology & Therapeutics* **46**, 377–394 (1990).
377. Reyhanoglu G, & Tadi, P. Etoposide. *StatPearls* https://www.ncbi.nlm.nih.gov/books/NBK557864/ (2020).
378. Bachelot, A., Chabbert-Buffet, N., Salenave, S., Kerlan, V. & Galand-Portier, M.-B. Anti-androgen Treatments. *Annales d'Endocrinologie* **71**, 19–24 (2010).
379. Huang, W.-Y., Ho, C.-L., Lee, C.-C., Hsiao, C.-W., Wu, C.-C., Jao, S.-W., Yang, J.-F., Lo, C.-H. & Chen, J.-H. Oral tegafur-uracil as metronomic therapy following intravenous FOLFOX for stage III colon cancer. *Plos one* **12**, e0174280–e0174280 (2017).
380. Bapiro, T. E., Sayi, J., Hasler, J. A., Jande, M., Rimoy, G., Masselle, A. & Masimirembwa, C. M. Artemisinin and thiabendazole are potent inhibitors of cytochrome P450 1A2 (CYP1A2) activity in humans. *European Journal of Clinical Pharmacology* **61**, 755–761 (2005).
381. Qiu, F., Wang, G., Zhao, Y., Sun, H., Mao, G., A, J. & Sun, J. Effect of danshen extract on pharmacokinetics of theophylline in healthy volunteers. *British Journal of Clinical Pharmacology* **65**, 270–274 (2008).
382. Gorski, J. C., Huang, S.-M., Pinto, A., Hamman, M. A., Hilligoss, J. K., Zaheer, N. A., Desai, M., Miller, M. & Hall, S. D. The Effect of Echinacea (Echinacea purpurea Root) on Cytochrome P450 Activity in Vivo. *Clinical Pharmacology & Therapeutics* **75**, 89–100 (2004).
383. Faber, M. S., Jetter, A. & Fuhr, U. Assessment of CYP1A2 Activity in Clinical Practice: Why, How, and When? *Basic & Clinical Pharmacology & Toxicology* **97**, 125–134 (2005).
384. Oscarson, P. Information Security Fundamentals BT - Security Education and Critical Infrastructures. in (eds. Irvine, C. & Armstrong, H.) 95–107 (Springer US, 2003).
385. Lam, Y. W. F. Chapter one - Principles of Pharmacogenomics: Pharmacokinetic, Pharmacodynamic, and Clinical Implications. in (eds. Lam, Y. W. F. & Scott, S. A. B. T.-P. (Second E.) 1–53 (Academic Press, 2019). doi:https://doi.org/10.1016/B978-0-12-812626-4.00001-2.
386. Alsanosi, S. M. M., Skiffington, C. & Padmanabhan, S. Pharmacokinetic

Pharmacogenomics. in *Handbook of Pharmacogenomics and Stratified Medicine* (ed. Padmanabhan, S. B. T.-H. of P. and S. M.) 341–364 (Academic Press, 2014). doi:https://doi.org/10.1016/B978-0-12-386882-4.00017-7.

387. Gurusamy, U. & Shewade, D. G. Pharmacogenomics in India. in (ed. Padmanabhan, S. B. T.-H. of P. and S. M.) 1037–1059 (Academic Press, 2014). doi:https://doi.org/10.1016/B978-0-12-386882-4.00046-3.
388. Wright, C. & Moore, R. D. Disulfiram treatment of alcoholism. *The American Journal of Medicine* **88**, 647–655 (1990).
389. Methoxyflurane. in *Meyler's Side Effects of Drugs* (ed. Aronson, J. K. B. T.-M. S. E. of D. (Sixteenth E.) 913 (Elsevier, 2016). doi:https://doi.org/10.1016/B978-0-444-53717-1.01061-1.
390. Lewis, D. F. V. 57 varieties: the human cytochromes P450. *Pharmacogenomics* **5**, 305–318 (2004).
391. Komatsu, H., Kinoshita, M. & Murakami, I. Neural Responses in the Retinotopic Representation of the Blind Spot in the Macaque V1 to Stimuli for Perceptual Filling-In. *The Journal of Neuroscience* **20**, 9310 LP–9319 (2000).
392. Rettie, A. E. & Jones, J. P. Clinical and toxicological relevance of CYP2C9: Drug-Drug Interactions and Pharmacogenetics. *Annual Review of Pharmacology & Toxicology* **45**, 477–494 (2004).
393. Soars, M. G., Gelboin, H. V, Krausz, K. W. & Riley, R. J. A comparison of relative abundance, activity factor and inhibitory monoclonal antibody approaches in the characterization of human CYP enzymology. *British Journal of Clinical Pharmacology* **55**, 175–181 (2003).
394. Bibi, Z. Retracted : Role of cytochrome P450 in drug interactions. 1–10 (2008).
395. Pirmohamed, M. Warfarin: almost 60 years old and still causing problems. *British Journal of Clinical Pharmacology* **62**, 509–511 (2006).
396. Owattanapanich, W., Owattanapanich, N., Kungwankiattichai, S., Ungprasert, P. & Ruchutrakool, T. Efficacy and Toxicity of Idarubicin Versus High-dose Daunorubicin for Induction Chemotherapy in Adult Acute Myeloid Leukemia: A Systematic Review and Meta-analysis. *Clinical Lymphoma Myeloma & Leukemia* **18**, 8148–21.e3 (2018).
397. Rosenkranz, Bernd Fasinu and Pius Bouic, P. An Overview of the Evidence and Mechanisms of Herb–Drug Interactions. *Frontiers in Pharmacology* **3**, 69 (2012).

398. Izzo, A. A. Interactions between Herbs and Conventional Drugs: Overview of the Clinical Data. *Medical Principles & Practice* **21**, 404–428 (2012).
399. Fugh-Berman, A. Herb-drug interactions. *The Lancet* **355**, 134–138 (2000).
400. Izzo, A. A. Herb–drug interactions: an overview of the clinical evidence. *Fundamental & Clinical Pharmacology* **19**, 1–16 (2005).
401. Richens, A. Pharmacokinetic and pharmacodynamic drug interactions during treatment with vigabatrin. *Acta Neurologica Scandinavica* **92**, 43–46 (1995).
402. Meng, Q. & Liu, K. Pharmacokinetic interactions between herbal medicines and prescribed drugs: focus on drug metabolic enzymes and transporters. *Current Drug Metabolism* **15**, 791—807 (2014).
403. Sharma, R. A., McLelland, H. R., Hill, K. A., Ireson, C. R., Euden, S. A., Manson, M. M., Pirmohamed, M., Marnett, L. J., Gescher, A. J. & Steward, W. P. Pharmacodynamic and Pharmacokinetic Study of Oral Curcuma Extract in Patients with Colorectal Cancer. *Clinical Cancer Research* **7**, 1894 LP – 1900 (2001).
404. Zhou, S.-F. Structure, function and regulation of P-glycoprotein and its clinical relevance in drug disposition. *Xenobiotica* **38**, 802–832 (2008).
405. Dean, M., Hamon, Y. & Chimini, G. The human ATP-binding cassette (ABC) transporter superfamily. *Journal of Lipid Research* **42**, 1007–1017 (2001).
406. Thiebaut, F., Tsuruo, T., Hamada, H., Gottesman, M. M., Pastan, I. & Willingham, M. C. Cellular localization of the multidrug-resistance gene product P-glycoprotein in normal human tissues. *Proceedings of the National Academy of Sciences of the United States of America* **84**, 7735–7738 (1987).
407. Tian, X., Li, Z., Lin, Y., Chen, M., Pan, G. & Huang, C. Study on the PK profiles of magnoflorine and its potential interaction in Cortex phellodendri decoction by LC-MS/MS. *Analytical and Bioanalytical Chemistry* **406**, 841–849 (2014).
408. Ma, J., Zheng, L., Deng, T., Li, C.-L., He, Y.-S., Li, H.-J. & Li, P. Stilbene glucoside inhibits the glucuronidation of emodin in rats through the down-regulation of UDP-glucuronosyltransferases 1A8: Application to a drug–drug interaction study in Radix Polygoni Multiflori. *Journal of Ethnopharmacology* **147**, 335–340 (2013).
409. Sun, S., Wang, Y., Wu, A., Ding, Z. & Liu, X. Influence Factors of the Pharmacokinetics of Herbal Resourced Compounds in Clinical Practice. *Evidence-Based Complementary & Alternative Medicine* **2019**, 1983780 (2019).

410. Thummel, K. E. Gut instincts: CYP3A4 and intestinal drug metabolism. *The Journal of Clinical Investigation* **117**, 3173–3176 (2007).

411. Thummel, K. E., Kunze, K. L. & Shen, D. D. Enzyme-catalyzed processes of first-pass hepatic and intestinal drug extraction. *Advanced Drug Delivery Reviews* **27**, 99–127 (1997).

412. Martignoni, M., Groothuis, G. & de Kanter, R. Comparison of mouse and rat cytochrome p450-mediated metabolism in liver and intestine. *Drug Metabolism and Disposition* **34**, 1047 LP – 1054 (2006).

413. Pal, D. & Mitra, A. K. MDR- and CYP3A4-mediated drug–herbal interactions. *Life Sciences* **78**, 2131–2145 (2006).

414. Morgan, D. J. Clinical Pharmacokinetics of β-Agonists. *Clinical Pharmacokinetics* **18**, 270–294 (1990).

415. Lázaro, E., Lowe, P. J., Briand, X. & Faller, B. New Approach To Measure Protein Binding Based on a Parallel Artificial Membrane Assay and Human Serum Albumin. *Journal of Medicinal Chemistry* **51**, 2009–2017 (2008).

416. Kratochwil, N. A., Huber, W., Müller, F., Kansy, M. & Gerber, P. R. Predicting plasma protein binding of drugs: a new approach. *Biochemical Pharmacology* **64**, 1355–1374 (2002).

417. Banker, M.J. & Clark, T. H. Plasma/serum protein binding determinations. *Current Drug Metabolism* **9**, 854–859 (2008).

418. Borst, P. & Elferink, R. O. Mammalian ABC Transporters in Health and Disease. *Annual Review of Biochemistry* **71**, 537–592 (2002).

419. Alrefai, W. A. & Gill, R. K. Bile Acid Transporters: Structure, Function, Regulation and Pathophysiological Implications. *Pharmaceutical Research* **24**, 1803–1823 (2007).

420. Zhou, S.F., Liu, J.P., Wei, M.Q. & Duan, W. Role of multidrug resistance associated proteins in drug development. in *Multidrug Resistance: A Global Concern* (ed. Asad U. Khan, R. Z.) 3 (Bentham eBooks, 2012).

421. Zhou, S.F., Wang, L.L., Di, Y.M., Xue, C.C., Duan, W., Li, C.G. & Li, Y. Substrates and inhibitors of human multidrug resistance associated proteins and the implications in drug development. *Current Medicinal Chemistry* **15**, 1981–2039 (2008).

422. Maddison, J. E., Page, S. W. & Dyke, T. M. Clinical pharmacokinetics. in *Small Animal Clinical Pharmacology* (eds. Maddison, J. E., Page, S. W. & Church, D.

B. B. T.) 27–40 (W.B. Saunders, 2008). doi:https://doi.org/10.1016/B978-070202858-8.50004-X.

423. Amin, M. L. P-glycoprotein Inhibition for Optimal Drug Delivery. *Drug Target Insights* **7**, 27–34 (2013).

424. Chandrasekaran, B., Abed, S. N., Al-Attraqchi, O., Kuche, K. & Tekade, R. K. Computer-Aided Prediction of Pharmacokinetic (ADMET) Properties. in Advances in Pharmaceutical Product Development and Research. in *Advances in Pharmaceutical Product Development and Research* (ed. Tekade, R. K. B. T.) 731–755 (Academic Press, 2018). doi:https://doi.org/10.1016/B978-0-12-814421-3.00021-X.

425. Tang, H., Wu, Y., Xiao, F., Wang, B., Asenso, J., Wang, Y., Sun, W., Wang, C. & Wei, W. Regulation of CP-25 on P-glycoprotein in synoviocytes of rats with adjuvant arthritis. *Biomedicine & Pharmacotherapy* **119**, 109432 (2019).

426. Wilkens, S. Structure and mechanism of ABC transporters. *F1000Prime Reports* **7**, 14 (2015).

427. Choi, Y. H. & Yu, A.-M. ABC transporters in multidrug resistance and pharmacokinetics, and strategies for drug development. *Current Pharmaceutical Design* **20**, 793–807 (2014).

428. Esim, O., Sarper, M., Ozkan, C. K., Oren, S., Baykal, B., Savaser, A. & Ozkan, Y. Effect simultaneous delivery with P-glycoprotein inhibitor and nanoparticle administration of doxorubicin on cellular uptake and *in vitro* anticancer activity. *Saudi Pharmaceutical Journal* **28**, 465–472 (2020).

429. Nabekura, T., Kawasaki, T., Jimura, M., Mizuno, K. & Uwai, Y. Microtubule-targeting anticancer drug eribulin induces drug efflux transporter P-glycoprotein. *Biochemistry & Biophysics Reports* **21**, 100727 (2020).

430. Ma, Y., Wang, Y., Xu, Z., Wang, Y., Fallon, J. K. & Liu, F. Extreme low dose of 5-fluorouracil reverses MDR in cancer by sensitizing cancer associated fibroblasts and down-regulating P-gp. *PLOS ONE* **12**, e0180023 (2017).

431. Narayanan, G., Merrill, D., An, R., Nolte, D. D. & Turek, J. J. Intracellular Doppler Spectroscopy detects altered drug response in SKOV3 tumor spheroids with silenced or inhibited P-glycoprotein. *Biochemical & Biophysical Research Communications* **514**, 1154–1159 (2019).

432. Yuan, Z., Shi, X., Qiu, Y., Jia, T., Yuan, X., Zou, Y., Liu, C., Yu, H., Yuan, Y., He, X., Xu, K. & Yin, P. Reversal of P-gp-mediated multidrug resistance in colon

cancer by cinobufagin. *Oncology Reports* **37**, 1815–1825 (2017).

433. Beklen, H., Gulfidan, G., Arga, K. Y., Mardinoglu, A. & Turanli, B. Drug Repositioning for P-Glycoprotein Mediated Co-Expression Networks in Colorectal Cancer. *Frontiers in Oncology* **10**, 1273 (2020).
434. Turkmenoglu, F. P., Kutsal, Y. G., Dolgun, A. B., Diker, Y. & Baydar, T. Evaluation of herbal product use and possible herb–drug interactions in Turkish elderly. *Complementary Therapies in Clinical Practice* **23**, 46–51 (2016).
435. Azwanida, N. N. A Review on the Extraction Methods Use in Medicinal Plants, Principle, Strength and Limitation. *Journal of Medicinal and Aromatic Plants* **4**, doi:10.4172/2167-0412.100019. (2015).
436. Cheng, K., Gao, H., Wang, R.-R., Liu, Y., Hou, Y.-X., Liu, X.-H., Liu, K. & Wang, W. Evaluation of Extraction and Degradation Methods to Obtain Chickpeasaponin B1 from Chickpea (Cicer arietinum L.). *Molecules* **22**, 332 (2017).
437. Kotzé, M., Eloff, J. N. & Houghton, P. J. Extraction of antibacterial compounds from Combretum microphyllum (Combretaceae). *South African Journal of Botany* **68**, 62–67 (2002).
438. Harborne, J. B. *Phytochemical methods: A guide to modern techniques of plant analysis.* (Chapman and Hall, 1998).
439. Kokate, K. C. Delhi: Vallabh Prakashan. *Practical Pharmacognosy* 218 (1997).
440. Benzie, I. F. F. & Strain, J. J. The Ferric Reducing Ability of Plasma (FRAP) as a Measure of “Antioxidant Power”: The FRAP Assay. *Analytical Biochemistry* **239**, 70–76 (1996).
441. Martínez-Maqueda, D., Miralles, B. & Recio, I. HT29 Cell Line BT - The Impact of Food Bioactives on Health: *in vitro* and *ex vivo* models. in (eds. Verhoeckx, K. et al.) 113–124 (Springer International Publishing, 2015). doi:10.1007/978-3-319-16104-4_11.
442. Hekmati, M., Ben-Shaul, Y. & Polak-Charcon, S. A morphological study of a human adenocarcinoma cell line (HT29) differentiating in culture. Similarities to intestinal embryonic development. *Cell Differentiation & Development* **31**, 207–218 (1990).
443. Le Bivic, A., Hirn, M. & Reggio, H. HT-29 cells are an *in vitro* model for the generation of cell polarity in epithelia during embryonic differentiation. *Proceedings of the National Academy of Sciences of the United States of America* **85**, 136–140 (1988).

444. de Gorter, D. J. J., van Dinther, M. & ten Dijke, P. Chapter fifteen - Measurement of Constitutive Activity of BMP Type I Receptors. in *Constitutive Activity in Receptors and Other Proteins, Part A* (ed. Conn, P. M. B. T.-M. in E.) **484**, 281–293 (Academic Press, 2010).

445. Mosmann, T. Rapid colorimetric assay for cellular growth and survival: Application to proliferation and cytotoxicity assays. *Journal of Immunological Methods* **65**, 55–63 (1983).

446. Kuete, V., Karaosmanoğlu, O. & Sivas, H. Anticancer Activities of African Medicinal Spices and Vegetables. in *Medicinal Spices and Vegetables from Africa* (ed. Kuete, V. B. T.-) 271–297 (Academic Press, 2017). doi:https://doi.org/10.1016/B978-0-12-809286-6.00010-8.

447. Wu, D. & Yotnda, P. Production and detection of reactive oxygen species (ROS) in cancers. *Journal of Visualized Experiments* **3357**, (2011) doi:10.3791/3357.

448. Sivandzade, F., Bhalerao, A. & Cucullo, L. Analysis of the Mitochondrial Membrane Potential Using the Cationic JC-1 Dye as a Sensitive Fluorescent Probe. *Bio-protocol* **9**, e3128 (2019).

449. Perelman, A., Wachtel, C., Cohen, M., Haupt, S., Shapiro, H. & Tzur, A. JC-1: alternative excitation wavelengths facilitate mitochondrial membrane potential cytometry. *Cell Death & Disease* **3**, e430–e430 (2012).

450. Schindelin, J., Arganda-Carreras, I., Frise, E., Kaynig, V., Longair, M., Pietzsch, T., Preibisch, S., Rueden, C., Saalfeld, S., Schmid, B., Tinevez, J.-Y., White, D. J., Hartenstein, V., Eliceiri, K., Tomancak, P. & Cardona, A. Fiji: an open-source platform for biological-image analysis. *Nature Methods* **9**, 676–682 (2012).

451. Hussain, H., L., S. R., Ahmad, S., Abd. Razak, M. F., Wan Mohamud, W. N., Bakar, J. & Ghazali, H. M. Determination of cell viability using acridine orange/propidium iodide dual-spectrofluorometry assay. *Cogent Food & Agriculture* **5**, 1582398 (2019).

452. Thomé, M. P., Filippi-Chiela, E. C., Villodre, E. S., Migliavaca, C. B., Onzi, G. R., Felipe, K. B. & Lenz, G. Ratiometric analysis of Acridine Orange staining in the study of acidic organelles and autophagy. *Journal of Cell Science* **129**, 4622 LP – 4632 (2016).

453. Yang, Y., Xiang, Y. & Xu, M. From red to green: the propidium iodide-permeable membrane of Shewanella decolorationis S12 is repairable. *Scientific Reports* **5**,

18583 (2015).

454. Lakshmanan, I. & Batra, S. K. Protocol for Apoptosis Assay by Flow Cytometry Using Annexin V Staining Method. *Bio-protocol* **3**, e374 (2013).

455. Pereyra-Vergara, F., Olivares-Corichi, I. M., Perez-Ruiz, A. G., Luna-Arias, J. P. & García-Sánchez, J. R. Apoptosis Induced by (-)-Epicatechin in Human Breast Cancer Cells is Mediated by Reactive Oxygen Species. *Molecules* **25**, 1020 (2020).

456. Pozarowski, P. & Darzynkiewicz, Z. Analysis of cell cycle by flow cytometry. *Checkpoint Controls & Cancer*, 301–311 (2004).

457. Wishart, D. S., Feunang, Y. D., Guo, A. C., Lo, E. J., Marcu, A., Grant, J. R., Sajed, T., Johnson, D., Li, C., Sayeeda, Z., Assempour, N., Iynkkaran, I., Liu, Y., Maciejewski, A., Gale, N., Wilson, A., Chin, L., Cummings, R., Le, D., Pon, A., Knox, C. & Wilson, M. DrugBank 5.0: a major update to the DrugBank database for 2018. *Nucleic Acids Research* **46**, D1074–D1082 (2018).

458. Venter, P., Malemela, K., Mbazima, V., Mampuru, L.J., Muller, C.J.F., & Riedel, S. An RP-LC-UV-TWIMS-HRMS and Chemometric Approach to Differentiate between *Momordica balsamina* Chemotypes from Three Different Geographical Locations in Limpopo Province of South Africa. *Molecules* **26**, (2021).

459. Ferlay, J., Colombet, M. & Soerjomataram, I. Global and Regional Estimates of the Incidence and Mortality for 38 Cancers. *GLOBOCAN 2018.* (2018).

460. Alves Martins, B. A., de Bulhões, G. F., Cavalcanti, I. N., Martins, M. M., de Oliveira, P. G. & Martins, A. M. A. Biomarkers in Colorectal Cancer: The Role of Translational Proteomics Research. *Frontiers in Oncology* **9**, 1284 (2019).

461. Qi, F., Yang, Y., Zhang, H. & Chen, H. Long non-coding RNAs: Key regulators in oxaliplatin resistance of colorectal cancer. *Biomedicine & Pharmacotherapy* **128**, 110329 (2020).

462. Longley, D. B., Harkin, D. P. & Johnston, P. G. 5-Fluorouracil: mechanisms of action and clinical strategies. *Nature Reviews Cancer* **3**, 330–338 (2003).

463. Wyatt, M. D. & Wilson 3rd, D. M. Participation of DNA repair in the response to 5-fluorouracil. *Cellular & Molecular Life Sciences* **66**, 788–799 (2009).

464. Vodenkova, S., Buchler, T., Cervena, K., Veskrnova, V., Vodicka, P. & Vymetalkova, V. 5-fluorouracil and other fluoropyrimidines in colorectal cancer: Past, present and future. *Pharmacology & Therapeutics* **206**, 107447 (2020).

465. Liu, D., Zhang, L., Duan, L., Wu, J., Hu, M., Liu, Z. & Wang, C. Potential of

herb-drug / herb interactions between substrates and inhibitors of UGTs derived from herbal medicines. *Pharmacological Research* **150**, 104510 (2019).

466. Souda, S., George, S., Mannathoko, N., Goercke, I. and Chabaesele, K. Antioxidant and Antibacterial Activity of Methanol Extract of *Momordica balsamina*. *IRA International Journal of Applied Sciences* **10**, 7–17 (2018).

467. van de Venter, M., Roux, S., Bungu, L. C., Louw, J., Crouch, N. R., Grace, O. M., Maharaj, V., Pillay, P., Sewnarian, P., Bhagwandin, N. & Folb, P. Antidiabetic screening and scoring of 11 plants traditionally used in South Africa. *Journal of Ethnopharmacology* **119**, 81–86 (2008).

468. Rocha E Silva, L. F., Ramalhete, C., Nogueira, K. L., Mulhovo, S., Ferreira, M.-J. U. & Pohlit, A. M. *In vivo* evaluation of isolated triterpenes and semi-synthetic derivatives as antimalarial agents. *European Journal of Medicinal Chemistry* **102**, 398–402 (2015).

469. Ramalhete, C., Mulhovo, S., Lage, H. & Ferreira, M.J.U. Triterpenoids from *Momordica balsamina* with a Collateral Sensitivity Effect for Tackling Multidrug Resistance in Cancer Cells. *Planta Medica* **84**, 18, 1372–1379 (2018).

470. Thakur, M., Singh, K. & Khedkar, R. Phytochemicals: Extraction process, safety assessment, toxicological evaluations, and regulatory issues. in *Functional and Preservative Properties of Phytochemicals* (ed. Prakash, B. B. T.) 341–361 (Academic Press, 2020). doi:https://doi.org/10.1016/B978-0-12-818593-3.00011-7.

471. Orlich, M. J., Siapco, G. & Jung, S. Vegetarian Diets and the Microbiome. in *Vegetarian and Plant-Based Diets in Health and Disease Prevention* (ed. Mariotti, F. B. T.) 429–461 (Academic Press, 2017). doi:https://doi.org/10.1016/B978-0-12-803968-7.00024-1.

472. Masoko, P., Mmushi, T. J., Mogashoa, M. M., Mokgotho, M. P., Mampuru, L. J. & Howard, R. L. *In vitro* evaluation of the antifungal activity of *Sclerocarya birrea* extracts against pathogenic yeasts. *African Journal of Biotechnology* **7**, 3521–3526 (2008).

473. Eloff, J. N., Ntloedibe, D. T. & van Brummelen, R. A simplified but effective method for the quality control of medicinal plants by planar chromatography. *African Journal of Traditional, Complementary, & Alternative Medicines* **8**, 1–12 (2011).

474. Zahan, S., Mowla, T.-E.-, Uddin, S. M. N., Hossain, M. K., Mannan, A. B.,

Rahman, M., Chen, U., Mazumder, T., Uddin, A. H. M. M., Arefin, S. & Hussain, M. S. Evaluation of phytochemical and pharmacological properties of seeds of *Momordica charantia*. *Avicenna Journal of Phytomedicine* **10**, 448–459 (2020).

475. Engelhardt, U. & Winterhalter, P. Countercurrent Chromatography | Flavonoids. in *Encyclopedia of Separation Science* (ed. Wilson, I. D. B. T.) 1–9 (Academic Press, 2007). doi:https://doi.org/10.1016/B978-012226770-3/10718-6.
476. Plumb, G. W., Price, K. R. & Williamson, G. Antioxidant properties of flavonol glycosides from tea. *Redox Report* **4**, 13–16 (1999).
477. Rha, C.-S., Jeong, H. W., Park, S., Lee, S., Jung, Y. S. & Kim, D.-O. Antioxidative, Anti-Inflammatory, and Anticancer Effects of Purified Flavonol Glycosides and Aglycones in Green Tea. *Antioxidants* **8**, 278 (2019).
478. Lea, M. A. Flavonol Regulation in Tumor Cells. *Journal of Cellular Biochemistry* **116**, 1190–1194 (2015).
479. Semwal, D. K., Semwal, R. B., Combrinck, S. & Viljoen, A. Myricetin: A Dietary Molecule with Diverse Biological Activities. *Nutrients* **8**, 90 (2016).
480. Nomura, S., Monobe, M., Ema, K., Matsunaga, A., Maeda-Yamamoto, M. & Horie, H. Effects of flavonol-rich green tea cultivar (*Camellia sinensis L*.) on plasma oxidized LDL levels in hypercholesterolemic mice. *Bioscience, Biotechnology, & Biochemistry* **80**, 360–362 (2016).
481. Senggunprai, L., Thammaniwit, W., Kukongviriyapan, V., Prawan, A., Kaewseejan, N. & Siriamornpun, S. *Cratoxylum formosum* Extracts Inhibit Growth and Metastasis of Cholangiocarcinoma Cells by Modulating the NF-κB and STAT3 Pathways. *Nutrition & Cancer* **68**, 328—341 (2016).
482. Fraczkowska, K., Bacia, M., Przybyło, M., Drabik, D., Kaczorowska, A., Rybka, J., Stefanko, E., Drobczynski, S., Masajada, J., Podbielska, H., Wrobel, T. & Kopaczynska, M. Alterations of biomechanics in cancer and normal cells induced by doxorubicin. *Biomedicine & Pharmacotherapy* **97**, 1195–1203 (2018).
483. Thiagarajan, S., Arapoc, D. J., Husna Shafie, N., Keong, Y. Y., Bahari, H., Adam, Z. & E, T. *Momordica charantia* (Indian and Chinese Bitter Melon) Extracts Inducing Apoptosis in Human Lung Cancer Cell Line A549 via ROS-Mediated Mitochodria Injury. *Evidence-Based Complementary & Alternative Medicine* **2019**, 2821597 (2019).
484. Ofuegbe, S.O., Oyagbemi, A.A., Omobowale, T.O., Fagbohun, O.S., Yakubu, M.A. & Adedapo, A. A. Anti-proliferative and cytotoxic effects of methanol extract

of the leaves of Momordica charantia L.(Cucurbitaceae) on vascular smooth muscle cells (VSMC) and HT-29 cell lines. *Journal of Medicinal Plants Research* **11**, 665-672 (2017).

485. Ghasemzadeh, A., Jaafar, H. Z. E., Rahmat, A. & Devarajan, T. Evaluation of Bioactive Compounds, Pharmaceutical Quality, and Anticancer Activity of Curry Leaf (*Murraya koenigii* L.). *Evidence-Based Complementary & Alternative Medicine* **2014**, 873803 (2014).
486. Nouri, Z., Fakhri, S., Nouri, K., Wallace, C. E., Farzaei, M. H. & Bishayee, A. Targeting Multiple Signaling Pathways in Cancer: The Rutin Therapeutic Approach. *Cancers* **12**, (2020).
487. Liao, W., Chen, L., Ma, X., Jiao, R., Li, X. & Wang, Y. Protective effects of kaempferol against reactive oxygen species-induced hemolysis and its antiproliferative activity on human cancer cells. *European Journal of Medicinal Chemistry* **114**, 24–32 (2016).
488. Wu, P., Meng, X., Zheng, H., Zeng, Q., Chen, T., Wang, W., Zhang, X. & Su, J. Kaempferol Attenuates ROS-Induced Hemolysis and the Molecular Mechanism of Its Induction of Apoptosis on Bladder Cancer. *Molecules* **23**, 2592 (2018).
489. Moradzadeh, M., Tabarraei, A., Sadeghnia, H. R., Ghorbani, A., Mohamadkhani, A., Erfanian, S. & Sahebkar, A. Kaempferol increases apoptosis in human acute promyelocytic leukemia cells and inhibits multidrug resistance genes. *Journal of Cellular Biochemistry* **119**, 2288–2297 (2018).
490. Riahi-Chebbi, I., Souid, S., Othman, H., Haoues, M., Karoui, H., Morel, A., Srairi-Abid, N., Essafi, M. & Essafi-Benkhadir, K. The Phenolic compound Kaempferol overcomes 5-fluorouracil resistance in human resistant LS174 colon cancer cells. *Scientific Reports* **9**, 195 (2019).
491. Jeong, J. C., Kim, M. S., Kim, T. H. & Kim, Y. K. Kaempferol Induces Cell Death Through ERK and Akt-Dependent Down-Regulation of XIAP and Survivin in Human Glioma Cells. *Neurochemical Research* **34**, 991–1001 (2009).
492. Yi, X., Zuo, J., Tan, C., Xian, S., Luo, C., Chen, S., Yu, L. & Luo, Y. Kaempferol, A Flavonoid Compound From Gynura Medica Induced Apoptosis And Growth Inhibition In MCF-7 Breast Cancer Cell. *African Journal of Traditional, Complementary, & Alternative Medicines* **13**, 210–215 (2016).
493. Li, J. G. Wang, S. D. Research progress on antitumor effect and mechanism of

isorhamnetin. *Shanxi Medical Journal* **40**, 1215–1217 (2011).

494. Yang, C.L., Wang, Z.R., Tao, D.C. and Peng, T. Effect of isorhamnetin on bcl-2 gene expression of HeLa cell. *West China Medical Journal* **1**, 196–198 (2003).

495. Wei, J., Su, H., Bi, Y., Li, J., Feng, L. & Sheng, W. Anti-proliferative effect of isorhamnetin on HeLa cells through inducing G2/M cell cycle arrest. *Experimental & Therapeutic Medicine* **15**, 3917–3923 (2018).

496. Li, C., Yang, X., Hu, J.B. & Liao, J. Z. Isorhamnetin suppresses the growth of gefitinib resistant human lung cancer PC9 cells. Journal of *Herbal Medicine* **31**, 831–834 (2012).

497. Zhu, L., Wang, Z., Zhou, L., Yang, C., Zhang, Z., Xiao, J. & Ren, F. Effects and mechanisms of isorhamnetin on lung carcinoma. *Space Medicine & Medical Engineering* **18**, 381 (2005).

498. Ruan, Y., Hu, K. & Chen, H. Autophagy inhibition enhances isorhamnetin-induced mitochondria-dependent apoptosis in non-small cell lung cancer cells. *Molecular Medicine Reports* **12**, 5796–5806 (2015).

499. Antunes-Ricardo, M., Moreno-García, B. E., Gutiérrez-Uribe, J. A., Aráiz-Hernández, D., Alvarez, M. M. & Serna-Saldivar, S. O. Induction of Apoptosis in Colon Cancer Cells Treated with Isorhamnetin Glycosides from Opuntia Ficus-indica Pads. *Plant Foods for Human Nutrition* **69**, 331–336 (2014).

500. Jaramillo, S., Lopez, S., Varela, L. M., Rodriguez-Arcos, R., Jimenez, A., Abia, R., Guillen, R. & Muriana, F. J. G. The Flavonol Isorhamnetin Exhibits Cytotoxic Effects on Human Colon Cancer Cells. *Journal of Agricultural & Food Chemistry* **58**, 10869–10875 (2010).

501. Hu, J., Zhang, Y., Jiang, X., Zhang, H., Gao, Z., Li, Y., Fu, R., Li, L., Li, J., Cui, H. & Gao, N. ROS-mediated activation and mitochondrial translocation of CaMKII contributes to Drp1-dependent mitochondrial fission and apoptosis in triple-negative breast cancer cells by isorhamnetin and chloroquine. *Journal of Experimental & Clinical Cancer Research* **38**, 225 (2019).

502. Hu, S., Huang, L., Meng, L., Sun, H., Zhang, W. & Xu, Y. Isorhamnetin inhibits cell proliferation and induces apoptosis in breast cancer via Akt and mitogen-activated protein kinase kinase signaling pathways. *Molecular Medicine Reports* **12**, 6745–6751 (2015).

503. Hu, S. & Deng, Y. C. The Mechanism of Isorhamnetin on Breast Cancer Cells. *Journal of China Pharmaceutical University* **44**, 563–567 (2013).

504. Wang, J.-L., Quan, Q., Ji, R., Guo, X.-Y., Zhang, J.-M., Li, X. & Liu, Y.-G. Isorhamnetin suppresses PANC-1 pancreatic cancer cell proliferation through S phase arrest. *Biomedicine & Pharmacotherapy* **108**, 925–933 (2018).

505. Luo, H.Q., Li, X.Y., Guan, C.N. & Lin, G. P. Effect of isorhamnetin on the growth and proliferation of nasopharyngeal carcinoma cells. *Journal of Guangdong Medical College* **29**, 119–121 (2011).

506. Chenchun, J., Yi, X. and Yong, Z. Effects of Isorhamnetin on the Proliferous Cycle and Apoptosis of Human Hepatoma HepG-2 Cells: An Experimental Study. *Journal of Military Surgeon in Southwest China* **3**, 17 (2012).

507. Li, Y.P. Wang, H. Z. The inhibitory effect of isorhamnetin on growth of human gastric carcinoma cells. *China Primary Health Care* **6**, 58–59 (2008).

508. Lin, K.-W., Yang, S.-C. & Lin, C.-N. Antioxidant constituents from the stems and fruits of *Momordica charantia*. *Food Chemistry* **127**, 609–614 (2011).

509. Liu, J.Q., Chen, J.C., Wang, C.F. and Qiu, M. H. One new cucurbitane triterpenoid from the fruits of *Momordica charantia*. *European Journal of Chemistry* **1**, 294–296 (2010).

510. Cheng, B.H., Chen, J.C., Liu, J.Q., Zhou, L. & Qiu, M. H. Cucurbitane-Type Triterpenoids from *Momordica charantia*. *Helvetica Chimica Acta* **96**, 1111–1120 (2013).

511. Harinantenaina, L., Tanaka, M., Takaoka, S., Oda, M., Mogami, O., Uchida, M. & Asakawa, Y. *Momordica charantia* Constituents and Antidiabetic Screening of the Isolated Major Compounds. *Chemical & Pharmaceutical Bulletin* **54**, 1017–1021 (2006).

512. Tan, M.-J., Ye, J.-M., Turner, N., Hohnen-Behrens, C., Ke, C.-Q., Tang, C.-P., Chen, T., Weiss, H.-C., Gesing, E.-R., Rowland, A., James, D. E. & Ye, Y. Antidiabetic Activities of Triterpenoids Isolated from Bitter Melon Associated with Activation of the AMPK Pathway. *Chemistry & Biology* **15**, 263–273 (2008).

513. Keller, A. C., Ma, J., Kavalier, A., He, K., Brillantes, A. M. B. & Kennelly, E. J. Saponins from the traditional medicinal plant *Momordica charantia* stimulate insulin secretion *in vitro*. *Phytomedicine* **19**, 32–37 (2011).

514. Liu, C.-H., Yen, M.-H., Tsang, S.-F., Gan, K.-H., Hsu, H.-Y. & Lin, C.-N. Antioxidant triterpenoids from the stems of *Momordica charantia*. *Food Chemistry* **118**, 751–756 (2010).

515. Akihisa, T., Higo, N., Tokuda, H., Ukiya, M., Akazawa, H., Tochigi, Y., Kimura,

Y., Suzuki, T. & Nishino, H. Cucurbitane-Type Triterpenoids from the Fruits of *Momordica charantia* and Their Cancer Chemopreventive Effects. *Journal of Natural Products* **70**, 1233–1239 (2007).

516. Pitchakarn, P., Ogawa, K., Suzuki, S., Takahashi, S., Asamoto, M., Chewonarin, T., Limtrakul, P. & Shirai, T. *Momordica charantia* leaf extract suppresses rat prostate cancer progression *in vitro* and *in vivo*. *Cancer Science* **101**, 2234–2240 (2010).
517. Pitchakarn, P., Suzuki, S., Ogawa, K., Pompimon, W., Takahashi, S., Asamoto, M., Limtrakul, P. & Shirai, T. Induction of G1 arrest and apoptosis in androgen- *Momordica charantia* (bitter melon) reduces obesity-associated macrophage and mast cell infiltration as well as inflammatory cytokine expression in adipose tissues dependent human prostate cancer by Kuguacin. *Cancer Letters* **306**, 142-150 (2011).
518. Hasani-Ranjbar, S., Nayebi, N., Larijani, B. & Abdollahi, M. A systematic review of the efficacy and safety of herbal medicines used in the treatment of obesity. *World Journal of Gastroenterology* **15**, 3073–3085 (2009).
519. Bao, B., Chen, Y.-G., Zhang, L., Na Xu, Y. L., Wang, X., Liu, J. & Qu, W. *Momordica charantia* (Bitter Melon) reduces obesity-associated macrophage and mast cell infiltration as well as inflammatory cytokine expression in adipose tissues. *Plos one* **8**, e84075–e84075 (2013).
520. Yasui, H., Kato, A. & Yazawa, M. Antifeedants to Armyworms, Spodoptera lituraand Pseudaletia separata,from Bitter Gourd Leaves, *Momordica charantia*. *Journal of Chemical Ecology* **24**, 803–813 (1998).
521. Phillips, D.H. and Arlt, V. M. Genotoxicity: damage to DNA and its consequences. *Molecular, Clinical & Environmental Toxicology* **1**, 87–110. (2009).
522. Fernandes de Sá Ferreira, I. C. & Ferrão Vargas, V. M. Mutagenicity of medicinal plant extracts in-Salmonella/microsome assay. *Phytotherapy Research* **13**, 397–400 (1999).
523. Barboza, G.E., Cantero, J.J., Núñez, C., Ariza Espinar, L. & Pacciaroni, A. D. V. Medicinal plants: A general review and a phytochemical and ethnopharmacological screening of the native Argentine Flora. *Museo Botanica* **34**, 1–2 (2009).
524. Sohni, Y. R., Mutangadura-Mhlanga, T. & Kale, P. G. Bacterial mutagenicity of

eight medicinal herbs from Zimbabwe. *Mutation Research/Genetic Toxicology* **322**, 133–140 (1994).

525. Basaran, A. A., Yu, T.-W., Plewa, M. J. & Anderson, D. An investigation of some Turkish herbal medicines in *Salmonella typhimurium* and in the COMET assay in human lymphocytes. *Teratogenesis, Carcinogenesis, & Mutagenesis* **16**, 125–138 (1996).
526. Romero-Jiménez, M., Campos-Sánchez, J., Analla, M., Muñoz-Serrano, A. & Alonso-Moraga, Á. Genotoxicity and anti-genotoxicity of some traditional medicinal herbs. *Mutation Research/Genetic Toxicology & Environmental Mutagenesis* **585**, 147–155 (2005).
527. Maréchal, A. & Zou, L. DNA damage sensing by the ATM and ATR kinases. *Cold Spring Harbor Perspectives in Biology* **5**, a012716 (2013).
528. Kwok, M. & Stankovic, T. Targeting the Ataxia Telangiectasia and Rad3 Signaling Pathway to Overcome Chemoresistance in Cancer. in *Cancer Sensitizing Agents for Chemotherapy* (ed. Johnson, D. E. B. T.) **3** 203–230 (Academic Press, 2019).
529. Bonner, W. M., Redon, C. E., Dickey, J. S., Nakamura, A. J., Sedelnikova, O. A., Solier, S. & Pommier, Y. γH2AX and cancer. *Nature Reviews Cancer* **8**, 957–967 (2008).
530. Palla, V.-V., Karaolanis, G., Katafigiotis, I., Anastasiou, I., Patapis, P., Dimitroulis, D. & Perrea, D. gamma-H2AX: Can it be established as a classical cancer prognostic factor? *Tumor Biology* **39**, 1010428317695931 (2017).
531. Yar Khan, H., Zubair, H., Fahad Ullah, M., Ahmad, A. & Mumtaz Hadi, S. A prooxidant mechanism for the anticancer and chemopreventive properties of plant polyphenols. *Current Drug Targets* **13**, 1738–1749 (2012).
532. Finkel, T. Signal transduction by reactive oxygen species. *Journal of Cell Biology* **194**, 7–15 (2011).
533. Mittler, R. ROS Are Good. *Trends in Plant Science* **22**, 11–19 (2017).
534. Pizzino, G., Irrera, N., Cucinotta, M., Pallio, G., Mannino, F., Arcoraci, V., Squadrito, F., Altavilla, D. & Bitto, A. Oxidative Stress: Harms and Benefits for Human Health. *Oxidative Medicine & Cellular Longevity* **2017**, 8416763 (2017).
535. Klein, J. A. & Ackerman, S. L. Oxidative stress, cell cycle, and neurodegeneration. *The Journal of Clinical Investigation* **111**, 785–793 (2003).
536. Cross, C.E., Halliwell B, Borish ET, Pryor WA, Ames BN, Saul RL, McCord JM,

and H. D. Oxygen radicals and human disease. *Annals of Internal Medicine* **107**, 526–545 (1987).

537. Chedea, V. S., Braicu, C., Chirilă, F., Ogola, H. J. O., Pelmuş, R. Ş., Călin, L. G. & Socaciu, C. Antioxidant/Prooxidant and Antibacterial/Probacterial Effects of a Grape Seed Extract in Complex with Lipoxygenase. *BioMed Research International* **2014**, 313684 (2014).

538. Aggarwal, V., Tuli, H. S., Varol, A., Thakral, F., Yerer, M. B., Sak, K., Varol, M., Jain, A., Khan, M. A. & Sethi, G. Role of Reactive Oxygen Species in Cancer Progression: Molecular Mechanisms and Recent Advancements. *Biomolecules* **9**, 735 (2019).

539. Morse, D., Lin, L., Choi, A. M. K. & Ryter, S. W. Heme oxygenase-1, a critical arbitrator of cell death pathways in lung injury and disease. *Free Radical Biology & Medicine* **47**, 1–12 (2009).

540. Ryter, S. W. & Choi, A. M. K. Heme Oxygenase-1: Redox Regulation of a Stress Protein in Lung and Cell Culture Models. *Antioxidants & Redox Signaling* **7**, 80–91 (2004).

541. Heasman, S.-A., Zaitseva, L., Bowles, K. M., Rushworth, S. A. & Macewan, D. J. Protection of acute myeloid leukaemia cells from apoptosis induced by front-line chemotherapeutics is mediated by haem oxygenase-1. *Oncotarget* **2**, 658–668 (2011).

542. Martin, D., Rojo, A. I., Salinas, M., Diaz, R., Gallardo, G., Alam, J., de Galarreta, C. M. R. & Cuadrado, A. Regulation of Heme Oxygenase-1 Expression through the Phosphatidylinositol 3-Kinase/Akt Pathway and the Nrf2 Transcription Factor in Response to the Antioxidant Phytochemical Carnosol. *Journal of Biological Chemistry* **279**, 8919–8929 (2004).

543. Wegiel, B., Nemeth, Z., Correa-Costa, M., Bulmer, A. C. & Otterbein, L. E. Heme oxygenase-1: a metabolic nike. *Antioxidants & Redox Signaling* **20**, 1709–1722 (2014).

544. Ng, C. J., Wadleigh, D. J., Gangopadhyay, A., Hama, S., Grijalva, V. R., Navab, M., Fogelman, A. M. & Reddy, S. T. Paraoxonase-2 Is a Ubiquitously Expressed Protein with Antioxidant Properties and Is Capable of Preventing Cell-mediated Oxidative Modification of Low Density Lipoprotein*. *The Journal of Biological Chemistry* **276**, 44444–44449 (2001).

545. Altenhöfer, S., Witte, I., Teiber, J. F., Wilgenbus, P., Pautz, A., Li, H., Daiber,

A., Witan, H., Clement, A. M., Förstermann, U. & Horke, S. One enzyme, two functions: PON2 prevents mitochondrial superoxide formation and apoptosis independent from its lactonase activity. *The Journal of Biological Chemistry* **285**, 24398–24403 (2010).

546. Martinelli, N., Consoli, L., Girelli, D., Grison, E., Corrocher, R. & Olivieri, O. Chapter three - Paraoxonases: Ancient Substrate Hunters and Their Evolving Role in Ischemic Heart Disease. in *Advances in Clinical Chemistry* (ed. Makowski, G. S. B. T.-A. in C. C.) **59,** 65–100 (Elsevier, 2013).

547. Xin, G., DU, J., Wang, Y.-T. & Liang, T.-T. Effect of oxidative stress on heme oxygenase-1 expression in patients with gestational diabetes mellitus. *Experimental & Therapeutic Medicine* **7**, 478–482 (2014).

548. Ulyanova, T., Szél, A., Kutty, R. K., Wiggert, B., Caffé, A. R., Chader, G. J. & van Veen, T. Oxidative Stress Induces Heme Oxygenase-1 Immunoreactivity in Müller Cells of Mouse Retina in Organ Culture. *Investigative Ophthalmology & Visual Science* **42**, 1370–1374 (2001).

549. Sommer, J., Mahli, A., Freese, K., Schiergens, T. S., Kuecuekoktay, F. S., Teufel, A., Thasler, W. E., Müller, M., Bosserhoff, A. K. & Hellerbrand, C. Analysis of molecular mechanisms of 5-fluorouracil-induced steatosis and inflammation *in vitro* and in mice. *Oncotarget* **8**, 13059–13072 (2017).

550. Numazawa, S., Sugihara, K., Miyake, S., Tomiyama, H., Hida, A., Hatsuno, M., Yamamoto, M. & Yoshida, T. Possible Involvement of Oxidative Stress in 5-Fluorouracil-Mediated Myelosuppression in Mice. *Basic & Clinical Pharmacology & Toxicology* **108**, 40–45 (2011).

551. Concetta Scuto, M., Mancuso, C., Tomasello, B., Laura Ontario, M., Cavallaro, A., Frasca, F., Maiolino, L., Trovato Salinaro, A., Calabrese, E. J. & Calabrese, V. Curcumin, Hormesis and the Nervous System. *Nutrients* **11**, 2417 (2019).

552. Chen, D., Wu, C., Qiu, Y., Chu, Q., Sun, X., Wang, X., Chen, J., Lu, M., Chen, D. & Pang, Q. Curcumin ameliorates hepatic chronic inflammation induced by bile duct obstruction in mice through the activation of heme oxygenase-1. *International Immunopharmacology* **78**, 106054 (2020).

553. Chen, M.-H., Lee, M.-Y., Chuang, J.-J., Li, Y.-Z., Ning, S.-T., Chen, J.-C. & Liu, Y.-W. Curcumin inhibits HCV replication by induction of heme oxygenase-1 and suppression of AKT. *International Journal of Molecular Medicine* **30**, 1021–1028 (2012).

554. Gaedeke, J., Noble, N. A. & Border, W. A. Curcumin blocks fibrosis in anti-Thy 1 glomerulonephritis through up-regulation of heme oxygenase 1. *Kidney International* **68**, 2042–2049 (2005).

555. D'Arcy, M. S. Cell death: a review of the major forms of apoptosis, necrosis and autophagy. *Cell Biology International* **43**, 582–592 (2019).

556. Ly, J. D., Grubb, D. R. & Lawen, A. The mitochondrial membrane potential (Δψm) in apoptosis; an update. *Apoptosis* **8**, 115–128 (2003).

557. Izyumov, D. S., Avetisyan, A. V, Pletjushkina, O. Y., Sakharov, D. V, Wirtz, K. W., Chernyak, B. V & Skulachev, V. P. "Wages of Fear": transient threefold decrease in intracellular ATP level imposes apoptosis. *Biochimica et Biophysica Acta - Bioenergetics* **1658**, 141–147 (2004).

558. Wyllie, A. H., Morris, R. G., Smith, A. L., & Dunlop, D. Chromatin cleavage in apoptosis: association with condensed chromatin morphology and dependence on macromolecular synthesis. *The Journal of Pathology* **142**, 67–77 (1984).

559. Zwaal, R. F. A., Comfurius, P. & Bevers, E. M. Surface exposure of phosphatidylserine in pathological cells. *Cellular & Molecular Life Sciences* **62**, 971–988 (2005).

560. Henderson, C. J., Aleo, E., Fontanini, A., Maestro, R., Paroni, G. & Brancolini, C. Caspase activation and apoptosis in response to proteasome inhibitors. *Cell Death & Differentiation* **12**, 1240–1254 (2005).

561. Shi, Y. Caspase activation, inhibition, and reactivation: a mechanistic view. *Protein Science : A Publication of the Protein Society* **13**, 1979–1987 (2004).

562. Li, H., Zhu, H., Xu, C. & Yuan, J. Cleavage of BID by Caspase 8 Mediates the Mitochondrial Damage in the Fas Pathway of Apoptosis. *Cell* **94**, 491–501 (1998).

563. Thornberry, N. A. & Lazebnik, Y. Caspases: Enemies Within. *Science* **281**, 1312 LP–1316 (1998).

564. Kitamura, Y., Shimohama, S., Kamoshima, W., Ota, T., Matsuoka, Y., Nomura, Y., Smith, M. A., Perry, G., Whitehouse, P. J. & Taniguchi, T. Alteration of proteins regulating apoptosis, Bcl-2, Bcl-x, Bax, Bak, Bad, ICH-1 and CPP32, in Alzheimer's disease. *Brain Research* **780**, 260–269 (1998).

565. Takashi Hattori Rikiya Fujita, Kunihiko Fukuchi, N. O. Heterodimerization of Bcl-2 and Bcl-XL with Bax and Bad in Colorectal Cancer. *Acta Oncologica* **39**, 495–500 (2000).

566. Azimian, H., Dayyani, M., Toossi, M. T. B. & Mahmoudi, M. Bax/Bcl-2

expression ratio in prediction of response to breast cancer radiotherapy. *Iranian Journal of Basic Medical Sciences* **21**, 325–332 (2018).

567. Yang, J., Liu, X., Bhalla, K., Kim, C. N., Ibrado, A. M., Cai, J., Peng, T.-I., Jones, D. P. & Wang, X. Prevention of Apoptosis by Bcl-2: Release of Cytochrome c from Mitochondria Blocked. *Science* **275**, 1129 LP – 1132 (1997).
568. Cai, J., Yang, J. & Jones, D. Mitochondrial control of apoptosis: the role of cytochrome c. *Biochimica et Biophysica Acta - Bioenergetics* **1366**, 139–149 (1998).
569. Tan, Y., Demeter, M. R., Ruan, H. & Comb, M. J. BAD Ser-155 Phosphorylation Regulates BAD/Bcl-XL Interaction and Cell Survival. *Journal of Biological Chemistry* **275**, 25865–25869 (2000).
570. Yang, E., Zha, J., Jockel, J., Boise, L. H., Thompson, C. B. & Korsmeyer, S. J. Bad, a heterodimeric partner for Bcl-xL and Bcl-2, displaces bax and promotes cell death. *Cell* **80**, 285–291 (1995).
571. Jones, J. M., Datta, P., Srinivasula, S. M., Ji, W., Gupta, S., Zhang, Z., Davies, E., Hajnóczky, G., Saunders, T. L., Van Keuren, M. L., Fernandes-Alnemri, T., Meisler, M. H. & Alnemri, E. S. Loss of Omi mitochondrial protease activity causes the neuromuscular disorder of mnd2 mutant mice. *Nature* **425**, 721–727 (2003).
572. Kroemer, G., Galluzzi, L. & Brenner, C. Mitochondrial membrane permeabilization in cell death. *Physiological Reviews* **87**, 99–163 (2007).
573. Martinez-Ruiz, G., Maldonado, V., Ceballos-Cancino, G., Grajeda, J. P. R. & Melendez-Zajgla, J. Role of Smac/DIABLO in cancer progression. *Journal of Experimental & Clinical Cancer Research* **27**, 48 (2008).
574. Locksley, R. M., Killeen, N. & Lenardo, M. J. The TNF and TNF Receptor Superfamilies: Integrating Mammalian Biology. *Cell* **104**, 487–501 (2001).
575. Hsu, H., Xiong, J. & Goeddel, D. V. The TNF receptor 1-associated protein TRADD signals cell death and NF-κB activation. *Cell* **81**, 495–504 (1995).
576. Berthelet, J. & Dubrez, L. Regulation of Apoptosis by Inhibitors of Apoptosis (IAPs). *Cells* **2**, 163–187 (2013).
577. Gyrd-Hansen, M. & Meier, P. IAPs: from caspase inhibitors to modulators of NF-κB, inflammation and cancer. *Nature Reviews Cancer* **10**, 561–574 (2010).
578. Liston, P., Fong, W. G. & Korneluk, R. G. The inhibitors of apoptosis: there is more to life than Bcl2. *Oncogene* **22**, 8568–8580 (2003).
579. Hrdinka, M. & Yabal, M. Inhibitor of apoptosis proteins in human health and

disease. *Genes & Immunity* **20**, 641–650 (2019).

580. Zhang, H., Kim, J. K., Edwards, C. A., Xu, Z., Taichman, R. & Wang, C.-Y. Clusterin inhibits apoptosis by interacting with activated Bax. *Nature Cell Biology* **7**, 909–915 (2005).

581. Scott, F.L., Denault, J.B., Riedl, S.J., Shin, H., Renatus, M. & Salvesen, G. S. XIAP inhibits caspase-3 and-7 using two binding sites: evolutionarily conserved mechanism of IAPs. *The European Molecular Biology Organization Journal* **24**, 645-655 (2005).

582. Srinivasula, S.M., Hegde, R., Saleh, A., Datta, P., Shiozaki, E., Chai, J., Lee, R.A., Robbins, P.D., Fernandes-Alnemri, T., Shi, Y. & Alnemri, E. S. A conserved XIAP-interaction motif in caspase-9 and Smac/DIABLO regulates caspase activity and apoptosis. *Nature* **410**, 112–116 (2001).

583. Zumbrägel, F.K., Machtens, D.A., Curth, U., Lüder, C.G., Reubold, T.F. & Eschenburg, S. Survivin does not influence the anti-apoptotic action of XIAP on caspase-9. *Biochemical & Biophysical Research Communications* **482**, 530-535 (2017).

584. Gottfried, Y., Rotem, A., Lotan, R., Steller, H. & Larisch, S. The mitochondrial ARTS protein promotes apoptosis through targeting XIAP. *The European Molecular Biology Organization Journal* **23**, 1627-1635 (2004).

585. Vucic, D., Deshayes, K., Ackerly, H., Pisabarro, M.T., Kadkhodayan, S., Fairbrother, W.J. & Dixit, V. M. SMAC negatively regulates the anti-apoptotic activity of melanoma inhibitor of apoptosis (ML-IAP). *Journal of Biological Chemistry* **277**, 12275-12279 (2002).

586. Shin, H., Renatus, M., Eckelman, B.P., Nunes, V.A., Sampaio, C.A. & Salvesen, G. S. The BIR domain of IAP-like protein 2 is conformationally unstable: implications for caspase inhibition. *Biochemical Journal* **385**, 1-10 (2005).

587. Abukhdeir, A. M. & Park, B. H. P21 and p27: roles in carcinogenesis and drug resistance. *Expert Reviews in Molecular Medicine* **10**, e19–e19 (2008).

588. Dohoney, K. M., Guillerm, C., Whiteford, C., Elbi, C., Lambert, P. F., Hager, G. L. & Brady, J. N. Phosphorylation of p53 at serine 37 is important for transcriptional activity and regulation in response to DNA damage. *Oncogene* **23**, 49–57 (2004).

589. El-Deiry, W.S., Harper, J.W., O'Connor, P.M., Velculescu, V.E., Canman, C.E.,

Jackman, J., Pietenpol, J.A., Burrell, M., Hill, D.E., Wang, Y. & Wiman, K. G. WAF1/CIP1 is induced in p53-mediated G1 arrest and apoptosis. *Cancer Research* **54**, 1169–1174 (1994).

590. Harper, J.W., Elledge, S.J., Keyomarsi, K., Dynlacht, B., Tsai, L.H., Zhang, P., Dobrowolski, S., Bai, C., Connell-Crowley, L. and Swindell, E. Inhibition of cyclin-dependent kinases by p21. *Molecular Biology of the Cell* **6**, 387–400 (1995).
591. Xiong, Y., Hannon, G.J., Zhang, H., Casso, D., Kobayashi, R. & Beach, D. p21 is a universal inhibitor of cyclin kinases. *Nature* **366**, 701–704 (1993).
592. Dulić, V., Kaufmann, W.K., Wilson, S.J., Tisty, T.D., Lees, E., Harper, J.W., Elledge, S.J. & Reed, S. I. p53-dependent inhibition of cyclin-dependent kinase activities in human fibroblasts during radiation-induced G1 arrest. *Cell* **76**, 1013–1023 (1994).
593. Di Leonardo, A., Linke, S.P., Clarkin, K. & Wahl, G. M. DNA damage triggers a prolonged p53-dependent G1 arrest and long-term induction of Cip1 in normal human fibroblasts. *Genes & Development* **8**, 2540–2551 (1994).
594. Yadav, V., Sultana, S., Yadav, J. & Saini, N. Gatifloxacin induces S and G2-phase cell cycle arrest in pancreatic cancer cells via p21/p27/p53. *Plos one* **7**, e47796–e47796 (2012).
595. Agnantis, N. J., Goussia, A., Zagorianakou, P. & Bai, M. 19 - Alterations of the Cell Cycle Regulating Proteins in Invasive Breast Cancer: Correlation with Proliferation, Apoptosis, and Clinical Outcome. in *Molecular Genetics; Lung and Breast Carcinomas* (ed. Hayat, M. A. B. T.-H. of I. and in S. H. of H. C.) **1** 425–438 (Academic Press, 2002).
596. Campos, A. & Clemente-Blanco, A. Cell Cycle and DNA Repair Regulation in the Damage Response: Protein Phosphatases Take Over the Reins. *International Journal of Molecular Sciences* **21**, 446 (2020).
597. Bernstein, C., Bernstein, H., Payne, C. M. & Garewal, H. DNA repair/pro-apoptotic dual-role proteins in five major DNA repair pathways: fail-safe protection against carcinogenesis. *Mutation Research/Reviews in Mutation Research* **511**, 145–178 (2002).
598. Zhu, H., Zhang, L., Wu, S., Teraishi, F., Davis, J. J., Jacob, D. & Fang, B. Induction of S-phase arrest and p21 overexpression by a small molecule 2[[3-(2,3-dichlorophenoxy)propyl] amino]ethanol in correlation with activation of ERK. *Oncogene* **23**, 4984–4992 (2004).

599. Herkel, J. & Cohen, I. R. p53 Autoantibodies. in *Autoantibodies* (eds. Shoenfeld, Y., Gershwin, M. E. & Meroni, P. L. B. T.) 271–276 (Elsevier, 2007). doi:https://doi.org/10.1016/B978-044452763-9/50040-8.

600. Dornan, D., Shimizu, H., Perkins, N. D. & Hupp, T. R. DNA-dependent Acetylation of p53 by the Transcription Coactivator p300. *Journal of Biological Chemistry* **278**, 13431–13441 (2003).

601. Toledo, F. & Wahl, G. M. Regulating the p53 pathway: *in vitro* hypotheses, *in vivo* veritas. *Nature Reviews Cancer* **6**, 909–923 (2006).

602. Vousden, K. H. & Lane, D. P. p53 in health and disease. *Nature Reviews Molecular Cell Biology* **8**, 275–283 (2007).

603. Saito, S., Goodarzi, A. A., Higashimoto, Y., Noda, Y., Lees-Miller, S. P., Appella, E. & Anderson, C. W. ATM Mediates Phosphorylation at Multiple p53 Sites, Including Ser46, in Response to Ionizing Radiation. *Journal of Biological Chemistry* **277**, 12491–12494 (2002).

604. Olsson, A., Manzl, C., Strasser, A. & Villunger, A. How important are post-translational modifications in p53 for selectivity in target-gene transcription and tumour suppression? *Cell Death & Differentiation* **14**, 1561–1575 (2007).

605. Castrogiovanni, C., Waterschoot, B., De Backer, O. & Dumont, P. Serine 392 phosphorylation modulates p53 mitochondrial translocation and transcription-independent apoptosis. *Cell Death & Differentiation* **25**, 190–203 (2018).

606. Semple, J. I., Smits, V. A. J., Fernaud, J.-R., Mamely, I. & Freire, R. Cleavage and degradation of Claspin during apoptosis by caspases and the proteasome. *Cell Death & Differentiation* **14**, 1433–1442 (2007).

607. Sar, F., Lindsey-Boltz, L. A., Subramanian, D., Croteau, D. L., Hutsell, S. Q., Griffith, J. D. & Sancar, A. Human Claspin Is a Ring-shaped DNA-binding Protein with High Affinity to Branched DNA Structures. *Journal of Biological Chemistry* **279**, 39289–39295 (2004).

608. Takayama, S., Reed, J. C. & Homma, S. Heat-shock proteins as regulators of apoptosis. *Oncogene* **22**, 9041–9047 (2003).

609. Mehlen, P., Kretz-Remy, C., Préville, X. & Arrigo, A. P. Human hsp27, Drosophila hsp27 and human alphaB-crystallin expression-mediated increase in glutathione is essential for the protective activity of these proteins against TNFalpha-induced cell death. *The European Molecular Biology Organization Journal* **15**, 2695–2706 (1996).

610. Rogalla, T., Ehrnsperger, M., Preville, X., Kotlyarov, A., Lutsch, G., Ducasse, C., Paul, C., Wieske, M., Arrigo, A.-P., Buchner, J. & Gaestel, M. Regulation of Hsp27 Oligomerization, Chaperone Function, and Protective Activity against Oxidative Stress/Tumor Necrosis Factor α by Phosphorylation. *Journal of Biological Chemistry* **274**, 18947–18956 (1999).

611. Garrido, C., Bruey, J.-M., Fromentin, A., Hammann, A., Patrick Arrigo, A. & Solary, E. HSP27 inhibits cytochrome c-dependent activation of procaspase-9. *The Federation of American Societies for Experimental Biology Journal* **13**, 2061–2070 (1999).

612. Bruey, J.-M., Ducasse, C., Bonniaud, P., Ravagnan, L., Susin, S. A., Diaz-Latoud, C., Gurbuxani, S., Arrigo, A.-P., Kroemer, G., Solary, E. & Garrido, C. Hsp27 negatively regulates cell death by interacting with cytochrome c. *Nature Cell Biology* **2**, 645–652 (2000).

613. Gupta, S. & Knowlton, A. . Cytosolic Heat Shock Protein 60, Hypoxia, and Apoptosis. *Circulation* **106**, 2727–2733 (2002).

614. Beere, H. M., Wolf, B. B., Cain, K., Mosser, D. D., Mahboubi, A., Kuwana, T., Tailor, P., Morimoto, R. I., Cohen, G. M. & Green, D. R. Heat-shock protein 70 inhibits apoptosis by preventing recruitment of procaspase-9 to the Apaf-1 apoptosome. *Nature Cell Biology* **2**, 469–475 (2000).

615. Saleh, A., Srinivasula, S. M., Balkir, L., Robbins, P. D. & Alnemri, E. S. Negative regulation of the Apaf-1 apoptosome by Hsp70. *Nature Cell Biology* **2**, 476–483 (2000).

616. Swaminathan, S. Drugs used in tuberculosis and leprosy. in *Side Effects of Drugs Annual 28* (ed. Aronson, J. K. B. T.) **28**, 342–345 (Elsevier, 2005).

617. Wilkinson, G. R. Drug Metabolism and Variability among Patients in Drug Response. *New England Journal of Medicine* **352**, 2211–2221 (2005).

618. Slaughter, R. L. & Edwards, D. J. Recent Advances: the Cytochrome P450 Enzymes. *Annals of Pharmacotherapy* **29**, 619–624 (1995).

619. Sheweita, S. A. Drug-metabolizing enzymes mechanisms and functions. *Current Drug Metabolism* **1**, 107–132 (2000).

620. Fontana, E., Dansette, P.M. & Poli, S. M. Cytochrome p450 enzymes mechanism based inhibitors: common sub-structures and reactivity. *Current Drug Metabolism* **6**, 413–451 (2005).

621. Bradford, L. D. CYP2D6 allele frequency in European Caucasians, Asians,

Africans and their descendants. *Pharmacogenomics* **3**, 229–243 (2002).

622. Meyer, U. A. Pharmacogenetics and adverse drug reactions. *The Lancet* **356**, 1667–1671 (2000).

623. Komatsu, T., Yamazaki, H., Shimada, N., Nakajima, M. & Yokoi, T. Roles of Cytochromes P450 1A2, 2A6, and 2C8 in 5-Fluorouracil Formation from Tegafur, an Anticancer Prodrug, in Human Liver Microsomes. *Drug Metabolism & Disposition* **28**, 1457 LP–1463 (2000).

624. Yamamiya, I., Yoshisue, K., Ishii, Y., Yamada, H. & Yoshida, K.-I. Enantioselectivity in the cytochrome P450-dependent conversion of tegafur to 5-fluorouracil in human liver microsomes. *Pharmacology Research & Perspectives* **1**, e00009–e00009 (2013).

625. Brickell, K., Porter, D. & Thompson, P. Phenytoin toxicity due to fluoropyrimidines (5FU/capecitabine): three case reports. *British Journal of Cancer* **89**, 615–616 (2003).

626. Miura, K., Kinouchi, M., Ishida, K., Fujibuchi, W., Naitoh, T., Ogawa, H., Ando, T., Yazaki, N., Watanabe, K., Haneda, S., Shibata, C. & Sasaki, I. 5-FU metabolism in cancer and orally-administrable 5-FU drugs. *Cancers* **2**, 1717–1730 (2010).

627. Binkhathlan, Z. & Lavasanifar, A. P-glycoprotein inhibition as a therapeutic approach for overcoming multidrug resistance in cancer: current status and future perspectives. *Current Cancer Drug Targets* **13**, 326–346 (2013).

628. Holohan, C., Van Schaeybroeck, S., Longley, D.B. & Johnston, P. G. Cancer drug resistance: an evolving paradigm. *Nature Reviews Cancer* **13**, 714–726 (2013).

629. Nanayakkara, A. K., Follit, C. A., Chen, G., Williams, N. S., Vogel, P. D. & Wise, J. G. Targeted inhibitors of P-glycoprotein increase chemotherapeutic-induced mortality of multidrug resistant tumor cells. *Scientific Reports* **8**, 967 (2018).

630. Ferreira, R. J., dos Santos, D. J. V. A. & Ferreira, M.-J. U. P-glycoprotein and membrane roles in multidrug resistance. *Future Medicinal Chemistry* **7**, 929–946 (2015).

631. Lehne, G. P-glycoprotein as a drug target in the treatment of multidrug resistant cancer. *Current Drug Targets* **1**, 85–99 (2000).

632. Ramalhete, C., Molnár, J., Mulhovo, S., Rosário, V. E. & Ferreira, M.-J. U. New potent P-glycoprotein modulators with the cucurbitane scaffold and their

synergistic interaction with doxorubicin on resistant cancer cells. *Bioorganic & Medicinal Chemistry* **17**, 6942–6951 (2009).

633. Ramalhete, C., Mulhovo, S., Molnar, J. & Ferreira, M.-J. U. Triterpenoids from *Momordica balsamina*: Reversal of ABCB1-mediated multidrug resistance. *Bioorganic & Medicinal Chemistry* **24**, 5061–5067 (2016).

Chapter 7

7. Appendices

Annexure A – Mitochondrial membrane potential

The number of green and red fluorescent cells was quantified using the ImageJ (32 bit) software application (imagej.nih.gov/ij/list.html), version 1.52a. The following procedure was used for quantifying;

1. After opening the image, the background was subtracted by selecting;
   - Process > Subtract background with rolling ball
2. The multi-colour image (RGB) was converted to grayscale (8-bit) by selecting;
   - Image > Type > 8-bit
3. The relative size of the cells was set as 100 µm obtained from the burnt scale on the images
4. A copy of the image was made by selecting;
   - Image > Duplicate
5. A binary image was then created by selecting;
   - Image > Adjust > Threshold > Apply
   - In “Threshold”, the cells of interest were highlighted
6. Particles that were merged together were corrected for by selecting;
   - Process > Binary > Watershed
7. Counting of cells was done by selecting;
   - Analyse > Analyse particles
   - Objects matching the specified shape and size were highlighted
   - The summary of the total number and area of cells was then presented on a separate window

Annexure B – AO/PI

The intensity of the red fluorescence was quantified using the ImageJ (32 bit) software application (imagej.nih.gov/ij/list.html), version 1.52a. The following procedure was used for quantifying;

1. The multi-colour images (RGB) were split to grayscale images by selecting;
   - Image > Colour > Split channels
2. A copy of the image was made by selecting;
   - Image > Duplicate
3. A binary image was then created by selecting;
   - Image > Adjust > Threshold > Apply
   - In “Threshold”, all structures of interest were highlighted
4. The background was subtracted by selecting;
   - Process > Subtract background with a rolling ball
5. Particles that were merged were corrected for by selecting;
   - Process > Binary > Watershed
6. Measurements for intensity values were set by selecting;
   - Analyse > Set Measurements
   - Under “Set Measurements” the “Redirect to” line was set to the name of the copy of the image still in grayscale
7. Particles of the binary image were then analysed by selecting;
   - Analyse > Analyse particles
   - The summary of the intensity measurement of particles was then presented on a separate window

Annexure C – Annexin V/PI

Cells treated with the MeOH extract at IC_{50} concentration was used for setting the gates and compensation due to autofluorescence.

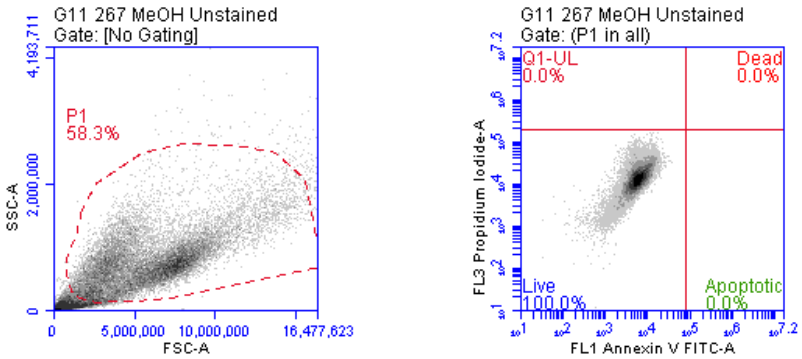

A B

Figure 7.1: Representative image of gating applied to forward and side scatter plots.

A – A polygonal gating was drawn around the cell population in the forward/side scatter lot (P1). The quadrant gate was set in the FL1/FL3 plot using an unstained cell sample treated with the MeOH extract, which displayed autofluorescence in the FL3 channel.

For determination of colour compensation settings, the cells treated with the MeOH extract were stained with Annexin and PI separately. The Annexin/PI template used already contained compensation settings which were adjusted so that the median values for FL3 in the live and apoptotic quadrat were similar (Fig 7.2 and table 7.1)

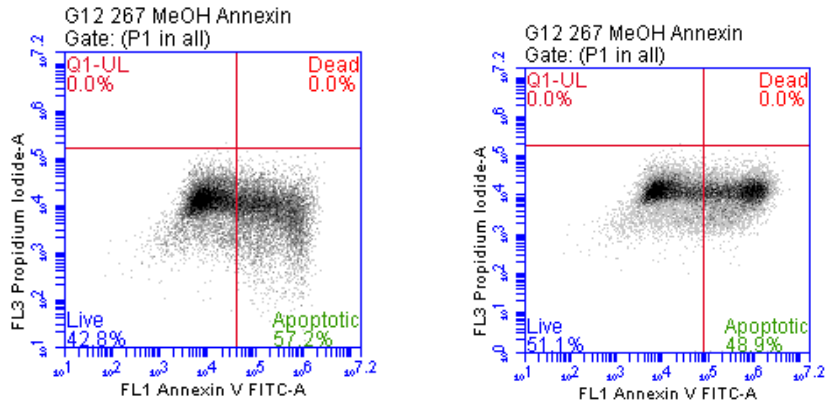

A B

Figure 7.2: Representative image for compensation of Annexin V stained sample.

A – The compensation setting of the template (correct FL3 by subtracting 2.6% of FL1) did not results in equal median values, which were reduced to 1.6% (B)

FL1 was corrected in a similar way. The MeOH extract-treated cells stained with PI only were then used to Check the compensation settings for FL1. The median values for the Q1-UL and live quadrants were again slightly overcompensated and the percentage was reduced to 0.28% to make the median value for FL1 for both quadrants (Fig 7.3).

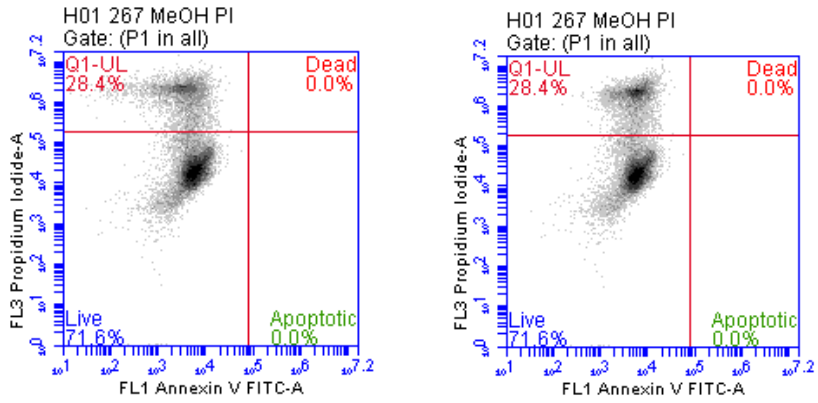

Figure 7.3: Representative image for compensation of PI stained samples.

A – before adjusting FL1 compensation (0.4%) – B after adjusting compensation (0.28%).

Table 7. 1: Before and after compensation median values for FL3 and FL1

	Median values (Before)	Median values (After)
FL3	11356.0 and 3230.0	11599.0 and 11458.0
FL1	3308.5 and 5440.0	5501.0 and 5468.0

Annexure D – Cell cycle analysis

Cell cycle analysis was done using the FlowJo analysis software application, version 10.6.2 (https://www.flowjo.com). The Watson Pragmatic algorithm univariate modelling was used to create a fit to the cell cycle data. The procedure was as follows;

1. Cell population of interest were identified using the forward vs side scatter (FSC vs SSC) gating.
2. The forward scatter height vs side scatter area (FSC-H vs SSC-A) density plot was used to exclude doublets by gating singlets using the polygonal gating tool

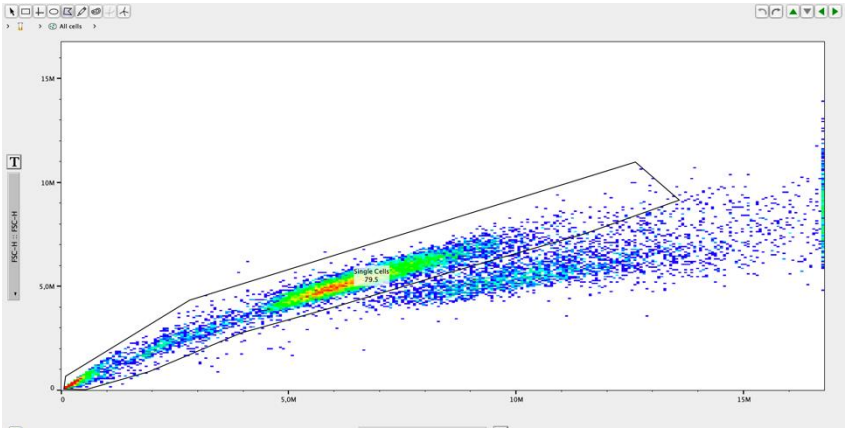

Figure 7.4: Representative image of doublet exclusion.

A polygonal gate was drawn around singlet cells from a FSC-H vs FSC-A density plot.

3. Single parameter histograms were then generated to distinguish cells in different cell cycle phases.

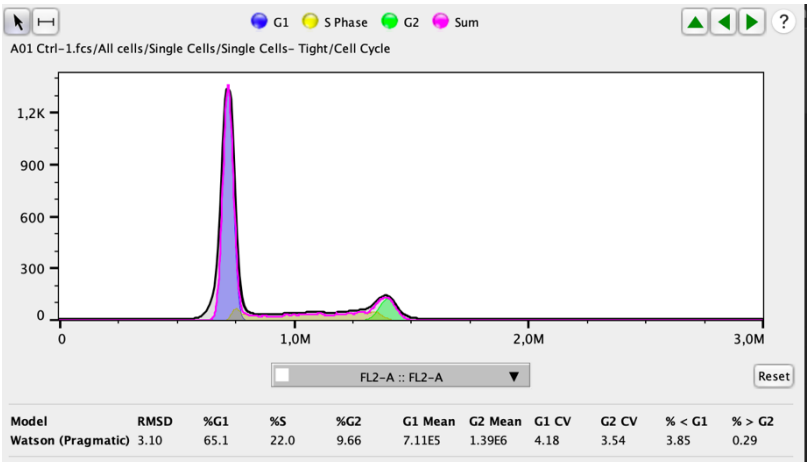

Figure 7.5: Representative image of single parameter histogram.

The single parameter histogram was generated using FL2-A to distinguish cells in different phases of the cell cycle.

Annexure E - Effect of *M. balsamina* MeOH extract on the efficacy of 5-Fluorouracil on activity of P450 enzymes

Methodology

The effect of the *M. balsamina* H_2O and MeOH extracts on the efficacy of 5-FU on CYP1A2, CYP2A6 and CYP2C8 activity was assessed using the Vivid® CYP450 Screening kits, following the manufacturer's description (Thermo Fisher Scientific, Waltham, USA). The assay was conducted as in 3.12 and cells treated with a range of 5-FU concentrations together with IC_{50} concentrations of the MeOH extract obtained for each CYP. The concentrations were 0.8 to 80 µg/ml of 5-FU with 154 µg/ml of the MeOH extract for CYP1A2, 93 µg/ml of the MeOH extract for CYP2A6 and 14 µg/ml of the MeOH extract for CYP2C8.

Results

The results showed that the *M. balsamina* MeOH extract had no effect on the efficacy of 5-FU regarding activity of CYP1A2, CYP2A6 and CYP2C8 (Figure 7.7). This was made evident by the MeOH IC_{50} concentrations having the same percentage inhibition with the combination treatment with 5-FU, thereby elucidating that the extract did not promote nor interfere with the efficacy of 5-FU.

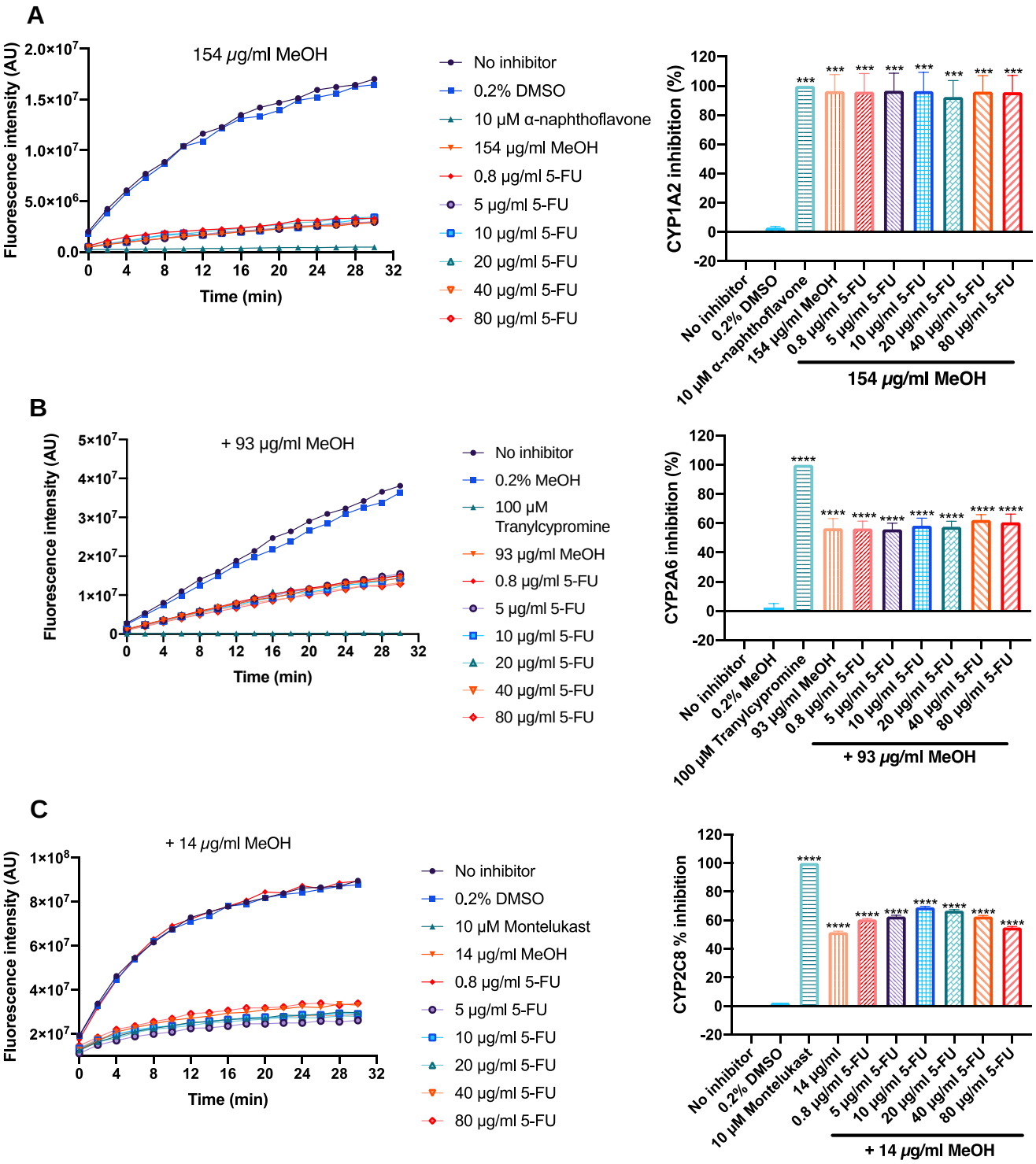

Figure 7.6: Effect of the *M. balsamina* methanol extract on the efficacy of 5-Fluorouracil on activity of CYPs 1A2, 2A6 and 2C8.

CYP activity was assessed by spectrophotometry using the Vivid® CYP450 Screening Kits. Tested 5-FU concentrations ranged from 0.8 to 80 µg/ml. DMSO or methanol at 0.2% served as a vehicle control and 10 µM α-naphthoflavone, 100 µM tranylcypromine or 50 µM of sulfaphenazole, as a positive inhibitor. Each data point represents the S.E.M of two independent experiments, performed in duplicate. *** $p \leq 0.001$ and **** $p \leq 0.0001$ indicate significant differences to the DMSO/MeOH control.

Annexure F – IC_{50} graphs

MTT 24 h (MeOH)

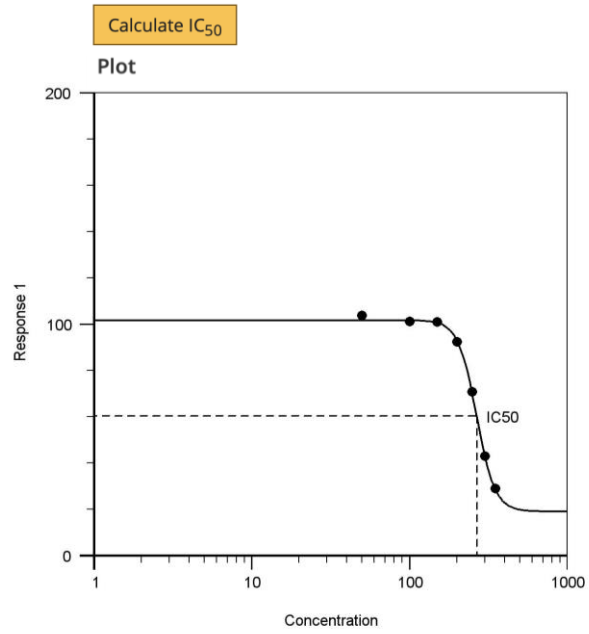

Figure 7.7: *M. balsamina* MeOH extract IC_{50} graph (24h).

The IC_{50} value for the *M. balsamina* MeOH extract on HT-29 colon cancer cells was determined using AAT Bioquest from MTT data obtained after 24h of treatment.

MTT 72 h (5-FU)

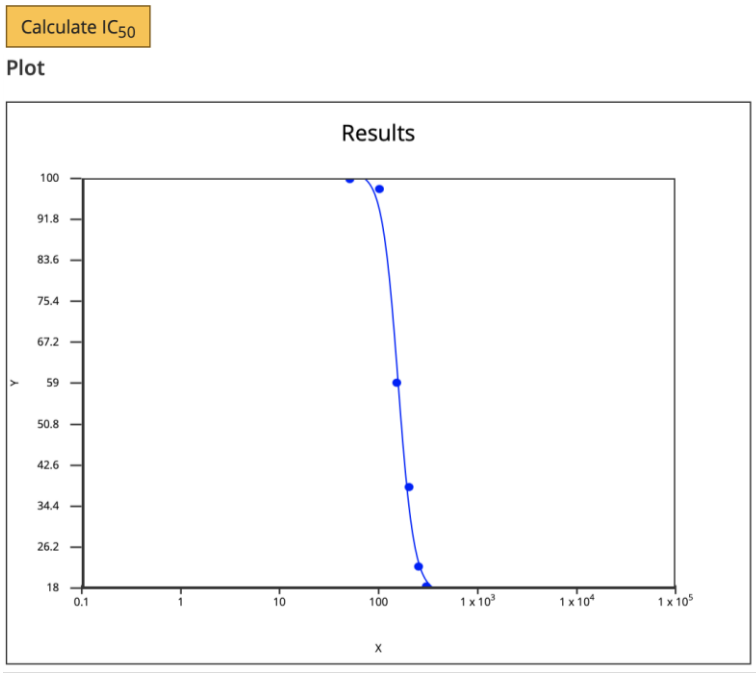

Figure 7.8: *M. balsamina* MeOH extract IC_{50} graph (72h).

The IC_{50} value for the *M. balsamina* MeOH extract on HT-29 colon cancer cells was determined using AAT Bioquest from MTT data obtained after 72h of treatment.

MTT 72 h (5-FU)

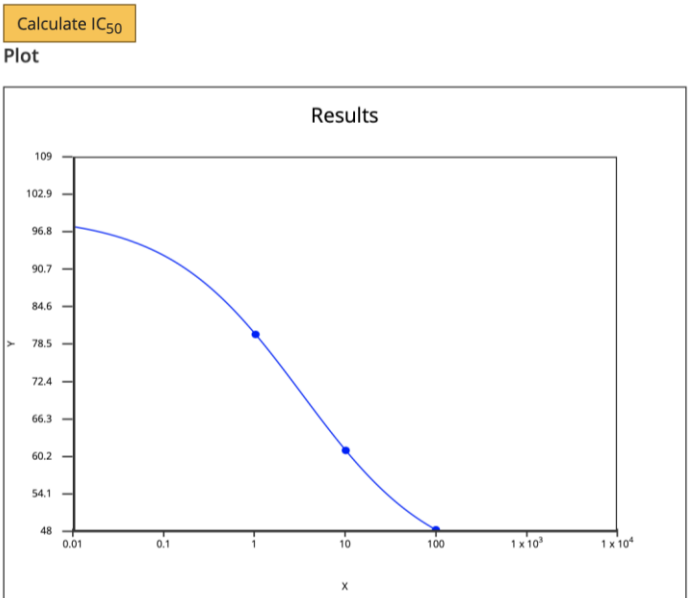

Figure 7.9: 5-Fluorouracil IC_{50} graph.

The IC_{50} value for 5-Fluorouracil on HT-29 colon cancer cells was determined using AAT Bioquest from MTT data obtained after 24h of treatment.

Annexure G – List of reagents and main equipment

Reagents

- Methanol (cat# 34860), butanol (cat# B7906), acetic acid (cat# A6283), chloroform (cat# C2432), ethyl acetate (cat# 270989), formic acid (cat# F0507), benzene (cat# 270709), ethyl acetate (cat# 270989), ammonium hydroxide (cat# 221228), Iron (III) chloride (cat# 157740), Sodium hydroxide (cat# S8045), lead (IV) acetate (cat# 185191), α-naphthol (cat# N1000), acetic anhydride (cat# 242845), sulfuric acid (cat# 339741) ascorbic acid (cat#A92902) acridine orange (cat# A6014), 5-Fluorouracil (5-FU) (cat# F6627-1G), Curcumin (cat# C1386-5G), 3-(4,5-dimethylthiazol-2-yl)-2,5-diphenyltetrazolium (MTT) (cat# M2003-1G), 2',7'-dichlorodihydrofluorescein diacetate (DCFH-DA) (cat# D6883), HEPES (cat# 83264-500ML-F), α-naphthoflavone (cat# N5757), Tranylcypromine (cat# P8511), Sulfaphenazole (cat# NS0758) and Dimethyl sulfoxide (cat# 276855) (Sigma-Aldrich, St. Louis, USA)
- Aluminium-backed silica gel 60 F_{254} plates (MilliporeSigma, cat# 10554, Burlington, USA)
- (PBS) (Lonza, cat# BE17-516F, Basel, Switzerland)
- Dulbecco's Modified Eagle's Medium (DMEM) (HyClone Laboratories, cat# SH30285.03, South Logan, USA)
- Propidium iodide (PI) (Invitrogen, cat# p3566, Life Technologies, Carlsbad, USA)
- (FBS) (Gibco, cat# 10500064, Life Technologies, Carlsbad, USA).
- Dulbecco's phosphate-buffered saline (DPBS) (Gibco, cat# 14040133, Life Technologies, Carlsbad, USA).
- trypsin (Gibco, cat# 25200072, Life Technologies, Carlsbad, USA)
- Trypan blue (Invitrogen, cat# T10282, Carlsbad, USA)
- Muse™ Multi-Colour DNA Damage kit (MilliporeSigma, cat# MCH200107, Burlington, USA)
- 5,5′,6,6′-tetrachloro-1,1′,3,3′-tetraethylbenzimi-dazolylcarbocyanine iodide (JC-1) (Sigma, cat#T4069-5MG, Steinheim, Germany)
- Caspase-8 colourimetric assay kit (cat# K119-100) Caspase-9 colourimetric assay kit (cat# K113-100) (R&D Systems, Minneapolis, USA)
- Pierce™ BCA Protein Assay kit (ThermoFisher Scientific™, cat# 23225 Waltham, USA).
- RNase A (Qiagen, cat# 19101, Hilden, Germany)

- Vivid® CYP450 screening kits CYP1A2 (cat# P2863), CYP2A6 (cat# PV6140), CYP2C8 (cat# P2861) and CYP2C9 (cat# P2860) (Thermo Fisher Scientific, Waltham, USA)
- Montelukast (cat# AB142323, Abcam, Cambridge, UK)
- P-gp-Glo™ Assay Systems with P-glycoprotein (Promega, cat# V3591, Madison, USA)

Equipment

- Freeze-dryer (Labconco, Labotec, Cape Town)
- Microtiter plate reader (GloMax®-Multi+Detection system, Promega, Madison, USA)
- Milli-Q water purification system (Millipore, Milford, USA)
- Filter unit ((0.22 µm polyethersulfone) (Millipore, cat#SLGPO33RS Watford, UK)
- Filter paper with a pore size of 12-15 µm (Munktell, UK)
- LC/MS (Agilent Technologies, Santa Clara, USA)
- Inverted phase-contrast microscope (Olympus CKX31, Tokyo, Japan).
- SpectraMax i3x (Molecular Devices, LLC, Sunnyvale, CA, USA).
- Centrifuge (SL16R; Thermo Fischer Scientific, Johannesburg, South Africa)
- BD Accuri™ C6 flow cytometer (BD Biosciences, Johannesburg, South Africa)
- Inverted fluorescent microscope (Nikon Eclipse Ti/S Fluorescence Microscope (Nikon, Minato City, Tokyo, Japan))
- ChemiDoc MP system (Bio-Rad, Hercules, USA)
- TissueLyser (Qiagen™, Hilden, Germany)

Turnitin report

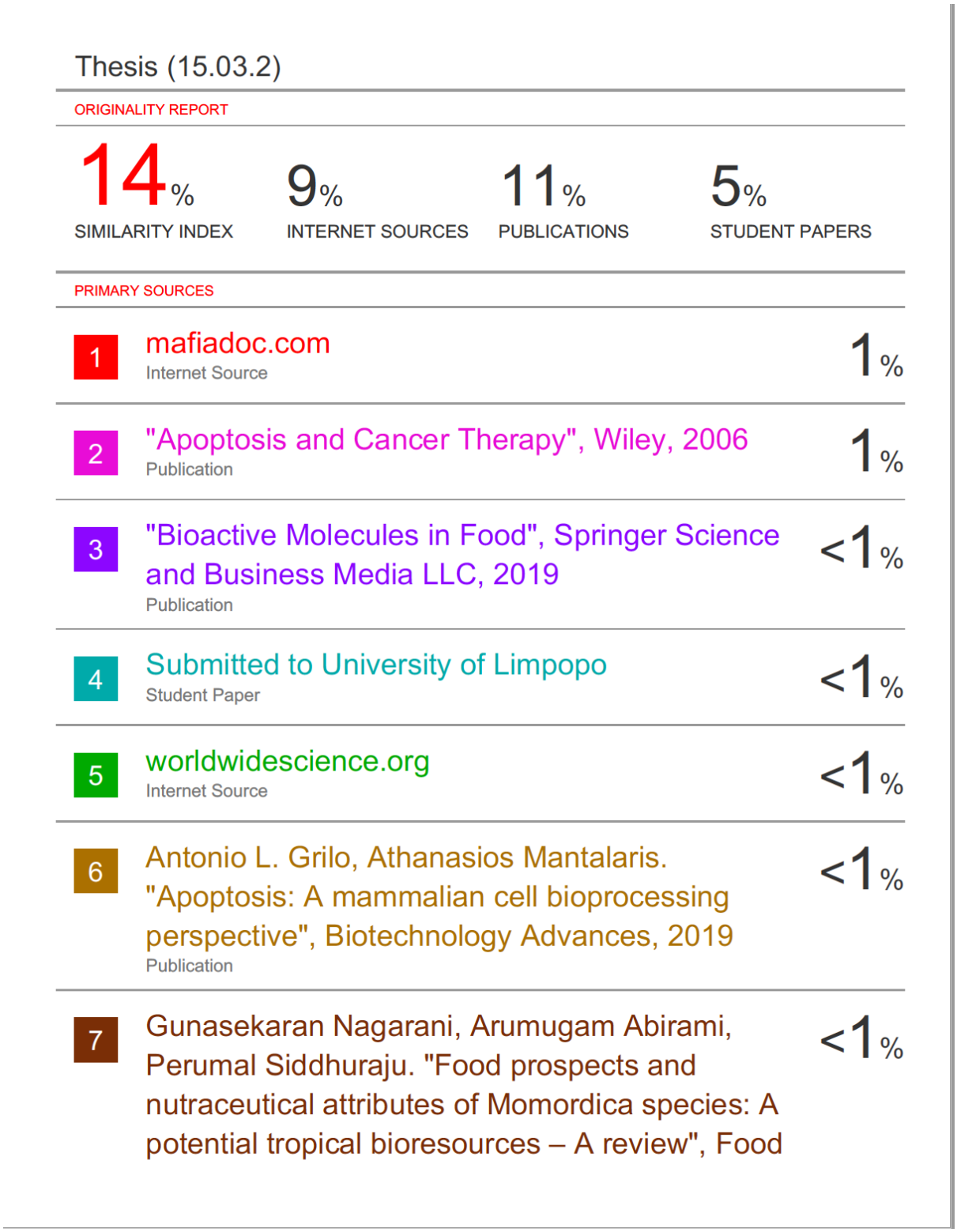

Thesis (15.03.2)

ORIGINALITY REPORT

14%	9%	11%	5%
SIMILARITY INDEX	INTERNET SOURCES	PUBLICATIONS	STUDENT PAPERS

PRIMARY SOURCES

1	mafiadoc.com Internet Source	1%
2	"Apoptosis and Cancer Therapy", Wiley, 2006 Publication	1%
3	"Bioactive Molecules in Food", Springer Science and Business Media LLC, 2019 Publication	<1%
4	Submitted to University of Limpopo Student Paper	<1%
5	worldwidescience.org Internet Source	<1%
6	Antonio L. Grilo, Athanasios Mantalaris. "Apoptosis: A mammalian cell bioprocessing perspective", Biotechnology Advances, 2019 Publication	<1%
7	Gunasekaran Nagarani, Arumugam Abirami, Perumal Siddhuraju. "Food prospects and nutraceutical attributes of Momordica species: A potential tropical bioresources – A review", Food	<1%